The Role of Immunoglobulin M in Immune Evasion by *Plasmodium falciparum*

Thesis submitted in accordance with the requirements of the University of Liverpool for the degree of Doctor in Philosophy

by Katy Lloyd

May 2015

If we knew what it was
we were doing, it
would not be called
research, would it?

Albert Einstein

Abstract

Plasmodium falciparum parasites have evolved numerous ingenious methods to subvert immune recognition, in order to survive within the human host. One such immune evasion mechanism features the expression of ligands which bind to the Fc-portion of human IgM. The binding of IgM to *P. falciparum*-encoded PfEMP1 molecules expressed on infected erythrocyte surfaces has been well characterised. Recently, two novel IgM-binding proteins expressed on merozoites were identified, known as DBLMSP and DBLMSP2. The aim of this project was to characterise the binding of these merozoite surface proteins to IgM, and to investigate what advantage IgM binding may afford *P. falciparum* merozoites.

Although DBLMSP and DBLMSP2 have been implicated in camouflaging critical epitopes from immune responses, it is unknown whether these proteins function to alter the binding of IgM to IgM-receptors, such as the human Fcμ receptor. A panel of domain-swap antibodies, in which homologous domains are exchanged between human IgA and IgM, identified the Cμ4 domain of human IgM as the target of both the DBLMSP proteins and hFcμR. Despite this, the binding of DBLMSP and DBLMSP2 to IgM did not prevent its binding to hFcμR, suggesting the malarial proteins recognise an alternative region on IgM than that recognised by hFcμR. In fact, DBLMSP and DBLMSP2 engaged IgM bound to both hFcμR and DC-SIGN, which was found to facilitate interactions of these malarial proteins with IgM-positive human lymphocytes. However, binding of recombinant DBLMSP and DBLMSP2 *per se* did not induce proliferation or apoptosis of human lymphocytes. A possible explanation for this is that DBLMSP and DBLMSP2 were found to exist in complex with IgM and other unidentified parasite molecules. This suggests that these proteins associate with other merozoite surface proteins *in vivo*, which could potentially induce functional consequences upon lymphocyte binding. This thesis lays the foundation for future research into how native IgM-parasite protein complexes may function to bind to lymphocytes and modulate host immune responses.

This thesis also presents data that hFcμR functions as an endocytosis receptor for human IgM, in which the binding and internalisation of human IgM occurs in a glycan-independent manner.

Declaration statement

I declare that the work on which this thesis is based is my original work, except where acknowledgements indicate otherwise. I further declare that this work has not been previously submitted for a degree at the University of Liverpool or any other institution.

List of publications generated as part of this thesis

I. **Lloyd, K.A.** *et al.* Investigating the role of *P. falciparum* IgM binding proteins DBLMSP and DBLMSP2 on IgM receptor interactions. In preparation.

II. **Lloyd, K.A.** *et al.* Glycosylation of human IgM does not affect binding or internalisation by hFcμR. In preparation.

III. Czajkowsky, D.M., Andersen, J., Fuchs, A., Wilson, T., Mekhaiel, D.N., Colonna, M., He, J., Shao, Z., Mitchell, D.A., Wu, G., Dell, A., Haslam, S., **Lloyd, K.A.**, Moore, S., Sandlie, I., Blundell, P. and Pleass, R.J. (2015) Developing the Hexa-Fc scaffold for drug and vaccine application. Scientific Reports, **5**: 9526.

Acknowledgements

First of all, I would like to thank Professor Pleass for not only giving me the opportunity to work in his laboratory, but also for the support and guidance he has provided over the course of my PhD. Thanks to Dr Pat Blundell for help with the cloning experiments and for coming to the rescue on many occasions of crisis. A special thanks to my colleagues Shona Moore and Jenna Gritzfeld, for the unity and countless stress-relieving chats which helped me through this process. I would also like to thank Dr Britta Urban for supervision, and Dr Pilar Requena and Dr Daniel Muema for helpful discussions and technical advice.

This project would not have been possible without the contribution of numerous collaborators. I would like to thank to Dr Gavin Wright and Dr Cecile Crosnier at the Sanger Institute for the recombinant DBLMSP and DBLMSP2 proteins, Dr Daniel Czajkowsky and Jiabin Wang from Shangai University for their contributions to the molecular dynamic stimulations, and to Dr Daniel Mitchell from University of Warwick for surface plasmon resonance experiments.

To all of my family, friends, and loved ones, I cannot thank you enough for all that you have done.

Table of Contents

List of figures

List of tables

Abbreviations

Å	angstrom
Ab	antibody
Ag	antigen
AMA	apical membrane antigen
AP	alkaline phosphatase
APC	allophycocyanin
ASN	asparagine
BCR	B cell receptor
BSA	bovine serum albumin
CDR	complementary determining region
CHO	chinese hamster ovary
CIDR	cysteine-rich interdomain region
CLL	chronic lymphocytic leukaemia
CPG	c-phosphate-g
CSA	chondroitin sulphate antigen
CSP	circumsporozoite protein
DBL	duffy binding-like
DBLMSP	duffy binding-like merozoite surface protein
DBLMSP2	duffy binding-like merozoite surface protein2
DC-SIGN	dendritic cell-specific intercellular adhesion molecule-3-grabbing non-integrin
DMSO	dimethyl sulphoxide
DNA	deoxyribonucleic acid
EBL	erythrocyte binding ligand
EDTA	ethylenediaminetetraacetic acid
ELISA	enzyme-linked immunosorbent assay
Fab	fragment antigen binding
FACS	fluorescence activated cell sorting
FAIM3	fas apoptotic inhibitory molecule 3
FBS	foetal bovine serum
Fc	fragment crystallizable
FcR	fc receptor
FITC	fluorescenin isothiocyanate
FPLC	fast protein liquid chromatography
GFP	green fluorescence protein
GLCNAC	*n*-acetylglucosamine
GMFI	geometric mean intensity fluorescence
HBSS	hank's balanced salt solution
HEK	human embryonic kidney
HEPES	2-[4-(2-hydroxyethyl)piperazin-1-yl]ethanesulfonic acid

HIV	human immunodeficiency virus
HR	hour
HRP	horse radish peroxidase
IC	immune complex
ICAM	intergrin cell adhesion molecule
IE	infected erythrocyte
Ig	immunoglobulin
IL	interleukin
ITAM	immunoreceptor tyrosin-based activation motif
ITIM	immunoreceptor tyrosin-based inhibitory motif
IVIG	intravenous immunoglobulin
KDA	kilodalton
LPS	lipopolysaccharide
mAb	monoclonal antibody
MHC	major histocompatibility complex
MSP	merozoite surface protein
MW	molecular weight
NK	natural killer
OD	optical density
PBS	phosphate buffered saline
PBMC	peripheral blood mononuclear cell
PHA	phytohaemagglutinin
PE	phycoerythrin
PFEMP1	*Plasmodium falciparum* erythrocyte membrane protein 1
PFRH	*Plasmodium falciparum* reticulocyte binding homologue
*Pv*DBP	*Plasmodium vivax* duffy binding protein
PKC	protein kinase c
PNGASE	peptide-n-glycosidase
PV	parasitophorous vacuole
RON	rhoptry neck protein
SD	standard deviation
SIGNR1	c-type lectin, mouse homolog of dc-sign
SPAM	secreted polymorphic antigen merozoite
SPR	surface-plasmon resonance
TAE	tris-acetate edta
TLR	toll like receptor
TMB	3,3’,5,5’-tetramethylbenzidine substrate
TD	thymus-dependent
TGN	trans-golgi network
TRAP	thrombospondin-related anonymous protein
TRIM21	tripartite motif-containing 21
VAR	variant genes
VMD	visual molecular dynamics

Chapter 1: Introduction

1.1. Malaria

Malaria is a disease caused by the protozoan parasite of the genus *Plasmodium*, which is transmitted by the bites of infected female *Anopheles* mosquitoes. Many different species of *Plasmodium* infect a wide range of animals, ranging from birds to humans [1]. The four species of *Plasmodium* which cause malaria in humans are *Plasmodium falciparum, Plasmodium vivax, Plasmodium ovale,* and *Plasmodium malariae*. Recently, *Plasmodium knowlesi* was confirmed as the fifth species to cause naturally acquired infections in humans [2].

1.2. Malaria infections in humans

Malaria is an ancient disease thought to have evolved alongside the human race [3, 4]. Approximately 3.4 billion people, almost half of the World's population, are at risk of malaria infection every year, one third of which are at high risk [5]. In 2012 alone there were ~207 million clinical malaria cases and ~627,000 deaths reported, 90% of which occurred in sub-Saharan Africa [5]. The majority of deaths are in children under the age of five, and it is predicted that a child dies every minute from the disease [5]. The most common species eliciting infections in humans are *P. falciparum* and *P. vivax,* whereby *P. falciparum* cause severe malarial disease and subsequent mortality. Other *Plasmodium* species generate significant morbidity in infected individuals residing in endemic regions [1]. Due to the high prevalence and mortality of malaria caused by *P. falciparum*, this thesis will focus on *P. falciparum* infections.

1.3. Life cycle of *Plasmodium falciparum*

The lifecycle of *P. falciparum* is complex and multi-staged, occurring in both human and mosquito hosts. In the human host, infections are dichotomised into pre-erythrocytic and erythrocytic stages (Figure 1.1). Due to the complexity of initial infection and dissemination of the parasite, mouse models of malaria (*P. yoelli* and

P. berghei) have been utilised to investigate the pre-erythrocytic stage. Malaria infection is initiated when an infected female *Anopheles* mosquito injects a small number of parasites (~20 sporozoites) under the subcutaneous tissue of the mammalian host, and less frequently directly into the bloodstream, when taking a blood meal [6-8]. Within one hour of injection, some sporozoites leave the area of the bite and glide through the dermis to a blood vessel whereby they migrate through the circulatory system to reach the liver [7, 9]. An alternative hypothesis proposes that sporozoites arrive at the liver via the lymphatic systems [10, 11]. However, subsequent research showed that although ~30% of migrating sporozoites entered the lymphatic system, the majority were trapped in lymph nodes and digested by dendritic cells [6]. Further research is required to confirm whether sporozoites migrate through the lymphatic system to reach the liver. Sporozoites are thought to cross the sinusoidal barrier of the liver principally by traversing kupffer cells [12]. Sporozoites engage host cells via the binding of the circumsporozoite protein (CSP) and thrombospondin-related anonymous protein (TRAP) expressed on sporozoite surfaces with heparan sulphate proteoglycans of liver cells [13-15]. Subsequently, sporozoites traverse through several hepatocytes before settling within one, resulting in the formation of a parasitophorous vacuole which surrounds the parasite [16]. Inside the hepatocyte, each sporozoite replicates and differentiates into thousands of asexual merozoites prior to their release into the bloodstream upon hepatocyte rupture [17].

The erythrocytic stage of the life cycle is initiated once merozoites re-enter the bloodstream following heptacyte rupture [1, 18, 19]. Merozoites then invade uninfected erythrocytes and develop through ring-shaped immature trophozoites to mature trophozoites (Figure 1.2). Subsequent intraerythrocytic asexual replication of the parasite transforms the trophozoites into schizonts, which consist of ~16-30 daughter merozoites. Schizonts rupture and release the merozoites into the periphery, each of which has the ability to invade other erythrocytes and repeat the cycle of schizogony. The rupture of *P. falciparum* infected erythrocytes evokes the clinical symptoms of malaria, such as fever and rigor. Each cycle of schizogony takes approximately 48hr in *P. falciparum*, and the infection is amplified roughly 20-fold during each cycle in non-immune humans. The lifecycle continues until some merozoites escape the cycle to differentiate into the sexual parasitic stages, known as male and female gametocytes. A large proportion of gametocytes sequester in the extravascular space

of the bone marrow, whereby they undergo development before migrating to the circulation [20]. The gametocytes then circulate in the blood until they are ingested by a mosquito taking a blood meal, thus completing the human stage of the *Plasmodium* life cycle [21].

A pivotal step in the erythrocytic cycle is the invasion of erythrocytes by extracellular merozoites (Figure 1.2). The development of a fast and efficient invasion process has contributed to the evolutionary success of *Plasmodium*, since it limits the exposure of parasitic antigens to the host immune system [1]. The invasion process commences with the egress of parasites from an infected cell, which occurs due to protease secretions and mounting intracellular pressure from merozoite growth [22, 23]. Approximately 60 seconds after egress, merozoites quickly recognise, attach to, and invade uninfected erythrocytes [1]. Multiple antigens expressed on merozoite surfaces, such as merozoite surface protein 1 (MSP1), members of the erythrocyte binding ligand (EBL) and *P. falciparum* reticulocyte binding homologue (PfRH) protein families, initiate primary attachment of the merozoite to erythrocytes [24-27]. These are referred to as adhesins as they function to bind directly to specific ligands expressed on erythrocyte surfaces [28]. Although little is known about the receptor-ligand interactions which permit attachment of the merozoite to erythrocytes, the interaction between PfRH5 and Ok blood group antigen basigin was recently found to be essential for erythrocyte invasion in all tested *P. falciparum* strains [25].

Following primary attachment, the apical end of the merozoite orientates towards the erythrocyte surface forming an irreversible attachment, referred to as tight junction formation [29, 30]. Tight junction formation between the merozoite and erythrocyte is mediated by parasitic invasins, such as apical membrane antigen 1 (AMA1) or rhoptry neck protein (RON) complex [31, 32]. These interact with the actinomyosin system of the merozoite and are translocated towards its posterior end, which propels the parasite in a forward motion into the erythrocyte. The parasite then induces invagination of the erythrocyte membrane around itself and enters a parasitophorous vacuole within the erythrocyte. Upon invasion, proteases cleave antigens from the merozoite surface coat resulting in their release into the periphery [33].

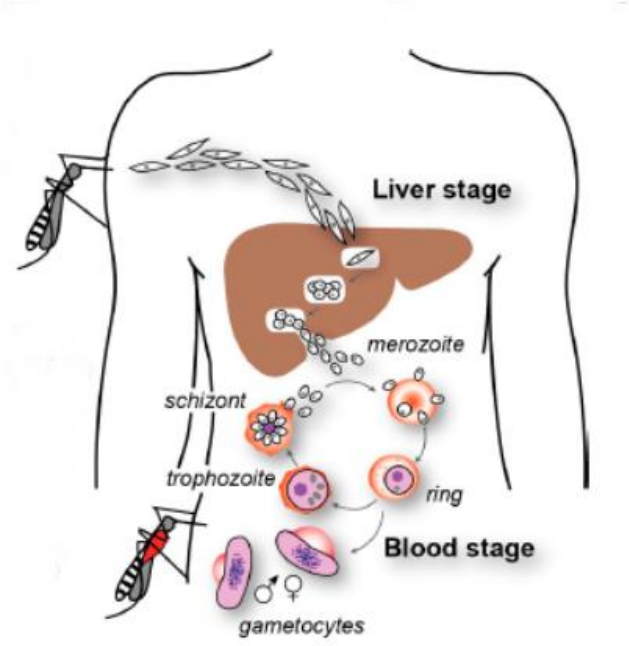

Figure 1.1 ***P. falciparum*** **life cycle in the human host.** The *Anopheles* mosquito bites a human and deposit sporozoites under the dermis. These migrate to the liver to invade hepatocytes (liver stage), whereby they transform into exoerythrocytic merozoites which are released into the blood stream upon hepatocyte rupture. In the blood, merozoites quickly invade erythrocytes to form early rings, which then develop into trophozoites and mature schizonts (blood stage). Next, erythrocytes burst and release merozoites which reinvade uninfected erythrocytes. During the blood stage, some merozoites differentiate into gametocytes which are subsequently ingested by a feeding mosquito during the blood meal [28].

Each stage of the *P. falciparum* life cycle in humans is a possible target for therapeutics and/or targeting by vaccines. The erythrocytic stage of the life cycle has received much attention to date as antigens on the merozoite surface are exposed to the host immune system during this stage. Furthermore, the obligation of *P. falciparum* to invade host erythrocytes in order to survive represents an attractive weakness of the parasite which can be exploited in therapeutic or vaccine design [1]. Designing therapeutics or specific antibodies (Abs) to block the entry of *P. falciparum* into erythrocytes can prevent its replication and amplification within cells. However, a greater understanding of host-parasite interactions is required for the development of new treatments and to identify potential vaccine candidates.

1.4. Epidemiology of malaria

There is marked variation in the risk of *P. falciparum* infection globally. The disease is most prevalent in sub-Saharan Africa (Figure 1.3), whereby transmission intensity helps to classify countries or regions as endemic, holo-endemic, or meso-endemic [34]. There are numerous factors contributing to differences in geographical epidemiology of *P. falciparum*, including local vector species, transmission intensities, housing conditions and population densities [35-37]. Another factor includes human genetic variation. A growing number of genes have been associated with conferring a degree of protection against *P. falciparum* infection and severe disease [38, 39]. Early studies revealed that blood-related disorders which correlated with the historic incidence of malaria, such as sickle-cell trait and thalassaemia, confer protection against the disease [40-42]. Polymorphisms in major histocompatibility complex (MHC) genes have been associated with tolerance or susceptibility of infection, as presentation of malarial epitopes on MHC molecules expressed by infected cells is essential for T cell recognition and priming of pre-erythrocytic immunity to malaria [43-47]. Furthermore, certain polymorphisms within genes encoding Fcγ receptors (FcγRIIA and FcγRIIB) have also been shown to associate with both protection from and susceptibility to clinical malaria [48, 49], most likely as a consequence of altered binding of IgG subclasses to these receptors. Co-infections in hosts are also confounding factors of the disease. In areas of stable malaria transmission, infections with HIV and visceral leishmania increase susceptibility of *P. falciparum* infection and disease

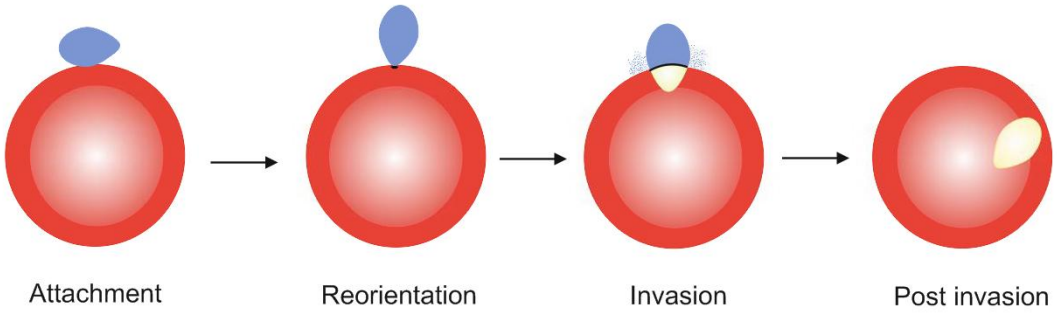

Figure 1.2 Invasion of red blood cells by merozoites. Invasion is initiated with attachment of the merozoite to the erythrocyte surface via low-affinity interactions, followed by the reorientation process in which the apical end of the merozoite is positioned adjacent to the erythrocyte surface to facilitate tight junction formation. The formation of high-affinity ligand-receptor interactions secures the merozoite whilst the tight junction moves from the apical to posterior end. The merozoite surface coat is shed upon erythrocyte invasion, creating a parasitophorous vacuole within the erythrocyte [1].

severity [50, 51]. Moreover, immune responses against *P. falciparum* cause decreased resistance to invasive non-typhoid Salmonella, a common and often fatal complication in malaria patients [52].

The majority of the reported deaths occur in sub-Saharan Africa, where children under five and pregnant women are particularly susceptible to severe disease [5]. Malaria has devastating consequences in addition to direct effects of mortality and morbidity, including impaired intellectual development due to reduced school attendance and productivity, onset of developmental abnormalities following cerebral malaria, and reduced yearly gross national product in malaria endemic countries [53-55]. In endemic regions, pregnant women have a 2- to 3-fold increased risk of developing severe malarial disease compared to non-pregnant women [32]. Furthermore, pregnancy-associated malaria causes adverse consequences such as maternal anaemia, intrauterine growth retardation, spontaneous abortions, low-birth weight, and infant mortality [56, 57]. International travellers who visit endemic regions are also highly susceptible to malaria infection, as approximately 10,000 cases and 150 deaths are reported each year [58]. In addition, individuals who emigrate from malaria endemic countries to more developed countries are at higher risk of infection when they return to their country of origin [59]. Disease susceptibility in these vulnerable populations is thought to be associated with a decrease in clinical immunity against the parasite [37, 59].

1.5. Pathology of malaria

The clinical symptoms of malaria typically appear a week following an infective mosquito bite, and some of the most common clinical symptoms include fever, chills, headache, vomiting and splenomegaly [60]. The severity of malarial disease is classified into three categories; severe and complicated, mild and uncomplicated, and asymptomatic [61, 62]. Severe disease accounts for the mortality of *P. falciparum* infection, resulting from disease manifestations such as cerebral malaria, severe anaemia, acute renal failure, metabolic acidosis, hypoglycaemia, and pulmonary oedema [61].

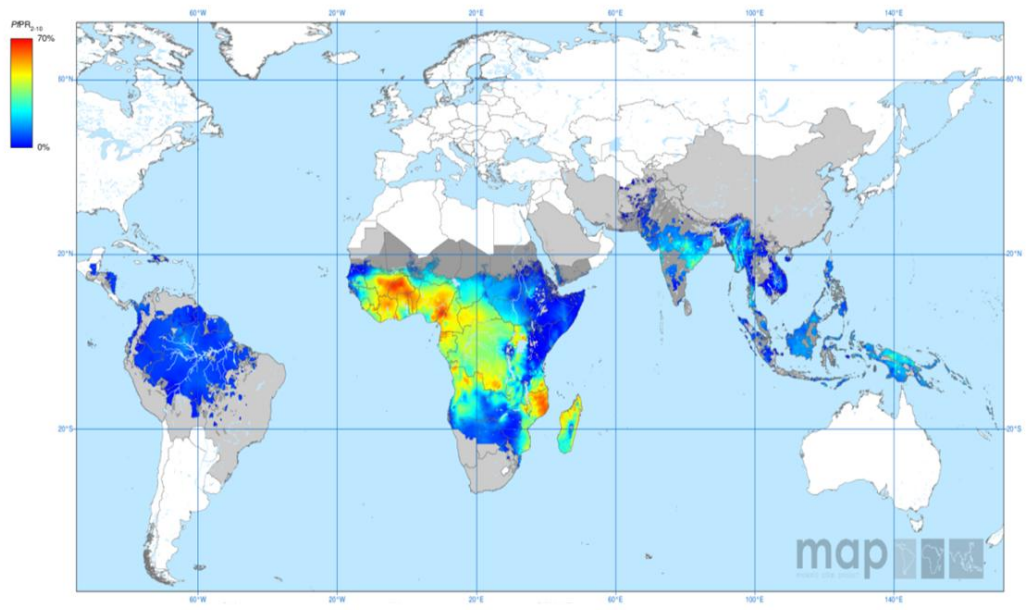

Figure 1.3 Global distribution of *P. falciparum* malaria endemicity in 2010. Heat-map depicting mean point estimates of the age-standardised annual mean *P. falciparum* parasite rate in 2-10 year olds (PfPR$_{2\text{-}10}$) in areas of stable transmission. Light grey areas on the map represent *P. falciparum* free geographic areas and dark grey as areas of no risk or unstable risk (MAP, Accessed 11th October 2014 from: http://www.map.ox.ac.uk/client_media/png/Pf_mean_2010/Pf_mean_2010_World.png).

A prominent characteristic of the pathogenesis of *P. falciparum* infection involves the parasite's ability to cause infected erythrocytes (IEs) to adhere to the endothelium of capillaries. The sequestration of IEs to microvasculature contributes to severe malaria by obstructing blood flow through tissues resulting in hypoxia and inadequate tissue perfusion [63]. Pathogenesis is also mediated by the destruction of erythrocytes. The direct rupture of IEs and indirect destruction of non-parasitised erythrocytes has been associated with the development of severe anaemia [64, 65]. Furthermore, the delivery of oxygen to organs is compromised with the destruction of erythrocytes, which may account for the observed hypoxia. The mechanisms governing *P. falciparum* pathogenesis are complex and are likely to involve numerous contributing factors. However, rapid expansion of IEs, erythrocyte destruction, microvascular obstruction, and ensuing inflammatory responses are considered key events in severe disease [66].

1.6. Control of *P. falciparum* infections

Increased efforts to control malaria have resulted in a global malaria incidence decrease of 17% and decreased malaria mortality rates of 26% between 2000-2010 [5]. This success was largely owing to the launch of the Roll Back Malaria Initiative by WHO [67], which has been widely endorsed [68]. The strategy of this programme involved aggressive vector control in highly endemic regions to help lower transmission, increased research into potential vaccines and anti-malarial drug, improved diagnostic measures, and intervention through indoor residual spraying with insecticides and mass administration of bed nets [5, 67].

Despite recent advances, the burden of malaria is still great and drug-resistance in *P. falciparum* is on the rise [5, 69]. The emergence of drug-resistance in *P. falciparum* populations threatens to thwart global malaria elimination. Chloroquine resistance is widespread, and resistance to sulfadoxine-pyrimethamine has grown in countries utilizing the drug as a replacement for chloroquine [70]. In a bid to reduce the emergence and spread of resistance, combination therapy composed of drugs with different modes of actions was adopted. Artemisinin-based combination treatments is the most widely promoted combination therapy and has shown promising efficacy in both Asia and Africa [71, 72]. However, resistance to artemisinin and its derivatives is

well established in South-east Asia and poses the risk of spreading [5, 69]. Furthermore, resistance to pyrethroids has rapidly emerged due to large-scale distribution of insecticide-treated bednets [73].

Vaccination has proved to be the most effective method for the prevention of infectious diseases to date [74]. However, a licensed malaria vaccine is still unavailable and initial findings from human trials for the leading vaccine candidate RTS,S/AS01 reported moderate efficacy of 30-50% [75, 76]. Moreover, the mechanisms by which this vaccine confers protection are poorly understood. The recent discovery of cross-strain dependency on the interaction between basigin and PfRH5 for erythrocyte invasion offers an exciting avenue for the development of new therapeutics to combat the disease [25]. The elimination of malaria requires a multifaceted approach, enlisting effective insecticides, chemotherapy and the development of an affordable yet efficacious vaccine [77]. Our limited understanding of the biology of *P. falciparum* and how the parasite interacts with the immune system contributes to the difficulty in generating an effective vaccine [78]. These gaps in knowledge need to be filled in order to facilitate malaria elimination efforts.

1.7. Immunity to *P. falciparum*

Immune protection from malaria is extremely complex and poorly understood. In areas of intense *P. falciparum* transmission, severe malaria disease is mainly a feature of childhood (Figure 1.4) [5]. After several episodes of malaria, individuals develop incomplete immunity which helps to control parasitemia and protects from severe disease and death [18]. Malaria in immune adults is regarded as "uncomplicated" and is characterised by low-grade parasitemia, fever, chills and rigors, however sterilizing immunity is most likely never achieved and wanes in the absence of re-exposure [18, 79]. This suggests that continued exposure to *P. falciparum* antigens is required to generate and maintain immunity against malaria. Innate, cellular and humoral immune responses have all been implicated in protection against the disease, although the underlying mechanisms which govern this are unclear [79].

In theory, any stage of the *P. falciparum* life cycle can be targeted by the host immune system. Nonetheless, responses against *P. falciparum* infection have been

traditionally divided into pre-erythrocytic and erythrocytic stages [27]. Protection against pre-erythrocytic stages is well documented and is mainly attributed to cellular responses, whereas humoral responses are required for erythrocytic-stage protection [27, 32]. Longitudinal studies in endemic regions highlighted that the pre-erythrocytic stages were unlikely to elicit naturally acquired immunity to *P. falciparum* infection [80]. Although immunity to pre-erythrocytic stages is limited, immunisation with irradiated sporozoites or vaccination with sporozoite antigens elicited considerable immune responses against *P. falciparum* [29, 81, 82]. In fact, these targets feature in the most advanced malaria vaccines available to date. For example, the leading vaccine candidate RTS,S is a recombinant antigen based on the *P. falciparum* circumsporozoite protein (CSP) and hepatitis B surface antigen [83]. Although RTS,S/AS02 vaccination initiates partial protection against *P. falciparum* infection, protection wanes with time, as protection was not found to extend to 5 years following vaccination [84]. This clearly highlights the need to further understand the complexities of immune responses against malaria, especially in regard to vaccine design.

During erythrocytic stages, exposed *P. falciparum*-derived antigens on free merozoites and IE surfaces present attractive targets for immune responses [85, 86]. Humoral immune responses are thought to govern naturally acquired immunity to erythrocytic stages as erythrocytes do not express MHC class I or II molecules on their cell surfaces [79]. Early studies revealed a role of Abs in mediating immunity to malaria, as severe malarial disease was successfully treated through passive administration of immunoglobulins from malaria-immune adults [87, 88]. Furthermore, broad antibody (Ab) responses against merozoite surface proteins (MSP2 and MSP3) were found to associate strongly with protection against clinical malaria [89]. In *P. falciparum* infections, Abs function to block erythrocyte invasion by merozoites [90], opsonise IEs to increase their clearance by phagocytes [86], and to mediate Ab-dependent cellular cytotoxicity [91].

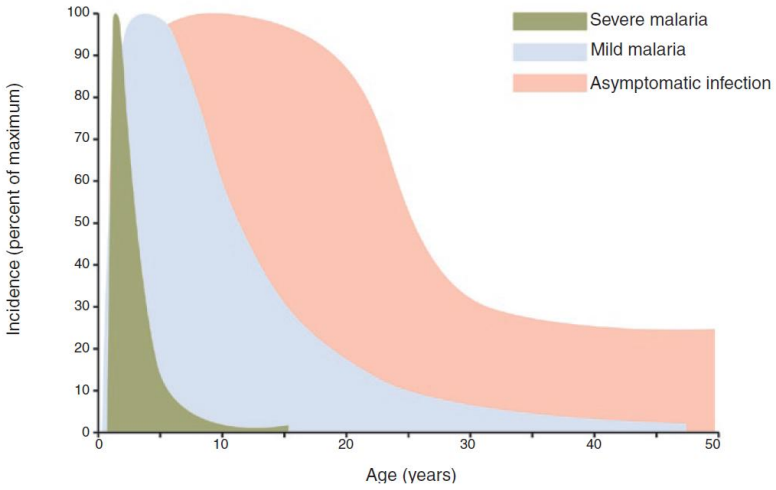

Figure 1.4 Population indices of naturally acquired immunity to *P. falciparum* in endemic regions. Severe malaria is a feature of childhood, as the slow acquisition of immunity against *P. falciparum* appears to result in the development of mild or asymptomic malaria [18].

Intriguingly, a recent study discovered differing Ab responses for induced and naturally acquired immunity against *P. falciparum* [92]. Strong humoral immune responses against pre-erythrocytic stage antigens CSP and liver stage antigen 1 (LSA1) were generated in individuals who were experimentally infected with *P. falciparum* whilst receiving chloroquine prophylaxis. Semi-immune individuals with naturally acquired immunity generated responses against numerous well-characterised merozoite and erythrocytic antigens, which were not observed in the experimentally-infected individuals [92]. This data implies that although vaccines targeting pre-erythrocytic stage are able to mount sufficient humoral responses when parasitemia was controlled by prophylaxis, immunity to erythrocytic stage antigens is pivotal for naturally acquired immunity. Therefore, vaccines targeting erythrocytic stages are more likely to generate long-lasting immunity against *P. falciparum* infections.

Although protection against erythrocytic-stage parasites has been traditionally ascribed to humoral responses, recent studies have implicated cellular immunity and interferon (IFN)-γ production in mediating protection. In the absence of Abs, cellular responses against IEs contribute to protection due to proliferative $CD8^+$ and $CD4^+$ T cell responses, IFN-γ and nitric oxide production [30, 93]. Furthermore, $CD4^+$ T cell help is essential in generating Ab responses against *P. falciparum* [94] and there is mounting evidence that $CD4^+$ T cell responses elicited through vaccination help protect against *P. falciparum* infections in humans [30].

Despite the great strides made in understanding immunity to *P. falciparum* in recent years, relatively few studies have investigated the combined effects of innate, humoral, and cellular responses in governing protection against malaria [95]. It is highly likely that these immune branches work synergistically to recognise, combat, and eliminate parasites in the human host. Understanding the low immunogenicity of *P. falciparum* is pivotal in the development of effective methods for malaria control, which include the design of efficacious vaccines.

1.8. Immune evasion mechanisms of *P. falciparum*

The slow acquisition of protective immunity against malaria is likely a result of the diverse immune evasion mechanisms which *P. falciparum* have evolved as a consequence of strong selection pressure [96, 97]. Immune evasion by *P. falciparum* is well researched and many comprehensive reviews have covered this topic in detail [96-100]. Briefly, *P. falciparum* immune evasion mechanisms characterised to date include intracellular parasitism, genetic polymorphism, IE adhesion, antigenic variation, camouflage, molecular smokescreens and immune response modulation.

Intracellular parasitism is an ingenious way pathogens have evolved to avoid host immune detection. It is particularly effective in the erythrocyte-stage of malaria as merozoites infect erythrocytes, which inherently lack MHC molecules, thus putting the parasite beyond the clutches of Abs and T cell recognition. The parasites themselves are highly polymorphic, whereby parasite populations express antigenically distinct alleles of a gene [101]. Extensive polymorphisms are common in parasite antigens which elicit immune responses, such as MSP1 and *P. falciparum* erythrocyte membrane 1 (PfEMP1) [34, 102, 103]. This allows parasites expressing mutated alleles to escape specific immune responses and selectively expand, much like HIV [104, 105]. Another way the parasite evades immunity is to trick the immune system into responding to an irrelevant antigen. Tandem repeats are often found in malaria antigens which are not targets of protective immunity [106], but function as immune-dominant B cell epitopes [97]. The generation of Ab responses against tandem repeats provide a smokescreen for epitopes crucial for mediating parasite function. Moreover, these repeats are able to cross-link surface immunoglobulins on B cell surfaces resulting in suppressed Ab responses [97].

Surface exposed *P. falciparum* antigens are vital for mediating host-parasite interactions, yet their extracellular location makes them targets of humoral responses. However, antigenic variation of these Ags allows parasites to evade humoral responses and elicit *P. falciparum* virulence mechanisms. For example, the expression of the highly polymorphic PfEMP1 molecule on IE surfaces mediates essential functions such as the adhesion of IEs to host endothelium [107, 108]. Whereas the majority of malaria erythrocytic antigens are encoded from one allele per locus, PfEMP1 variants are encoded by the *var* multigene family (~60 genes per genome)

present in multiple loci on different chromosomes [109, 110]. The transcription of *var* genes is mutually exclusive and only one PfEMP1 variant is expressed on the erythrocyte surface at a time, with the remaining *var* genes in a transcriptionally silent state [111]. However, *var* gene expression is able to switch during each reinvasion [112], which facilitates the parasite to switch the expression of PfEMP1 variants on the surface of the IE once Ab responses have been generated [107].

PfEMP1 molecules contribute to the pathogenesis of malaria by mediating cytoadhesion. This cytoadhesion either results in the sequestration of infected erythrocytes to host endothelia (preventing splenic clearance), in binding to non-IEs to form so-called rosettes, or in binding to platelets inducing platelet-mediated clumping [113]. Several human receptors have been shown to be involved in cytoadhesion mediated by PfEMP1 variants, including intercellular cell adhesion molecule 1 (ICAM-1), vascular cell adhesion molecule 1 (VCAM-1), complement receptor 1 (CR1), chondroitin sulphate antigen (CSA), endothelial protein C receptor (EPCR), CD36, and immunoglobulin M (IgM) [113, 114]. Which human receptor is being bound depends on which PfEMP1 variant is expressed on the surface of IEs. It is likely that other host receptors which bind PfEMP1 remain to be characterised.

The vast majority of the immune evasion mechanisms described above are mediated by interactions between parasite-derived proteins and host ligands. Central to a number of these mechanisms is the surprising ability of *P. falciparum* to bind human IgM in a non-cognate manner [100]. As it is impossible to cover the scope of the complex host-parasite interactions mediating immune evasion, the focal point of this thesis is in the understanding of how IgM-binding proteins facilitate immune evasion in *P. falciparum* infections.

1.9. Binding of non-immune IgM to *P. falciparum*-derived molecules

The neutralisation of pathogens by Abs is pivotal for humoral immune responses and protection against infection and disease. To evade Fc-mediated destruction, human pathogens have evolved to express ligands on their cell surfaces which bind the Fc region of host immunoglobulins. The functions of these ligands expressed by bacteria and viruses, such as *Staphylococcus aureus* protein A Cowman strain and herpes simplex virus gE-gI, have been well characterised [115-117]. However, surprisingly little is known about the role of immunoglobulin-binding molecules in parasitic infections.

A notable exception is the highly variable parasite antigen PfEMP1. PfEMP1 variants are composed of Duffy binding-like (DBL) domains categorised into six types (α-ζ) and cysteine-rich interdomain region domains (CIDR) categorised into three types (α-γ) [110]. A number of different domains from PfEMP1 variants have been shown to bind non-immune human IgM [100, 118], which are summarised in Table 1.1. The Cμ4 domain of IgM molecules bound PfEMP1 variants from six distinct parasites, suggesting distinct PfEMP1 variants from different parasite isolates utilise a conserved mechanism to adhere to IgM [118-120].

The reasons why PfEMP1 variants bind non-immune IgM are still being discovered. To date, PfEMP1 has been implicated in immune evasion mechanisms such as cytoadhesion [121, 122], immunomodulation [123], and camouflage [119]. Binding of non-immune IgM to PfEMP1 was shown to correlate with severe malaria in both laboratory strains and field isolates [120, 124]. Subsets of *P. falciparum* strains which bind non-immune IgM also possess specific phenotypes associated with virulence, such as rosetting [124] and CSA-binding in pregnancy-associated malaria [125, 126]. Intriguingly, IgM-binding is believed not to be a feature of other common phenotypes such as ICAM-1 or CD36 binding [124]. Studies investigating IgM binding by field isolates are rare and of insufficient coverage. In reality, it is not known how common or how important the IgM binding phenotype is to parasite virulence or survival.

Table 1.1 Known IgM-binding DBL domains in PfEMP1 variants adapted from [100, 118].

PfEMP1 variant	Domain
FCR3S1.2*var*1	CIDR
TM284S2*var*1	DBL2β
FCR3*var*1*csa*	DBL7ε
FCR3*var*2*csa*	DBL6ε
3D7*var*2*csa*	DBL2-X, DBL5ε, DBL6ε
TM284*var*1	DBL4β
HB3*var*6	DBLζ2

It is still unknown what advantage rosetting affords *P. falciparum* parasites [113]. Although not all rosetting variants bind non-immune IgM, the involvement of IgM in rosette formation appears to be essential for the strains that do, as rosetting frequencies in two different parasite strains (R+PA1 and HB3VAR6) were reduced when IgM was depleted from human serum [118, 122]. However, the presence of IgM alone did not restore rosetting frequency suggesting that other serum components are essential for rosette formation [118]. Exactly how IgM-binding is involved in rosette formation has not yet been clarified, but there have been several suggestions. The binding of non-immune IgM may stabilise rosettes by strengthening interactions between infected and uninfected erythrocytes [127]. For this to occur, IgM could either induce a conformational change in the PfEMP1 protein or bring several PfEMP1 proteins together increasing affinity or avidity [128]. In support of the latter hypothesis, a recent study found that one IgM molecule was able to bind two PfEMP1 molecules *in vitro* [118]. Another possibility is that IgM could interact with receptors on uninfected erythrocytes as well as with PfEMP1 on IE surfaces [124], however this has yet to be proven. Finally, IgM could promote rosetting by recruiting C1q which could subsequently interact with the complement receptor 1 (CR1) expressed on uninfected erythrocytes [120]. COS-7 cells expressing an IgM-binding PfEMP1 domain were still able to bind IgM in the presence of complement factors, suggesting that both C1q and PfEMP1 can bind to the same IgM molecule [120]. This was not the case for the non-rosetting, chondroitin sulfate A (CSA)-binding PfEMP1 variant VAR2CSA, as no binding was observed between C1q and IgM-opsonised VAR2CSA^{+}-infected erythrocytes [119]. However, this may be attributed to differences in IgM-binding between PfEMP1 variants or whether the IgM molecules already are bound to their epitopes or if they are in solution.

Whether the binding of IgM also strengthens cytoadhesion of non-rosetting variants is unknown. PfEMP1 variants involved in pregnancy-associated malaria, known as VAR2CSA, mediate adhesion to CSA in the intervillious space of the placenta [129]. Along with CSA adhesion, IEs expressing VAR2CSA also bind non-immune IgM, and the co-selection of CSA-and IgM-binding phenotypes is proposed to signify the role of non-immune IgM in parasite survival in the placenta [119, 125, 130]. The expression of a putative IgM receptor on the placenta has not been identified to date, although it has been suggested that multimeric IgM molecules may permit

interactions with CSA-rich syncytial 'knots' in the placental circulation [125]. The addition of non-immune IgM was not seen to increase binding of infected erythrocytes to placental cryosections [119]. However, the addition of normal human serum did increase binding, suggesting that other serum components can strengthen the binding or perhaps, as is the case for the rosetting variants, IgM coupled with additional serum component could account for the increase in binding.

P. falciparum parasites have also been shown to utilise non-immune IgM to shield immunogenic epitopes on the surface of IEs from PfEMP1-specific IgG recognition [119]. The pre-incubation of IEs expressing VAR2CSA with non-immune IgM prior to treatment with VAR2CSA-specific monoclonal antibodies (mAbs) was shown to significantly reduce their internalisation into phagocytic cells [119]. These IgM-opsonised IEs were subsequently able to interact with CSA in the placenta, suggesting that the masking effect of nonspecific IgM could conceal immunogenic epitopes whilst leaving epitopes critical for molecular functions exposed [119]. Little is known regarding IgM binding PfEMP1 variants other than VAR2CSA, but a recent study showed that IgM binding by the rosetting variant HB3VAR6 did not lower IE phagocytosis [118]. This suggests that the camouflage function of VAR2CSA is not a property shared by all IgM-binding PfEMP1 variants. Whether PfEMP1 variants bind IgM for different purposes, or if there is a common yet undiscovered purpose of IgM binding remains to be shown.

Humoral immune responses are pivotal for controlling *P. falciparum* malarial disease, but immunity is slow to develop and relatively short-lived [131]. This is partly attributed to antigenic diversity and complexity of the parasites, but there is emerging evidence that parasites actively alter B cell responses. Polyclonal B cell activation is often observed in malaria infections, resulting in hypergammaglobulinemia, elevated titres of autoAbs, and increased prevalence of B cell malignancies (e.g. Burkitt's lymphoma) [132, 133]. Dontai et al. demonstrated that the direct binding of IEs to peripheral B cells from non-immune donors resulted in T-cell independent polyclonal activation [123]. They identified the CIDR1α domain of the PfEMP1 variant FCR3S1.2 as a B cell mitogen. In addition to other proteins, non-immune IgM were shown to bind CIDR1α with low affinity, and its addition inhibited the binding of recombinant CIDR1α to B cells [123]. Further studies reported preferential activation of

memory B cells by CIDR1α [133], however the direct binding of CIDR1α to memory B cells was not shown. Gene expression profiling and functional data revealed that stimulation with recombinant CIDR1α induced tonsillar B cell survival and cell cycle progression [133]. This was hypothesised to confer protection against spontaneous cell death and provide a potential explanation for the increased risk of endemic Burkitt's lymphoma in areas of high transmission of *P. falciparum* [133]. These data led to the conclusion that CIDR1α stimulates B cell proliferation via the BCR [123]. However, in a more recent study the authors found that the phosphorylation profile of CIDR1α stimulated B cells differed substantially from B cell receptor-activated B cells, which led to the conclusion that B cell activation by CIDR1α does not proceed through the BCR [134]. This together with the observations that CIDR1α binding was never completely inhibited by IgM, along with the fact that the effect of anti-Ig on B cell binding was not shown, question whether the BCR is actually the main target in CIDR1α mediated B cell activation or if IgM binding simply sterically hinders the binding of CIDR1α to its receptor. Further studies should address these issues in order to clarify if CIDR1α is a bona fide IgM-binding molecule.

Whether PfEMP1 permits additional functional consequences is yet to be determined. Czajkowsky et al. hypothesised that PfEMP1 molecules may function to alter the binding of IgM to host effector proteins, such as complement components or IgM-receptors (depicted in Figure 1.5) [99]. IgM is a potent activator of complement due to its polymeric structure, which binds C1q via its Cμ3 domain [135]. Although the binding of PfEMP1 to the Cμ4 domain of IgM does not directly block binding of C1q [120], it may induce a conformational change in the central core of IgM to alter the C1q-binding site or may bind IgM in such an orientation to occlude the C1q-binding site [99]. However, this remains to be proven. Alternatively, *P. falciparum* DBL domains could function to interfere with IgM receptors, such as Fcμ, Fcα/μ receptor [100], or more recently the dendritic cell-specific intercellular adhesion molecule-3-grabbing non-integrin (DC-SIGN) [136].

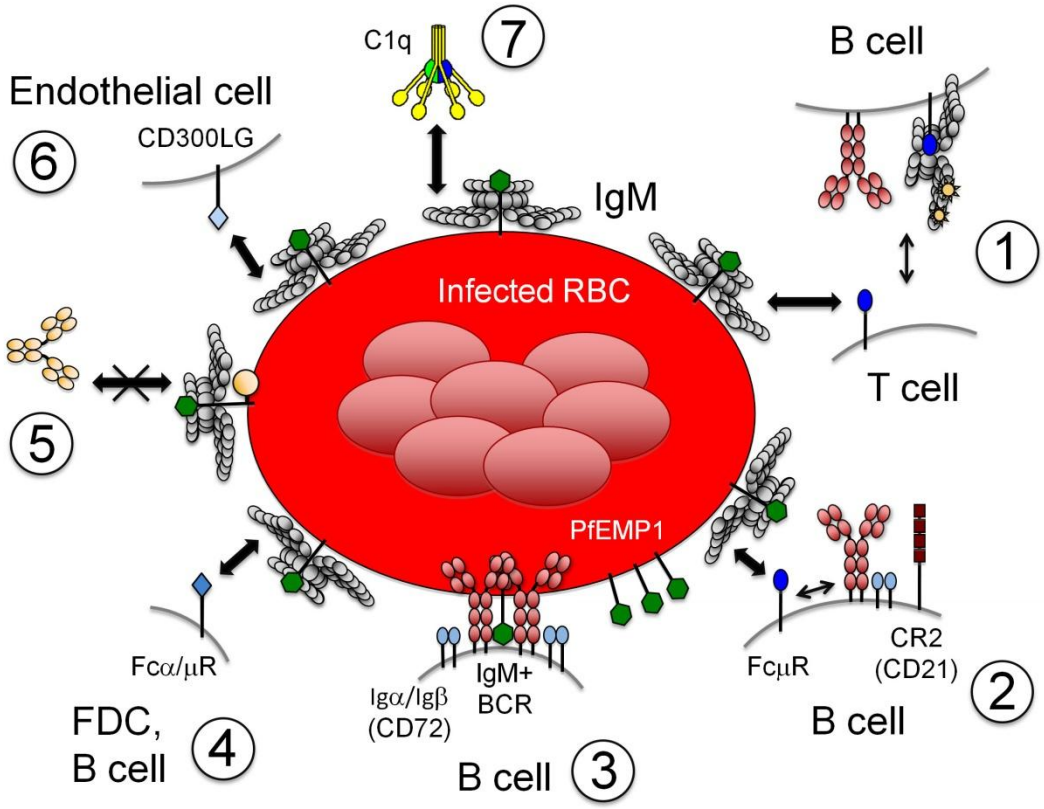

Figure 1.5 Hypothetical functional consequences of the IgM-PfEMP1 interaction. The diagram depicts several potential mechanisms by which IgM-DBL interactions could alter IgM-effector mechanisms, such as blocking immunological synapse formation mediated by FcμR expressed on T cells (1), or B cell activation by disrupting BCR-FcμR (and CR1/2) interactions (2). Further, the IgM-DBL interaction could affect interactions of IgM with Fcα/μR on FDC surfaces (4); the endothelial receptor CD300LG (6); or complement component C1q (7). The possibility for direct interaction between PfEMP1 molecules and BCR on B cell surfaces is also shown (3), which could result in B cell activation through receptor clustering, and the potential of IgM binding by PfEMP1 to shield immunogenic epitopes from humoral immune detection (5)[100].

The bona fide high-affinity Fc receptor for IgM (FcμR) expressed on $CD19^+$ B cells, $CD4^+$/$CD8^+$ T cells, and $CD56^+CD3^-$ NK cells has been implicated in promoting cell survival and proliferation of B cells [137, 138]. Therefore the binding of PfEMP1 to B cells via IgM bound to FcμR (and IgM^+ BCR) may alter signalling pathways to induce polyclonal B cell activation, resulting in observed hypergammaglobulinemias [139]. FcμR also triggers stimulatory intracellular signalling in NK cells [140], which could be hijacked by PfEMP1 to modulate IFN-γ secretion crucial in the early stage of infection [141, 142]. Although the function of FcμR on T cells is yet to be defined, its expression has been proposed to facilitate immune synapse formation with IgM^+ B cells and potentially enhance B cell activation and memory induction [100, 137]. Finally, Fcα/μR plays a role in mediating endocytosis of IgM-coated pathogens [143], antigen-presentation and B cell responses in the germinal center [144], and suppresses humoral immune responses against T-independent antigen by negatively regulating antigen retention by follicular dendritic cells (FDCs) in mice [145]. Therefore, the binding of IgM to PfEMP1 could significantly interfere with these receptor functions in order to confer a significant advantage to the parasite under immune attack. The functions of IgM receptors must be understood before these possibilities can be fully investigated.

A recent study using recombinant proteins and transgenic parasites characterised two *P. falciparum* proteins, DBLMSP and DBLMSP2, as novel IgM-binding proteins [146]. In contrast to PfEMP1 which is expressed on IEs, these proteins are found on the surface of free merozoites [146, 147]. DBLMSP and DBLMSP2 are members of the merozoite surface protein 3 (MSP3) family characterised by the presence of a NLR[K/N][A/G/N] motif at their N-terminus [147, 148]. Most proteins within this family also contain a C-terminal acidic or a secreted polymorphic antigen associated with merozoites (SPAM) domain [149] and a coiled-coil region believed to be involved in oligomerisation of the proteins [150]. As well as being highly polymorphic [151-153], DBLMSP and DBLMSP2 are unique from other MSP3-family members in containing a DBL domain [148, 149]. DBLMSP and DBLMSP2 directly and avidly bound the Cμ4 domain of non-immune IgM via their DBL domains, a function conserved across diverse strains and field isolates [146].

Several studies have proposed mechanisms by which PfEMP1 facilitates immune evasion, yet much less is known about the functional consequences of IgM-mediated

binding by DBLMSP and DBLMSP2. How IgM-binding by DBLMSP and DBLMSP2 could facilitate immune evasion will be explored further in this thesis. In particular, this thesis will focus on how these proteins may function to alter IgM-receptor interactions.

1.10. Immunoglobulin M

IgM is the oldest phylogenetic class of Ab which is expressed by all vertebrate species [154]. IgM is the first Ab to be produced during humoral responses, do not undergo somatic hypermutation or Ab class switching and are therefore of low affinity [155]. IgM exists as a membrane-bound form on B cells (BCR), in the circulation, and also on mucous membranes or in excretory gland secretions as secretory IgM [155]. Circulatory IgM is present at ~1-2mg/ml in the blood of healthy adults, principally as a pentamer and occasionally as a hexamer [156]. Unlike other immunoglobulin isotypes, circulatory IgM can be divided into non-immune and immune IgM [135]. Non-immune IgM molecules are low affinity and broadly reactive Abs which are generated by the B-1 subset of B cells in the absence of exogenous antigens [157, 158]. The multimeric structure of non-immune IgM compensates for the low antigen-binding affinity by creating 10 identical antigen-binding sites (Figure 1.6), which increase overall avidity when binding to multivalent antigens such as bacterial capsular polysaccharides [135, 156]. In addition, the multimeric structure of IgM facilitates complement activation in a highly efficient manner. Immune IgM is produced by B-2 cells in response to pathogenic exposure and differs from natural IgM in its affinity, specificity repertoire, range of function, and antigen-binding site structure [155]. The majority of circulating IgM molecules are considered to be non-immune IgM, as serum IgM levels are similar between animals grown in sterile conditions and normal animals [155]. However, both non-immune and antigen-specific IgM are crucial for Ab mediated responses against pathogens.

IgM molecules share similar structure to other Ab isotypes, whereby two heavy chains are linked with two light chains to form an immunoglobulin (Ig) subunit of approximately 190kDa (Figure 1.6). The heavy chains (μ) defining the IgM isotype are composed of one variable (V_μ) and four constant Ig domains ($C_\mu1$-$C_\mu4$) [155]. In addition, IgM molecules possess an 18-residue tail piece with no defined secondary

or tertiary structure [155]. Pentameric IgM is composed of five subunits joined by a joining (J-chain), whereas hexameric IgM is composed of six subunits which lack a J-chain [159, 160]. The J-chain is a 15kDa protein which covalently associates with pentameric IgM, through disulphide bond formation between cysteine residues in the J-chain and μ-tailpiece [161]. The J-chain was shown to regulate intracellular polymerisation of IgM [162], as well as mediating transport of secretory IgM across epithelia by binding to the polymeric Ig receptor (pIgR) [161, 163]. Hexameric IgM molecules lacking J-chains are unable to bind to pIgR, possibly owing to the fact that hexameric IgM activates complement 15-20 times more efficiently than pentameric IgM [164, 165]. If transported to the gut mucosa which contains high antigen loads, hexameric IgM could cause robust complement activation and ensuing inflammation, resulting in damage the host [166]. Therefore, it is possible that these sparse Abs have evolved without a J-chain to play a role in humoral rather than mucosal immunity [164, 165].

Attempts at obtaining a crystal structure of monomeric or polymeric IgM have been unsuccessful to date, most likely owing to the size and flexibility of IgM molecules [167]. As IgM shares basic domain architecture to IgE, a recent study utilised the similarities between the two immunoglobulins to build a homology-based structural model of pentameric IgM [135]. This model proposed a non-planar, mushroom-shaped complex for pentameric IgM, in which the central C-terminal domain portion protrudes out of the plane created by the Fab and Cμ2 domains [135]. Cryo-atomic force microscopy confirmed this unexpected conformation by imaging individual human IgM molecules. In this conformation, the protruding C-terminal domain could be targeted by Fc-binding proteins such as IgM receptors or IgM-binding malarial proteins [135]. Under this assumption, the protrusion would be directed towards the cell surface upon formation of polyvalent attachments with antigen on the cell surface, resulting in a table-like conformation that would permit the exposure of its C1q binding site to the surrounding solution. [135].

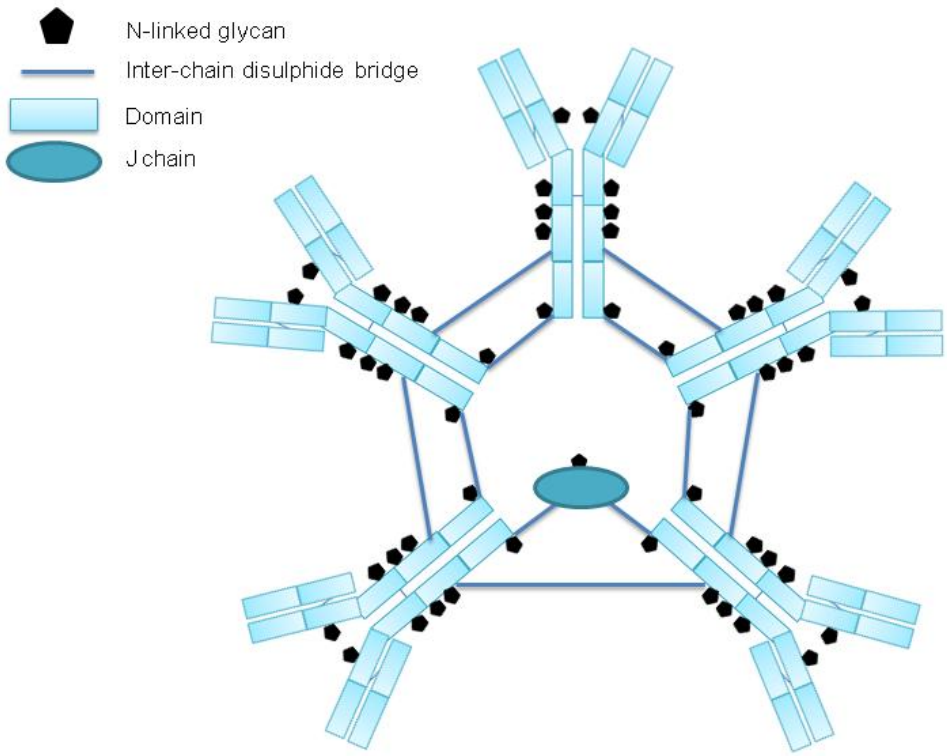

Figure 1.6 Human IgM is a glycoprotein. Pentameric IgM is composed of variable and constant heavy chain and light chain domains (V_H and C_H or V_L and C_L, respectively), and features a J-chain. Potential N-linked glycosylation sites are shown as black pentagons (adapted from [168]).

A recent study determined the atomic details of mouse IgM Fc domains using X-ray crystallography, SAXS, and NMR spectroscopy [167]. The structures of each domain (Cμ2, Cμ3, and Cμ4) were reconstructed to build a model for hexameric mouse IgM, which predicted a flexible star-shaped configuration around the inner Cμ4 core [167]. In this model, the core structure (~180Å) projected out of the plane created by the Cμ2 and Cμ3 domains [167], which supports previous structural data of human IgM [135]. Despite these recent advances, obtaining a crystal structure of human IgM will be pivotal to provide a better understanding of how the Fc region of the molecule mediates its effector functions.

There are five *N*-linked glycosylation sites present on each μ chain of circulatory IgM, located at Asn-171, Asn-332, Asn-395, Asn-402, and Asn-563. The light chains lack conserved *N*-linked glycosylation sites, and the J-chain contains a single site at Asn-48 (Figure 1.6). IgM is heavily glycosylated, as roughly 7-12% of the total mass of IgM is comprised of carbohydrates [155]. Glycosylation of IgM is important for the secretion of IgM and its presentation on B cell surfaces. Complex glycans predominantly terminating in sialic acid or galactose occupy Asn-171, Asn-332, Asn-395, whereas Asn-402 and Asn-563 are 100% and 17% occupied with $GlcNAc_2Man_{5\text{-}9}$-containing oligomannose glycans, respectively [168]. It is predicted that complex glycans are confined to the non-antigen binding face of IgM due to the mushroom-shape adopted by pentameric IgM [135, 168]. In this conformation, the glycans would be restricted from binding lectins once the Fab domain has bound antigens forcing IgM to adopt a crab-like conformation [135]. This hypothesis is supported by the finding mannose-binding lectin (MBL) does not bind to Ag-bound IgM molecules [168]. Therefore, these complex glycans may allow IgM to agglutinate lectin-containing microorganisms in the blood in the absence of specific antigen-binding [169]. In the case of non-immune IgM binding as seen with malaria Fcμ-binding proteins, the orientation of IgM with respect to the parasite or erythrocyte plasma membrane is unknown. Intuitively, the orientation would be opposite to that seen with Fab bound IgM, with the C1q binding sites facing the plasma membrane and the IgM glycans therefore facing towards the solution. However, more research is required to clarify the orientation of IgM with respect to parasite IgM binding proteins, whether this be on the surface of merozoites or IEs.

1.11. IgM-Fc receptors

The effector functions of IgM are primarily mediated through interactions of its Fc portion to cognate ligands, such as complement and IgM-receptors. Soluble IgM is known to bind at least seven ligands including: polymeric Ig receptor (pIgR)[170], Sp alpha [171], TRIM21 [172], Fcα/μR [173] and FcμR [137]. CD22 (an inhibitory co-receptor on B cells) [174] and serum mannan-binding lectin (MBL) [164] can also bind IgM through complex glycans found on IgM [168]. More recently work described in this thesis has shown DC-SIGN to be a novel receptor for human IgM [136]. These receptors generally bind IgM with nanomolar affinity as a consequence of the polymeric structure of IgM that endows this molecule with high avidity interactions. With an IgM serum concentration of 1-2mg/ml, most of these receptors *in vivo* would be saturated with IgM.

A receptor specific for the Fc portion of IgM was suggested over 40 years ago but remained unidentified until recently [137]. A *bona fide* receptor for the Fc portion of IgM (FcμR) was identified in humans and mice [137, 175]. In mice, FcμR expression is restricted to B cell lineages [23, 175], and in humans FcμR is expressed on B cells, T cells and NK cells [137]. Furthermore, FcμR expression is upregulated in patients with chronic lymphocytic leukaemia (CLL) [137, 176-178]. There has been controversy over the expression of FcμR on innate cells, which still remains to be resolved [137, 179-181]. The function of FcμR has largely been determined to-date using knock-out mouse models. FcμR-deficient mice exhibit raised levels of serum IgM, impaired germinal centre formation, altered B cell populations, reduced thymus-dependent Ab responses, and increased autoAb production [22, 138, 182]. These results suggest that FcμR mediates a significant portion of the effector functions of IgM, particularly the regulation of IgM homeostasis, autoimmune suppression and enhancing humoral immunity. Although these data may provide some insight into the function of FcμR, it is important to highlight that there may be functional and structural differences between human and murine FcμR. Significantly fewer studies have focused on the function of the human FcμR [140, 183], which still remains somewhat elusive (see Chapter 6).

1.12. Justification for study

Improving our understanding of host-parasite interactions is crucial to improve the control of malaria. In light of the extensive immune evasion mechanisms employed by *P. falciparum*, strategies to overcome this will have to be considered in order to develop highly effective vaccines, which has so far been difficult to attain.

With the recent discovery of two novel IgM-binding proteins expressed by *P. falciparum*, there is renewed interest into why the parasite expresses a number of molecules which selectively bind host immunoglobulins [146], particularly with respect to two different life cycle stages, the merozoite and/or infected erythrocytes. If IgM binding by merozoites serves the same purposes as binding by infected erythrocytes remains to be determined. The literature suggests numerous possible functions for one of these molecules, PfEMP1, in relation to how it may facilitate immune evasion [100]. Although merozoite DBLMSP and DBLMSP2 have been implicated in complement activation and camouflaging critical epitopes from immune responses, it is unknown whether the binding of these molecules to the Fc portion of IgM can affect subsequent interactions with IgM receptors. Further, the function of human FcμR remains unclear and whether there are hitherto unidentified receptors which can bind IgM remains to be determined.

This thesis aims to further characterise the DBLMSP-IgM interaction, and to determine why *P. falciparum* merozoites express DBL domains that bind non-immune human IgM. To achieve this, the specific objectives include:

I. Investigate the structural and biochemical requirements for DBLMSP and DBLMSP2 binding to human IgM
II. Determine if IgM-binding by DBLMSP and/or DBLMSP2 mediates immune evasion by:
    - Blocking interactions of IgM with receptors
    - Targeting IgM on hFcμR expressed on human lymphocytes
    - Promoting immunomodulation through binding lymphocytes
III. Investigate the structural and biochemical requirements for IgM binding to IgM-receptors
IV. Characterise the function(s) of human FcμR

Chapter 2: Materials and methods

This chapter describes materials and methods used throughout the thesis. The majority of chemicals and reagents used were from Fisher Scientific (Leicestershire, UK), Sigma-Aldrich (Dorset, UK), Life Technologies (Renfrewshire, UK), New England Biolabs (NEB: Herts, UK), Qiagen (West Sussex, UK), Promega (Madison, USA), GE Healthcare LifeSciences (Buckinghamshire, UK), DAKO (Cambridgeshire, UK), SouthernBiotech (Birmingham, AL), Biolegend (San Diego, CA), BioRad (Hertfordshire, UK), BD Biosciences (Oxford, UK), eBioscience Ltd. (Hatfield, UK), Eurofins Genomics (Eberseber, Germany), Abnova (Taipei, Taiwan) and Jackson ImmunoResearch Laboratories Inc. (West Grove, PA, USA).

2.1. Molecular biology techniques

2.1.1. Primer design

Primers used for sequencing were designed manually and by using OligoPerfect™ Designer (Life Technologies), taking into consideration the introduction of restriction endonuclease sites, base composition, length, and the avoidance of non-specific primer annealing. The primers were synthesized by Eurofins MWG Biotech AG.

2.1.2. Restriction endonuclease digests

Enzymatic digestions of DNA were performed using the BamHI and XhoI restriction endonucleases and reaction buffers purchased from NEB, according to the manufacturer's instructions. Diagnostic double digestion reactions typically consisted of 5µg plasmid DNA, 5µl of each restriction endonuclease, 10µl of 10x Buffer 3.1, made up to 100µl with nuclease-free water. To prepare plasmid DNA for subcloning, the DNA was double digested with a BamHI/ XhoI mixture as described above, digested at 37°C for 2hr or overnight, and dephosphorylated with Antarctic shrimp phosphatase (NEB) (5µl Antarctic phosphate buffer, 1µl Antarctic phosphatase, 4µl nuclease-free water) at 37°C for 30 min, followed by incubation at 70°C for 5 min to inactivate phosphatases. The success of the digestion was determined by DNA gel electrophoresis.

2.1.3. DNA gel electrophoresis

DNA samples were resolved by agarose gel electrophoresis. Agarose gels at 1% concentration were made by melting 1g of UltraPure Agarose (Life Technologies) in 100 ml tris-acetate-EDTA (TAE) buffer. The running buffer was TAE with 0.5μg/ml ethidium bromide. DNA samples were loaded with blue gel loading dye (NEB) and electrophoresed at 80V for 1hr. A 1kb DNA ladder (NEB) was used as a molecular DNA marker, according to manufacturer's instructions (Figure 2.1A). DNA samples were visualised using a UV illuminator (Biorad).

2.1.4. Agarose gel extraction

DNA bands were isolated from agarose gels using the QIAquick Gel Extraction kit, according to the manufacturer's instructions (Qiagen). Briefly, bands of interest were excised from the agarose gels, solubilised, and the DNA precipitated with isopropanol. Free DNA was captured on the membranes of QIAquick spin columns using centrifugation, washed and eluted with Tris-EDTA buffer. Final DNA concentrations were measured using a ND-1000 spectrophotometer.

2.1.5. DNA sequencing

DNA was sequenced to confirm the correct insertion of sequences into the expression plasmids, using automated sequencing services provided by Source Bioscience Lifescience (Nottingham, UK). The generated nucleotide sequences were analyzed using publicly available databases; ExPASy Bioinformatics Resource Portal, ClustalW2 (EMBL-European Bioinformatics Institute), and the basic local alignment search tool (BLAST).

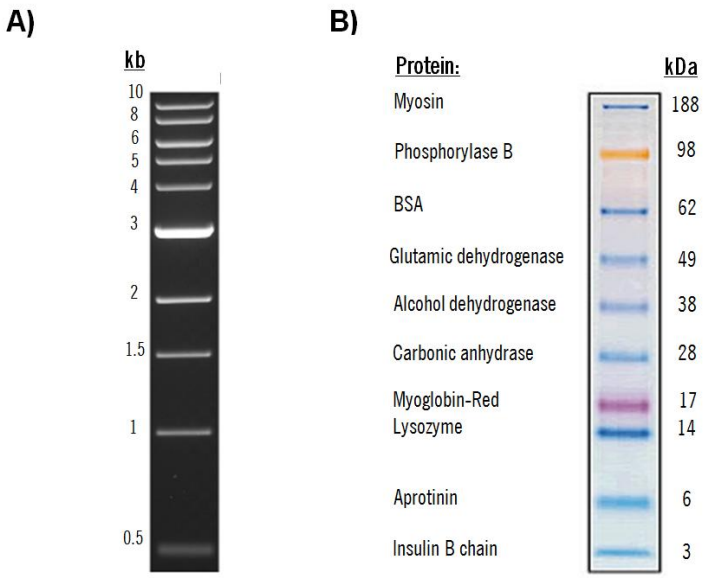

Figure 2.1 Molecular markers (A) NEB 1 kilobase (kb) DNA ladder. **(B)** Life Technologies SeeBlue® Plus2 Pre-stained Protein Standard, on a NuPAGE® Novex® 4-12% Bis-Tris Gel.

2.1.6. DNA Ligations

DNA ligations were conducted using T4 DNA ligase (NEB). A typical reaction consisted of the cloning vector, the insert of interest, T4 DNA ligase and T4 DNA ligase reaction buffer (NEB). To ensure high efficiency of ligation, 1:3 molar ratios of vector to insert were used. To calculate the required amount of insert, the following formula was used:

$$Insert\ (ng) = \frac{vector\ (ng)\ x\ insert\ (kbp)}{vector\ (kbp)}$$

Unless otherwise stated, all ligations were performed at 16° C for 16hr.

2.1.7. Transformation of competent cells with plasmid DNA

Ligated DNA (5µl of the ligation mix) was incubated on ice with 50µl of competent One Shot™ *E. coli* cells (TOP10 or DH5α, Life Technologies) for 30 min. The cells were heat-shocked for 30 sec at 42°C, then incubated on ice for 2 min. 250 µl of super optimal broth media (SOC; Life Technologies) was added to the bacteria which were then incubated for 1hr at 37°C in a shaking incubator. Transformed cells were plated onto LB-agar selection plates containing ampicillin (100µg/ml) or zeocin (25µg/ml), and incubated overnight at 37°C.

2.1.8. Isolation of plasmid DNA from bacterial cultures: miniprep and midiprep

Single bacterial colonies from selective LB plates were grown overnight at 37°C, in 5mls of LB medium with the relevant antibiotic, in a shaking incubator. Plasmid DNA was retrieved from the bacteria by alkaline lysis, according to the manufacturer's instructions (Qiagen miniprep kit) and typically gave 15-30µg of DNA in total. Variation in yield was dependent on plasmid copy number.

The plasmid DNA derived from minipreps were digested with relevant restriction endonucleases (section 2.1.2) and checked by DNA gel electrophoresis (section 2.1.3) to confirm the correct size of the inserts. DNA with correct inserts were sent for sequencing (section 2.1.5).

Plasmid DNA shown to be correct by sequencing were transfected again into competent bacteria, and 5ml LB + selection antibiotic cultures grown for several hours from single bacterial colonies. These cultures were used to inoculate 250ml LB containing relevant selection antibiotic, and this volume was grown overnight. Plasmid DNA was isolated by alkaline lysis (Qiagen midiprep kit), and yields were typically 300-500μg.

2.2. Protein production

2.2.1. Generation of DBLMSP and DBLMSP2 mammalian expression vectors

Mammalian expression vectors were generated that contain the chemically synthesised genes for DBLMSP and DBLMSP2, either full-length (FL) or lacking the DBL domains (C). Incorporation of these gene inserts into the mammalian expression vector pcDNA 3.1(+) (Life Technologies) was outsourced to GeneArt by Life Technologies. The genes were codon-optimised for expression in mammalian cells, and potential N-linked glycosylation sites were mutated to prevent inappropriate glycosylation of parasite proteins. Two c-myc tags and a 6x histidine (his) tag were placed downstream of the genes, and the inserts were flanked by the BamHI and XhoHI restriction enzyme sites.

To generate the pFUSE-MCS-DBLMSP/2 vectors, the genes for DBLMSP-FL/-C and DBLMSP2-FL/-C were excised from the pcDNA 3.1(+) vectors using BamHI and XhoHI restriction enzymes (section 2.1.2). Subcloning of the DBLMSP and DBLSMP2 genes was performed by Dr Pat Blundell. The mammalian expression vector pFUSE-MCS (Invivogen) was linearised by BamHI/ XhoI digestion and dephosphorylated (rSAP, NEB). Agarose gel electrophoresis (section 2.1.3) and gel elutions (section 2.1.4) were used to isolate the inserts and the linearised vector. The DBLMSP gene fragments were ligated into the linearised pFUSE-MCS vector (section 2.1.6), the ligation mixes were transformed into competent bacteria and plated onto selective LB agar plate. Plasmids with the correct insertions were isolated by the miniprep technique (Qiagen), and the correct sequences and vector maps are shown in Appendix II.

2.2.2. Preparation of DNA insert for mammalian cell transfection

Transfection of mammalian cells using FuGENE® transfection reagent (Promega) was performed according to the manufacturer's guidelines. Briefly, 3µg of maxiprep vector DNA was transferred to a clean Eppendorf tube containing 100µl DMEM complete medium (see section 2.1.8). Following mixing, 9µl of FuGENE® was added directly to the mix, vortexed and allowed to stand for 12 min. This mixture was then resuspended in CHO-K1 or HEK293T cells (5×10^5) in 10ml DMEM complete media, prior to transfer to a 100mm tissue culture dish and incubation for 24-48hr at 37˚C and 5% CO_2. Culture supernatant was then removed and replaced with selection media (DMEM complete media, 10% FBS and 400µg/ml zeocin). Cells were then cultured for up to 14 days at 37˚C to select for transfected cells.

To store these polyclonal transfected cell lines, cells were trypsinised (0.5% trypsin in EDTA for 2 min) and transferred to 175cm^2 flasks containing selection media, and at 70% confluency, the cell lines were frozen in fetal bovine serum (FBS)/ 10% DMSO for storage in liquid nitrogen For protein production, the cultures were grown to 70% confluency and the cells trypinised and passaged into 175cm^2 flasks in selection media at 1:200 dilution (cells:medium), in order to expand the population at volume and under selection pressure. Cells were then incubated at 37˚C at 5% CO_2 for up to14 days to allow for protein production.

2.2.3. Seeding for transfected CHO-K1 cell colonies

Transfected CHO-K1 cells were grown for four weeks under selection until isolated colonies began to appear. Cell colonies were selected using sterile filter paper and sterile tweezers. Each filter paper was then placed into 1ml selection media in a single well of a 24-well plate, and incubated at 37˚C at 5% CO_2 for up to14 days to allow for protein production. Immunoblotting was used to test for the presence of recombinant protein within culture supernatants.

2.2.4. Expression trials for recombinant protein in mammalian cells

Transfected cell culture media was harvested and filter sterilised (0.22µm), and 0.2% sodium azide added. Expression trials were then performed on culture supernatants

to detect secreted recombinant protein. For this, a mixture of immunoblotting, ELISA, SDS-PAGE and Western blotting techniques were used. The specific details for each protein expression trial are shown in Chapter 5.

2.2.5. Generation of DBLMSP and DBLMSP2 bacterial expression vectors

To generate bacterial expression vectors, the genes for DBLMSP-FL/-C and DBLMSP2-FL/-C were excised from the pFUSE-MCS-DBLMSP vectors using BamHI and XhoHI (section 2.1.2). These experiments were performed by Dr Pat Blundell. The pRSET-EmGFP vector (Life Technologies) was selected as it contains compatible restriction enzyme sites. Double digestion of this vector with BamHI/ XhoI resulted in the excision of the gene encoding the fluorescent protein. The DBLMSP genes were then cloned into the BamHI/XhoI sites (see Chapter 5 for further details).

2.2.6. Bacterial expression of DBLMSP and DBLMSP2

To initiate protein expression, the pRSET-DBLMSP plasmids (500ng) were transformed into BL21 Star (DE3) expression bacteria (Life Technologies) using the heat-shock method (section 2.1.7). Successfully transformed BL21 Star (DE3) colonies were picked off LB selection plates, and expanded to a volume of 5.5ml in LB medium supplemented with ampicillin. Cells were grown to mid-log phase (OD_{600}= 0.3-0.4) at 37˚C in a shaking incubator, then induced with 1mM isopropyl β-D-1-thiogalactopyranoside (IPTG) (see Chapter 5). Following induction, 0.5ml aliquots of cells were taken at 2hr intervals, pelleted and stored at -20˚C. Pelleted cells were then resuspended in 1x NuPAGE® reducing buffer (Life Technologies) and analyzed by SDS-PAGE and Western blotting (see Chapter 5).

2.3. Protein purification

2.3.1. Affinity chromatography

Recombinant proteins were purified on an anti-c-myc-sepharose column by affinity chromatography. Typically, 200-1000ml of filtered tissue culture supernatant was passed over the column using an ÄKTA Fine Performance Liquid Chromatography (FPLC) machine (GE Healthcare Life Sciences) at a flow rate of 0.5ml/ min. The

column was washed with 20ml of 1x Hank's Balanced Salt Solution (HBSS) buffer containing 0.1M sodium phosphate (pH7.4). The fractions were eluted using a linear gradient of 0.1M glycine (pH2) and neutralised using 1M Tris-HCl (pH9).

Fractions containing proteins were identified from the chromatogram profiles, ELISAs and dot blot assays (see Chapter 5).

2.3.2. Size exclusion chromatography

Proteins were assessed by size exclusion gel filtration using a Superdex 200 column (GE Healthcare Life Sciences) on an FPLC machine. The column was equilibrated in 1x HBSS buffer prior to loading proteins onto the column via a 100µl or 400µl loop. The proteins were eluted into fractions by running a pre-set program. The eluted proteins were passed through a UV flow cell (high performance monitor UPC-900) to measure their UV absorbance at 280nM using a charged-coupled device (CCD) detector. Absorbances of eluted proteins were recorded as peaks on a chromatogram. Chromatograms show the elution profile of purified proteins, whereby a symmetric profile (or peaks) indicates homogenous protein and asymmetric profiles indicate partially aggregated proteins.

Gel filtration standards (BioRad) were used to enable molecular weight (MW) predictions of proteins based on their elution fractions (Figure 2.2). These were run prior to each round of protein purification.

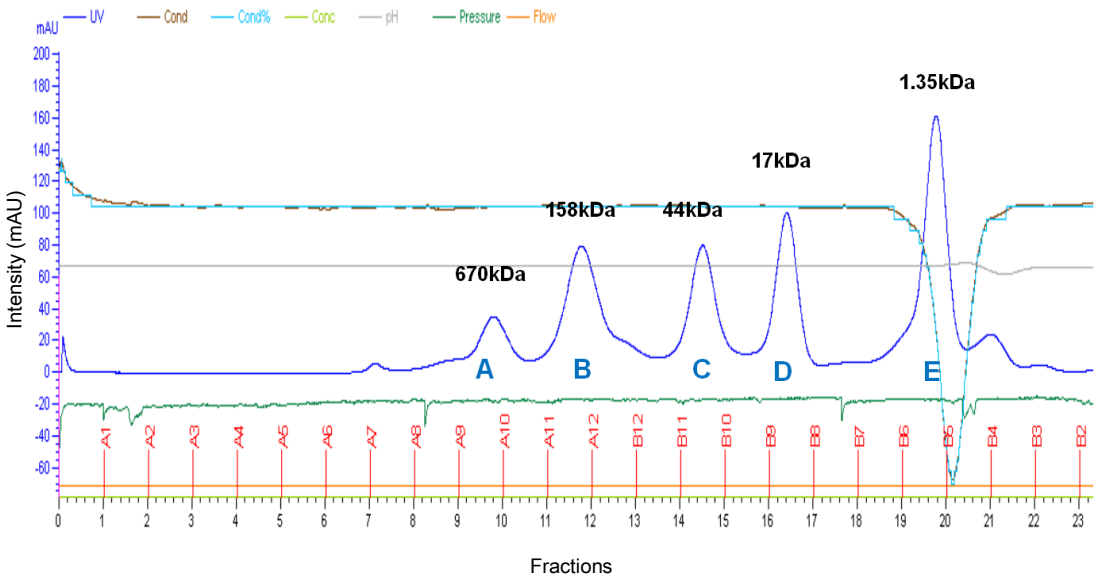

Figure 2.2 Size exclusion markers. Gel filtration standard (Biorad) was separated by size exclusion using a Superdex 200 column. Gel filtration standard components corresponding to peaks A-E included: thyroglobulin (670kDa); γ-globulin (158kDa); ovalbumin (44kDa); myoglobin (17kDa); vitamin B_{12} (1.35kDa).

2.4. Protein analysis techniques

2.4.1. Sodium Dodecyl Sulphate-Polyacrylamide Gel Electrophoresis (SDS-PAGE)

Protein samples were prepared with NuPAGE® sodium dodecyl sulphate (SDS) sample buffer (Life Technologies), and loaded either under reducing or non-reducing conditions, using dithiothreitol (DTT; 160mM) as a reducing agent. The samples were centrifuged at 27,396 g for 30 sec and then heated at 95°C for 2 min before loading 5-15µg of protein into the wells of a NuPAGE® Novex 4-12% Bis-Tris pre-cast gel. An XCellSureLock™ Mini-Cell electrophoresis system was used to run the gels in NuPAGE® MES SDS Running Buffer (Life Technologies) at 200V constant for 45 min. SeeBlue® Plus2 Pre-stained Protein Standard (Life Technologies) was used as a MW marker (Figure 2.1B). Gels were Coomassie stained (section 2.4.2) or transferred to a membrane for Western blotting (section 2.4.3).

2.4.2. Coomassie staining of gels

NuPAGE® Novex 4-12% Bis-Tris pre-cast gels were removed from their housing cassettes and stained in Coomassie Brilliant Blue R-250 (BioRad) on a platform shaker (Stovall Life Sciences Inc., Ringer, UK), before being washed twice in deionised water and left to destain overnight in Coomassie Brilliant Blue R-250 destaining buffer (BioRad). Protein bands were directly visualised on the destained gel and their respective molecular weights (kDa) were estimated by comparison with the molecular weight marker. Stained gels were scanned using an Epson Perfection 1260 flatbed scanner (Epson, Telford UK).

2.4.3. Western blotting

NuPAGE® Novex 4-12% Bis-Tris pre-cast gels were transferred to Protran nitrocellulose transfer membrane (GE Healthcare) in NuPAGE® transfer buffer (Life Technologies) at 40V for 1hr, using an XCell II™ blot module according to manufacturer's instructions (Life Technologies). To block non-specific binding, the membrane was rocked on a platform shaker with PBS-Tween (PBST; PBS with 0.1% Tween 20)/ 5% non-fat milk powder for 1hr, followed by at least three washes. Blocking, incubations and washings were performed in PBST. The membrane was

then incubated with primary Ab overnight on a rocker at room temperature (RT), followed by incubation with a secondary Ab conjugated to either horseradish peroxidase (HRP) or alkaline phosphatase (AP) for 3hr. Occasionally, the membrane was direct labelled with a conjugated Ab overnight.

Proteins were visualised by developing HRP-conjugated Abs with the chromogen 3',3'-Diaminobenzidine (DAB; DAKO), or AP-conjugated Abs with a developing buffer composed of 5-bromo-4-chloro-indolyl-phosphate/ Nitrobluetetrazolium (BCIP/NBT; 100mM Tris/HCl, pH 9.5, 100mM NaCl, 5mM $MgCl_2$), according to manufacturer's instructions (Sigma-Aldrich). Developed blots were then scanned and images stored.

2.4.4. Immunoblotting

Purified proteins or culture supernatants were dotted onto nitrocellulose membranes and air-dried for 30 min. Membranes were then blocked in PBST/5% non-fat milk powder for 1hr, washed three times in PBST and incubated with PBST-containing Abs to detect specific proteins and/ or tags. The presence of proteins on membranes was detected using the same method as for Western blots (section 2.4.3).

2.5. Protein-protein interaction techniques

2.5.1. Enzyme-linked immunosorbent assay (ELISA)

Appropriate target antigen or capture Ab were coated onto wells of Nunc-maxisorp microtitre plates (Fisher Scientific) overnight at 4°C in fresh carbonate/ bicarbonate buffer, pH 9.6 (Sigma-Aldrich). Unless otherwise stated, proteins were coated at 10µg/ml. Uncoated material was discarded and plate wells were washed extensively with PBST prior to being blocked with 200µl blocking buffer (PBST/ 5% non-fat milk powder) for 1hr at RT on a rocker. Following the incubation, the plate wells were washed with 200µl of PBST at least six times prior to incubation with an appropriate dilution primary Ab for at least 3hr at RT. The plates were washed in PBST and incubated with appropriate dilutions of detecting Abs for 3 hr at RT. Typically, HRP-conjugated Abs were used at 1:2000 dilutions in PBST, and AP-conjugated Abs at 1:5000 dilutions. HRP-conjugated Abs were detected using one tablet of 3,3',5,5'-tetramethylbenzidine substrate (TMB; Sigma-Aldrich) dissolved in

10ml of 0.1M citrate phosphate buffer, whereby 100µl of the solution per well was allowed to develop until the desired contrast between control and positive wells was achieved. The reaction was terminated by adding 50µl of 2M H_2SO_4 to each well immediately before the absorbance was read at 450nm (HRP) on an Expert Plus plate reader (Biochrom, SLS). AP-conjugated Abs were detected using p-Nitrophenyl phosphate (1mg/ml) in 0.2M Tris buffer containing 5mM magnesium chloride (Sigma-Aldrich), and read at 405nm. Optical density readings were blank-corrected against the mean of duplicate control wells containing a negative control such as PBS or secondary Ab alone.

2.5.2. Multi-channel surface plasmon resonance (SPR)

Surface plasmon resonance experiments were performed in collaboration with the laboratory of Dr Daniel Mitchell (University of Warwick). Recombinant human DC-SIGN was generated as described previously [184], as was IgM-Fc [185], mouse SIGNR1 was from R&D Systems (Abingdon, UK), and Pentaglobin™ was kindly provided by and Biotest UK. DC-SIGN or SIGNR1 were immobilised on GLM sensor chips (Bio-Rad) using amine coupling with sulfo-N-hydroxysuccinimide/1-Ethyl-3-[3-dimethylaminopropyl] carbodiimide. For IgM binding experiments, doubling dilutions (10µM-0.32µM) of IgM-Fc or Pentaglobin™ were injected at flow time 0, and replaced with buffer at 300 sec. To determine the binding of DBLMSP to IgM on DC-SIGN, human IgM was injected into flow at time 0 and replaced with buffer at 300 sec. Following this, DBLMSP or DBLMSP2 were injected at doubling dilutions from 10µM to 0.32µM into flow at time 900, and replaced with buffer at 1300 sec. Sensograms were recorded at 25˚C with the ProteOn XPR36 surface plasmon resonance biosensor (Bio-Rad) using a flow rate of 25µl/min. Kinetic parameters for protein-protein interactions were determined using the 1:1 Langmuir modeling algorithms included in the ProteOn Manager software suite (Bio-Rad).

2.6. Cell techniques

2.6.1. Mammalian cell culture

Human embryonic kidney (HEK) 293E and Chinese Hamster Ovarian (CHO-K1) cells were cultured in RPMI 1640 medium or DMEM containing 10% heat inactivated fetal bovine serum (FBS), 2mM L-glutamine, 100U/ml penicillin and 100μg/ml streptomycin, and 50mM 2-mercaptoethanol (Gibco by Life Technologies) (referred to as complete media).

Fcμ receptor cDNA-transfected cells (BW5147 T cells) were cultured in complete media supplemented with 0.1ng/ml puromycin [137]. Untransfected BW5147 T cells were used as a negative control, and were maintained in complete media. FcμR cDNA-transfected and untransfected BW5147 T cells were kindly donated by Dr Hiromi Kubagawa (University of Alabama at Birmingham).

Immature dendritic cells (iDCs) were derived from autologous-sorted $CD14^+$ blood monocytes by culture with granulocyte-macrophage colony stimulating factor (GM-CSF), interleukin (IL)-4 and tumor necrosis factor (TNF)-α for six days. These experiments were performed in the laboratory of Dr Britta Urban.

All cells were incubated at 37°C with 5% CO_2 for specific incubation periods or until semi-confluent. To prepare cells for freezing, cells (2×10^7 cells/ml) were resuspended in ice-cold FBS and allowed to stand on ice for 20 min. The same volume of ice cold FCS/20% DMSO was added to cells and gently mixed prior to aliquoting 1ml cell suspensions into cryovials. Cryovials were immediately put into freezing containers and stored at -80°C for 24hr, then transferred to liquid nitrogen for long-term storage.

2.6.2. Processing of blood samples and buffy coats

Trained clinical officers took 10ml blood samples from malaria-naïve volunteers, which was collected into heparin tubes and processed immediately. Methods were approved by the Ethical Review Committee of the Liverpool School of Tropical Medicine.

Buffy coats from blood of healthy, malaria-naïve individuals were obtained from the National Health Service (NHS) Blood and Transplant Service, under the Liverpool School of Tropical Medicine Research Tissue Bank Approval (REC ref 11/H1002/9) and were held under the Human Tissue Authority license number 12548.

Peripheral blood mononuclear cells (PBMCs) were isolated by Ficoll-Paque gradient centrifugation using Lymphoprep (Axis-Shield, Norway) and washed twice in RPMI/ 10% FBS. Cells were used immediately or cryopreserved at -140°C until use. Prior to each experiment, cells were rapidly thawed in a water bath at 37°C and washed three times in media. Cells were then rested for 3hr prior to trypan blue staining to determine cell viability and counts, and resuspended to desired concentrations.

2.6.3. *Plasmodium falciparum* parasite cultures

In vitro-adapted parasites used for this work include *P. falciparum* clones 3D7, ITGvar1, and ITGvar13. These experiments were kindly performed by Mohammad Alkurbi. Parasites were kept in continuous culture according to standard procedures [186]. Briefly, parasite strains were cultured in RPMI-1640 supplemented with 4mM hypoxanthine, 25mM HEPES and 20μg/ml gentamycin with erythrocytes (O^+) at 5% hemocrit and 10% AB^+ serum in buffered culture (pH 7.4). Parasites were maintained at ~5-8% parasitemia, and were synchronised prior to experimentation by two consecutive treatments with 5% sorbitol for 10 min [187], to ensure a synchrony window of 6hr. The culture medium was changed when parasites entered the trophozoite stage. To harvest the supernatant following merozoite egress (invasion of erythrocytes), parasites were cultured for another 14hr to allow schizonts to burst and merozoites to reinvade. The development of the parasite cycle was monitored by Giemsa staining (2% Giemsa in PBS) and thin blood film analysis (Figure 2.3). Parasite culture supernatant was harvested at this time point (early ring stage) by transferring the culture to a 50ml falcon tube and centrifuging at 500g for 5 min. The supernatant was transferred to a sterile falcon tube and stored at 4°C prior to use. In parallel, an equal quantity of uninfected erythrocytes were cultured and processed under the same conditions as above. The supernatant of the uninfected erythrocytes was used as a negative control.

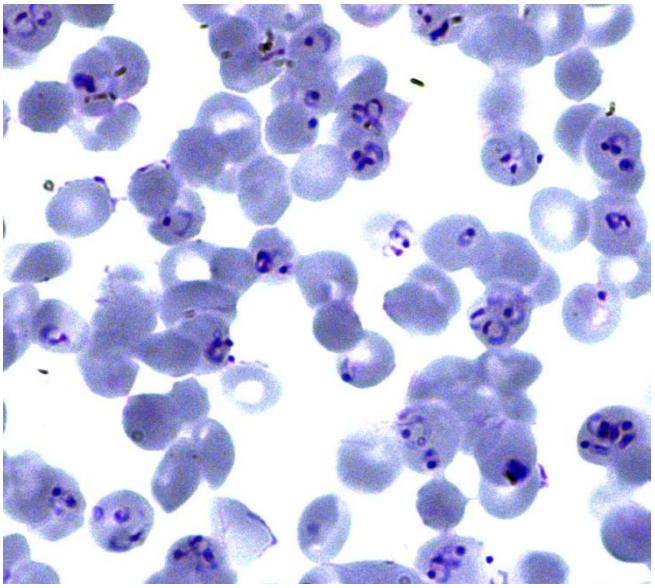

Figure 2.3 Highly synchronised *Plasmodium falciparum* culture. 3D7 strain of *P. falciparum* was grown at 5-8% parasitemia prior to experimentation and synchronised by two consecutive treatments with sorbitol. Parasite stage was determined by Giemsa staining (2% Giemsa in phosphate buffer for 30 min at RT) of thin blood films and examination by microscopy. Highly synchronised cultures were monitored and harvested at early ring stage for immunoprecipitation experiments.

2.7. Flow cytometry

2.7.1. Reagents

Abs to the following human antigens were used: fluoresceinisotheiocyanate (FITC)-conjugated Abs specific for CD4, CD8, CD19 and CD56, goat $F(ab')_2$ anti-human-IgM-RPE, goat $F(ab')_2$ anti-human lambda-RPE, and isotype controls were from SouthernBiotech. Anti-human CD4-Alexa-Fluor® 700 and anti-human CD19-PE-Cy7 were from eBioscience. Anti human CD19-Brilliant Violet™ 421, CD14-APC Cy7, CD8-PerCp, CD27-APC Cy7, CD21-Brilliant Violet™ 421, CD10-PE, CD38-Alexa-Fluor® 700, and anti-mouse IgG-APC were from Biolegend. Anti-CD27-PE-Cy5 was from Beckman Coulter. CellTrace™ Violet Cell Proliferation Kit was purchased from Life Technologies, as were LIVE/DEAD® Fixable Aqua Dead cell stain kit, propidium iodide, AbC™ anti-mouse and ArC™ amine reactive compensation bead kits. Anti-biotin-APC and anti-histidine (his)-PE Abs were from MilitenyiBiotec (Surrey, UK). 7-AAD, Annexin V-APC, and anti-human CD19-PE CF594, CD3-APC and CD3-Brilliant Violet™ 421 were from BD Pharmingen.

2.7.2. Generic technique

Unless otherwise stated, 2×10^5 cells were stained with fluorochrome-conjugated Abs in complete media or FACS buffer (PBS/ 0.1% BSA) for 1hr at 4°C, then washed three times in complete medium or FACs buffer by centrifugation at 598 g for 10 min. Following centrifugation, supernatants were discarded and cell pellets resuspended in FACs buffer. Flow cytometry was performed on BD LSRII flow cytometer with FACS Diva (BD) data acquisition.

For hFcμR-transfected cells, values of the untransfected cells (e.g. background) were removed from transfected cell data.

Live lymphocytes were identified on the basis of forward and side scatter, alongside the use of conjugated Abs specific for various lymphocyte populations. Data were analyzed using FlowJo software version 9.1. (FlowJoTreestar, OR, USA). Abs were titrated prior to use to determine optimal concentrations for staining. Typically, experiments were repeated at least three times using three different PBMC donors.

2.8. Production of recombinant DBLMSP and DBLMSP2

Recombinant DBLMSP and DBLMSP2 proteins of the 3D7 cloned strain of *Plasmodium falciparum* were kindly provided by Dr Cecile Crosnier (The Wellcome Trust Sanger Institute, Cambridge). Details of the protein production have been previously described [188]. Briefly, the coding sequence of full-length DBLMSP and DBLMSP2 (PF10_0348 and PF10_0355, respectively) were codon-optimised for expression in mammalian cells, so that any potential N-linked glycosylation sites (NXS/T sequence) were modified by substituting serine or threonine residues for an alanine (NXA). In some cases, the coding sequence of either the DBL domain or the C-terminal region containing the SPAM and coiled-coil domains (referred to as SPAM domain) was used [146]. Inserts were flanked with NotI/AscI restriction enzyme sites and cloned downstream of an exogenous signal sequence of murine origin [189]. The recombinant proteins feature a C-terminal rat Cd4-d3+4 tag [190] followed by either a biotinylation or a 6x-histidine (his) tag [25]. Recombinant proteins of the Cd4-d3+4 tag (referred to as Cd4-d3+4) alone were produced as a negative control. The proteins were produced recombinantly via transient transfection of HEK293E cells, which were cultured for six days at 37˚C with 5% CO_2. Cell culture supernatants were then harvested and filtered. Biotinylated protein culture supernatant was dialysed in HEPES-buffered saline (HBS; pH 7) for 48hr. Concentrations of biotinylated proteins in the culture supernatants were determined by ELISA using streptavidin-coated microtitre plates (Nunc), which were detected using an anti-rat Cd4 Ab (OX68, Serotec) followed by incubation with an anti-mouse-AP secondary Ab. The concentrations of biotinylated proteins were normalised using spin concentrators (Vivascience, 10k MWCO) or by dilutions with conditioned tissue culture supernatant or PBS containing 0.2% BSA [191]. His-tagged proteins were purified using His-Trap purification columns (GE Healthcare) on an ÄKTAxpress as previously described [144]. Recombinant protein quality was assessed by Coomassie staining and Western blot analysis (Figure 2.4).

In addition, recombinant DBLMSP and DBLMSP2 protein production was attempted in Chapter 5 (see Chapter for specific details).

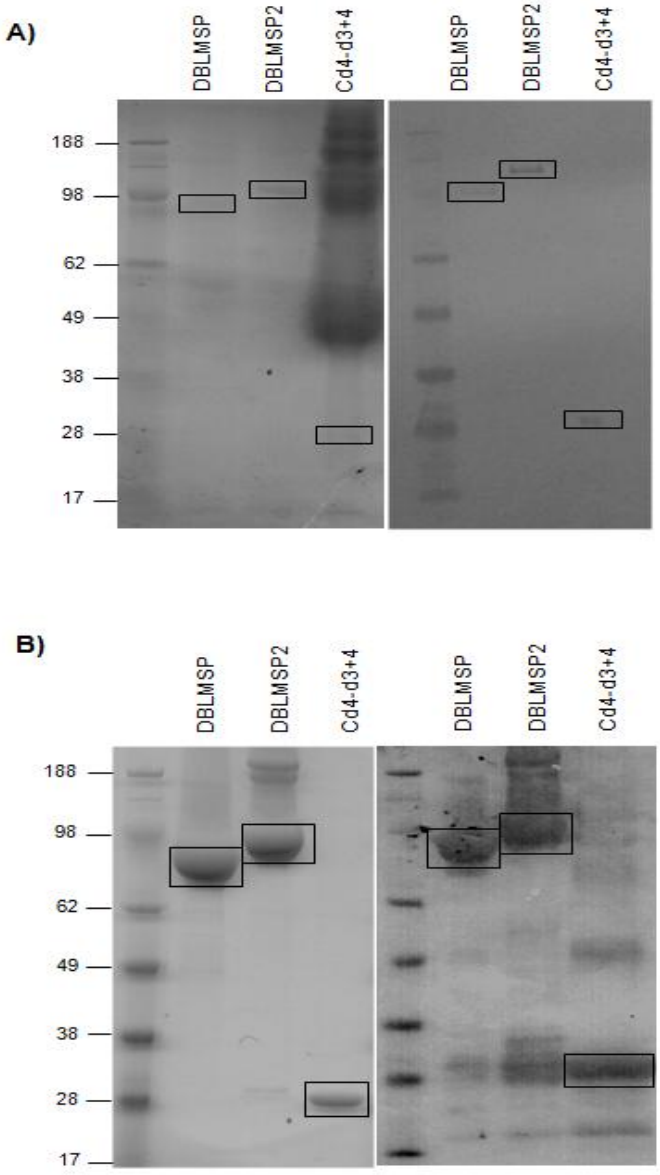

Figure 2.4 Recombinant DBLMSP and DBLMSP2 protein analysis. Coomassie staining (left panels) and Western blot analysis (right panels) of recombinant biotin-tagged **(A)** and his-tagged **(B)** DBLMSP, DBLMSP2 and Cd4-d3+4 proteins. Bands corresponding to DBLMSP, DBLMSP2 and Cd4-d3+4 are seen at ~80kDa, ~98kDa and ~25 kDa, respectively.

2.9. Determining the domain of human IgM binding DBLMSP and DBLMSP2 by ELISA

ELISA plates were coated with recombinant his-tagged DBLMSP, DBLMSP2, or Cd4-d3+4 proteins. After blocking, 10μg/ml human IgM was added to duplicate wells and incubated at RT for 3hr. In some experiments, a panel of domain-swap Abs described in a previous study [120] was used to determine which domain(s) of IgM bind DBLMSP and DBLMSP2 (performed by Professor Richard Pleass). For this, varying concentrations of domain-swap Abs were immobilised in duplicate onto microtitre plates (Nunc) and allowed to bind 10μg/ml recombinant his-tagged DBLMSP or DBLMSP2. Binding of IgM and domain-swap Abs was detected using anti-human IgM-HRP (Sigma-Aldrich).

The ability of the DBL and SPAM domains of DBLMSP and DBLMSP2 to bind human IgM was also investigated. Immobilised IgM was incubated with 100μl of normalised biotinylated DBL or SPAM domains, or biotinylated Cd4-d3+4, for 3hr at RT. Following washing, the binding of biotinylated proteins to IgM was detected using Extravidin®-Peroxidase.

2.10. Investigating the binding of DBLMSP and DBLMSP2 to FcμR

To determine if DBLMSP proteins blocked the binding of hIgM to FcμR, hFcμR-transfected cell lines were incubated with hIgM (15μg/ml) preincubated with varying concentrations of his-tagged DBLMSP and DBLMSP2 (see Chapter 4 for details). Cells were washed and labelled with $F(ab')_2$-anti-human IgM-RPE for flow cytometric analysis. These experiments were performed by Professor Richard Pleass.

To determine if DBLMSP proteins could engage IgM bound to FcμR, hFcμR-transfected cell lines were opsonised with 15μg/ml hIgM for 1hr at 4˚C, washed and incubated with 100μl of normalised biotinylated DBLMSP or DBLMSP2 for 1hr at 4˚C. Recombinant biotinylated DBLMSP, DBLMSP2 or Cd4-d3+4 proteins were initially titrated to determine working concentrations. Cells were washed three times with media and labelled with anti-biotin-APC.

Binding of DBLMSP proteins to PBMCs known to express FcμR, including $CD4^+$ and $CD8^+$ T cells, B cells, and NK cells [137], was also determined. For this, freshly isolated PBMCs (section 2.6.2) were incubated with complete media containing 100μl normalised biotinylated DBLMSP, DBLMSP2, or Cd4-d3+4 for 1hr at 4˚C. Cells were then washed and incubated with anti-biotin-APC, and subsequently labelled with FITC-conjugated Abs specific for human CD4, CD8, CD19, and CD56. In some experiments, cells were labelled with $F(ab')_2$-anti-human IgM-RPE to determine if DBLMSP co-localised with IgM on lymphocytes. Individual DBL or SPAM domains (section 2.8) were used to determine which region of the DBLMSP proteins mediated binding to IgM-opsonised on FcμR. For this, 100μl normalised biotinylated DBL or SPAM domains were incubated with hFcμR-transfected cell lines or PBMCs for 1hr at 4˚C, washed and labelled with anti-biotin-APC prior to flow cytometric analysis.

2.11. Staining of PBMCs with CellTrace™ Violet for determination of proliferation in culture

Proliferation of PBMCs was monitored by using the CellTrace™ Violet Cell Proliferation Kit (Life Technologies). PBMCs (10^7 cells/ml) were resuspended in 10ml pre-warmed PBS and labelled with 1μM CellTrace™ Violet Cell stain for 10 min at RT on a roller. Staining was quenched by adding 50ml of ice-cold media to the cells and immediate incubation on ice for 5 min. Cells were then washed three times by centrifugation before being placed into culture.

2.12. Functional assays to determine *in vitro* effects of DBLMSP and DBLMSP2

PBMCs isolated from malaria-naïve healthy donors were cultured at 2 x 10^5 cells per 200μl in U-bottomed 96-well culture plates (Nunc, Roskilde, Denmark) at 37˚C with 5% CO_2 and 95% humidity. All cultures were conducted in complete media. A schematic diagram of the experimental design for the functional assays is shown in Figure 2.5.

To determine the *in vitro* effects of DBLMSP proteins, PBMCs were incubated with varying concentrations of his-tagged recombinant DBLMSP, DBLMSP2, or Cd4-d3+4 proteins (see Chapter 4), which were either added directly to the culture medium or coated overnight in carbonate bicarbonate buffer (pH 9.6) onto round-bottom plates to induce receptor cross-linking [192]. In experiments where the ability of the DBLMSP proteins to induce cellular proliferation was assessed, CellTrace™ Violet-labelled cells were cultured with varying concentrations of his-tagged recombinant DBLMSP, DBLMSP2, or Cd4-d3+4 proteins for five days at 37˚C in a 5% CO_2 incubator. In some experiments, recombinant proteins were preincubated with human IgM (5:1 ratio), or with PHA or CpG ODN 2006, for 30 min at RT prior to culture. Cells cultured with PHA (5μg/ml; Life Technologies) or CpG ODN 2006 (1μg/ml; Hycult Biotech) were used as positive controls for T cell and B cell proliferation, respectively. Unstimulated cells cultured in complete media alone or in media supplemented with varying concentrations of bovine serum albumin (BSA) were used as negative controls. Following five days of culture, cells were harvested and washed prior to labelling with anti-CD4-Alexa Fluor® 700, anti-CD8-FITC, and anti-CD19-PE Cy7. Proliferation of gated lymphocytes was shown by depletion of CellTrace™ Violet staining by flow cytometry (Figure 2.6).

Apoptosis assays were set up alongside proliferation assays. For this, PBMCs were cultured with 50μg/ml of his-tagged DBLMSP, DBLMSP2 or Cd4-d3+4 proteins for 24hr or 48hr at 37˚C with 5% CO_2. PBMCs were harvested and labelled with Abs specific for anti-human CD3-Brilliant Violet™, anti-human CD19-FITC, and anti-human CD8-FITC (Figure 2.6B for gating strategy). To quantify apoptotic cells, PBMCs were labelled with Annexin V-APC and 7-AAD according to the manufacturer's instructions (BD Pharmingen). Briefly, cells were washed twice with ice cold PBS and resuspended in 1x Binding Buffer containing Annexin V-APC and 7-AAD (1:10) and incubated for 15 min at RT in the dark. Following incubation, labelled cells were immediately analyzed by flow cytometry. UV irradiation-induced apoptosis in PBMCs was used as a positive control [193], whereby cells were harvested and subject to UV-radiation for 30 min at a wavelength of 230nm (UV transilluminator, UVP) prior to labelling.

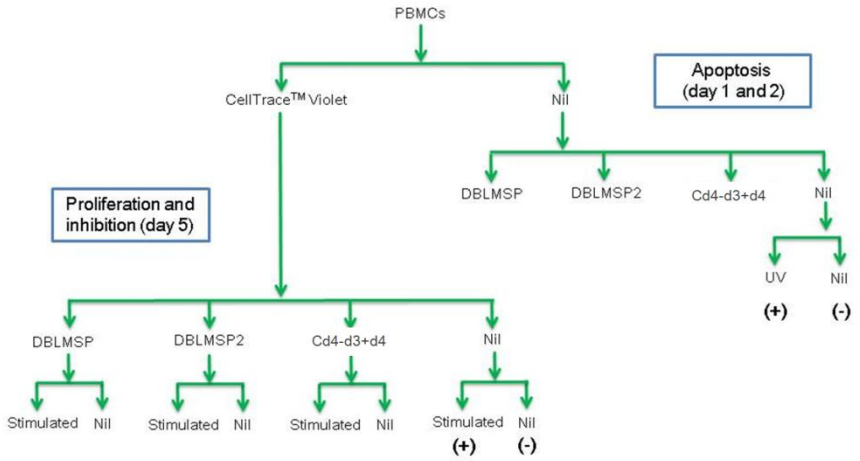

Figure 2.5 Experimental design for the determination of the *in vitro* effects of DBLMSP and DBLMSP2. Cells were placed into culture on day 0, apoptosis was determined on days 1 and day 2, and proliferation and inhibition of proliferation were determined on day 5. Positive and negative controls are shown as (+) and (-), respectively.

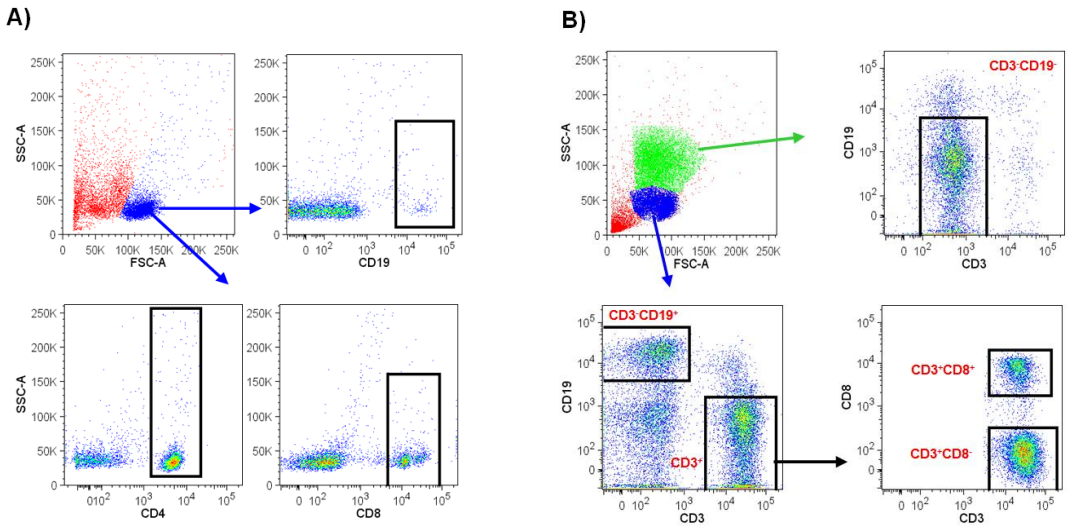

Figure 2.6 Gating strategies for PBMCs in functional assays. (A) Lymphocytes were identified on side scatter (SSC) and forward scatter (FSC) plot (shown by blue dots). Lymphocytes were further gated into $CD4^+$ and $CD8^+$ T cells and B cells based on expression of human CD4, CD8, and CD19, respectively. **(B)** Within the lymphocyte gate (shown as blue dots), cells were gated into $CD19^+$ and $CD3^+$. The $CD3^+$ cell population was further gated into $CD8^+$ T cells ($CD3^+CD8^+$) and $CD8^-$ T cells ($CD3^+CD8^-$). Monocytic cells were identified on SSC and FSC plot (shown by green dots), which were further gated into $CD3^-CD19^-$ monocytic cells (shown as a black gate).

2.13. Parasite culture immunoprecipitation analysis

To investigate if other malarial proteins are present within the DBLMSP-IgM complex, culture supernatant was harvested from *P. falciparum* parasite strains 3D7, ITGvar1, and ITGvar13 grown in the presence of 10% human serum (section 2.6.3) by centrifugation at 266 g for 10 min. Media from uninfected RBC cultures was used as a negative control. Anti-human IgM-agarose beads (Sigma-Aldrich) were incubated with culture supernatants in excess (to precipitate all of the IgM from the supernatants) for 2hr on a roller. Beads were pelleted by centrifugation (266 g, 5 min), washed five times in PBS to remove unbound proteins, then added to reducing and non-reducing SDS-PAGE sample buffer and boiled for 5 min. Samples were separated by SDS-PAGE and transferred to nitrocellulose membrane by Western blotting (section 2.4.3). After blocking, blots were incubated with either 10μg/ml of IVIG (GammaGard®, Baxter Healthcare; purified from 3000 healthy donors) or 10μg/ml of hyperimmune purified IgG from Malawians in malaria-endemic regions (immune sera; purified from 360 donors) in PBST overnight at RT. Blots were extensively washed in PBST and incubated with anti-human IgG-AP for the detection of immunoreactive parasite proteins. In some experiments, membranes were incubated with polyclonal rabbit anti-DBLMSP Abs (kindly provided by Dr Cecile Crosnier) and anti-rabbit IgG peroxidase (1:1000; Sigma-Aldrich) to detect DBLMSP/ DBLMSP2.

To determine if IgM-parasite protein complexes could still engage FcμR, 50μl of culture supernatants (predicted to contain 5μg hIgM) were incubated with hFcμR-transfected cells for 1hr at 4˚C, washed extensively and labelled with $F(ab')_2$-anti-human IgM-RPE and analysed by flow cytometry.

2.14. IgM binding to cell surfaces

The binding of hIgM to GFP-gated hFcμR-transfected cells (Figure 2.7) was determined by labelling with F(ab')$_2$-anti-human IgM-RPE. To determine the optimal concentration of hIgM for subsequent binding assays, hFcμR-transfected cells were incubated with media alone or media supplemented with varying concentrations of hIgM (see Chapter 3), labelled with F(ab')$_2$-anti-human IgM-RPE and analyzed by flow cytometry. The optimal concentration of IgM was determined as 15μg/ml. In some experiments, a panel of domain-swap Abs, in which the domains of IgA were replaced with domains of IgM [120], were used to determine the domain(s) of IgM which bind hFcμR, detected using F(ab')$_2$-anti-human lambda-RPE. The ability of gated lymphocytes to bind 15μg/ml hIgM or 10% human serum was also investigated (see Chapter 3).

2.15. Immunofluorescence microscopy to determine IgM levels on lymphocyte surfaces

PBMCs from healthy donors were incubated for 1hr on ice with media alone or media supplemented with 15μg/ml human IgM. Cells were washed three times in media to remove unbound IgM. After washing, 1 x 10^5 PBMCs per sample were prepared on Superfrost plus slides using the Shandon Cytospin 4 (Fisher Scientific) to generate cytospins. Protective coverslips were mounted on the slides, and the PBMC cytospins were permeabilised in methanol for 5 min. Cytospins were washed three times in PBS, blocked in complete media and washed three more times. After air drying, PBMCs were labelled with a cocktail of Abs including anti-human CD4/8/19/56-FITC and F(ab')$_2$-anti-human IgM-RPE for 1hr at 4°C. Cytospins were washed three times in PBS, air-dried, then stained with the Prolong Gold anti-fade reagent with DAPI (Life Technologies) according to manufacturer's guidelines. Cytospins were examined using a Zeiss Axioskop microscope and Carl Zeiss AIM software (Carl Zeiss Microscopy). For each cytospin, ten individual images were taken at random points to determine overall levels of surface IgM on lymphocytes.

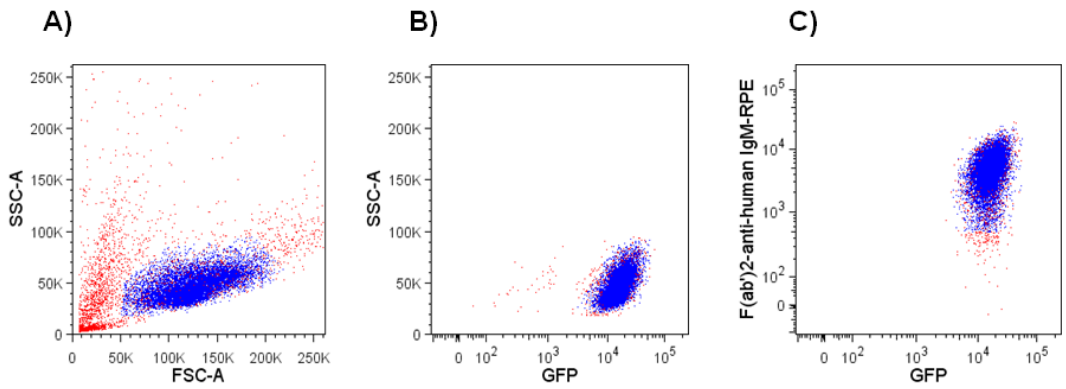

Figure 2.7 Gating strategy for IgM binding to GFP$^+$ human FcμR-transfected cell lines. (A) Live cells were identified on side scatter (SSC) and forward scatter (FSC) plot (shown by blue dots). **(B)** Within the live cell gate, hFcμR-transfected cells were identified based on the expression of green fluorescent protein (GFP) (shown as blue dots) which **(C)** were further gated to IgM$^+$ cells (shown by blue dots) to determine mean intensity fluorescence values for IgM binding.

2.16. Flow cytometry analysis to determine FcμR-mediated internalisation of IgM

Internalisation of IgM via FcμR was investigated using a previously described protocol with modifications [183]. Briefly, hFcμR-transfected cells or PBMCs were incubated for 1hr on ice with media alone or media supplemented with 15μg/ml human IgM or 10% human serum. In some experiments, artificially-induced IgM immune complexes (15μg/ml) formed using heat-aggregation (62˚C for 30 min) [194] were used to determine if IgM-immune complexes could bind to and be internalised by hFcμR. Cells were then washed in ice-cold media and incubated at 37˚C for varying periods to allow for receptor internalisation. Samples maintained on ice were used as a control for maximal binding of IgM (time 0). The immediate addition of ice-cold media to cells and incubation on ice was used to halt internalisation. Cells were washed twice and labelled with $F(ab')_2$-anti-human IgM-RPE.

To investigate IgM internalisation into lymphocyte subsets, a lymphocyte staining panel was formed. For this, Abs were initially titrated to determine relevant working concentrations. The panel consisted of anti-CD19-Brilliant Violet™ 421, anti-CD3-APC, anti-CD4-Alexa Fluor® 700, anti-CD8-PerCP, and anti-CD56-FITC to differentiate B cells, T cells, and NK cells (see Chapter 6). Internalisation assays were performed as above.

2.17. Flow cytometry analysis to determine FcμR internalisation

hFcμR-transfected cells were incubated with 1μg anti-hFcμR mAb (Abnova) for 1hr at 4˚C prior to internalisation assays (section 2.16). Following internalisation, cells were washed and labelled with anti-mouse IgG-APC for 1hr at 4˚C, labelled with $F(ab')_2$-anti-human IgM-RPE and analyzed by flow cytometry.

2.18. Determination of expression of FcμR on lymphocytes

Lymphocyte subsets expressing FcμR were determined in PBMCs by flow cytometry (see Chapter 6). The expression of hFcμR on cells was determined using an anti-FAIM3 (hFcμR) mAb (1μg; Abnova) and secondary anti-mouse IgG-APC Ab for

labelling. To determine expression on B cell subsets, the following Abs were used: anti-CD19-PE CF594, anti-CD10-PE, anti-CD38-Alexa Fluor® 700, anti-CD21-Brilliant Violet™ 421, and anti-CD27-APC Cy7 (B cell panel). Expression on T cells and NK cells were determined with anti-CD3-Brilliant Violet™ 421, anti-CD4-FITC, anti-CD8-PerCp and anti-CD56-Alexa Fluor® 700 (T/NK cell panel). Cell viability was determined with LIVE/DEAD® Fixable Aqua Dead Cell staining according to the manufacturer's instructions (Life Technologies).

2.19. Cellular activation of PBMCs to determine effects on IgM internalisation

Purified PBMCs were activated in order to investigate the effect of cellular activation on IgM internalisation. Stimulants were added to PBMCs at predetermined concentrations (Table 2.1), on ice immediately before incubation at 37°C for internalisation assays.

Induction of PBMC activation was measured alongside the internalisation assay. To determine cellular proliferation, CellTrace™ Violet stained cells (2 x 10^5 cells/well) were stimulated and incubated for five days at 37˚C with 5% CO_2. Following incubation, cells were harvested, washed, and labelled with anti-CD19-Brilliant Violet™ 421 and anti-CD3-APC.

2.20. Endoglycosidase treatment of human IgM

Glycans were removed from hIgM using peptide-N-glycosidase F (PNGase F), α1-6 mannosidase, and neuraminidase according to the manufacturer's protocol (NEB). Briefly, 50μg of hIgM was incubated overnight at 37˚C with appropriate endoglycosidase and buffer solutions. Solutions of hIgM and buffer alone were used as controls (non-treated IgM). The success of endoglycosidase treatment was determined by separating 5μg of treated or untreated IgM under reducing and non-reducing conditions by SDS-PAGE, followed by Coomassie staining (section 2.4.2 and section 2.4.3, respectively).

Table 2.1 Details of various stimulants used to activate lymphocytes. The working concentrations, cellular targets, and mechanisms of action are highlighted.

Stimulant	Target	Mechanism of action	Concentration
PHA	T cells	Unknown	5µg/ml
Anti-CD3	T cells	Receptor cross-linking	1:3000 dilution
Anti-IgM	T/ B cells	Surface Ig/ receptor cross-linking	2µg/ml
Anti-IgA+IgG+IgM	T/ B cells	Surface Ig/ receptor cross-linking	2µg/ml
CpG ODN 2006	B cells	TLR 9 agonist	1µg/ml
LPS	B cells	TLR 4 agonist	10µg/ml

2.21. Glycan assays

To determine the role of glycans in mediating IgM-FcμR interactions, endoglycosidase-treated IgM was incubated with hFcμR-transfectants for 1hr on ice, then washed and labelled with $F(ab')_2$-anti-human IgM-RPE. Untreated IgM was used as a positive control for binding.

To determine if glycans are required to mediate interactions between DBLMSP proteins and IgM, his-tagged recombinant DBLMSP and DBLMSP2 and Cd4-d3+4 proteins were immobilised onto 96-well Maxisorb microplates (Nunc) in triplicate. Following blocking, plates were incubated with varying concentrations of endoglycosidase treated- and non-treated hIgM for 3hr. Plates were washed, and binding was detected with anti-human IgM-AP.

The ability of PNGase-cleaved hIgM and IVIG to bind DC-SIGN was assessed by ELISA. For this, recombinant DC-SIGN was coated to microtitre wells (Nunc). The wells were washed and blocked with TSM (20mM Tris-HCl, 150mM NaCl, 2mM $CaCl_2$, 2mM $MgCl_2$, 5% BSA) buffer (pH 7.4) for 2hr at RT, prior to four washes with TSM and overnight incubation at 4˚C with 10μg/ml digested (+) or undigested (-) Abs in duplicate. After overnight incubation, wells were washed and incubated with anti-human IgM-AP for 3hr, then developed as in section 2.5.1.

2.22. Flow cytometry analysis to determine FcμR-mediated internalisation of endoglycosidase-treated IgM

hFcμR-transfected cells or PBMCs were incubated with 15μg/ml endoglycosidase-treated or non-treated IgM for 1hr at 4°C prior to internalisation assays, as described in section 2.16. Cells were then washed and labelled with $F(ab')_2$-anti-human IgM-RPE, anti-CD19-FITC, anti-CD3-Brilliant Violet™ 421, anti-CD4-AF700, anti-CD8-PerCp, prior to analysis by flow cytometry.

2.23. Stimulant binding ELISA

The binding of human immunoglobulins (Ig) to various stimulants was assessed by ELISA. Goat anti-human IgM $Fc_{5\mu}$ fragment-specific and goat anti-human IgA+IgG+IgM (H+L) Abs were from Jackson ImmunoResearch Laboratories Inc. (West Grove, PA, USA). Horseradish peroxidase- and alkaline phosphatase-conjugated Abs against hIgM, hIgG, and hIgA were purchased from Sigma-Aldrich, as were IgM from human serum, lectin from *Phytolaccaamericana* (pokeweed, PWM), lectin from *Phaseolus vulgaris* (phytohaemagglutinin, PHA), and lipopolysaccharide from *Escherichia coli* (LPS). Human IgG and IgA from plasma were from Calbiochem (La Jolla, CA, USA). CpG B-DNA (ODN 2006) was from Hycult Biotech (Uden, The Netherlands).

For this, stimulants were coated in duplicate onto wells of a microtitre plate (Nunc). Plates were washed extensively and blocked. After three washes with PBST, 10μg/ml of human IgM, IgG or IgA were added to wells and incubated for 3hr at RT. Subsequent washes with PBST were used to remove unbound Igs. Binding of immunoglobulins to stimulants was detected using mouse anti-human Ig-HRP Abs specific for each Ig isotype.

2.24. Molecular dynamic simulations

Molecular dynamic simulations were performed in collaboration with the laboratory of Dr Daniel Czajkowsky at the Shanghai Jiao Tong University. The homology model of DBLMSP was generated based on the known structures of members of the DBL family [195, 196]. The working atomic model of IgM and the model of the IgM/DBL interaction have been described previously [197, 198]. The on-line server, Phyre2, was used to produce homology models of FcμR [199]. This server identified two regions of FcμR that exhibited homology with proteins with known structures, with exceptional confidence. One region is the expected transmembrane domain of FcμR [200] that exhibited homology (predicted with ~70% confidence) to the transmembrane domain of ErbB2 receptor tyrosine kinases (pdb: 2KS1)[201]. The other region, expected to be an Ig-like domain that directly contacts IgM [200, 202-204], exhibited homology (predicted with 99.6% confidence) to the extracellular domain of the IREM-1 (PDB: 2NMS)[205]. The putative dimer of the Ig-like region was generated

based on the Cα3 domains of human IgA1 (PDB:1OW0) using Deep View/ Swiss-PdbViewer)[206], although other dimeric Ig domains produce similar results. Homology models were evaluated with Ramachandran plots using VMD [207-209].

2.25. Statistical analysis

The data were analysed using the GraphPad Prism 6 statistical software. P values below 0.05 were considered to be significant, and those below 0.01 as highly significant. Data that were skewed were subject to non-parametric tests for comparisons between groups. In particular, the Mann-Whitney test was used to compare percentages of IgM on cell surfaces during internalisation assays, and Dunn's multiple comparison tests were used to investigate statistical significance in the binding of DBLMSP and/or DBLMSP2 to endoglycosidase-treated and non-treated IgM. Multiple t-tests were used for the comparison of binding or percentage positive cells in normally distributed data

Chapter 3: Characterizing the binding of human IgM to receptors

3.1. Literature review

3.1.1. IgM

The varied roles of IgM are still being discovered after a century of investigation. The characteristics and functions of IgM are well established and have been extensively reviewed [155, 156, 210]. As selective IgM deficiencies are rare in humans, studies utilizing knock-out mice, which lack secretory IgM ($sIgM^{-/-}$) have highlighted the importance of IgM in immunity [211, 212]. These mice are more susceptible to viral [213], parasitic [214, 215], fungal [216, 217] and bacterial [218, 219] infections, exhibited impaired germinal centre (GC) formation and reduced responses to T cell dependent antigens [212, 220]. Other well-documented effector functions of IgM include:

- Agglutination of pathogens and pathogenic-products [181]
- Activation of the classical and lectin complement pathways [135, 165]
- Regulating the development and survival of B cells in naïve mice [221, 222]
- Clearance of apoptotic cells and apoptotic microparticles released from dying cells [223-226]
- Maintaining immune homeostasis and reinforcing immune tolerance [227-229]
- Regulating autoimmunity and atherosclerosis [159, 161, 162, 230]

The profound effect of IgM on both protective immunity and immune homeostasis is attributed to interactions of its Fc region with effector molecules such as complement and Fc receptors (FcRs). FcRs mediate a plethora of biological functions including phagocytosis of Ab-opsonised pathogens, induction of cellular cytotoxicity, regulation of hypersensitive responses, and B cell activation [160, 231, 232]. The elusive receptor for the Fc portion of IgM (FcμR) was recently identified by screening for immunoglobulin (Ig) domain sequences with homology to the other known IgM receptors, including the Fcα/μR and polymeric Ig receptor (pIgR) [137, 175].

3.1.2. FcμR

FcμR is a 60kDa type-I integral membrane protein containing a single V-set Ig-like domain [137, 175]. It is encoded by a single copy gene (*FCMR*) located on the same region of chromosome 1 (1q32.3) as Fcα/μR and pIgR [175]. Mouse FcμR shares 36% and 43% amino acid sequence homology with Fcα/μR and pIgR respectively, and there is 57.7% homology between human and mouse FcμR [175]. FcμR cDNA is predicted to encode a 390 amino acid (aa) protein, with signal peptide (17aa), extracellular region (236aa), transmembrane region (19aa), and a cytoplasmic tail (118aa) (Figure 3.1) [137]. The extracellular region has no identifiable domain characteristic except for a single V-set Ig-like domain, which shares sequence homology with pIgR and Fcα/μR within its N-terminal region. Pentameric IgM binds to FcμR via its Fc portion ($Fc_5\mu$), which occurs at a high affinity (10.8 ± 9.2nM) when assuming a 1:1 stoichiometry [137]. Due to this high affinity, it is predicted that FcμR is occupied by IgM *in vivo* [137]. Neuraminidase treatment of hFcμR-transfected cells slightly enhanced IgM binding, suggesting the involvement of sialic acid in the interaction [137].

FcμR differs from the other IgM receptors as it binds soluble IgM, but not IgA or IgG [175]. Kubagawa et al. hypothesised that this was owing to a shorter complementarity determining region 1 (CDR1) loop, predicted to contact the Ig ligands, for FcμR compared to Fcα/μR or pIgR, which contained non-charged residues (Met, Leu, or Thr) at the corresponding IgA docking site in pIgR (position Arg31) [137]. The cytoplasmic tail of FcμR is relatively long and contains nine conserved serine residues, which are potential sites for protein kinase C (PKC) phosphorylation or casein kinase 2 phosphorylation, and three conserved tyrosine residues which do not match signalling motifs such as immunoreceptor tyrosine-based inhibitor motif (ITIM), immunoreceptor tyrosine-based activation motif (ITAM), or switch motifs [137]. Phosphorylation of these residues occurred within three minutes of receptor cross-linking by IgM molecules, whereby phosphorylation of the serine residues was more prominent after 30 min whereas tyrosine phosphorylation had subsided by that time [137]. Murakami et al. identified the DDYINV motif at the end of the FcμR cytoplasmic tail as a potential signalling motif, as fits the criteria for the hemi-ITAM (hemITAM) and Ig-tail tyrosine (ITT) signalling motifs [140].

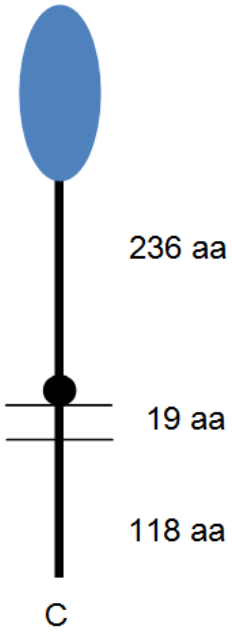

Figure 3.1 Predicted protein structure of human FcμR. Human FcμR cDNA encodes a type 1 transmembrane protein with a peptide core of ~41kDa. Numbers indicate amino acid residues of the signal peptide in the extracellular (236aa), transmembrane (19aa), and cytoplasmic (118aa) domains. The N-terminal portion of the extracellular region contains a single V-set Ig-like domain (blue oval), and the remaining region has no known domain structure adapted from [137].

Receptor ligation with mouse IgM resulted in phosphorylation (PLCγ2 and ERK) of FcμR in the natural killer (NK) cell line YTS and human NK cells [140]. Maximal stimulation of ERK was observed 30 min following ligation of FcμR with murine IgM [140], similar to that observed for serine phosphorylation in FcμR-transfected cells [137]. Together this data supports the role of FcμR in the propagation of signalling pathways, although the downstream effects of FcμR-mediated signalling are currently being resolved.

FcμR contains no N-linked glycosylation motifs, but is heavily O-glycosylated [137, 175, 183]. Three sites of extensive O-glycosylation were identified on the 60kDa form of FcμR, and mutations in these sites were found to disrupt trafficking of FcμR to the cell surface [183]. In addition to its cell surface localisation, a substantial quantity of FcμR was found to reside intracellularly, where it co-localised extensively with the trans-Golgi network (TGN) and less so with early or late endosomes [183]. It is unknown whether this localisation serves as an intracellular storage site capable of rapidly releasing FcμR under certain conditions [183]. However, FcμR is not trans-located to TGN following its internalisation in FcμR-transfected HeLa cells [183].

Unique to other FcRs, the expression of FcμR is restricted to adaptive immune cells [137]. *FCMR* mRNA is strongly expressed in the spleen, thymus, and peripheral blood leukocytes in humans, and in the spleen, thymus, bone marrow and lymph node of mice [175]. In mice, FcμR is expressed on the surfaces of B cells, but not T cells, dendritic cells (DCs) or macrophages [175]. In humans, the receptor is expressed on the surface of B cells, $CD4^+$ and $CD8^+$ T cells, and at low densities on $CD56^+/CD3^-$ NK cells. Kubagawa et al. reported no detectable FcμR expression on the surface of erythrocytes, platelets, $CD14^+$ monocytes, or $CD13^+$ granulocytes [137]. Intriguingly, FcμR is the only FcR constitutively expressed on T cells, and there is no clear demarcation between T cells positive and negative for FcμR [137]. In addition to CD22, FcμR is the only IgM-binding ligand identified to date that is expressed on the surface of B cells [137, 233].

There has been controversy over the expression of FcμR on innate immune cells. Kubagawa et al. reported no detectable surface levels FcμR on innate cells, even following overnight culture in IgM-free media to induce FcμR expression [137]. However, Lang et al. disputed this by claiming that FcμR (Toso) was expressed on

innate cells such as monocytes and granulocytes in mice [180]. They proposed that Toso maintains activation thresholds for reactive oxygen species (ROS) production in granulocytes, regulates cytokine production, and mediates phagocytosis [180]. In response to these findings, Honjo et al. further analysed the expression of FcμR on innate immune cells and found no surface expression of FcμR on granulocytes or macrophages from the bone marrow or spleen of wild-type mice [179]. Neither could they find any detectable expression of FcμR by myeloid cells at both protein and RNA levels using reverse transcription (RT)-PCR. They concluded that the expression of FcμR on myeloid cells as reported by Lang et al. could be an artefact due to non-specific reactivity of murine mAbs specific for FcμR due to a lack of FcγR blocking [179].

Despite the recent characterisation of a *bona fide* Fc receptor for IgM, the mechanism by which IgM binds to human FcμR (hFcμR) is yet to be determined. In order to understand why *P. falciparum* binds non-immune IgM, it is essential to know how IgM binds to its receptors. In this chapter, the binding of IgM to hFcμR is investigated through the identification of the domain(s) of IgM which mediate binding, and by determining features of IgM which govern the interaction. Furthermore, the structural aspects of IgM binding to hFcμR are evaluated using molecular dynamic simulations.

3.2. Objectives

Characterise the binding of human IgM to hFcμR through structural and biochemical analysis. The specific objectives were:

I. To determine the mechanisms by which human IgM bind hFcμR
II. To generate a structural model of human hFcμR
III. To identify novel ligand(s) for human IgM

3.3. Results

3.3.1. Human FcμR is a receptor for IgM

Although FcμR has been characterised as a *bona fide* Fc receptor for IgM [137, 140], it is unknown whether IgM-immune complexes (ICs) can bind to the receptor. Here, we confirm human IgM (hIgM) and heat-aggregated IgM bind to BW5147 cells transfected with hFcμR (kindly provided by Professor Kubagawa). The ability of human IgM (hIgM) to bind to green fluorescent protein (GFP)-positive hFcμR-transfected cell lines [137] was analysed by flow cytometry. For this, GFP^+ live cells were gated (Figure 3.2) and IgM binding was determined by staining cells with $F(ab')_2$-anti-human IgM-RPE. Initially, hIgM was titrated to determine the optimal concentration to be used for subsequent binding assays (Figure 3.3A), which was determined to be 15μg/ml.

To study the interaction of immune complexes with hFcμR, IgM-ICs were formed by heat-aggregation, as previously described [194]. Size exclusion chromatography verified IgM-IC formation, which contained oligmers of higher molecular mass relative to hIgM alone (shown as a pink trace) (Figure 3.4). The predicted molecular mass of IgM is 900kDa: the major peak for heat-aggregated hIgM (shown as a blue trace) lies within the void volume of the column used, while uncomplexed hIgM appears at ~900kDa. Although hIgM did not complex completely, heat-aggregation was found to successfully complex ~50% of hIgM molecules.

The binding of heat-aggregated hIgM (15μg/ml) to hFcμR-transfected cell lines was assessed by flow cytometry. As shown in Figure 3.3B, IgM-ICs bind hFcμR, which appeared to bind significantly better than the same concentration of uncomplexed IgM (Figure 3.3A). The observed increase in RPE fluorescence could be explained by the enhanced ability of IgM-ICs to bind to hFcμR-transfected cells, via cross-linking of cell surface receptors, or it may be that IgM-ICs bound to a single FcμR would provide more targets for the detecting Ab. Regardless the data confirms the ability of IgM-ICs to engage hFcμR.

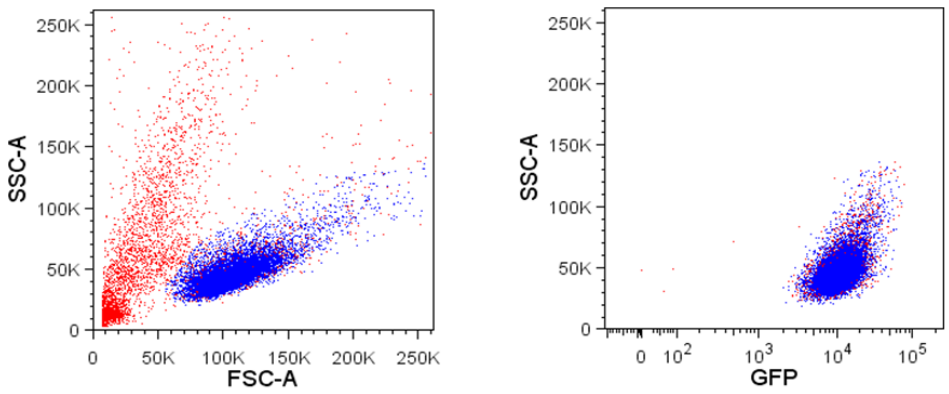

Figure 3.2 Gating strategy for GFP$^+$ human FcμR-transfected BW5147 cell lines. Live cells were identified on side scatter (SSC) and forward scatter (FSC) plot (left panel; shown by blue dots). Within the live cell gate, hFcμR-transfected cells were identified based on the expression of green fluorescent protein (GFP) (right panel; shown by blue dots). Data are representative of more than 10 repeat experiments.

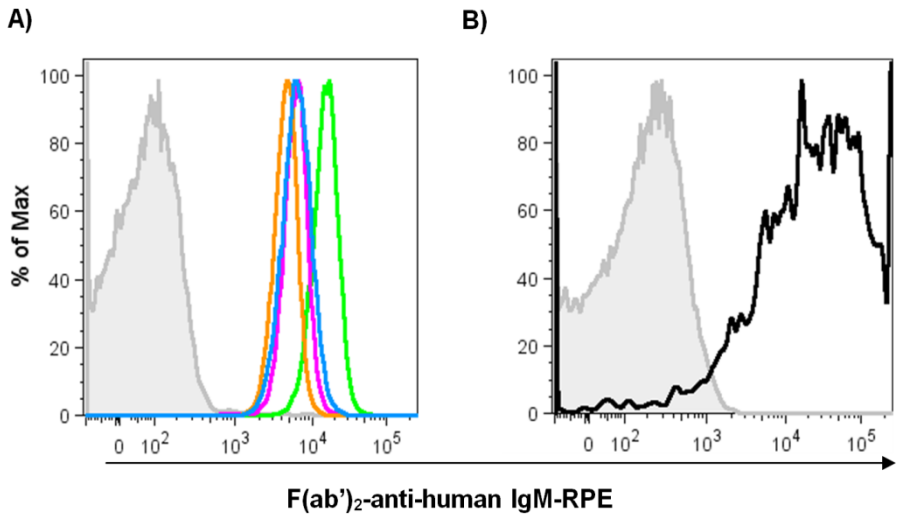

Figure 3.3 Human FcμR is a receptor for IgM. (A) Human IgM binds to hFcμR-transfected cells in a concentration dependent manner. hFcμR-transfected cells were incubated with media alone (grey trace), or media supplemented with 150μg/ml (green trace), 75μg/ml (orange trace), 37.5μg/ml (pink trace) or 15μg/ml (blue trace) hIgM for 1hr at 4˚C. Cells were washed extensively and labelled with F(ab')$_2$-anti-human IgM-RPE to detect IgM binding to hFcμR by flow cytometry. (**B)** IgM-immune complexes (ICs) bind hFcμR. IgM-ICs were formed by heat-aggregation by incubating hIgM at 63˚C for 20 min. Complex formation was then confirmed by size exclusion chromatography (Figure 3.4). hFcμR-transfected cells were then incubated with 15μg/ml heat-aggregated hIgM for 1hr at 4˚C, washed and labelled with F(ab')$_2$-anti-human IgM-RPE prior to flow cytometric analysis (n=3).

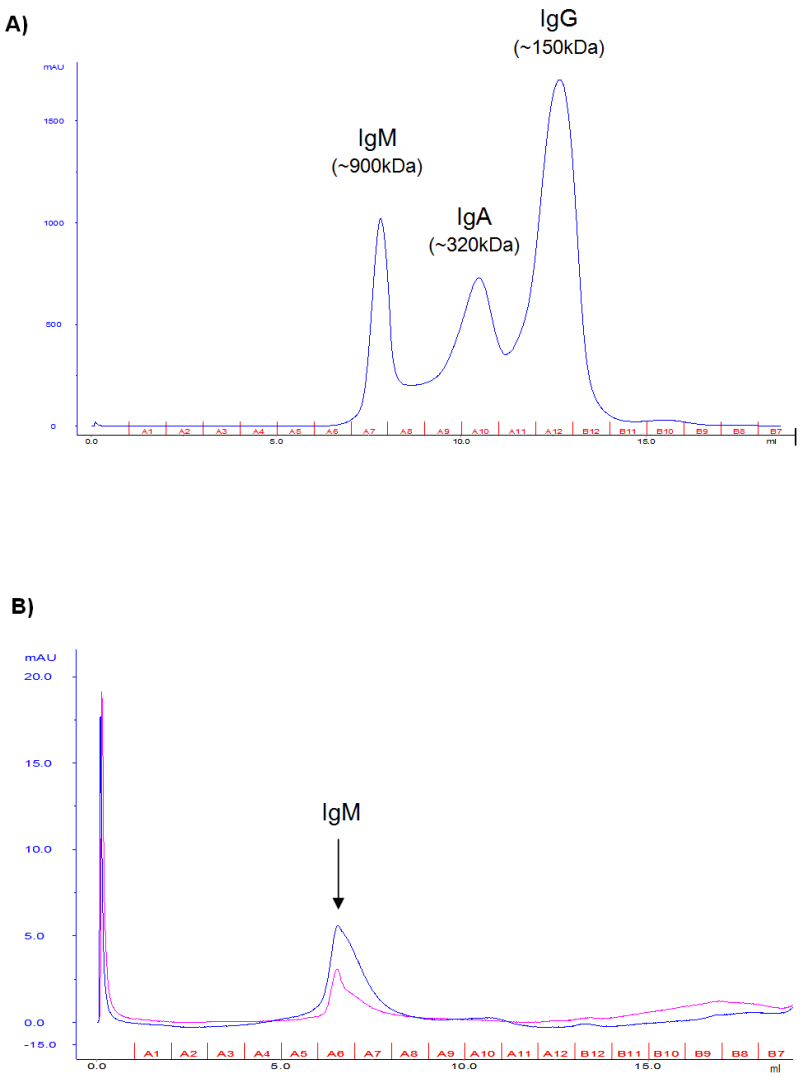

Figure 3.4 Size exclusion of IgM-immune complexes. (A) Pentaglobin™ (12% IgM, 12% IgA and 76% IgG by weight) was separated by size exclusion chromatography on a Superdex® 200 column, and used as a marker to predict the fraction at which hIgM was eluted. **(B)** Overlay of the hIgM (Sigma-Aldrich; shown as blue trace) and heat-aggregated IgM (shown as pink trace) size exclusion chromatogram profiles. Untreated hIgM appears to be aggregated compared to the IgM of Pentaglobin™ (as shown in A). Heat-aggregation of hIgM resulted in the formation of oligomers of high molecular mass, as depicted by a ~50% reduction in the peak corresponding to ~900kDa (fraction A6) when compared to hIgM (blue trace). The major peak for heat-aggregated hIgM lies within the void volume for the column used. Data are representative of two repeat runs.

3.3.2. The Cμ4 domain of IgM forms the binding site for human FcμR

Previous studies showed the Fc region of pentameric IgM ($Fc_5\mu$) bound hFcμR [137]. To determine the domain of the IgM-Fc molecule critical for interaction with hFcμR, a panel of domain-swapped Abs described in a previous study [120] were used, in which homologous domains are exchanged between human IgA and IgM (Figure 3.5). The ability of gated hFcμR-transfected cells to bind domain-swapped Abs was analyzed by flow cytometry (Figure 3.5). Abs that contained only the Cμ4 domain were able to interact with hFcμR, whereas no binding was observed with human IgA and only weak binding was seen with the α1μ2μ3α3 domain-swap Abs lacking the Cμ4 domain. This shows that the Cμ2 and/or Cμ3 domains are involved in binding hFcμR, although the contribution of either of these domains is less important than the Cμ4 domain. The slight reduction in binding of α1α2μ4 compared to hIgM or α1μ2μ3μ4 suggests that the Cμ2 and/or Cμ3 domain, in conjunction with the Cμ4 domain, enhance binding of hIgM to hFcμR.

3.3.3. IgM glycosylation is not involved in FcμR binding

Since glycosylation of the Fc region of immunoglobulins can modulate Fc receptor binding [169], we sought to determine whether glycosylation of IgM-Fc is crucial for permitting interactions with hFcμR. IgM molecules are heavily glycosylated [168]. The Cμ4 domain of IgM containing a single N-linked glycan attachment site at Asn563 that is occupied with $GlcNAc_2Man_{5\text{-}9}$ oligosaccharide types, whereas the Cμ3 domain contains N-linked glycan sites at Asn395 and Asn402 which are occupied with sialic acid- or galactose-terminating complex glycans and $GlcNAc_2Man_{5\text{-}9}$-containing oligomannose glycans, respectively [168].

To investigate if glycans contribute to the binding of hIgM to hFcμR, these carbohydrates were removed from hIgM with a range of endoglycosidases including peptide N-glycosidase (PNGase) F, α1-6 mannosidase, and neuraminidase (Figure 3.6), and their ability to bind hFcμR investigated by flow cytometry (Figure 3.7). De-glycosylated hIgM was still able to bind hFcμR demonstrating that PNGase F, α1-6 mannosidase or neuraminidase susceptible glycan(s), such as the aforementioned high mannose or sialic acid residues, do not contribute to hIgM binding of hFcμR.

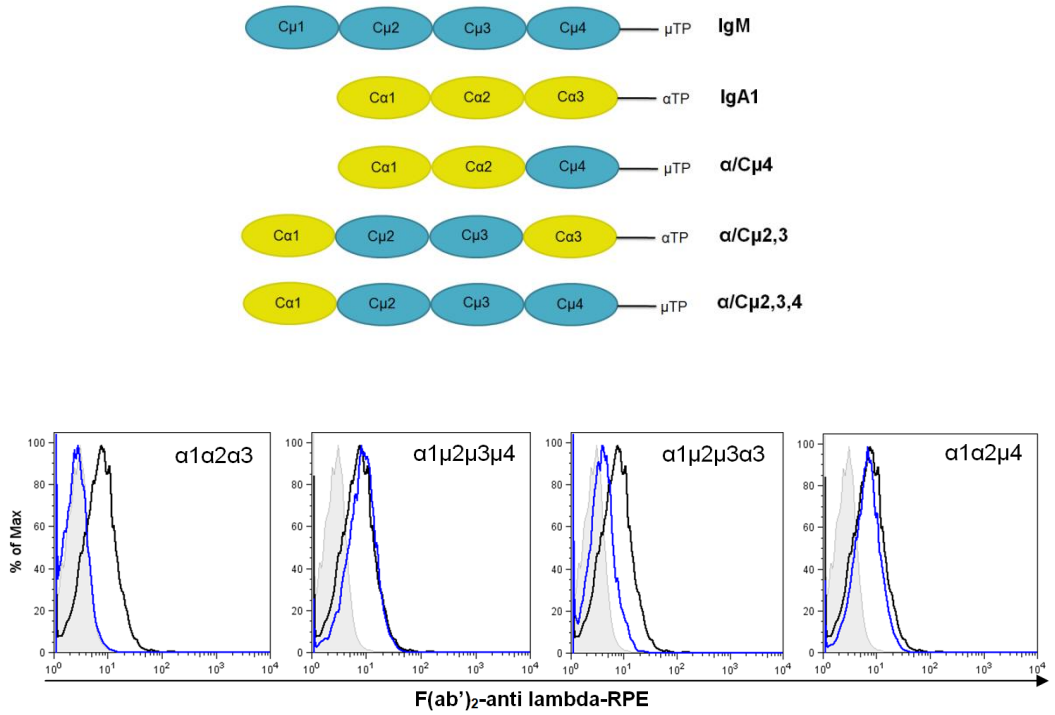

Figure 3.5 The Cμ4 domain of IgM binds to human FcμR. hFcμR-transfected cells were incubated with media supplemented with domain-swap Abs (blue trace), hIgM (black trace), or media alone (grey trace) for 1hr at 4°C, then washed extensively. Binding of Abs was determined by staining with $F(ab')_2$-anti lambda-RPE and subsequent flow cytometry analysis. The binding of domain swap Abs containing the Cμ4 domain of IgM (α1μ2μ3μ4 and α1α2μ4) to hFcμR was comparable to hIgM, and partial binding was observed with domain-swap Abs containing the Cμ2 and Cμ3 domains (α1μ2μ3 α3). Data are representative of three repeat experiments (performed by Professor Pleass).

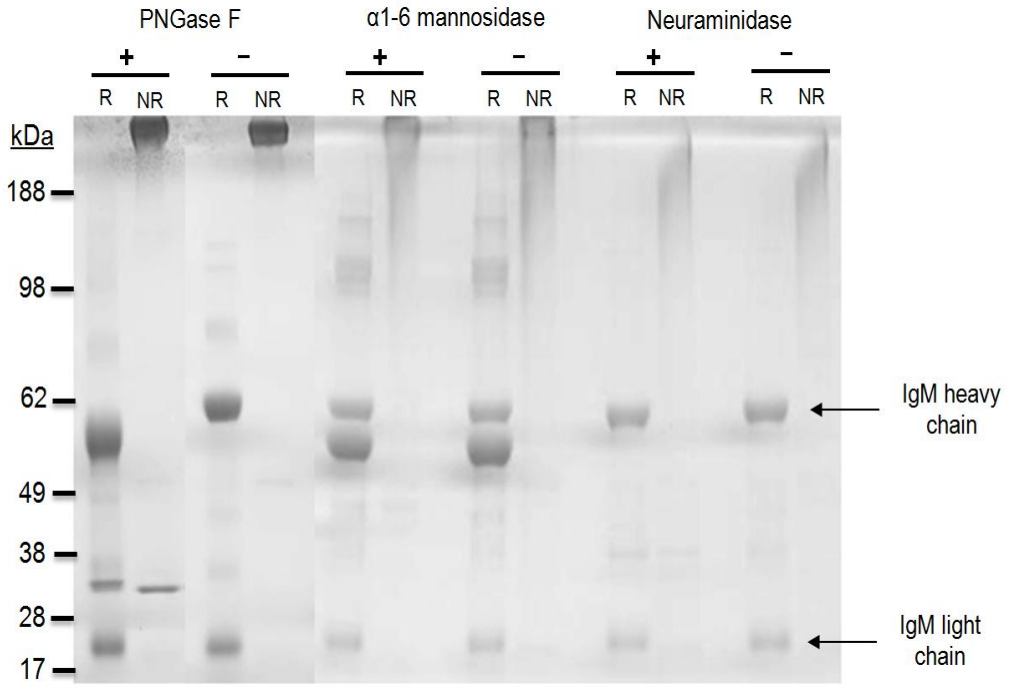

Figure 3.6 Endoglycosidase digestion of human IgM. Human IgM (50µg; Sigma-Aldrich) was digested in the presence (+) or absence (-) of 10µl (5,000 units) of PNGase F, α1-6 mannosidase, or neuraminidase according to manufacturer's instructions (New England Biolabs). After overnight incubation at 37˚C, 5µg of each Ab preparation was run under reducing (R) or non-reducing (NR) conditions into wells of a 4-12% Bis-Tris gradient gel (Novex) together with Seeblue Plus2 pre-stained protein standards (Life Technologies). De-glycosylation of hIgM by PNGase F resulted in a decrease in the molecular weight (MW) of the IgM heavy chain (from ~62kDa to ~55kDa) and light chain (~25kDa to ~23kDa), and reductions in MW for the heavy chain with neuraminidase treatment (~62kDa to ~60kDa), which signify the removal of glycans from hIgM molecules. There appears to be no obvious differences in MW between α1-6-mannosidase-treated and non-treated hIgM.

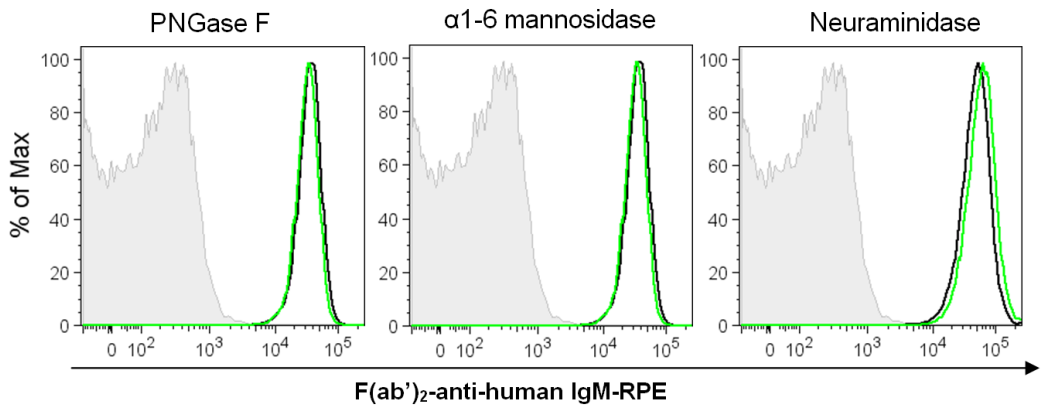

Figure 3.7 Glycans do not mediate interactions between IgM and hFcμR. hFcμR-transfected cell were incubated with media supplemented with endoglycosidase-treated (green trace) and –non-treated (black trace) hIgM, or buffer only (grey trace) for 1hr on ice. Binding of hIgM to cells was detected using $F(ab')_2$-anti-human IgM-RPE. Data shown is representative of one of three repeat experiments.

3.3.4. Human IgM binds to lymphocytes expressing FcμR

In humans, FcμR is predominantly expressed by adaptive immune cells including $CD19^+$ B cells, $CD4^+$ and $CD8^+$ T cells, and $CD56^+CD3^-$ natural killer (NK) cells [137]. Since hIgM was shown to bind to hFcμR-transfected cells, the ability of hIgM to bind lymphocyte subsets known to express FcμR was next investigated. Peripheral blood mononuclear cells (PBMCs) were isolated from healthy donors and labelled with markers to differentiate lymphocyte subsets (Figure 3.8). IgM binding to lymphocyte subsets was detected by labelling with exogenous hIgM and $F(ab')_2$-anti-human IgM-RPE, whereas the levels of IgM on lymphocyte surfaces were determined by staining with $F(ab')_2$-anti-human IgM-RPE alone (Figure 3.9). There was clear binding of exogenous IgM to $CD3^+$ T cells and $CD56^+CD3^-$ NK cells, whereas binding to $CD19^+$ B cells was moderate. Endogenous surface levels of IgM were high for $CD19^+$ B cells and $CD56^+CD3^-$ NK cells, but not $CD3^+$ T cells, indicating differential binding of IgM between subsets expressing hFcμR *in vivo*. The presence of endogenous IgM on the surfaces of isolated lymphocytes was also confirmed by immunofluorescence microscopy (Figure 3.10). Together, these results show that IgM is present on the surfaces of isolated B cells and NK cells, which support previous findings [140]. For B cells, the observed high levels of IgM on cell surfaces are contributed at least in part to cross-reactivity of the $F(ab')_2$-anti-human IgM-RPE with IgM^+ B cell receptors (BCR).

Curiously, the monocytic cell population was also found to be positive for cell surface IgM (Figure 3.11C). Circulating monocytes were shown to retain IgM on their surface following purification (Figure 3.11C, grey trace), and were able to bind exogenous IgM (Figure 3.11C, aqua trace). These data suggest that monocytes express a hitherto unidentified cell surface receptor for hIgM, or could possibly suggest that hFcμR is expressed on human monocytes, in conjunction with several reports of FcμR expression on murine monocytes [180, 234, 235].

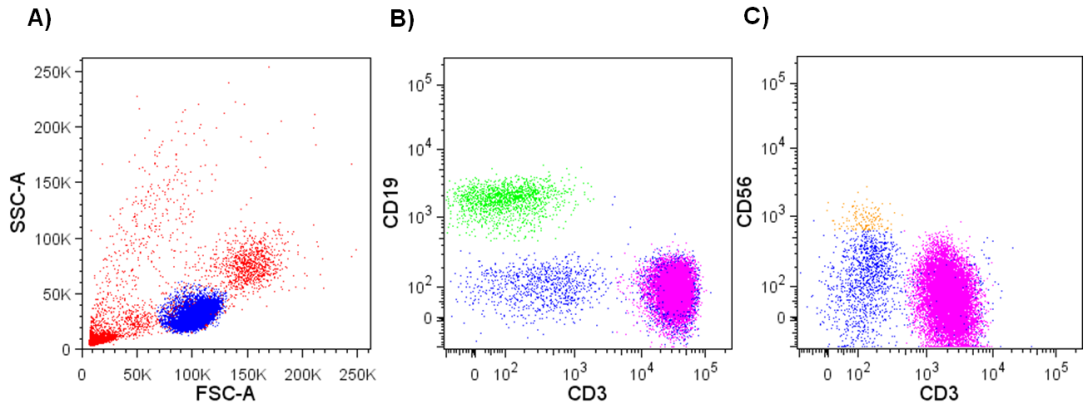

Figure 3.8 Gating strategy for lymphocyte subsets. (A) Lymphocytes (shown as blue dots) were gated from human PBMCs by side (SSC) and forward (FSC) scatter profiles. Within the lymphocytes gate, B cells ($CD19^+CD3^-$; shown as green dots), T cells ($CD3^+CD19^-$; shown as pink dots). **(B)** and natural killer cells ($CD56^+CD3^-$; shown as orange dots) **(C)** were identified based on the surface expression of CD19, CD3 and CD56.

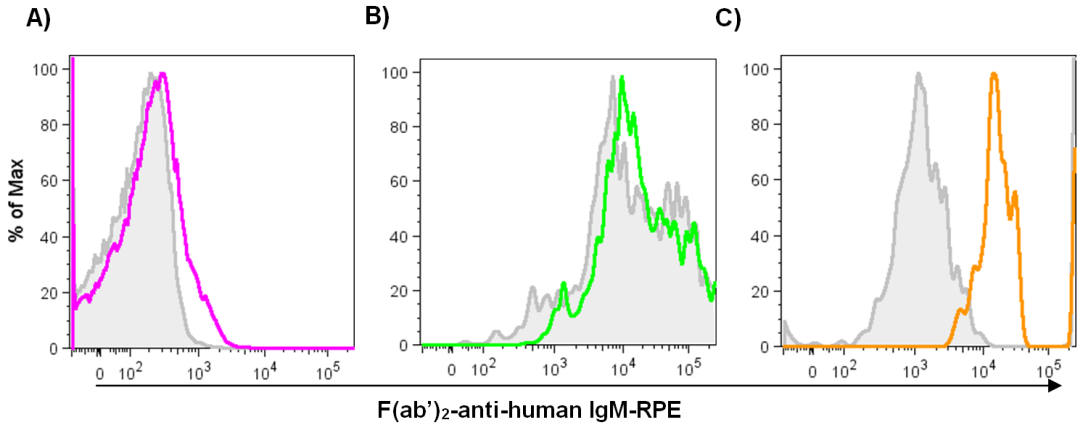

Figure 3.9 Lymphocyte subsets known to express FcμR bind exogenous hIgM. FcμR is expressed on human B cells, T cells, and natural killer (NK) cells. To determine if exogenous hIgM could bind to these cell populations, PBMCs isolated from healthy donors were incubated with 15μg/ml hIgM at 4˚C for 1hr. Cells were washed and labelled with anti-human CD3-APC, anti-human CD19-Brilliant Violet™ 421, anti-human CD56-FITC and $F(ab')_2$-anti-human IgM-RPE prior to flow cytometry. Exogenous hIgM was shown to bind to $CD3^+CD19^-$ T cells **(A)**, $CD3^-CD19^+$ B cells **(B)** and $CD3^-CD56^+$ NK cells **(C)**, respectively shown as pink, green, and orange traces. In addition, endogenous IgM levels on cell surfaces were high for B cells and NK cells but not T cells (shown as grey traces). Data are representative of three repeats.

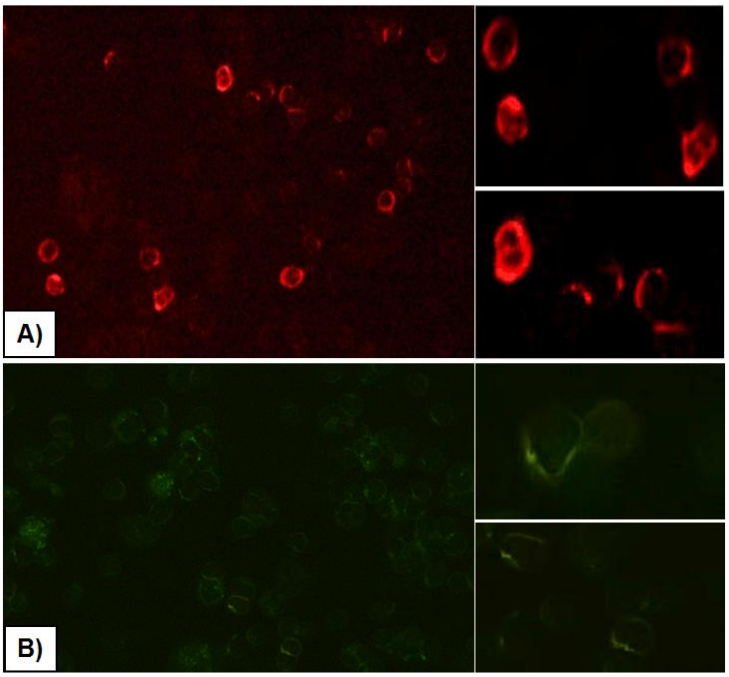

Figure 3.10 Human IgM is present on lymphocyte surfaces. PBMCs were cytospun onto slides and labelled with **(A)** F(ab')$_2$-anti-human IgM-RPE (shown as red) or with **(B)** anti-CD4/CD8/CD19/CD56-FITC (shown as green) for 1hr at 4˚C and washed before cell surface levels of hIgM were visualised by immunofluorescence microscopy (20x and 40x magnification for left and right panels, respectively). Images were taken from the same field of view. Images quality was improved by adjusting the contrast and brightness of the images.

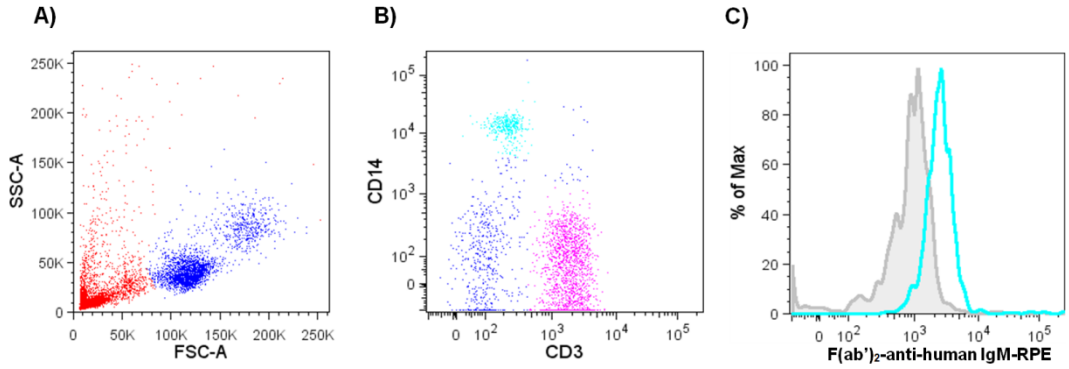

Figure 3.11 Exogenous human IgM binds to monocytes. (A) PBMC population was gated based on forward (FSC) and side scatter (SSC) profiles (shown as blue dots). **(B)** Gating strategy for monocytes. PBMCs were labelled with anti-human CD14-APC Cy7 and anti-human CD3-Brilliant Violet™ 421 to differentiate monocytic cell populations ($CD3^{-}CD14^{+}$; shown as aqua dots). **(C)** Exogenous hIgM binding to monocytes. PBMCs were incubated with media alone (grey trace) or media supplemented with 15µg/ml hIgM (aqua trace) at 4˚C for 1hr, prior to washing and labelling with $F(ab')_2$-anti-human IgM-RPE to detect IgM binding to gated monocytes by flow cytometry. Data are representative of three repeats.

3.3.5. DC-SIGN is a novel receptor for IgM-Fc

As hIgM bound to monocytes, we hypothesised that monocytes expressed a cell surface receptor specific for hIgM. Although there has been controversy over the expression of FcμR on innate cells in mice [179-181], there is strong evidence to suggest that hFcμR is not expressed on innate cells [137]. Furthermore, hFcα/μR expression is restricted to human mesangial cells [236], follicular dendritic cells in germinal centres and pre-germinal B cells (IgD^+CD38^+) [144]. Therefore, the identity of the hIgM-binding receptor on monocyte surfaces was investigated.

Dendritic cell-specific ICAM-3grabbing nonintegrin (DC-SIGN) is a C-type lectin membrane protein which is expressed by a subset of $CD14^+$ cells in the periphery [167, 237]. As multimeric IgM is known to form highly valent interactions, it was hypothesised that the expression of DC-SIGN on $CD14^+$ monocytes may account for the observed binding of hIgM. To test this hypothesis, the ability of human DC-SIGN to bind CHO cell-derived hexameric IgM-Fc [238] was investigated by multichannel surface plasmon resonance (SPR). These experiments were performed in the laboratory of Dr Daniel Mitchell (University of Warwick). The binding of IgM-Fc to SIGNR1, the mouse orthologue of DC-SIGN [166], was also investigated by SPR. As shown in the sensogram in Figure 3.12, IgM-Fc bound DC-SIGN with nanomolar affinity (K_d ~0.26μM) and bound strongly to SIGNR1 (K_d ~2.2μM). Furthermore, the ability of Pentaglobin® to bind to DC-SIGN and SIGNR1 was investigated to see if this binding could be duplicated with native Abs. Pentaglobin® is a licensed IVIG preparation which is enriched for polymeric immunoglobulins (12% IgM, 12% IgA and 76% IgG by weight) [239]. Pentaglobin® bound strongly to DC-SIGN but unlike IgM-Fc, no binding was observed with SIGNR1 (Figure 3.12). A possible explanation for this is that the expression of IgM-Fc in CHO cells may alter glycan composition of IgM or result in undetermined posttranslational modifications that could affect binding [136].

The ability of hIgM to bind to native DC-SIGN was confirmed by flow cytometry experiments analysing hIgM to monocyte-derived immature dendritic cells (iDCs), which showed marginal binding of hIgM to iDCs (Figure 3.13).

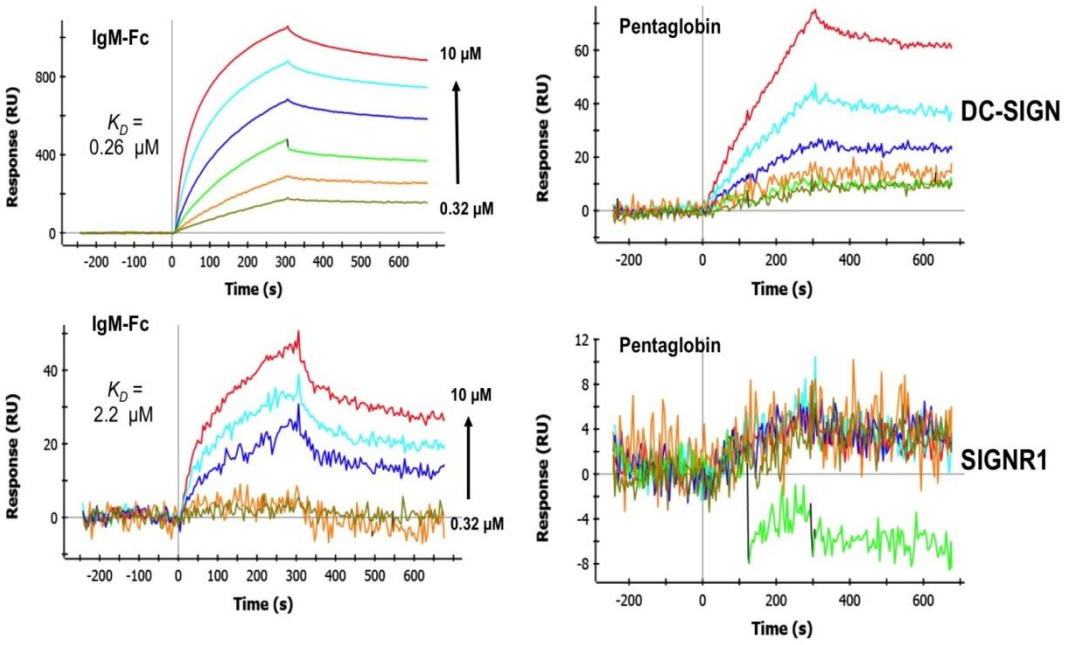

Figure 3.12 Binding of IgM to DC-SIGN by multi-channel surface plasmon resonance. To determine if DC-SIGN is a receptor for IgM-Fc, recombinant human DC-SIGN or mouse SIGNR1 were immobilised onto a sensor chip. Doubling dilutions (10µM-0.32µM) of IgM-Fc or Pentaglobin® were injected at flow time 0, and replaced with buffer at 300 sec. The sensograms depict the association and dissociation curves of IgM-Fc and Pentaglobin® binding to DC-SIGN and SIGNR1, which include dissociation constants (K_d) values for IgM-Fc binding. Data are representative of duplicate experiments (performed in the laboratory of Dr Mitchell).

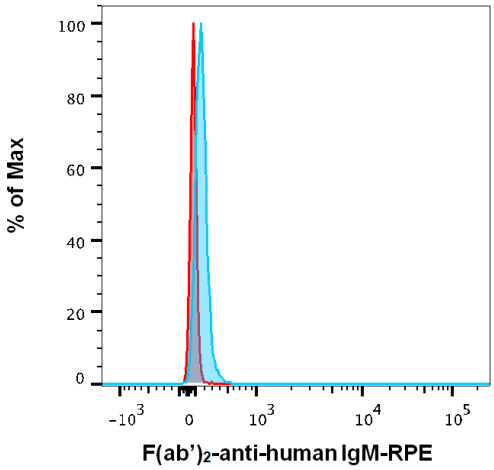

Figure 3.13 Dendritic cells bind human IgM. Immature dendritic cells (iDCs) were derived from autologous-sorted $CD14^+$ blood monocytes by culture with granulocyte-macrophage colony stimulating factor (GM-CSF), IL-4 and tumor necrosis factor (TNF)-α for six days. iDCs and hIgM were investigated in the laboratory of Dr Britta Urban. Following culture, iDCs were incubated with media only (red trace) or media supplemented with hIgM (blue trace) for 1hr on ice. The binding of hIgM to gated iDCs was assessed by staining with $F(ab')_2$-anti-human IgM-RPE and subsequent flow cytometric analysis.

DC-SIGN is C-type lectin which possesses high affinity for high mannose structures [136, 240]. As IgM is heavily mannosylated [168], it is possible that the interaction between DC-SIGN and IgM is mannose dependent. To test this theory, glycans were cleaved from human IgM and/or IVIG with PNGase F (Figure 3.14). Subsequently, the ability of de-glycosylated Abs to bind to DC-SIGN was assessed by ELISA (Figure 3.15). PNGase F treatment reduced the binding of hIgM and IVIG to DC-SIGN by ~30% and 50%, respectively (Figure 3.15). This suggests that PNGase F susceptible glycans do contribute to the binding of IgM to DC-SIGN.

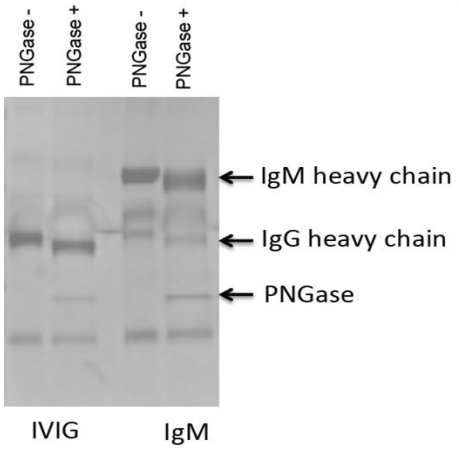

Figure 3.14 Removal of glycans from IgM by PNGase F treatment. Human IgM (50µg; Sigma-Aldrich) and IVIG (50µg; GammaGard) were incubated overnight at 37˚C in the presence (+) or absence (-) of PNGase F in accordance with the manufacturer's instructions (NEB). Following incubation, 5µg of each Ab preparation was run under reducing conditions on a 4-12% Bis-Tris gradient gel (Novex) with Seeblue Plus2 pre-stained protein standards (Life Technologies).

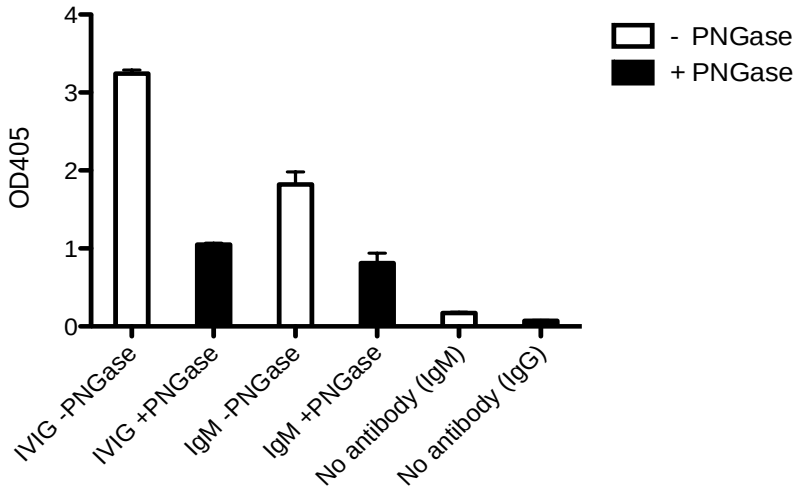

Figure 3.15 DC-SIGN binds to glycans on IgM. The ability of PNGase cleaved hIgM and IVIG to bind DC-SIGN was assessed by ELISA. For this, 10µg/ml recombinant DC-SIGN was coated to microtitre wells (Nunc) in carbonate buffer (pH9) overnight at 4˚C. The wells were then washed and blocked with TSM (20mM Tris-HCl, 150mM NaCl, 2mM $CaCl_2$, 2mM $MgCl_2$, 5% BSA) buffer (pH 7.4) for 2hr at room temperature (RT), prior to four washes with TSM and overnight incubation at 4˚C with 10µg/ml digested (+) or undigested (-) Abs in duplicate. After overnight incubation, wells were washed and incubated with anti-human IgM-alkaline-phosphatase (1:1000) for 2hr at RT, then developed with 100µl of the substrate p-nitrophenyl phosphate after further washing. Absorbance was measured at 405nm. Data are representative of the mean ±SEM of two independent repeats.

3.3.6. Modelling of IgM binding to hFcμR

Molecular dynamic simulations were used to provide structural insights into how IgM engages hFcμR, which were generated in collaboration with the laboratory of Dr Daniel Czajkowsky (Shanghai Jiao Tong University, China). For this, a recently resolved homology-based structural model of hIgM [135] was used to model the interaction between hIgM and hFcμR. As there is no known structure for hFcμR, we searched for possible structural homologs using the Phyre2 Server (http://www.sbg.bio.ic.ac.uk/phyre2/html/page.cgi?id=index), as previously described [199]. The server identified homologs for two regions of hFcμR. The first segment consists of residues Phe252 to Val272, which exhibited striking homology to the transmembrane region of the epiderminal growth factor receptor known as erbb1 [201]. Intriguingly, erbb1 is expressed on the cell surface as a dimer, mediated by its transmembrane region [201, 241], suggesting that hFcμR may also exist as a dimer. The second segment (residues Val33 to Gly105) was found to be homologous to numerous Ig-like domains (Figure 3.16), including those for the IgM receptors pIgR and Fcα/μR [137, 203, 242-245]. These receptors were shown to bind IgM via the complementarity determining region (CDR1-3) loops present in the Ig-like domain [203]. Owing to the sequence homologies between hFcμR and pIgR/ Fcα/μR, the CDR region of the Ig-like domains of hFcμR was investigated as the binding region for IgM. Further, interactions of IgM with a dimeric version of hFcμR were also evaluated (Figure 3.17), with adjacent monomers localised as in known for dimeric Ig-domain structures [206]. The finding that glycosylation was not involved in mediating interactions between hFcμR and IgM (Figure 3.7), and the likely involvement of two IgM domains (Cμ2/Cμ4 or Cμ3/Cμ4) (Figure 3.5) provide constraints on the potential binding sites of hFcμR. Moreover, as all known interactions between Abs and their receptors occur via the C-terminal end of Ig domains [244, 246], these region were chosen to generate the model. The FcμR Ig-like domain was positioned so that its CDR loops completely covered the Cμ2/Cμ4 interface, characteristic of type I engagement of Ab-receptor interactions [244].

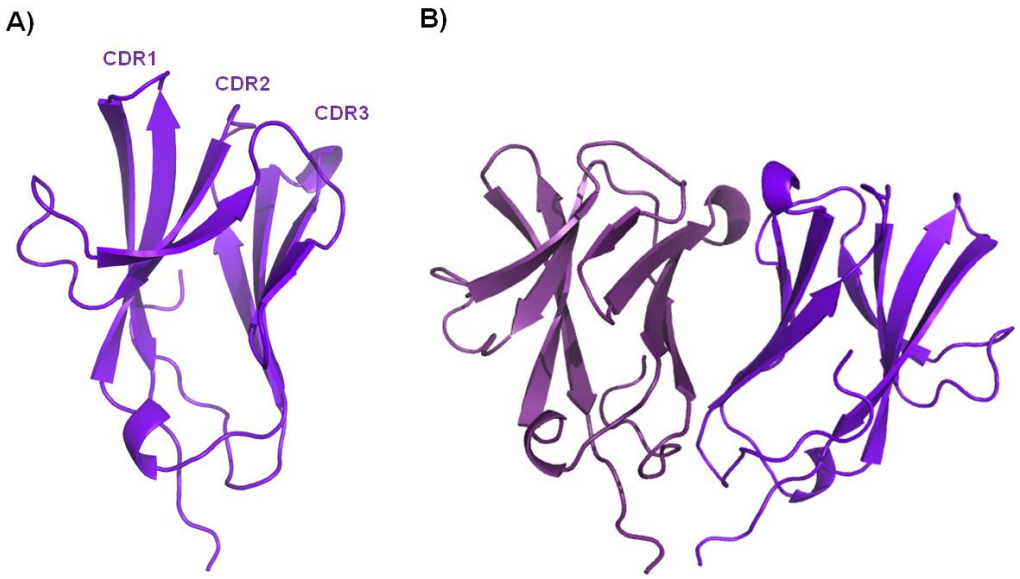

Figure 3.16 Model of hFcμR. Molecular dynamic simulation of hFcμR (performed in the laboratory of Dr. Czajkowsky), represented as a monomer **(A)** and as a dimer **(B)**, which contains a single Ig-like domain composed of three complementarity determining regions (CDR).

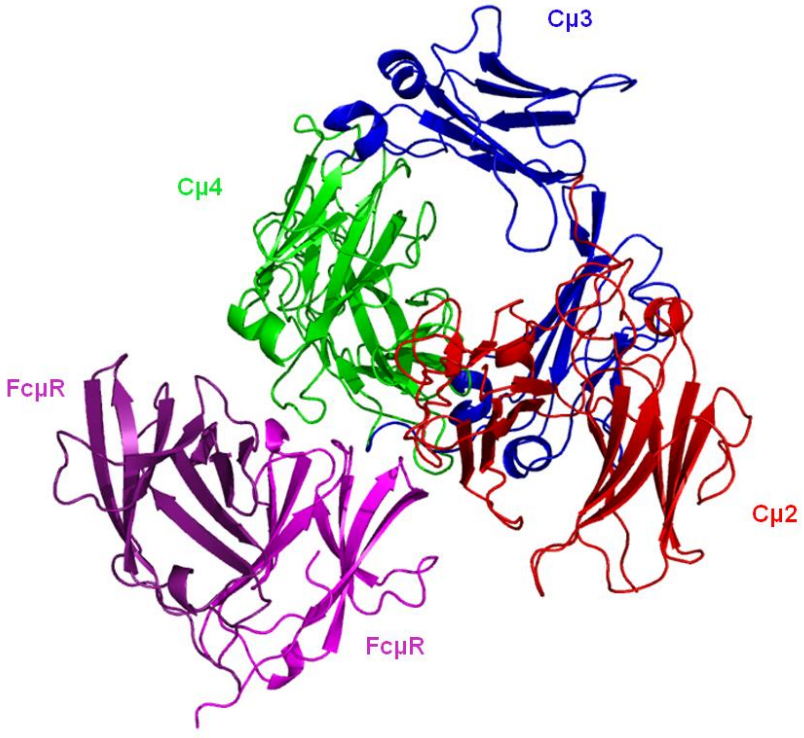

Figure 3.17 Model of hFcμR-IgM interaction. Molecular dynamic simulations depicting the interaction between dimeric hFcμR (shown in magenta) and the heavy chain of IgM. The Cμ2, Cμ3 and Cμ4 domains of IgM are shown as red, blue, and green ribbons, respectively.

Closer inspection of the interface between the monomeric hFcμR Ig-like domain and Cμ2/Cμ4 domains revealed several charged and hydrophobic residues that could play a significant role in mediating this interaction (Figure 3.18). In particular, there are two pairs of charged residues (Arg344 and His327 in IgM and Asp94 and Glu24 in hFcμR), and a pair of polar residues within hydrogen bonding distance from each other (Glu345 in IgM and Asn92 in hFcμR) that surround a hydrophobic pocket (consisting of Leu326 and Leu343 in IgM and Met91 in hFcμR) that could be important in mediating the interaction between Cμ4 and hFcμR. Additionally, the hydrophobic patch involving Val159 and Val324 in IgM and Met25 and Val27 in hFcμR, could be important for the simultaneous interaction between Cμ2 and hFcμR.

Overall, consideration of the available structural information of these proteins indeed provides a physical means to explain the experimental results generated in this Chapter. Additional experimental data featured in Chapter 4 provides further insight into how IgM docks onto hFcμR.

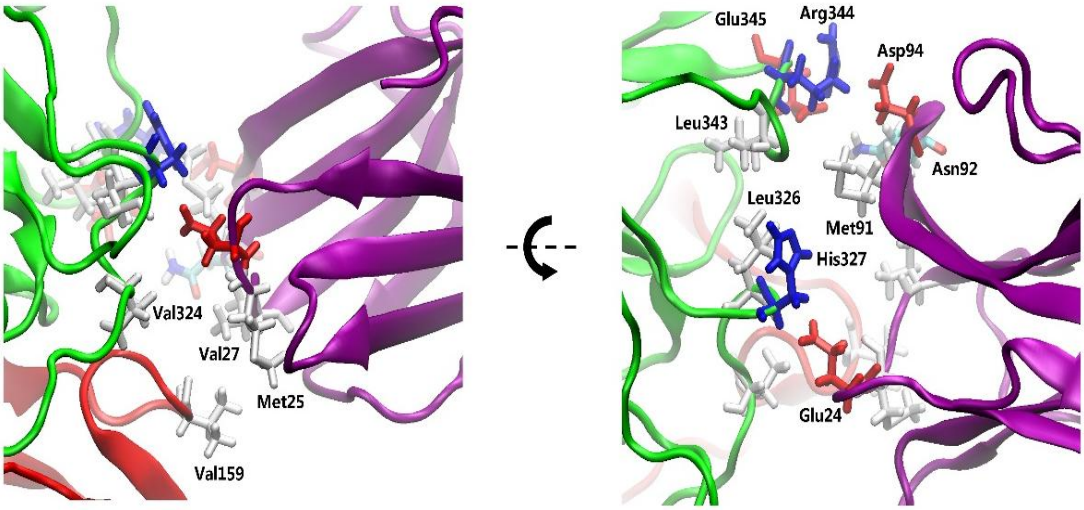

Figure 3.18 Closer inspection of hFcμR-IgM interaction. The binding sites and key residues of two proteins are shown in stick representation. The colouring of hFcμR and the domains of IgM are as in Figure 3.17, and the hydrophobic, positively charged, and negatively charged residues are depicted as white, blue, and red sticks, respectively.

3.4. Discussion

In this chapter, the biochemical nature of IgM binding to hFcμR was investigated. Several intriguing features were identified: (1) The Cμ4 domain of IgM mediates binding to FcμR, which does not involve glycans. (2) Heat-aggregated IgM ICs are able to bind FcμR. (3) FcμR is proposed from modelling with homologous proteins to form a dimer on cell surfaces.

A panel of domain-swap IgM and IgA Abs [120] was used to determine regions vital for hFcμR binding. The Cμ4 domain of hIgM was identified as the domain which bound cell-surface hFcμR expressed on transfected cell lines, with a partial contribution made by the Cμ2 and/or Cμ3 domain. Although the Cμ2 and/or Cμ3 domain alone exhibited weak binding to hFcμR, the absence of these domains in domain-swap Abs containing the Cμ4 domain resulted in a reduction in binding when compared to pentameric IgM. One interpretation is that the Cμ2, Cμ3 and Cμ4 domains form a binding interface for hFcμR. Alternatively, the Cμ2 and Cμ3 domain may enable stabilisation of the Fc region. The Cμ3 and Cμ4 domains feature as ligands for other IgM receptors. For example, the binding of IgM to hFcα/μR was also shown to require contributions from both the Cμ3 and Cμ4 domains [247]. Furthermore, the observation that the extracellular portion of pIgR (known as secretory component) blocked IgM binding to hFcα/μR also implicated these domains in governing IgM-pIgR interactions [247, 248]. Together, the findings reported here support and extend the previous discovery that the $Fc_5\mu$ fragment of IgM governs interactions with hFcμR [137].

The discovery of the Cμ4 domain of pentameric IgM as the ligand for hFcμR is particularly intriguing given that this domain is also the target of *P. falciparum*-derived IgM-binding molecules PfEMP1, DBLMSP and DBLMSP2 [120, 146]. Whether non-specific binding of IgM by these molecules prohibits interactions between IgM and hFcμR remains to be determined (see Chapter 4). As FcμR has been implicated in modulating immune responses [138], preventing the binding of hIgM to this receptor could be crucial for the survival of the parasite in the host. This interesting question will be explored further in Chapter 4.

The Cμ3 and Cμ4 domains of IgM contain N-linked glycosylation sites at Asn-395, Asn-402, and Asn-563 which are predominantly occupied with complex glycans or oligomannose-type glycans [168]. The removal of these glycans did not perturb hIgM binding to hFcμR, which differs from other FcRs which require Ig glycosylation for optimal binding [169]. The fact that the single N-linked site in the Cμ4 domain is only ~17% occupied could offer one explanation as to why endoglycosidase treatment of IgM did not impact on binding to hFcμR (Arnold 2005). As the glycosylation of IgM molecules is critical for permitting interactions with mannose-binding lectin (MBL), it is tempting to speculate that the IgM-hFcμR interaction evolved in a glycan-independent manner to allow IgM-MBL-Ag immune complexes to bind hFcμR.

An intriguing finding was that IgM-ICs are able to bind hFcμR expressed on transfected cells, as this could suggest that the receptor plays a role in priming immune responses. The formation of ICs through agglutination of pathogens by IgM is pivotal for immune responses against infection. Further, internalisation of ICs results in the removal of pathogens and antigen presentation to the adaptive immune system via MHC class I molecules. For example, murine B cells were shown to internalise *Staphylococcus aureus*-IgM-ICs in a Fcα/μR-dependent manner [143], and FcγRIIA and FcRn have been implicated on the internalisation and cross-presentation of antigens on dendritic cells (DCs) [249, 250]. The data reported here, in support of previous data which showed the role of FcμR in IgM internalisation [183], highlights the potential of the receptor to initiate cross-presentation of IgM-ICs on antigen presenting cells such as B cells. However, whether Ag-specific IgM-ICs can bind to and be internalised by hFcμR remains to be determined, especially as IgM is predicted to adopt a different confirmation upon antigen binding [135]. Alternatively, hFcμR may function to bind and internalise non-specific IgM-ICs to promote their removal. In support of this hypothesis, experiments using knock-out mice ($Fc\mu R^{-/-}$) suggested that FcμR regulates IgM levels in the periphery [182] and IgM internalised via FcμR is shuttled to endosomes for degradation [183]. Finally, the binding of IgM-ICs by FcμR may function to initiate cross-linking of receptors, similar to that observed for CD22 and the BCR on murine B cells [233]. This cross-linking was shown to trigger a negative feedback mechanism for B cell activation through CD22-mediated BCR-signalling suppression. Curiously, FcμR was implicated in lowering the threshold of BCR signalling as B cell proliferation in response to anti-IgM

stimulation was reduced in FcμR$^{-/-}$ mice [138]. Furthermore, cross-linking of FcμR enhanced survival of B cells in response to BCR cross-linking [138]. It will therefore be of interest to further investigate significance of IgM-IC binding to hFcμR, especially in relation to how Ag-specific IgM-ICs may modulate B cell responses via FcμR and BCR cross-linking.

Studies using knockout mice (FcμR$^{-/-}$) have generated the majority of insight into the biological function of FcμR [138, 180, 182], or from studies which use mouse IgM to investigate the role of FcμR in humans [140]. As a result of this, little is known about the interaction of hIgM to hFcμR. Moreover, there has been controversy on whether FcμR functions to inhibit apoptosis [178, 210] or to act as an IgM receptor [137]. Here, we confirm that hFcμR is a receptor for hIgM and show that exogenous hIgM can bind to lymphocytes known to express FcμR. Moreover, isolated B cells and NK cells were found to have high levels of cell-surface IgM, which were not so pronounced for T cells. This data supports a recent study which reported IgM on the surface of circulating NK cells [140]. The high affinity of the IgM-FcμR interaction (K_d ~10.8nM) may offer one explanation for this observed effect, as hFcμR may be opsonised with IgM on circulating B cells and NK cells. Under this assumption, hFcμR expressed on T cells would not be occupied with IgM. The high surface levels of IgM and marginal binding of exogenous IgM to B cells suggests that FcμR is fully occupied on these cells. However, the expression of IgM$^+$ BCR may account for the observed high levels of IgM on B cell surfaces. Further work is required to clarify the persistence of IgM bound to FcμR on lymphocyte surfaces. Although B cells, T cells and NK cells bound exogenous hIgM, there was differential binding between the lymphocyte subsets. The reasons for this are still unclear, however the high surface levels of IgM on purified B cells and low surface levels on T cells, coupled with the ability of T cells to bind exogenous IgM, supports the hypothesis that T-B cell interactions can be formed via the interactions of FcμR on T cells with IgM$^+$ BCR or IgM-Ag complexes on B cells [137].

Surprisingly, IgM was also observed to bind to monocytes. The presence of a receptor for IgM on the surface of human monocytes was suggested by an earlier study, determined by the ability of monocytes to form rosettes with sheep erythrocytes (SRBC) in the presence of anti-SRBC Abs of the IgM isotype [251].

However, a later study repeated these experiments and observed no rosette formation [252]. The study concluded that human monocytes do not express Fcμ receptors and that the previous findings may have been contributed to contaminating IgG Abs in the IgM preparations [252]. However, the discussion over the expression of FcμR on monocytes remains controversial. Numerous studies have published conflicting data on the expression of hFcμR on human monocytes recently [137, 179, 180, 235, 242], and the debate remains unresolved. Therefore, there is a possibility that the observed binding of IgM to monocytes could be due to the expression of hFcμR. To resolve this issue, future studies should aim to clarify whether hFcμR is expressed on monocytic cell populations.

The identification of DC-SIGN as a novel ligand for IgM could offer an alternative explanation as to how monocytes bind hIgM. However, expression of DC-SIGN on $CD14^+$ cells which bind hIgM needs to be confirmed. Although a subset of monocytes express DC-SIGN [167, 237], given the observed high levels of IgM binding to monocytes, it seems unlikely that these cells contribute to the proportion of IgM binding observed here. Therefore, it is tempting to speculate that another unidentified receptor expressed on monocyte surfaces can also bind IgM. Despite the identity of this receptor being unknown, numerous candidate mannose-binding ligands are expressed on monocytes subsets, including mannose receptor (MR) and DC-SIGN [253, 254]. MR is constitutively expressed by multiple monocyte-derived cell populations, such as immature monocyte-derived DCs and alternatively activated M2 macrophages [255, 256]. Moreover, the attenuation of ricin toxin-induced apoptosis of THP-1 monocytes by anti-MR Abs suggests expression of MR on monocytes surfaces [254, 257]. Selectins (e.g. CD62e, CD621) which bind complex N-glycans via sialyl Lewix x (sLe^x) motifs were also proposed as mannose ligands on monocytes [254, 258]. The mannose-dependent binding of type I fimbriated *E. coli* by Mac1 (CD11b/CD18) [259], and the high affinity of $CD11b^+$ monocytes for mannosylated glycopolymers [260], implicate Mac1 as a potential mannose-binding ligand expressed on monocytes [254]. Repeating the aforementioned binding assays with glycan cleavage IgM would confirm whether the binding of IgM to monocytes is mediated via glycan receptors.

Whether the expression of DC-SIGN by monocytes can account for the observed IgM binding is still unknown. Nonetheless, IgM-Fc or IgM-enriched IVIG bound DC-SIGN and SIGNR1 with high-affinity. These data confirm DC-SIGN as a novel receptor for hIgM [136]. The interaction of DC-SIGN with IgM was found to be dependent upon glycosylation of IgM [136]. IgM glycosylation has previously been shown to significantly enhance receptor binding to another lectin receptor, namely CD22 on B cells [261, 262]. Furthermore, the extent of IgM-glycosylation was shown to correlate with the binding of recombinant DC-SIGN to IgM^+ BCR follicular lymphoma B cells [263]. The cross-linking of IgM^+ BCR by recombinant DC-SIGN led to the induction of signalling in these malignant B cells, highlighting the potential importance of the interaction between IgM and DC-SIGN. However, in-depth knowledge of the functional consequence of IgM binding by DC-SIGN remains to be determined. Given the abundant expression of DC-SIGN on monocyte-derived dendritic cells [167], it is tempting to speculate that the binding and internalisation of IgM-ICs to the receptor could function to enhance immune responses through antigen presentation. Moreover, binding of IgM by DC-SIGN could govern clearance of IgM-opsonised apoptotic cells and production of anti-inflammatory IL-10 by dendritic cells [264]. It will be of interest to further investigate the IgM-DC-SIGN interaction.

Molecular dynamic simulations proposed that hFcμR could exist as a dimer on cell surfaces, as its transmembrane region shared sequence homology with erbb1, which was previously shown to form dimers [241]. In support of dimer formation for this IgM receptor, Fcα/μR is known to form a stable homo-dimer on cell surfaces via ε-(γ-glutamyl) lysine isopeptide bond formation between the ε-amino group of lysine residues and γ-carboxamide group of glutamic acid residues [144]. Given the large molecular weight of IgM, it is tempting to speculate that dimerisation of FcμR could contribute to avidity interactions and account for its high affinity for IgM [137]. However, whether FcμR exists as a dimer is still to be determined experimentally. Future studies could utilise two-colour quantum-dot tracking for the visualisation of dimer formation, as previously described [241]. Here, we provide a structural insight into the possible interaction between hFcμR and the Fc portion of IgM based on experimental data. This topic will be further expanded in Chapter 4.

Chapter 4: Determining why *P. falciparum* merozoites express proteins which bind non-immune IgM

4.1. Literature review

4.1.1. MSP3 family

The merozoite surface protein 3 (MSP3) multi-gene family encodes six MSP3-like proteins expressed on the merozoite surface; MSP 3 (MSP 3.1), MSP6 (MSP 3.2), H101 (MSP 3.3), DBLMSP (MSP 3.4), H103 (MSP 3.7) and DBLMSP2 (MSP 3.8) [148]. MSP3-like family proteins are synthesised simultaneously in schizont-stage parasites, which undergo proteolytic cleavage in parasitophorous vacuoles during merozoite maturation [265, 266]. The majority of the cleaved fragments are released into the culture supernatant upon schizont rupture, however a small proportion of fragments associate non-covalently to the merozoite surface by mechanism(s) yet to be resolved [265, 267].

Members of the MSP3 multi-gene family were grouped due to similarities in the organisation of their C-terminal regions compared to MSP3 (Figure 4.1) [148]. Although the N-terminal regions of MSP3-like proteins were found to be highly polymorphic [265, 268, 269], the C-terminal regions shared sequence homologies and are highly conserved among parasite isolates [148], implying that these proteins may play a role in parasite survival [270]. The conservation of C-terminal sequences within the MSP3 multi-gene family contributed to the ability of Abs raised against one member of the family to cross-react with other members of the gene family [148]. These cross-reactive Abs promoted Ab-dependent cellular inhibition (ADCI) of parasite growth [148, 271]. Moreover, immune sera from individuals living in endemic regions also recognised the C-terminal domain of different members of the MSP3-gene family [148, 270], and anti-MSP3 Abs have been shown to correlate with protection in field studies [272-274]. These results highlight the importance of MSP3-like proteins in eliciting protective immunity against malaria.

4.1.2. DBLMSP and DBLMSP2

Duffy-binding like (DBL) domains play a crucial role in disease severity in malaria by mediating a number of pathogenic mechanisms including erythrocyte invasion and cytoadhesion [66, 275]. These cysteine-rich DBL domains are encoded by a variety of genes within the *P. falciparum* genome, including members of the erythrocyte-binding ligand (*EBL*) and *var* gene superfamilies [110].

A recent study characterised the expression of DBL domains by two members of the MSP3 multi-gene family [149]. Two closely-related members of the MSP3-family, DBLMSP and DBLMSP2, were found to contain a central DBL domain in addition to a C-terminal secreted polymorphic antigen associated with merozoites (SPAM) domain [147, 149]. Whereas the majority of the MSP3-gene family contain a single SPAM domain [148, 266], the presence of a single central DBL domain is unique to DBLMSP and DBLMSP2 (aa residue 143-443 and 161-457, respectively) [147, 149]. DBL domains of DBLMSP and DBLMSP2 share 38% sequence identity and 62% similarity, whereas the SPAM domains share 30 and 53%, respectively [147]. SPAM domains are composed of a glutamic acid-rich region and a leucine-zipper-like region, which are thought to form large oligomers that could extent to potentially allow for improved interactions with erythrocyte membrane proteins [147, 276]. Recently, the SPAM domains of DBLMSP and DBLMSP2 were resolved as high molecular weight oligomers by size-exclusion chromatography, suggesting that the C-terminal domain of these proteins facilitates oligmerisation [146]. This intriguing feature will be explored more in Chapter 5.

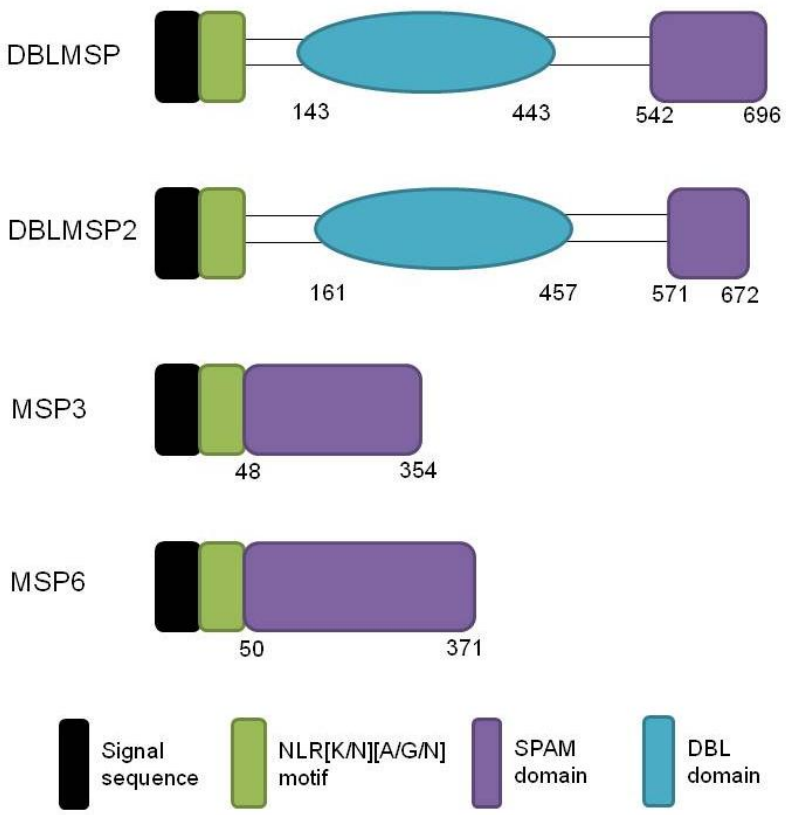

Figure 4.1 Structure of the MSP3-like family proteins. The schematic diagram depicts the presence of SPAM domains common to all MSP3-like family members, whereas the DBL domain is exclusive to DBLMSP and DBLMSP2 adapted from [147]. The numbers depict amino acid (aa) residues.

4.1.3. Structure of DBLMSP and DBLMSP2

The three-dimensional structure of the DBL domain of DBLMSP2 was recently resolved by X-ray crystallography, which was subsequently used as a template to build a homology-based structure of the DBL domain of DBLMSP [147]. DBLMSP2 was found to contain a canonical DBL fold with an α-helical core composed of three subdomains which adopted a boomerang-like shape (Figure 4.2). Inter-chain disulphide linkages were found to stabilise DBLMSP2, and the disulphide bond architecture of DBLMSP and DBLMSP2 was proposed to be unique to that of the DBL proteins of the PfEMP1 and EBL family [147]. Further, DBLMSP2 showed structural similarities with DBL domains from PfEMP1, including VAR2CSA DBL6e, DBL3X and *Pf*EBA-175 F2 DBL [147]. Although other DBL-containing proteins have been suggested to form dimers [277], the domain architecture and structure of DBLMSP2 did not satisfy the requirements for this kind of dimerisation [147]. However, as the structure of the full-length protein has yet to be resolved, the oligomerisation status of DBLMSP and DBLMSP2 remains unknown.

DBLMSP is expressed on merozoites surfaces in all schizonts, whereas DBLMSP2 is expressed on a very small subset (≤1%) of schizonts [151]. However, numerous studies have confirmed the presence of DBLMSP and DBLMSP2 on merozoite surfaces [147, 149]. Due to the lack of GPI-anchor motifs or transmembrane domains, DBLMSP and DBLMSP2 are thought to associate with other proteins on the surface of merozoites [147, 149]. Hodder et al. hypothesised that processing by the parasite serine protease *Pf*SUB1 may account for incorporation of DBLMSP and DBLMSP2 onto the merozoite surface [147]. In support of this, the N-terminus regions of these proteins contain potential *Pf*SUB1 cleavage sites and saponin-processing revealed that two forms of the proteins exist [147], and the integration of MSP6 into the MSP1 complex was found to be dependent on *Pf*SUB1 processing [278, 279]. However, further research is required to elucidate the exact mechanism by which DBLMSP and DBLMSP2 associate with the merozoite surface, and clarify their interaction with other merozoite surface proteins.

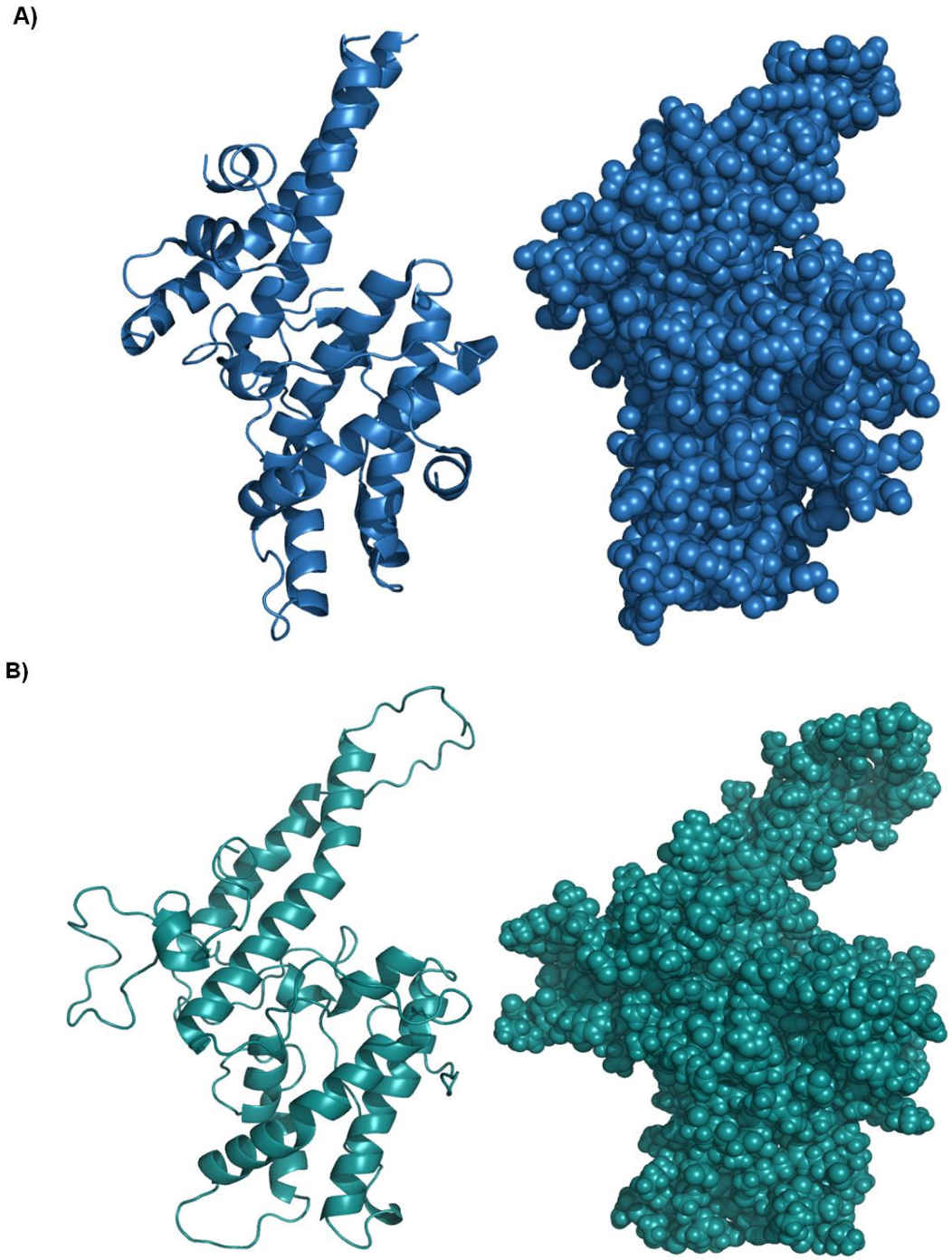

Figure 4.2 Structure of the DBL domains of DBLMSP and DBLMSP2 (A) Crystal structure of the DBL domain of DBLMSP2 domain (PDB accession code 3VUU). **(B)** Homology-based model of the DBL domain of DBLMSP was derived from the crystal structure of DBLMSP2. The structure of the DLB domain of DBLMSP2 was used as a template to build a model of the DBL of DBLMSP using the MODELLER program adapted from [147].

4.1.4. Vaccine candidate antigens

The striking polymorphisms in *dblmsp* and *dblmsp2*, particularly within the *dbl* region, indicates that these genes are likely to be subject to immense immune selection pressure, presumably owing to their expression on the merozoite surface [280]. This is supported by findings that full-length recombinant DBLMSP elicit specific Abs which inhibited erythrocyte invasion by *P. falciparum* merozoites [281]. These inhibitory Abs did not cross-react with the SPAM (C-terminal) domains of the other MSP3-family members, suggesting that they recognise regions outside of the SPAM domain of DBLMSP [281]. However, the role of the SPAM domain in protection has been documented in numerous studies [148, 271, 272]. Asymptomatic adults in endemic regions of Senegal exhibit high prevalence of Abs specific for the SPAM domain of DBLMSP [270], immune sera from individuals in India recognised both the DBL and SPAM domains of DBLMSP [149], and Abs against DBLMSP were isolated from sera of asymptomatic Thai adults [281]. The generation of Abs specific for DBLMSP irrespective of parasite isolate or endemic area signifies the potential importance of this protein in *P. falciparum* malaria. Additional research is required to assess the relationship between anti-DBLMSP Ab titres and clinical protection from malaria on a global scale, to help clarify the importance of these proteins in immunity to malaria [281]. Together, these data highlight the potential of DBLMSP and DBLMSP2 as attractive vaccine candidates. Understanding what role these proteins play in immunity to malaria could therefore help facilitate vaccine design.

4.1.5. DBLMSP and DBLMSP2 bind human IgM

Intriguingly, a recent study identified a previously unknown function of DBLMSP and DBLMSP2 whilst attempting to ascertain their immunoreactivity [146]. Full-length recombinant DBLMSP and DBLMSP2 exhibited non-specific immunoreactivity to both immune sera and unexposed control sera, suggesting that these proteins bind non-immune immunoglobulins [146]. Further analysis revealed that DBLMSP and DBLMSP2 bound non-immune human IgM, but not IgG, IgA, or IgE, and that this binding was human specific [146]. The Cμ4 domain of hIgM was identified as the target for DBLMSP and DBLMSP2, and these proteins were able to bind hIgM irrespective of whether it was bound to antigen or not. Although the presence of the J-chain in hIgM molecules was not essential for binding, the lack of a J-chain reduced binding

of DBLMSP2. The DBL domains of DBLMSP and DBLMSP2 govern binding to IgM, which occurs at high avidity (K_d = 0.3 and 1.1 nM, respectively). No binding to IgM was observed for the SPAM domains.

A variety of DBLMSP and DBLMSP2 DBL domains from different *P. falciparum* strains possess the IgM-binding phenotype, despite high levels of sequence polymorphisms [146]. The ability of native DBLMSP to bind IgM was confirmed since wild-type, but not *dblmsp*-deficient merozoites, had IgM bound to their surfaces following culture with human serum or purified human IgM [146]. These results identify DBLMSP and DBLMSP2 as novel IgM-binding *P. falciparum* proteins which are expressed on the surfaces of merozoites.

4.1.6. Functions of DBLMSP and DBLMSP2

Exactly why DBLMSP and DBLMSP2 variants bind non-immune hIgM remains unclear. To date, these proteins have been implicated in erythrocyte binding [147, 149] and camouflaging critical epitopes from immune detection through the binding of non-immune IgM [146].

Invasion of host erythrocytes is pivotal for *P. falciparum* replication and virulence. *P. falciparum* merozoites utilise numerous mechanisms to gain entry into host erythrocytes, including the expression of ligands which bind receptors on host cells [282]. The EBL family of proteins expressed on merozoite surfaces are well-characterised erythrocyte-binding ligands (EBL) which mediate erythrocyte invasion [283]. Since DBL domains are common in members of the EBL family, the ability of DBLMSP and DBLMSP2 to bind erythrocytes was investigated [147, 149]. COS-7 cells transfected with DBLMSP formed rosettes with uninfected erythrocytes, suggesting that DBLMSP may mediate merozoite attachment during erythrocyte invasion processes [149]. Hodder et al. further characterised DBLMSP and DBLMSP2 as erythrocyte-binding proteins, and highlighted the role of the DBL domains in this interaction [147]. They observed enhanced binding of recombinant DBL domain and full-length proteins in the presence of specific metal ions (Ca^{2+}, Cu^{2+}, Co^{2+}, and Zn^{2+}). This binding was not sensitive to trypsin and neuraminidase treatment of erythrocytes [147], contradicting earlier findings [149]. As well as the expression of DBL domains, the erythrocyte-binding phenotype is a unique feature of the DBLMSP

proteins as other MSP3-family members do not bind erythrocytes [147]. However, subsequent analysis revealed that the addition of DBLMSP-specific Abs had a modest inhibitory effect on erythrocyte invasion, and the ablation of *dblmsp* gene in knock-out parasites had no effect on erythrocyte invasion [146]. Therefore, although the DBLMSP proteins may help initiate interactions between merozoite and erythrocyte, their expression is not essential for invasion processes. More research is required to calrify the role of these proteins in erythrocyte invasion.

Despite high levels of sequence polymorphism, IgM-binding is a conserved phenotype of DBLMSP variants [146]. In total, ten representative DBL variants and six field isolates of DBLMSP, including the *P. reichenowi* ortholog for DBLMSP, and six representative DBL variants of DBLMSP2, were shown to bind IgM [146]. Curiously, the DBL domains of DBLMSP from variants 7G8 and 028 did not bind IgM, despite sharing sequence homology with the DBL domains of their DBLMSP2 counterparts [146]. The residues mediating interactions between DBL domains and IgM have yet to be determined. However, conservation of the IgM-binding between variants suggests that this phenotype could play an important role in malaria [146].

The DBL domains of DBLMSP and DBLMSP2 variants were found to be poorly immunogenic [146]. One explanation for this poor immunoreactivity could be that IgM-binding by DBLMSP and/or DBLMSP2 conceals critical epitopes from the host immune system, as previously described for the PfEMP1 variant VAR2CSA [284]. Immunoreactivity of full-length DBLMSP and DBLMSP2 to immune IgG was reduced in a dose-dependent manner when complexed with non-immune IgM. This effect was observed for numerous DBLMSP variants, suggesting that the camouflage of immune epitopes from Abs through non-immune IgM binding is a strain-transcending function [146].

Whether DBLMSP and/or DBLMSP2 permit additional functional consequences is yet to be determined, and therefore forms the focus of this chapter. Since MSP3 is shed from the merozoite surface upon erythrocyte invasion [265, 267], and given the high affinity of the DBLMSP proteins for human IgM [146], it is tempting to speculate that the formation of immune complexes of DBLMSP with IgM in the periphery could function to block IgM binding to its cognate receptors.

4.2. Objectives

To determine why *P. falciparum* merozoites express DBL domains which bind non-immune human IgM. The specific objectives were:

I. To identify requirements for the interaction between DBLMSP/ DBLMSP2 and human IgM
II. To establish whether DBLMSP and/or DBLMSP2 function to block IgM binding to host receptors
III. To determine if IgM-opsonised immune-cells are targets for DBLMSP and DBLMSP2, and the biological consequences of DBLMSPs binding
IV. To investigate the structural requirements for DBLMSP and DBLMSP2 interacting with IgM bound by FcμR

4.3. Results

4.3.1. Malaria DBL domains bind the Cμ4 domain of human IgM

DBLMSP and DBLMSP2 have been recently characterised to bind the Cμ4 domain of hIgM [146]. Since this domain is also bound by hFcμR (see Chapter 3), we sought to confirm which domain of hIgM the malarial proteins bind. Initially, the ability of full-length recombinant DBLMSP and DBLMSP2 proteins [146] to bind hIgM was assessed. DBLMSP and DBLMSP2 bound strongly to IgM in ELISAs, whereas no binding was observed for the control protein Cd4-d3+4 (Figure 4.3A; left panel). Further, the individual DBL domains of DBLMSP and DBLMSP2 were shown to bind to hIgM (Figure 4.3A; right panel).

A panel of domain-swap Abs generated in a previous analysis [120], and that were also used to characterise the interaction with VAR2CSA [284] were used to characterise the interaction of DBLMSP and DBLMSP2 with hIgM by ELISA. These experiments were performed by Professor Pleass (Liverpool School of Tropical Medicine). The Cμ4 domain was crucial for permitting DBLMSP and DBLMSP2 binding to domain-swap Abs (Figure 4.3B). No binding was detected with the α1μ2μ3α3 domain-swap Abs lacking the Cμ4 domain (Figure 4.3B). The presence of the Cμ2 and Cμ3 domains, in conjunction with the Cμ4 domain (α1μ2μ3μ4), enhanced binding of DBLMSP to the chimeric Abs, whereas the presence of these domains had less effect for DBLMSP2 binding (Figure 4.3B). These results confirm the ability of recombinant DBLMSP and DBLMSP2 to bind the Cμ4 domain (and partially via the Cμ2-Cμ3 domains) of hIgM.

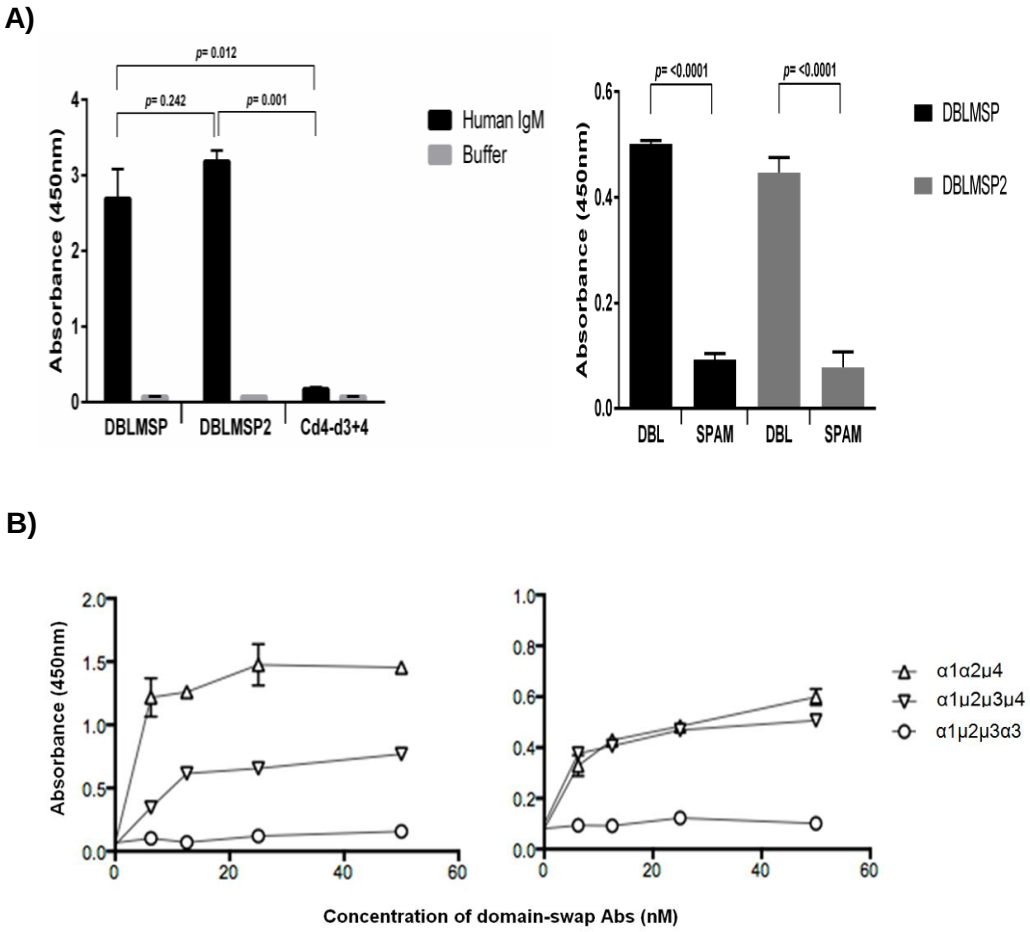

Figure 4.3 DBLMSP and DBLMSP2 bind to the Cμ4 domain of hIgM. (A) An indirect ELISA was used to confirm binding of recombinant full-length biotinylated DBLMSP and DBLMSP2 to hIgM (left panel). Biotinylated Cd4-d3+4 control protein did not bind to hIgM (left panel). Further, individual DBL domains of DBLMSP and DBLMSP2 bound hIgM, whereas no binding was observed with individual SPAM domains (right panel). The mean ± SD are shown for three repeat experiments. Unpaired *t* test was used to test for statistical significance ($p < 0.05$). **(B)** A panel of domain-swap Abs were used in which domains of IgA (shown as α) were substituted with domains of IgM (shown as μ) [120]. DBLMSP (right panel) and DBLMSP2 (left panel) bound to domain-swap Abs containing the Cμ4 domain (α1α2μ4 and α1μ2μ3μ4). No binding was observed for domain-swap Abs containing the Cμ2 and Cμ3 domains (α1μ2μ3α3). The mean ± SD are shown for two repeat experiments.

4.3.2. IgM glycosylation is not involved in DBLMSP and DBLMSP2 binding

Malaria antigens are typically not complex glycoproteins as *P. falciparum* lacks the biosynthetic machinery required for complex glycan synthesis [285]. We therefore wondered if DBLMSP and DBLMSP2 could interact with the glycans found on hIgM. For this, a range of endoglycosidases were used, including PNGase F, α1-6 mannosidase, and neuraminidase (which cleave N-glycans, mannose residues, and sialic-acid terminating glycans, respectively), which have previously been used to remove glycans from IgM [286, 287]. Endoglycosidase treatment had no significant effect on the binding of either DBLMSP or DBLMSP2 to hIgM (Figure 4.4). No binding of IgM was observed to the Cd4-d3+4 control. Together, these data suggest DBLMSP and DBLMSP2 bind hIgM in a glycan-independent manner.

4.3.3. Malaria DBL domains that also bind the Cμ4 domain of IgM do not block the interaction of IgM with hFcμR

Since the Cμ4 domain of IgM was also observed to be the target of hFcμR (see Chapter 3), we sought to investigate if these parasite proteins had evolved to block the interaction of IgM with hFcμR, as previously proposed [198]. Human IgM was incubated with varying concentrations of DBLMSP or DBLMSP2 and binding to hFcμR-transfected cell lines investigated by flow cytometry (Figure 4.5A,B). Saturating concentrations of DBLMSP2 had no significant effect ($p= 0.58$) on the interaction of hIgM with hFcμR (Figure 4.5A, right panel). DBLMSP at best could only block ~30% of the binding of hIgM to the hFcμR-transfected cells (Figure 4.5A, left panel), however this effect was not significant ($p= 0.09$).

In addition, prior binding of hIgM to the hFcμR-transfected cells did not prevent the interaction of either DBLMSP or DBLMSP2 with hIgM bound to the cell surface via FcμR (Figure 4.5B; left panel). This data also suggests that DBLMSP binds hIgM more strongly than DBLMSP2, a finding that has consistently been observed [146]. No binding of DBLMSP and DBLMSP2 to hFcμR was observed in the absence of hIgM (Figure 4.5B; right panel).

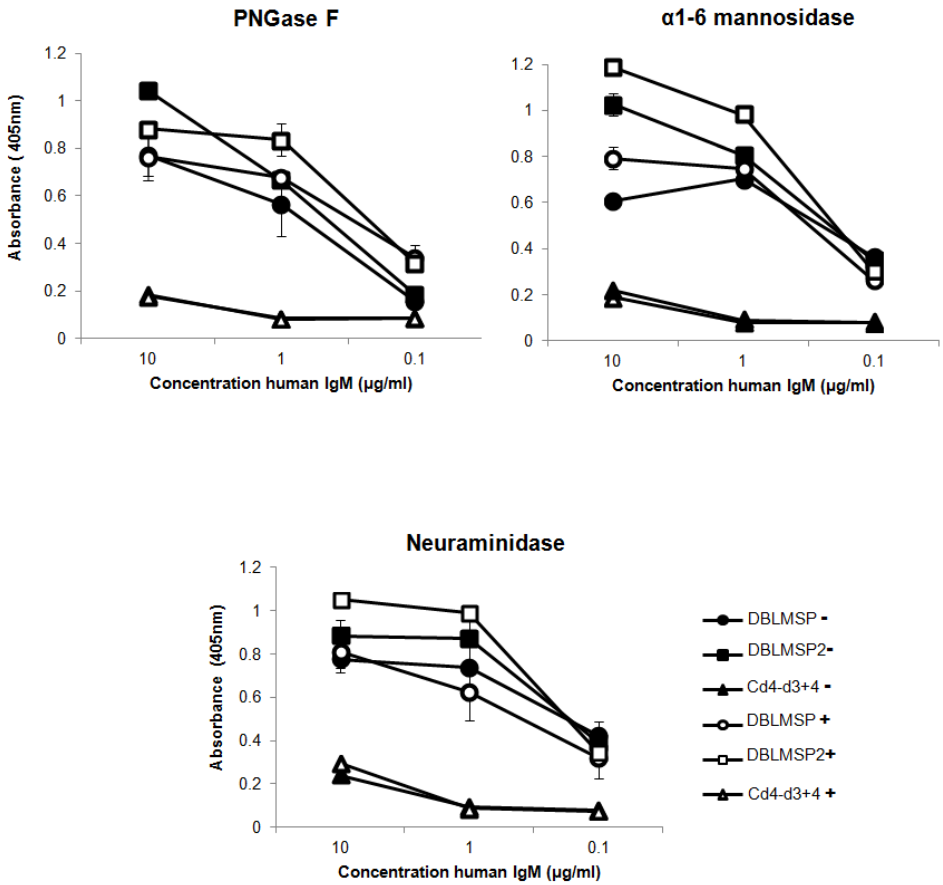

Figure 4.4 Endoglycosidase treatment of human IgM does not inhibit IgM binding to DBLMSP or DBLMSP2. Recombinant DBLMSP, DBLMSP2, and Cd4-d3+4 (10 µg/ml)were immobilised and incubated with varying concentrations of endoglycosidase-treated (non-filled markers; +) or non-treated (filled markers; -) hIgM. Dunn's multiple comparison tests revealed no statistical difference in binding of treated- or non-treated hIgM to DBLMSP or DBLMSP2. No binding was observed with Cd4-d3+4 control protein. Bars represent mean ± SD; *n* = 2.

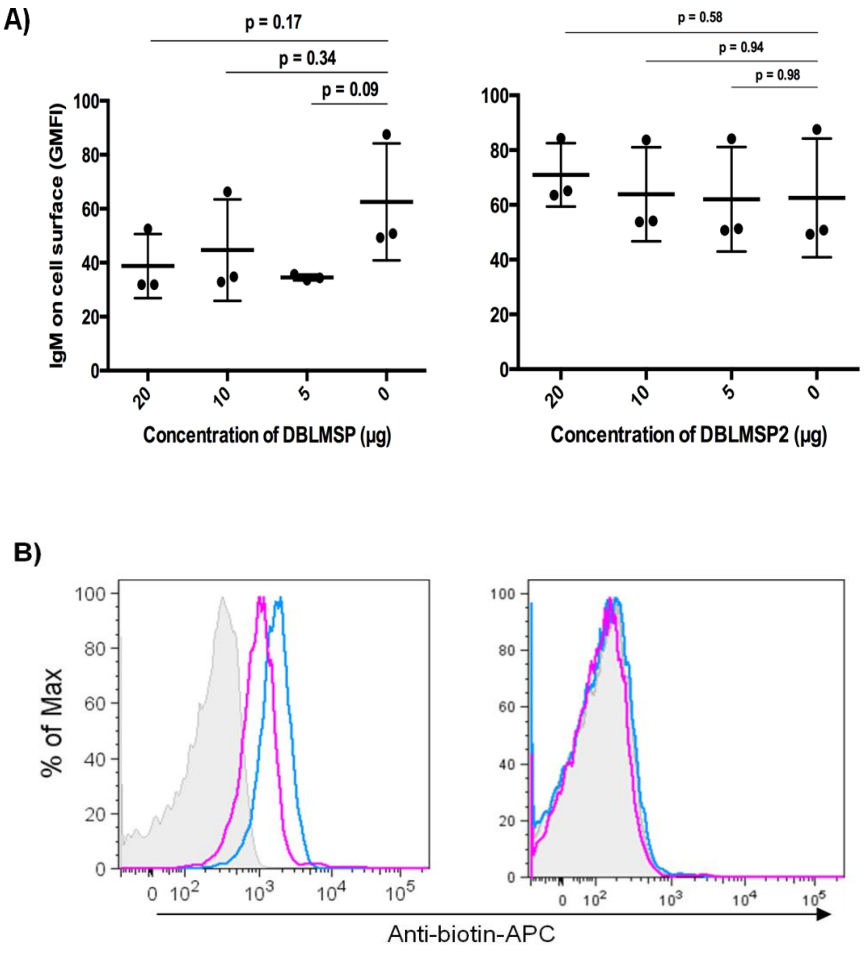

<u>Figure 4.5</u> DBLMSP and DBLMSP2 do not block the binding of human IgM to FcμR. (A) hFcμR-transfected cells were incubated with media supplemented with hIgM or media supplemented with hIgM preincubated with varying concentrations of DBLMSP or DBLMSP2 for 1hr on ice. Cells were washed and then labelled with $F(ab')_2$-anti-human IgM-RPE to detect IgM binding by flow cytometry. Percentage of hIgM on cell surfaces (GMFI) shows a trend for DBLMSP to block hIgM binding to hFcμR-transfected cells (albeit not significant), whereas no blocking was observed with DBLMSP2. The mean ± SD from three independent experiments is shown. Multiple t-tests were performed for the comparison of % IgM on cell surface (GMFI) values for hIgM preincubated with varying concentrations DBLMSP or DBLMSP2, and hIgM alone (0µg). Statistical significance was regarded as $p < 0.05$. **(B)** DBLMSP and DBLMSP2 engage hIgM bound to hFcμR-transfected cells. Normalised biotinylated DBLMSP or DBLMSP2 were incubated with hIgM-opsonised hFcμR-transfected cels on ice prior to flow cytometry analysis. In the overlay shown (left panel), binding of DBLMSP (blue trace) and DBLMSP2 (pink trace) to gated GFP^+ cells was detected using anti-biotin-APC. Background binding detected with anti-biotin-APC in the absence of biotinylated proteins (grey trace). No binding of either DBLMSP or DBLMSP2 to hFcμR-transfected cells was observed in the absence of hIgM (right panel). The results shown are representative of three independent experiments.

4.3.4. DBLMSP and DBLMSP2 interact with IgM bound to DC-SIGN

To test if DBLMSP and DBLMSP2 could interact with IgM bound to other known IgM receptors [136], the interaction of DBLMSP and DBLMSP2 with soluble recombinant human DC-SIGN tetramers by multichannel surface plasmon resonance analysis (MC-SPR) was investigated in the laboratory of Dr Daniel Mitchell (University of Warwick). The sensorgrams show that DBLMSP2 can still bind hIgM after hIgM has first engaged DC-SIGN (Figure 4.6). The high affinity for the interaction of DBLMSP2 for DC-SIGN-bound hIgM (K_d= 96nM) is approximately of the same order as those observed for the binding of DBLMSP and DBLMSP2 to IgM (K_d= 0.3nM and 1.1nM, respectively), as shown previously [146]. Given the multimeric nature of IgM, DC-SIGN and the two parasite proteins studied, these measurements reflect overall binding avidity and are not easily comparable with other monomeric protein interactions. The physiological concentration of IgM in human serum is around 1-2mg/ml (1-2μM), at least three orders of magnitude higher than the measured binding constants, implying that DBLMSP2 complexed to IgM would be rapidly and irreversibly bound by DC-SIGN and/or the FcμR.

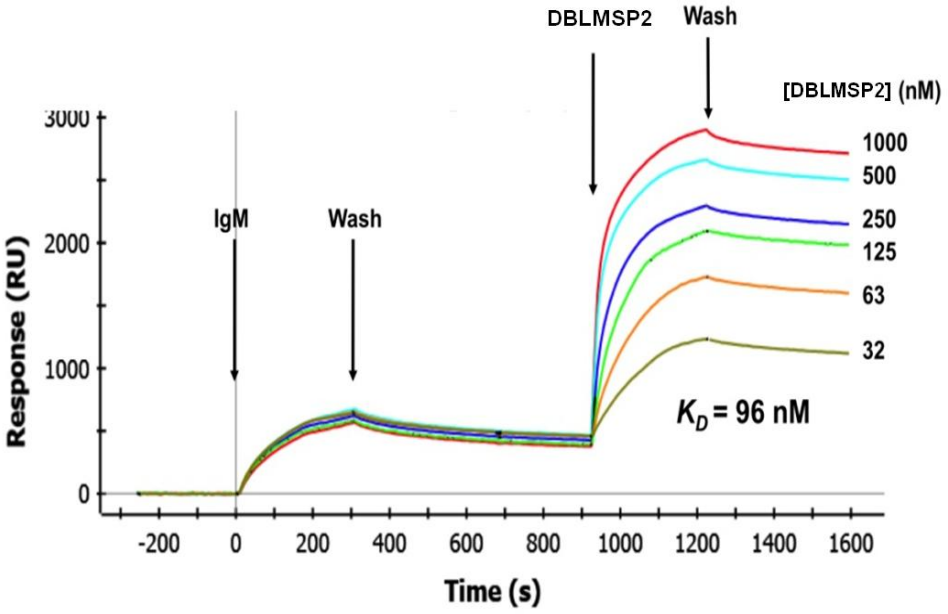

Figure 4.6 DBLMSP2 interact with IgM bound to DC-SIGN. Multi-channel surface plasmon resonance was conducted in the laboratory of Dr Daniel Mitchell (University of Warwick). Association and dissociation curves of DBLMSP2 binding to IgM bound to recombinant human DC-SIGN immobilised on a sensor chip. Human IgM was injected at doubling dilutions from 10μM to 0.32μM into flow at time 0, and replaced with buffer at 300 sec. DBLMSP2 was injected at doubling dilutions from 10μM to 0.32μM into flow at time 900, and replaced with buffer at 1300 sec. Data are representative of duplicate experiments. Similar results were observed for DBLMSP (data not shown).

4.3.5. DBLMSP and DBLMSP2 bind lymphocyte subsets that express hFcμR

As the hFcμR-transfected cell lines may not accurately reflect the expression of hFcμR *in vivo*, we next investigated the interaction of DBLMSP and DBLMSP2 with lymphocyte subsets previously shown to express hFcμR [137, 140].

Whether IgM^+ gated lymphocytes were also positive for DBLMSP and DBLMSP2 binding was first determined. For this, lymphocytes were first gated into IgM negative and positive populations, based on the use of controls (e.g. no detecting Ab). Three cell populations were observed (Figure 4.7); lymphocytes with no cell surface IgM (IgM^-), IgM positive lymphocytes (IgM^+), and highly positive lymphocytes (IgM^{++}). We hypothesised that cells with high levels of IgM on their surface are likely to be B cells expressing IgM^+ BCR. Importantly, all of the cells that bound DBLMSP and DBLMSP2 were also positive for cell surface IgM (Figure 4.7; overlays). In fact, binding of these proteins to lymphocytes appeared to correlate with the levels of surface IgM, as IgM^{++} lymphocytes exhibited the highest proportion of binding (Figure 4.7A). Moreover, there were significant differences in the binding of DBLMSP and DBLMSP2 to IgM positive ($^+$ and $^{++}$) lymphocytes when compared to IgM negative ($^-$) lymphocytes (Figure 4.7B; $p < 0.01$). Thus, the binding of DBLMSP and DBLMSP2 to lymphocytes appears to be dependent on the presence of surface IgM.

We next determined the subsets of lymphocytes that bound DBLMSP and DBLMSP2 (Figure 4.8). Both DBLMSP and DBLMSP2 bound to T cells ($CD4^+$ and $CD8^+$), $CD19^+$ B cells and $CD56^+$ NK cells, although binding of DBLMSP was always stronger. Interestingly, the great majority (>60% between at least three independent donors) of circulating peripheral $CD19^+$ B cells bound both DBLMSP and DBLMSP2, whereas only ~10-40% of circulating T lymphocytes and NK cells bound either protein (Figure 4.8 & 4.9). This supports the finding that lymphocytes with high levels of surface IgM (IgM^{++}) bound the highest proportion of DBLMSP and DBLMSP2, suggesting that these proteins may also engage the IgM^+ BCR, although this has yet to be determined.

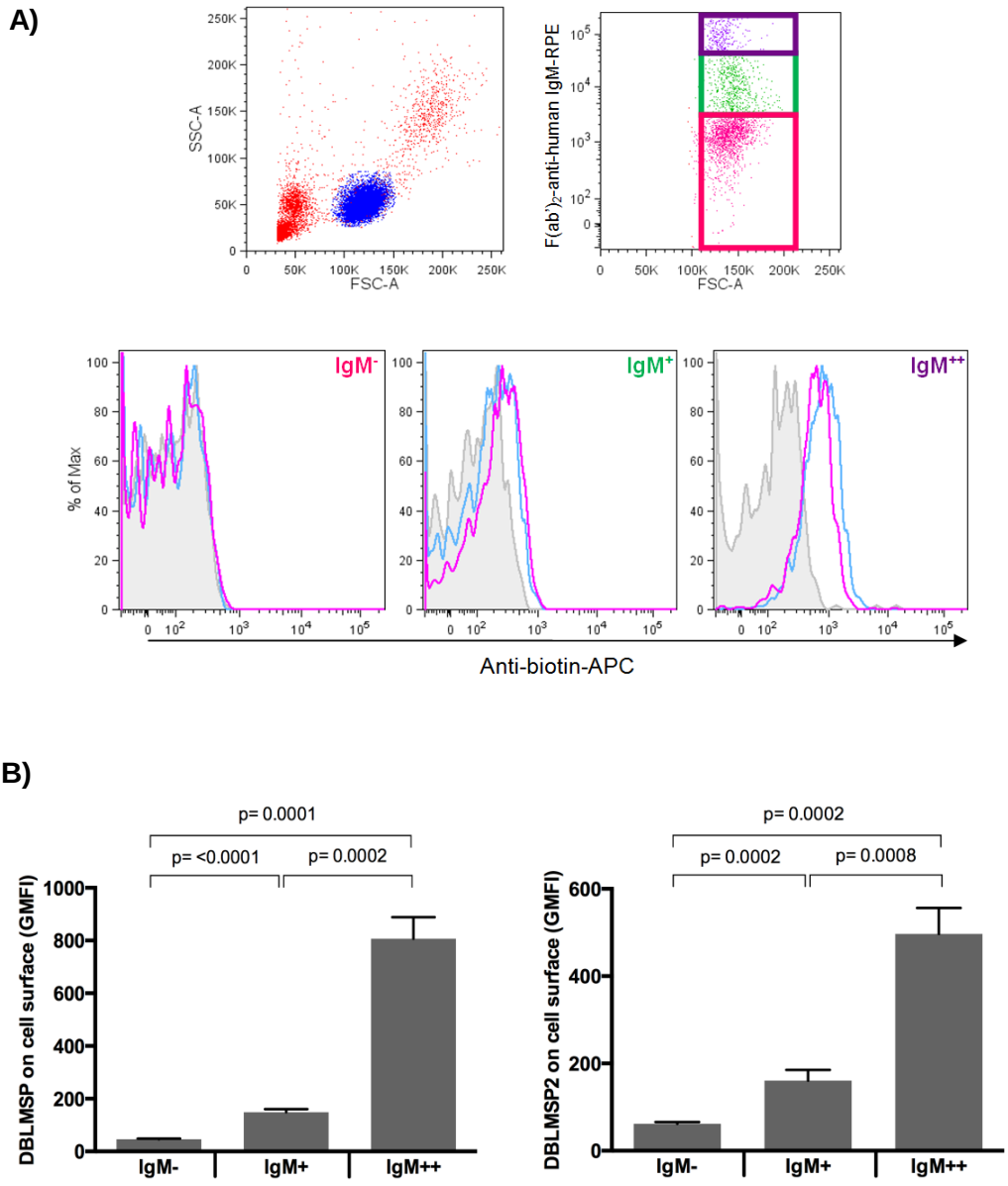

Figure 4.7 DBLMSP and DBLMSP2 bind to IgM-positive lymphocytes. Freshly isolated PBMCs were incubated with normalised amounts of biotinylated DBLMSP or DBLMSP2, washed and then incubated with anti-biotin-APC and $F(ab')_2$ goat anti-human IgM-RPE prior to flow cytometry analysis. **(A)** Lymphocytes were gated (blue dots), and further gated into IgM^- (magenta gate), IgM^+ (green gate), and IgM^{++} (purple gate) populations. Gates were set using negative controls (no detecting Ab). Binding of DBLMSP (blue trace) and DBLMSP2 (pink trace) to these populations are shown as traces. No binding was observed with the Cd4-d3+4 control protein (grey trace). **(B)** There was significant difference in binding of DBLMSP (left panel) and DBLMSP2 (right panel) to gated IgM^-, IgM^+, and IgM^{++} lymphocytes (as in *A*), as determined by multiple unpaired t-tests. The mean± SD of two repeats are shown.

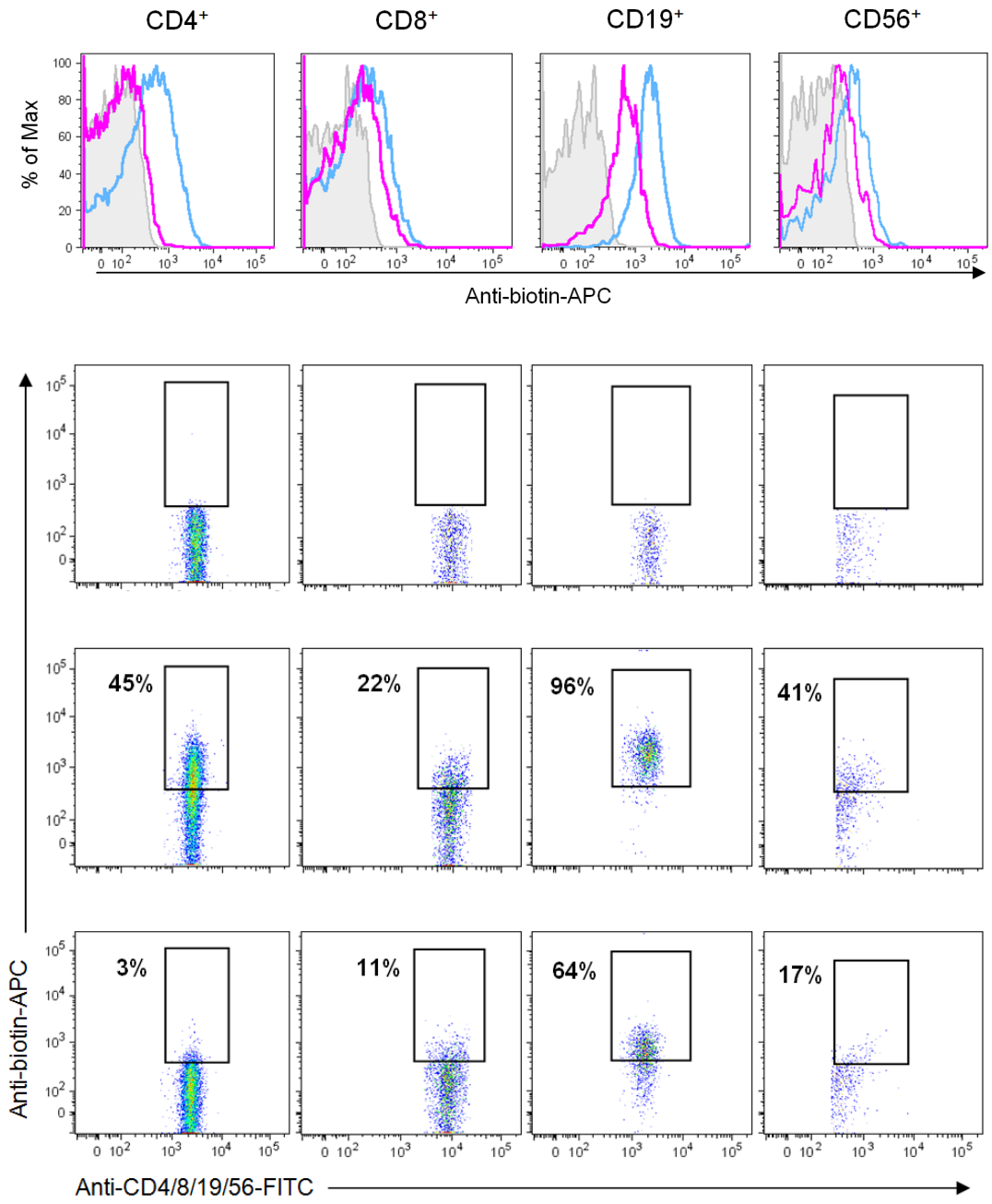

Figure 4.8 DBLMSP and DBLMSP2 bound to human lymphocytes. Freshly isolated PBMCs were incubated with normalised amounts of biotinylated DBLMSP, DBLMSP2 or Cd4-d3+4, and then with anti-biotin-APC along with the appropriate FITC-labelled mAbs specific for CD4, CD8, CD19, or CD56. Subsets of lymphocytes were gated and analyzed for binding of biotinylated DBLMSP (blue trace) and DBLMSP2 (pink trace). Percentages of gated lymphocytes positive for DBLMSP (middle panel) or DBLMSP2 (lower panel) binding are shown. Gates were set using the Cd4-d3+4 control (upper panel). Data is representative of one of three repeat experiments.

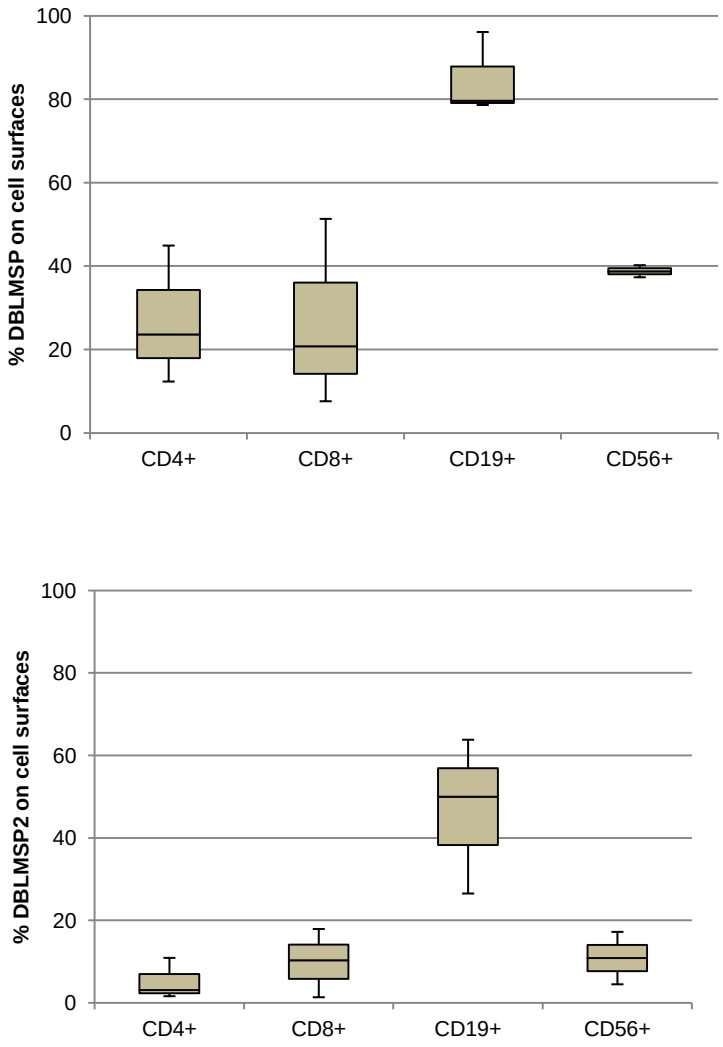

Figure 4.9 Quartile plots of variation in DBLMSP and DBLMSP2 binding to gated lymphocytes. Percentage of gated lymphocytes positive for DBLMSP or DBLMSP2 (*n*=3) are shown. Values are depicted as upper quartile, median and lower quartile (boxes) with minimum and maximum ranges.

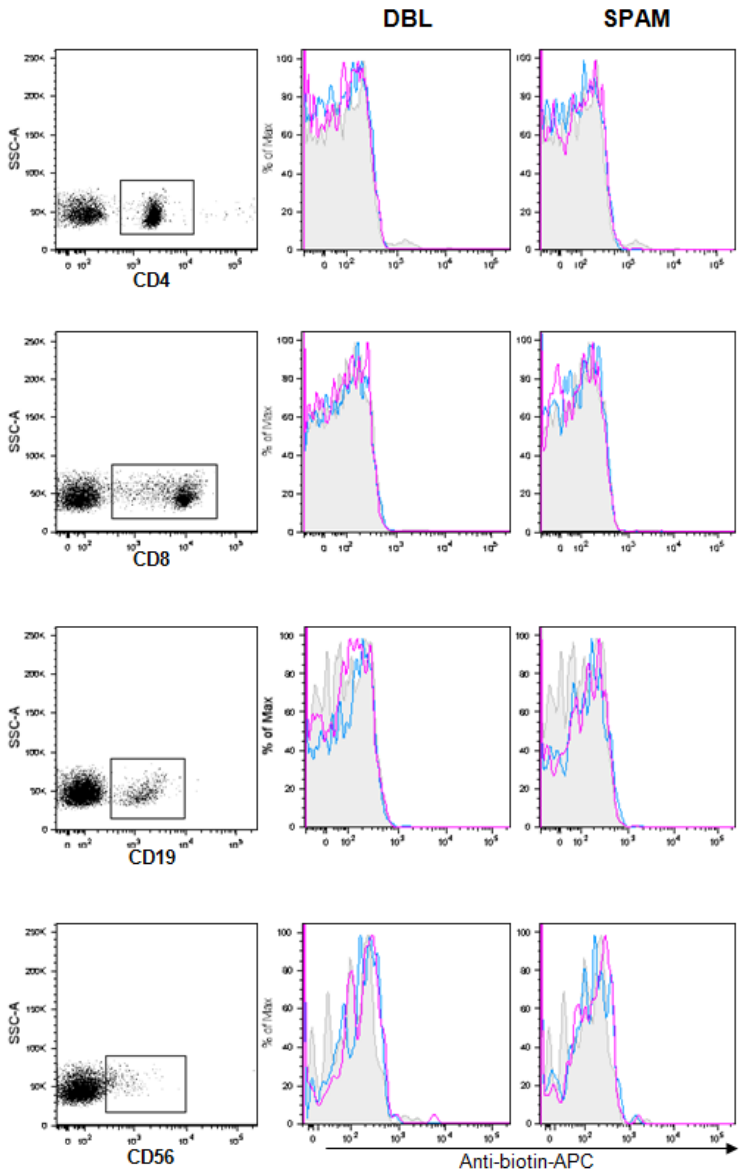

Figure 4.10 Individual domains of DBLMSP do not bind to lymphocytes. DBLMSP proteins are composed of Duffy-binding like (DBL) and secreted polymorphic antigen merozoite (SPAM) domains. To investigate which domain of the DBLMSP proteins mediated interactions with lymphocytes, normalised amounts of biotinylated DBL and SPAM domains were incubated with freshly isolated PBMCs and sequentially labelled with anti-biotin-APC and FITC-labelled Abs specific for human CD4, CD8, CD19, and CD56. The binding of DBL and SPAM domains of DBLMSP (shown as blue trace) and DBLMSP2 (shown as pink trace) to gated lymphocytes were assessed by flow cytometry. Neither DBL nor SPAM domains alone could bind to lymphocytes. Data are representative of one of three repeat experiments.

Although there was considerable variation in binding between donors, gated lymphocytes from all donors bound DBLMSP and DBLMSP2 but not the Cd4-d3+4 control (Figure 4.7 & 4.8). Intriguingly, individual DBL or SPAM domains of DBLMSP and DBLMSP2 expressed in isolation were unable to bind IgM^+ lymphocytes (Figure 4.10). The fact that the DBL domains alone were unable to engage IgM^+ lymphocytes supports the role of the SPAM domain in oligomerisation. Oligomerisation of the DBL domains in the full-length proteins may facilitate avidity interactions allowing DBLMSP/ DBLMSP2 to bind to IgM on lymphocyte surfaces.

There was also consistent binding of hIgM to $CD14^+$ monocytes (Figure 4.11A), and of the DBLMSP proteins to the monocytic cell population (Figure 4.11B), although this binding is likely to be mediated via an alternative IgM binding receptor as the debate regarding the expression of hFcμR by monocytes remains controversial [137, 179, 180, 235, 288].

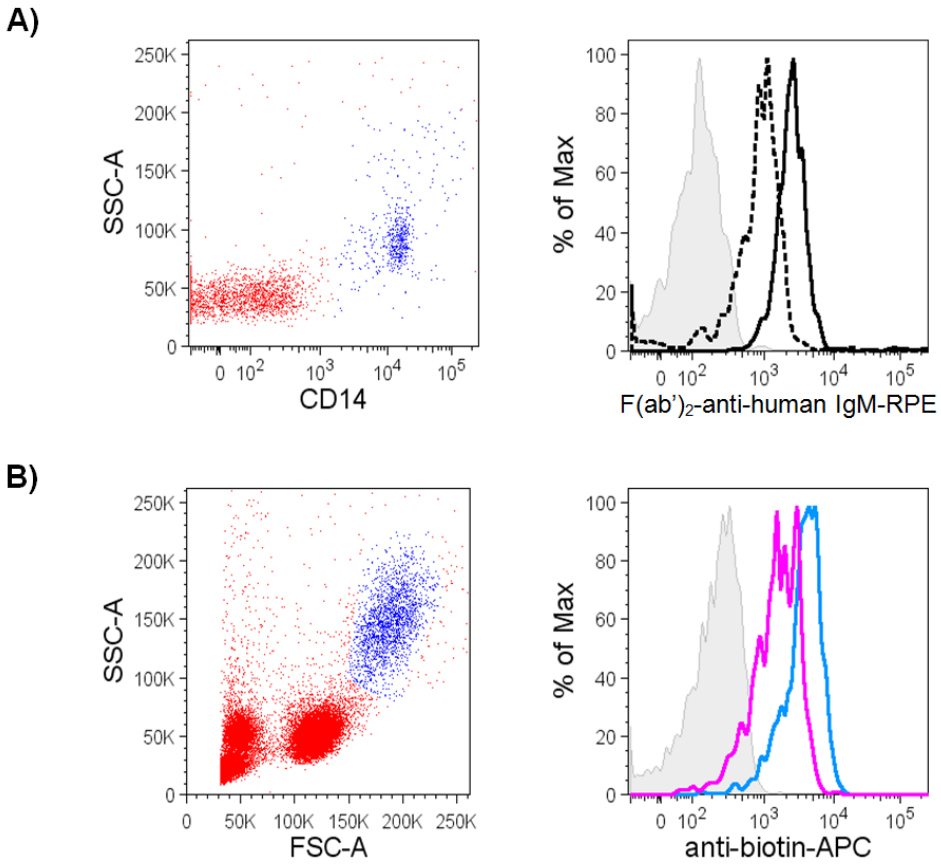

Figure 4.11 DBLMSP and DBLMSP2 bind to monocytic cells (**A)** Individual $CD14^+$ monocytes stained with anti-human CD14-APC Cy7 were gated (shown by blue dots, left panel). Binding of exogenous hIgM (black trace) to or cell surface levels of hIgM on cell surfaces (dotted trace) on gated $CD14^+$ monocytes were detected using $F(ab')_2$-anti-human IgM-RPE (right panel). (**B)** To investigate whether DBLMSP proteins bind to monocytic cells, monocytic cell population was gated based on forward (*FSC*) and side (*SSC*) scatter profiles of PBMCs (shown by blue dots, left panel). Binding of normalised biotinylated DBLMSP (blue trace) or DBLMSP2 (pink trace) to monocytic cells was detected using anti-biotin-APC (right panel). Data are representative of three repeat experiments.

4.3.6. DBLMSP and DBLMSP2 per se do not induce proliferation or apoptosis of human lymphocytes

Recent studies have suggested that chronic *P. falciparum* exposure induces immune dysfunction among B and T cell responses that may explain why immunity to malaria is slow to develop [289]. Immune dysfunction may include non-specific proliferation [290] and/or increased apoptosis [291] of immune cells. Since human lymphocytes, and B cells in particular, were shown to bind DBLMSP and DBLMSP2 we hypothesised that DBLMSP and DBLMSP2 may induce lymphocytes to proliferate or to undergo programmed cell death by apoptosis. Neither recombinant DBLMSP nor DBLMSP2 *per se* had any observable proliferative or apoptotic inducing functionality when co-cultured in the presence of human PBMCs (Figure 4.12 & 4.13, respectively). Similar results were obtained if DBLMSP or DBLMSP2 were complexed with IgM or coated directly to the surface of culture wells prior to incubation to with PBMCs to facilitate cross-linking of surface receptors (see appendix III; Figure A1).

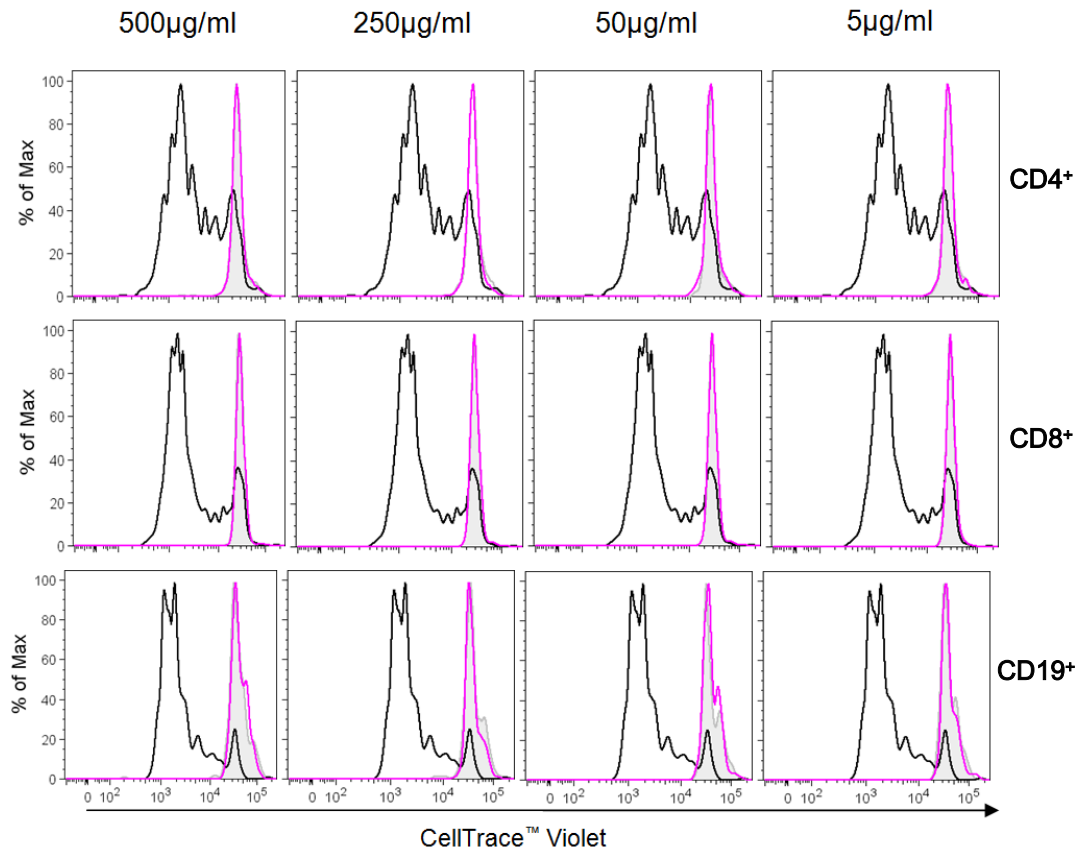

Figure 4.12 DBLMSP and DBLMSP2 do not induce cellular proliferation of lymphocytes. Purified CellTrace™ Violet-labelled PBMCs from malaria-naive individuals were co-cultured with varying concentrations of his-tagged DBLMSP (pink trace) or media only (grey trace). CellTrace™ Violet dilution of gated lymphocytes was examined five days post-incubation by flow cytometry. DBLMSP did not induce proliferation of gated $CD4^+$ (upper panel), $CD8^+$ (middle panel), or $CD19^+$ (lower panel) lymphocytes but was induced by the positive control, PHA (black trace). Similar results were observed with DBLMSP2 and Cd4-d3+4 control (data omitted for clarity). Data are representative of one of four repeat experiments.

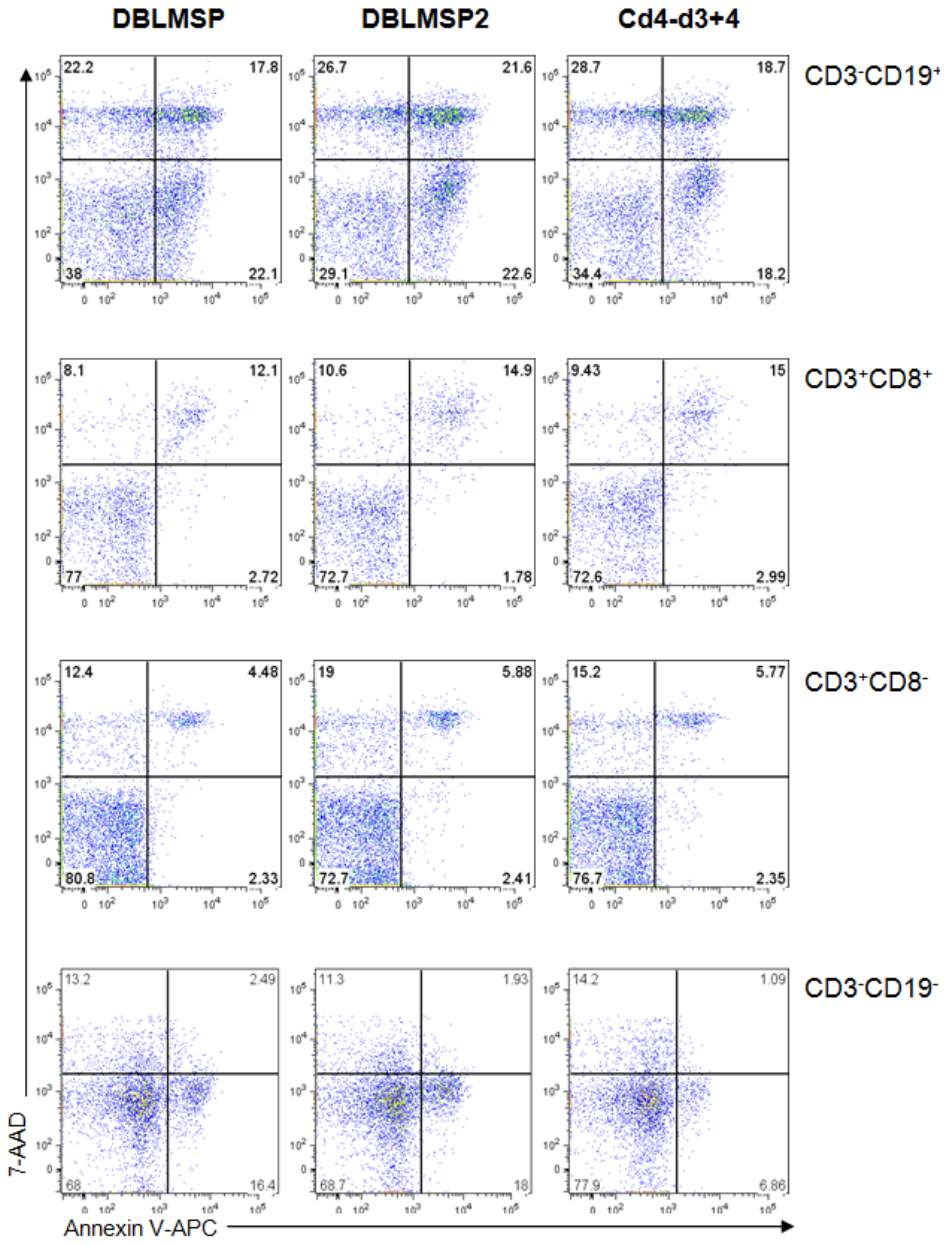

Figure 4.13 DBLMSP and DBLMSP2 do not induce apoptosis of lymphocytes. PBMCs were co-cultured with 50µg/ml his-tagged DBLMSP, DBLMSP2, or Cd4-d3+4 control for 24hr and analyzed for apoptosis by Annexin V and 7-AAD staining on gated lymphocyte populations. Apoptosis of lymphocytes are calculates as percentage of Annexin V^+7-AAD^- (early apoptosis), Annexin V^+7-AAD^+ (late apoptosis), or Annexin V^-7AAD^+ (dead) cells. Dot plots from one of three independent experiments are shown.

4.3.7. DBLMSP *per se* do not inhibit proliferation of human lymphocytes

FcμR has been previously implicated in enhanced B cell survival and proliferation following BCR cross-linking [138, 292]. Since the malaria proteins did not seem to initiate proliferation or apoptosis of PBMCs, it remained to be determined whether the binding of the malaria proteins to lymphocytes could function to inhibit cellular proliferation. For this, DBLMSP was preincubated with phytohaemagglutinin (PHA) or the TLR-9 agonist CpG ODN 2006 (CpG) for the induction of cellular proliferation of T cells and B cells, respectively, and then co-cultured in the presence of PBMCs. Preliminary data showed inhibition of cellular proliferation of $CD4^+/CD8^+$ T cells and $CD19^+$ B cells with saturating concentrations of DBLMSP but not Cd4-d3+4 (Figure 4.14). However, repeat experiment using two additional donors and further titrations of the recombinant proteins revealed a dose-dependent but protein non-specific inhibitory effect, owing to the inhibition observed at saturating concentrations of DBLMSP and Cd4-d3+4 (Figure 4.15).

Similar results were observed when DBLMSP was complexed to hIgM (Figure 4.16; upper panels). To our surprise, high concentrations of hIgM were also shown to inhibit the proliferation of $CD4^+/CD8^+$ T cells and $CD19^+$ B cells (Figure 4.16; middle panels). The specificity of IgM-mediated inhibition was confirmed in subsequent experiments, as proliferation of T cells and B cells was inhibited in a dose-dependent manner with cells co-cultured with high concentrations of hIgM but not BSA (see Chapter 6).

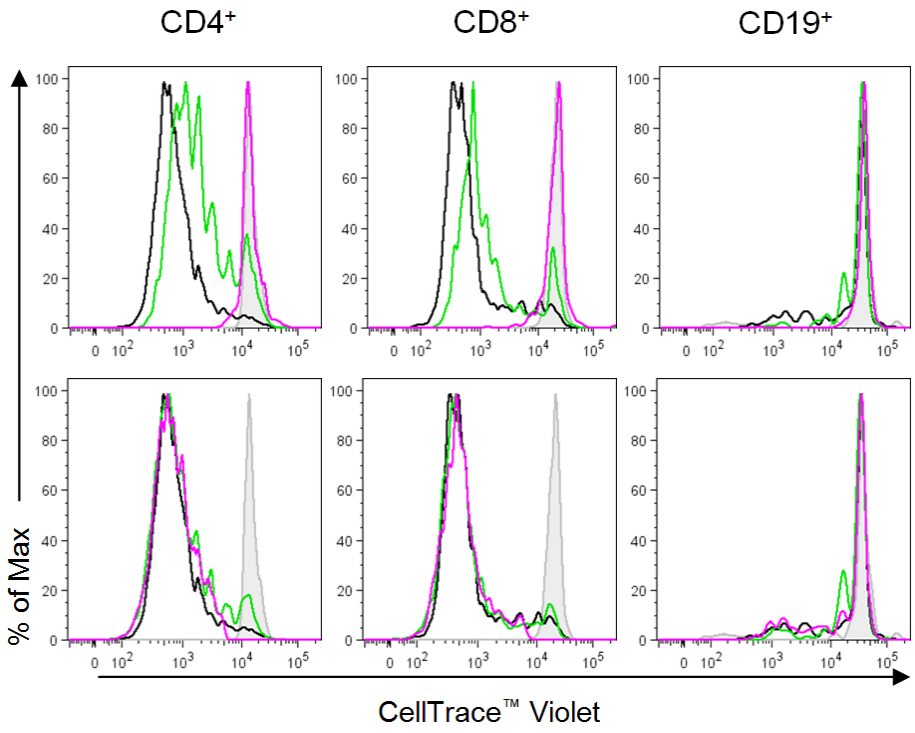

Figure 4.14 Saturating concentrations of DBLMSP appeared to inhibit proliferation in one donor. To investigate whether DBLMSP functions to inhibit cellular proliferation of T cells and/or B cells, varying concentrations of his-tagged DBLMSP or control protein Cd4-d3+4 were incubated with 5µg/ml PHA or 1µg/ml CpG for 30 min at 4˚C. CellTrace™ Violet-labelled PBMCs were then cultured for 5 days in media alone (grey filled trace) or with PHA (5µg/ml), CpG (1µg/ml), or PHA/DBLMSP, PHA/Cd4-d3+4, CpG/DBLMSP, and CpG/Cd4-d3+4 mixtures. Cellular proliferation of gated lymphocytes was investigated by flow cytometry. Saturating concentrations (500µg/ml) of DBLMSP (pink trace; upper panel) resulted in the inhibition of PHA-induced proliferation of $CD4^+$ and $CD8^+$ T cells, whereas slight inhibition was observed with Cd4-d3+4 (green trace; upper panel). Additionally, slight inhibition of CpG-induced proliferation of $CD19^+$ B cells by DBLMSP was observed at saturating concentrations (pink trace; upper panel). These effects were not observed at a lower concentration (50µg/ml), indicating that inhibition of cellular proliferation by DBLMSP was dose-dependent for this donor (*n*=1).

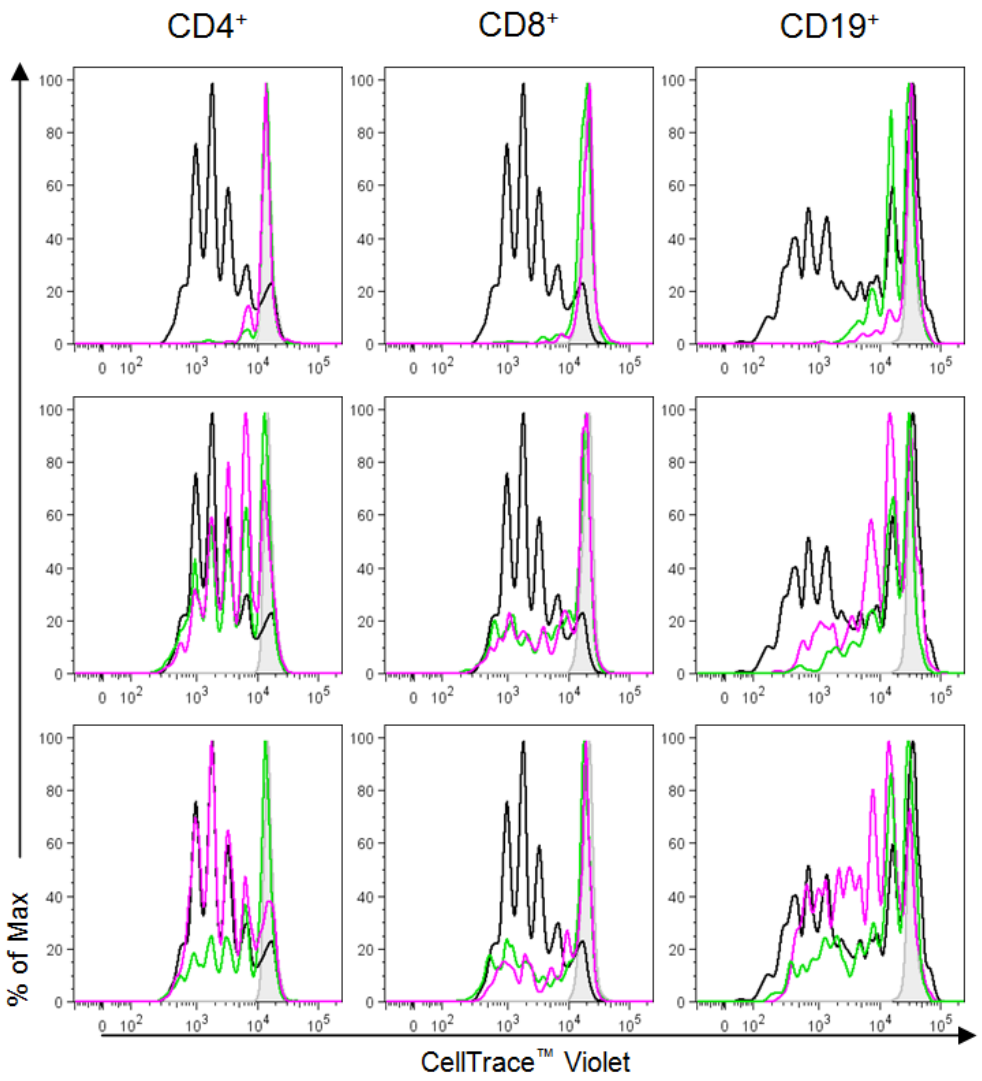

Figure 4.15 Inhibitory effect of DBLMSP is non-specific. To further investigate the ability of DBLMSP to inhibit cellular proliferation, the inhibition assay described above was repeated in another two donors and the concentrations of DBLMSP and Cd4-d3+4 his-tag proteins were further titrated. In these experiments, inhibition of PHA-induced proliferation of $CD4^+$ and $CD8^+$ T cells, and CpG-induced proliferation of $CD19^+$ B cells was observed for DBLMSP and Cd4-d3+4 at saturating concentrations (500µg/ml; top panels). This effect was dose-dependent, but not protein-specific, as the inhibitory effect decreased with decreasing protein concentrations (250µg/ml and 50µg/ml; middle and lower panels, respectively). Data are representative of two repeat experiments.

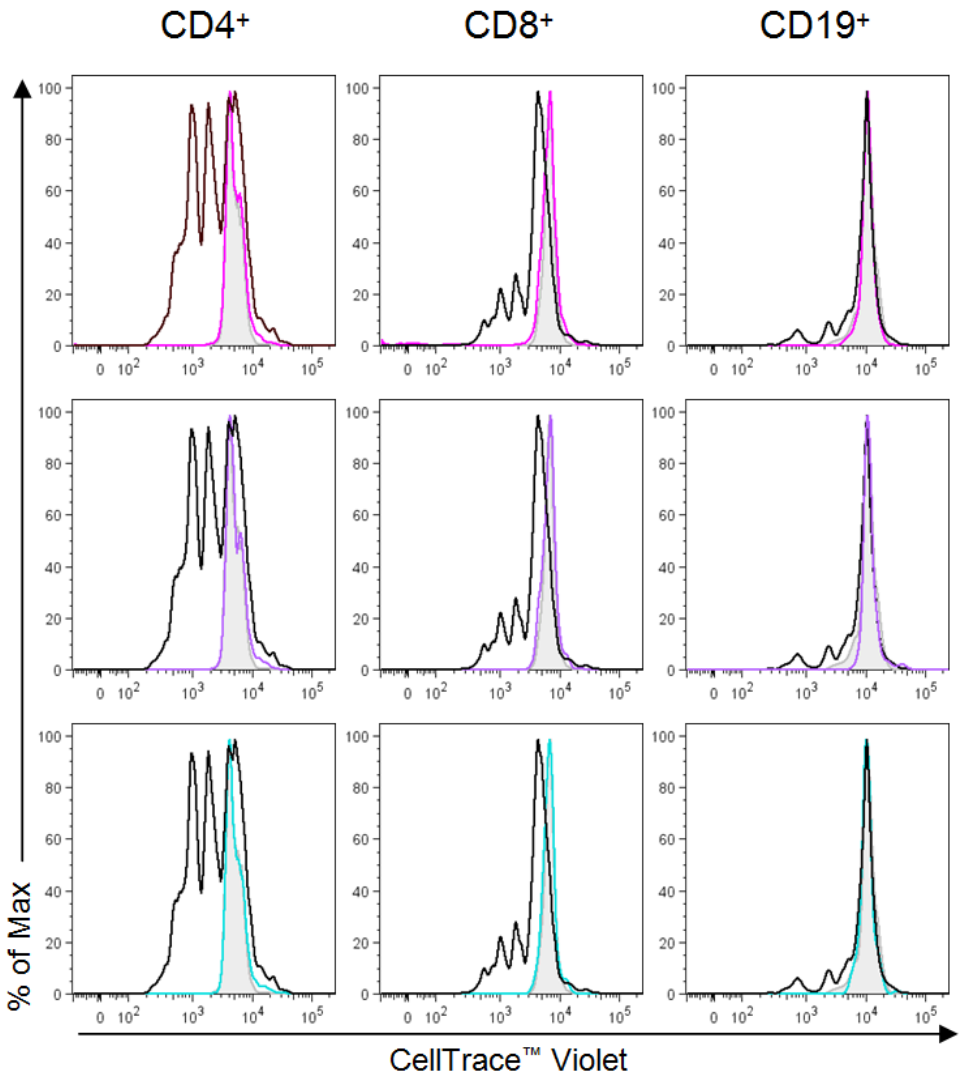

Figure 4.16 IgM/DBLMSP immune complexes inhibit cellular proliferation at saturating concentrations. Saturating concentrations of the IgM/DBLMSP complex (pink trace; upper panel), when co-cultured with PHA or CpG (5µg/ml and 1µg/ml, respectively), induce inhibition in gated lymphocytes. Co-culture of IgM with stimulants also initiated inhibition of cellular proliferation (purple trace; middle panel). IgM alone did not induce proliferation (aqua trace; lower panels).

4.3.8. Immunoglobulins bind stimulants

A striking finding was that hIgM inhibited cellular proliferation of stimulated lymphocytes (Figure 4.16). IgM molecules are heavily mannosylated, and the ability of oligomannose residues of hIgM to bind lectins, such as mannose-binding lectin (MBL), has been well characterised [168, 293]. Therefore, a possible explanation for the observed inhibition of proliferation by hIgM could be that IgM binds directly to PHA, and subsequently prevents their interaction with cellular receptors.

To test this hypothesis, the ability of human immunoglobulins (Ig) to bind various stimulants, including PHA, CpG, lipopolysaccharide (LPS) and pokeweed mitogen (PWM), was assessed by ELISA. As seen in Figure 4.17, a variety of stimulants bound human Igs. There was significant binding of PWM to human IgM, IgG, and IgA, with two-fold binding of IgM to PHA compared to IgG. IgM also bound PHA and LPS significantly. For hIgA, significant binding was observed with PHA and CpG. There was no significant binding of IgG to PHA, CpG, and LPS, when compared to the control (PBS) (Figure 4.17). These results show that PHA, LPS and PWM bind hIgM, which may account for the results observed in Figure 4.16.

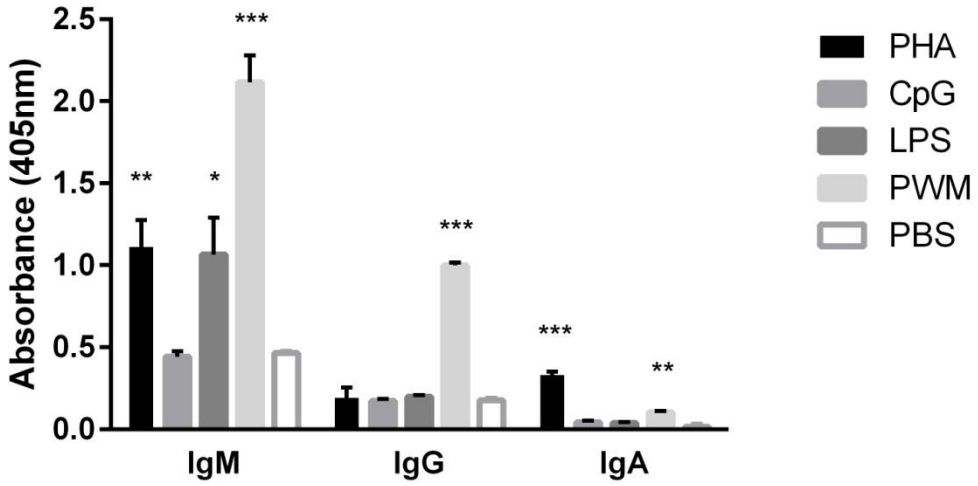

Figure 4.17 Immunoglobulins bind various stimulants by ELISA. The binding of coated stimulants (10µg/ml) to different Ig isotypes (10µg/ml) was detected using mouse anti-human Ig-HRP Abs specific for each Ig isotype. The mean ± SD for three replicates are shown (*n*=3). Significant differences were determined using a paired t-test, in which binding of Igs to stimulants was compared to binding to PBS: *****p <0.05, ****** p <0.01, and ******* p <0.001.

4.3.9. IgM exists in complex with DBLMSP/DBLMSP2 and other unidentified parasite molecules

One possible explanation for the lack of an observed effect of recombinant DBLMSP and DBLMSP2 *per se* may be that these proteins associate with other merozoite surface proteins during culture or *in vivo* that were not available in the functional assays with the recombinant proteins investigated here. For example, it is known that MSP3, MSP6, and MSP7 associate non-covalently with MSP1[294].

Therefore, IgM was immunoprecipitated from culture supernatants isolated from long-term *P. falciparum* ITGvar1 and ITGvar13 parasite cultures, or from negative controls without parasite, and their reactivity with DBLMSP-specific Abs (Figure 4.18A; left panel) or Malawian (malaria) immune sera (Figure 4.18A; right panel) was determined. A ~100kDa band corresponding to native DBLMSP could be detected with an anti-DBLMSP polyclonal Ab in the parasite cultures but not in the negative control (Figure 4.18A; left panel, boxed) consistent with previous observations [149, 281]. Immune sera from Malawians recognised additional parasite antigens that are also found in complex with IgM (Figure 4.18A; right panel). These data were also extended to pull-down experiments with 3D7 parasites from which these DBLMSP proteins were originally cloned (Figure 4.18B). Bands were observed at ~250kDa, 100kDa, 53kDa and 25kDa for IgM pull-downs from ITGvar1 and ITGvar13 cultures (Figure 4.18A; right panel), and ~250kDa, 140kDa, 100kDa, 80kDa, and 36kDa for IgM pull-downs from 3D7 culture (Figure 4.18B; right panel), which were not detected using non-immune sera. In these experiments, the detecting Ab appeared to cross-react with numerous other proteins present in the pull-down solution, including the heavy and light chains of IgM (Figure 4.18A; left panel). However, we identify suspected parasite proteins as bands that appeared for the parasite pull-down samples but not for the negative control.

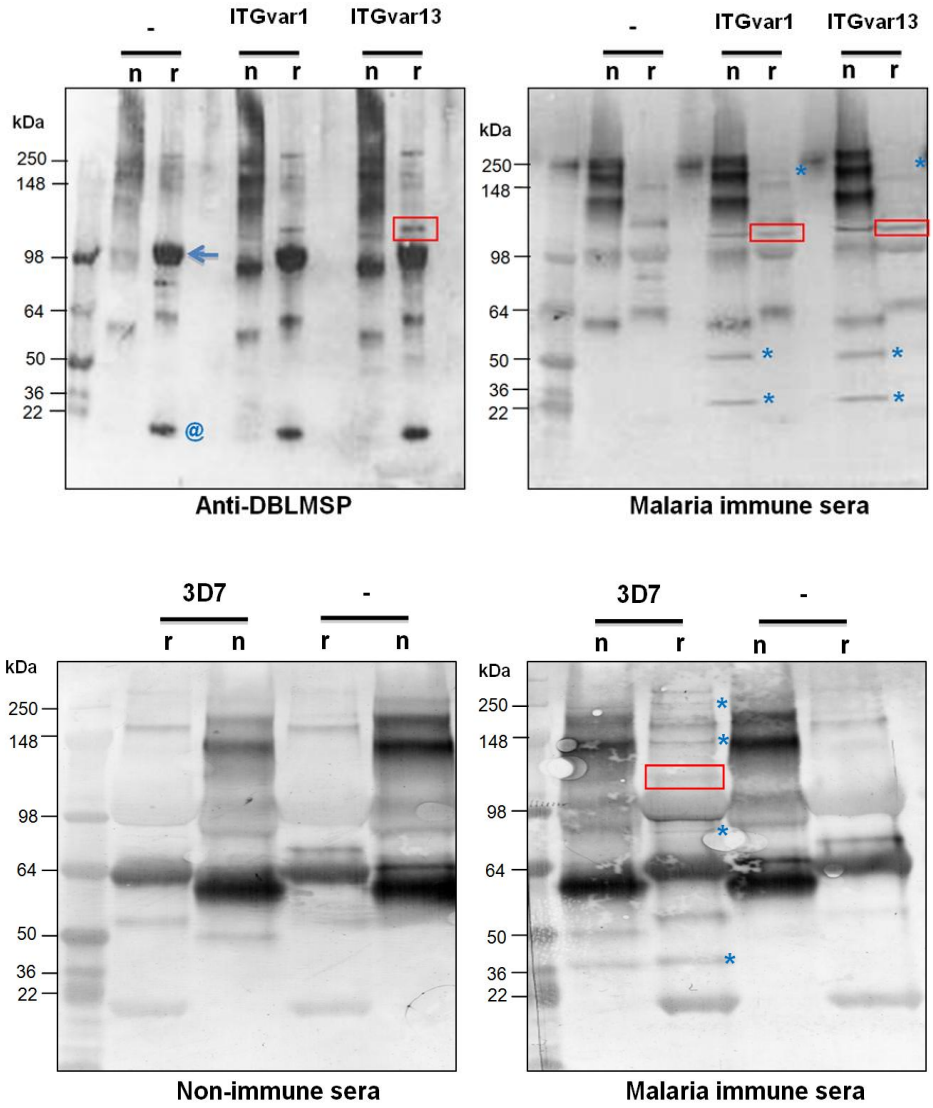

Figure 4.18 Additional parasite proteins are present in the IgM-DBLMSP complex. *P. falciparum* strains ITGvar1, ITGvar13, and 3D7 were cultured in the presence of 10% human AB serum (Sigma-Aldrich). IgM was immunoprecipitated from culture supernatant using anti-human IgM-agarose beads and washed three times in PBS. Non-reducing and reducing buffer was added to the beads, which were boiled for 5 min prior to being run on a 4-12% Bis-Tris gel. Following transfer to nitrocellulose membrane by Western blotting, membranes were blocked, washed extensively and incubated with rabbit anti-DBLMSP/2-mAbs or with sera for 3hr at RT. After extensive washing, parasite proteins in immunoprecipitations were detected using anti-rabbit IgG-peroxidase (1:1000; Sigma-Aldrich) or anti-human IgG-AP (1:2000; Sigma-Aldrich). Parasite proteins (shown as *) were regarded as bands present for the parasite strains that were absent from the negative control (-). The anti-rabbit IgG (whole molecule) cross-reacts with hIgM (arrow = IgM heavy chain, @ = light chain), detecting Ab was only absorbed against human IgG not IgM. However, this provided a good internal control for protein loading. Negative controls cultures (-) were incubated as for ITGvar1, ITGvar13, and 3D7 but without parasites. Suspected bands for DBLMSP/2 are boxed.

Alongside the IgM-immunoprecipitations, we investigated whether the presence of these additional parasite proteins within hIgM-DBLMSP complex blocked interactions of hIgM to hFcμR. IgM from parasite culture supernatants was still able to bind hFcμR-transfected cell, suggesting that the presence of additional parasite proteins within the complex does not affect its interactions with hFcμR (Figure 4.19).

Although these molecules remain to be identified, it does suggest that future experiments to determine the function of DBLMSP and/ or DBLMSP2 need to be undertaken with native material rather than with recombinant proteins alone, as the unidentified parasite proteins within complexes could initiate immunomodulatory effects such as the proliferation or apoptosis of lymphocytes.

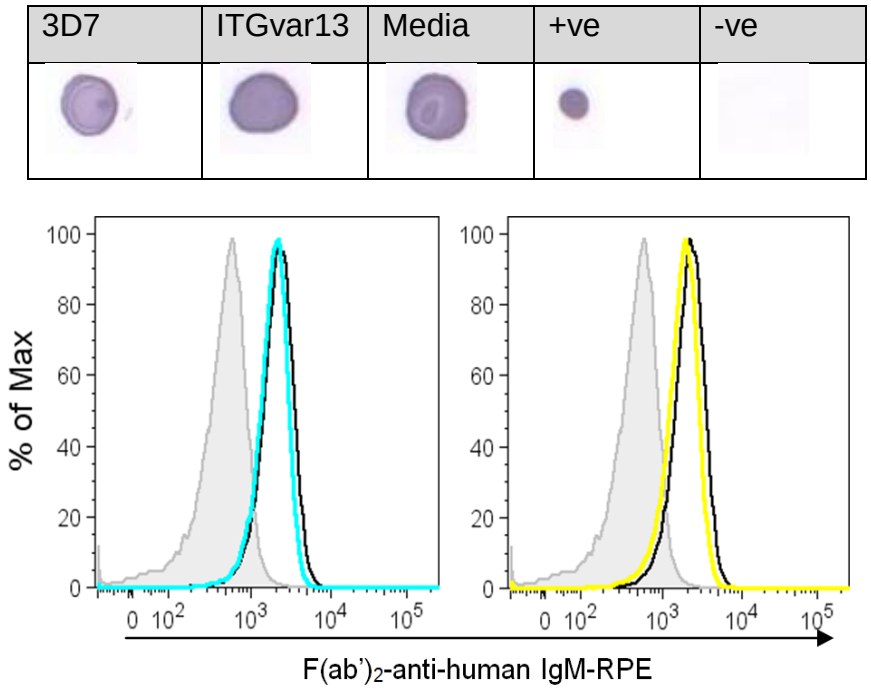

Figure 4.19 Parasite culture pull-down IgM can bind FcμR. Immunoblots were performed on *P. falciparum* 3D7 and ITGvar13 parasite culture supernatants to confirm presence of IgM. For this, 5µl culture supernatant was blotted onto nitrocellulose paper and allowed to dry, then blocked with PBST/5% milk powder for 1hr at RT. Following extensive washing, IgM was detected using mouse anti-human IgM-AP (1:5000 dilution).After confirming the presence of IgM in culture supernatants, 50µl of culture supernatant (predicted to contain 5µg hIgM) from each strain was incubated with hFcμR-transfected cells for 1hr at 4˚C, washed labelled with F(ab')2-anti-human IgM-RPE and analysed by flow cytometry. Binding of IgM isolated from 3D7 (aqua trace; left panel) or ITGvar13 (yellow trace; right panel) parasite cultures, or human IgM alone (5µg; black trace) are shown as overlays (*n*=2).

4.3.10. Molecular dynamic simulation of the IgM/FcμR/DBLMSP interaction

A working atomic model of the IgM/DBL interaction was recently characterised [100, 135]. Based on this structure, we investigated whether a physically plausible model of the IgM/FcμR/DBLMSP interaction could be produced that might provide insight into the results generated in this chapter.

A homology model of DBLMSP was generated using the known structures of members of the DBL family [196, 295], for which there is a high sequence similarity. This was used to build the IgM/FcμR/DBLMSP, alongside the previous model for IgM [135] and hFcμR (Chapter 3).

The binding of two DBLMSP proteins (maximally) to a single IgM monomer (within the pentameric or hexameric complex) severely restricts the potential binding sites on IgM for the FcμR. Furthermore, the fact that glycans are not required for this interaction and the likely involvement of two IgM domains (Cμ2/Cμ4 or Cμ3/Cμ4) (shown in Chapter 3) also provides constraints on these binding sites. Inspection of the IgM/DBLMSP model showed that the interface of Cμ3/Cμ4 is completely buried by the DBLMSP domains (Figure 4.20A). The N-linked glycosylation sites were positioned away from the predicted DBLMSP binding site, potentially explaining the findings that glycosylation of IgM did not affect DBLMSP binding (Figure 4.4).

As the FcμR interaction with IgM does not completely prevent DBLMSP interaction with IgM (Figure 4.5), we thus reasoned that FcμR contacts the Cμ2/Cμ4 interface (Figure 4.20B), similar to a type I engagement of Ab-receptor interactions [244]. In this orientation, CDR loops of the FcμR Ig-like domain completely cover the Cμ2/Cμ4 interface, resulting in a partial occlusion of one of the DBLMSP domains (Figure 4.20B & Figure 4.21). Such an occlusion is not extensive (involving only 5% of the residues in the DBLMSP and 16% in the FcμR Ig-like domain), and so would be expected to only perturb, but not completely prevent, the simultaneous association of DBLMSP and FcμR with IgM, as was observed experimentally (Figure 4.5). A similar association of dimeric FcμR with this Cμ2/Cμ4 interface also shows partial overlap with the DBLMSP (34% of the residues in the DBLMSP and 16% the FcμR Ig-like domain)(Figure 4.20C & Figure 4.21).

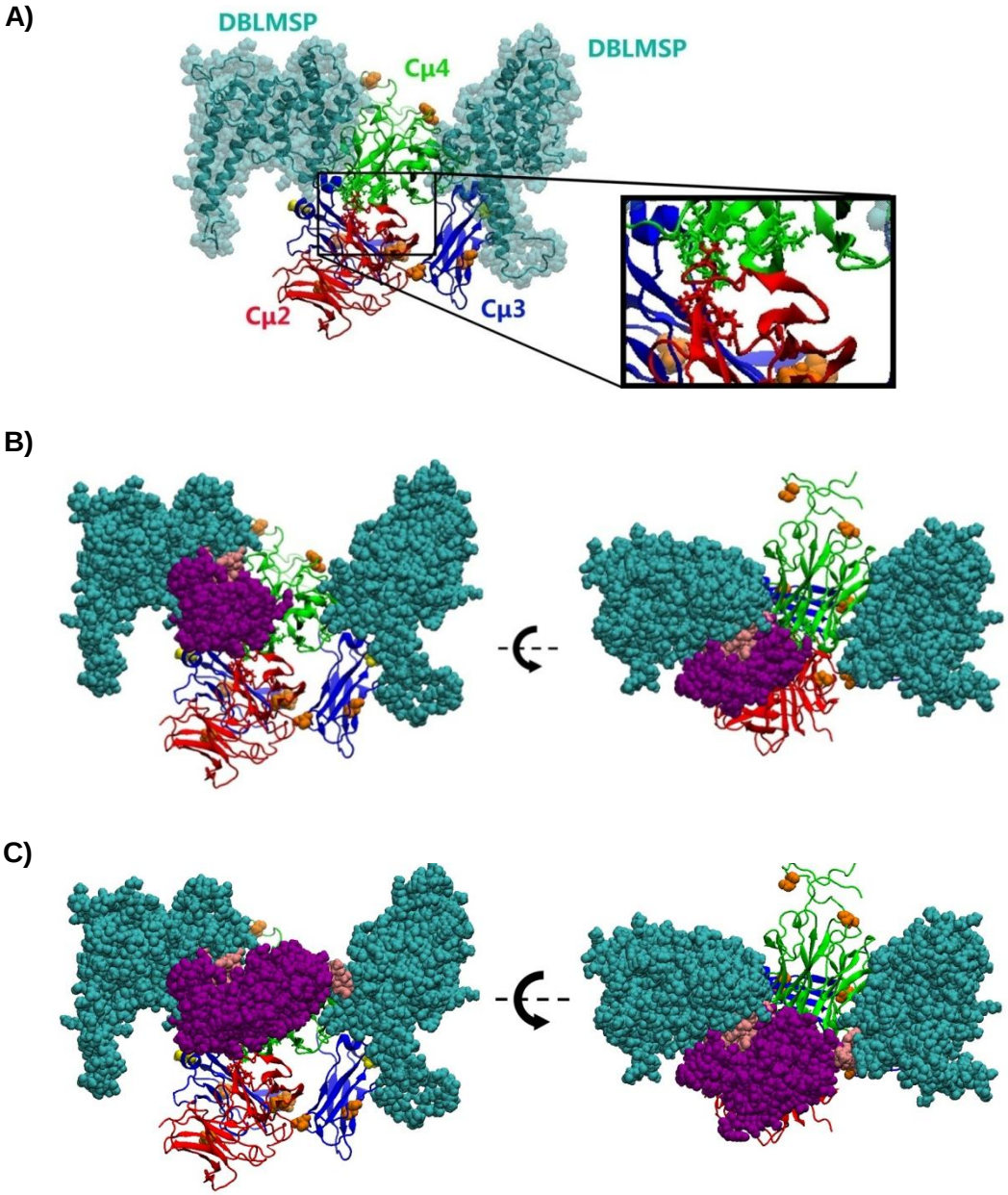

Figure 4.20 (A) Model of the interaction between IgM-Fc and two DBLMSP proteins, shows DBLMSP (shown in teal) can engage IgM-Fc principally via the Cμ4 domain (shown in green), and partially via the Cμ3 domain (shown in blue). N-linked glycans sites are depicted as van der Waals spheres (shown in orange), which are positioned outside of the IgM-DBLMSP binding site. The box depicts the predicted binding site of hFcμR. The interaction between the DBL domain of DBLMSP (shown in teal) and IgM-Fc (as in *A*) is also shown, in which hFcμR (shown in magenta) is depicted as monomer **(B)** or as a dimer **(C).** Note that in this orientation, there are residues within the Ig-like domains of hFcμR which occlude the DBLMSP proteins (shown as salmon spheres). The model suggests that DBLMSP proteins are able to engage IgM bound to hFcμR as a monomer or dimer, which occurs outside the glycosylated regions of IgM-Fc.

Together with the structural data presented in Chapter 3, we show here that is it physically viable for IgM-DBLMSP complexes to interact with hFcμR. This supports the experimental findings that the binding of DBLMSP and DBLMSP2 to IgM does not completely block subsequent interactions with the receptor.

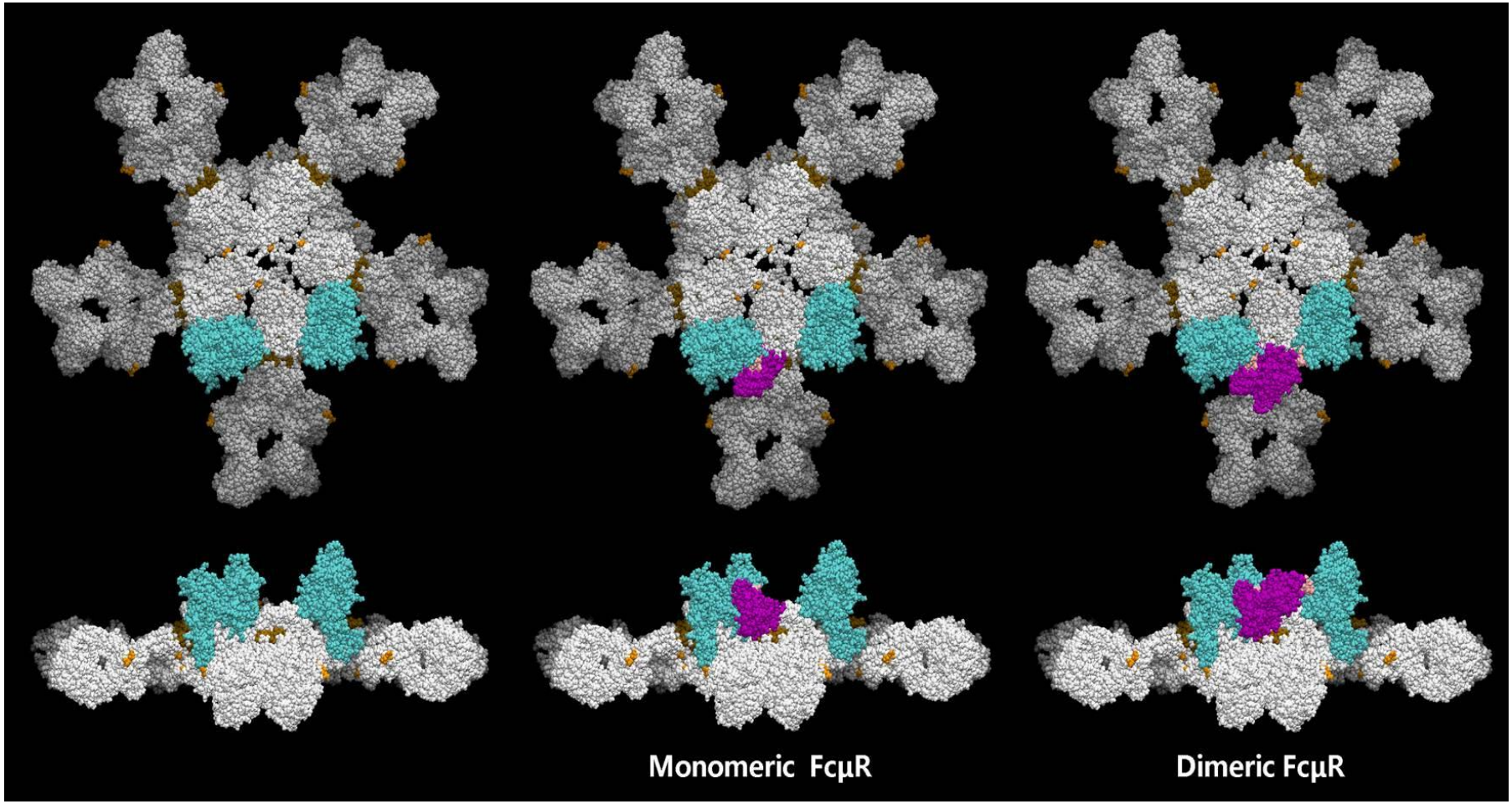

Figure 4.21 Model of the DBLMSP- pentameric IgM- hFcμR interaction. Interaction between DBL domain of DBLMSP (shown in teal), pentameric IgM (shown in white) and hFcμR (shown in magneta).

4.4. Discussion

DBLMSP and DBLMSP2 are two newly characterised *P. falciparum*-encoded proteins which avidly bind non-immune hIgM via their DBL domains, in order to mask immunogenic antigens on merozoite surfaces from humoral immune recognition [146]. However, whether these proteins perform additional functions is unknown. In this chapter, we show that DBLMSP and DBLMSP2 bind the same domain of hIgM as recognised by hFcμR, but do not completely block interactions between hIgM and hFcμR. In fact, full-length DBLMSP and DBLMSP2 were able to engage IgM^+ lymphocytes, but did not cause any biological consequences *per se*. This was possibly owing to the fact that additional parasite proteins are present in the DBLMSP-IgM complex.

In order to investigate why *P. falciparum* express IgM-binding proteins on merozoite surfaces, we first sought to confirm how these proteins recognise hIgM. The expression of the individual DBL and SPAM domains of DBLMSP and DBLMSP2 revealed that the DBL domain governs interactions with hIgM. A panel of domain-swap Abs [120] confirmed the Cμ4 domain of hIgM as the target of DBLMSP and DBLMSP2, as previously described [146]. In addition to the Cμ4 domain, the presence of the Cμ3 domain in domain-swap Abs significantly enhanced binding of DBLMSP and marginally enhanced binding of DBLMSP2 to IgM. Numerous PfEMP1 variants bind non-immune IgM via their DBL domains [118, 120], which also recognise the Cμ4 domain of hIgM [120]. This, together with the data presented here, highlights the potential importance of DBL domains in *P. falciparum* malaria and suggests that *P. falciparum*-encoded proteins utilise a conserved mechanism to bind non-immune hIgM. It will be of interest to explore the sequences of *P. falciparum* proteins which bind non-immune hIgM to see whether there are conserved sequences which govern this interaction. As the binding of non-immune hIgM by both PfEMP1 and DBLMSP variants has been implicated in the shielding of immunogenic epitopes from humoral immune responses [146, 284], the development of strain-transcending Abs which inhibit non-immune IgM-binding could be implicated in vaccine design to enhance vaccine efficacy.

Given that DBLMSP and DBLMSP2 recognise the same domain of hIgM as hFcμR (see Chapter 3), we hypothesised that these proteins may have evolved to block

interaction of hIgM with hFcμR. To investigate this, the ability of hIgM preincubated with full-length recombinant DBLMSP proteins to hFcμR-transfected cells was assessed by flow cytometry. DBLMSP partially (~15-30%) inhibited hIgM binding to hFcμR, whereas DBLMSP2 had no effect on binding, suggesting that these malaria proteins bind to the same domain but not the same residues of IgM as hFcμR. Although not significant, the blocking effect could have implications in malaria immunity since hFcμR has previously been shown to enhance B cell survival and Ab responses [137, 138, 182]. However, the effect of this partial blocking needs to be determined *in vivo*. In addition, as this effect was only observed at saturating concentrations, quantification of soluble DBLMSP in the periphery is required. Despite the observed inhibition, the majority of hIgM still bound to hFcμR suggesting that the function of these proteins is not to block IgM-hFcμR interactions.

As the binding of DBLMSP to hIgM did not significantly inhibit subsequent interactions with hFcμR, we next investigated whether these proteins utilised cell-surface IgM to bind to host cells. DBLMSP and DBLMSP2 bound to hIgM on hFcμR-transfected cells, whereas DBLMSP was found to consistently bind better to than DBLMSP2, possibly reflecting the difference in their affinity for IgM [146] or could signify that the proteins serve different biological functions during malaria infections. Similar results were observed for lymphocytes known to express hFcμR [137]. Due to the high affinity interaction between hIgM and hFcμR, the majority of purified lymphocytes are opsonised in hIgM. We therefore investigated if DBLMSP and DBLMSP2 could interact with hIgM bound to immune cells, and found that these proteins were only able to bind to IgM^+ lymphocytes. Strikingly, the majority of $CD19^+$ B cells bound both DBLMSP and DBLMSP2, whereas less binding observed for $CD4^+$/$CD8^+$ T cells and $CD56^+$ NK cells. One explanation for the high proportion of binding to $CD19^+$ B cells includes the binding of DBLMSP to IgM^+ BCR as well hFcμR. DBLMSP and DBLMSP2 also bound to the monocytic cell population, previously shown to bind hIgM (Chapter 3). However, the identity of the subsets binding these proteins remains unidentified, as does the receptor to which they bind. We also observed considerable variation in DBLMSP binding between donors, most likely owing to differential expression of hFcμR and/or surface levels of hIgM on lymphocytes. To confirm this, additional experiments should investigate whether the binding of DBLMSP to lymphocytes correlates with hFcμR expression.

In addition, lymphocyte subsets which bind these malarial proteins should be identified as disturbances in B cell homeostasis has been reported in *P. falciparum* infections [296, 297]. Regardless of donor variation, lymphocytes isolated from each donor bound recombinant full-length DBLMSP and DBLMSP2 but not the control protein, signifying the specificity of this interaction. To our knowledge, this is the first report of the conserved binding of malaria proteins binding directly to B cells, T cells, and NK cells.

Despite the fact that the DBL domains of DBLMSP and DBLMSP2 govern binding to hIgM [146], these domains alone were insufficient to permit binding to IgM^+ immune cells that express hFcμR. As the SPAM domain has been implicated in oligomerisation of DBLMSP and DBLMSP2 [146], as well as in MSP3 [276], it is possible that monomers of DBL domains do not generate sufficient avidity to interact with hIgM on hFcμR. This supports previous data which showed the affinities of DBLMSP and DBLMSP2 for IgM were decreased ~200- to 550- fold in the absence of the SPAM domain [146]. The requirement of oligomerisation for receptor binding has also been proposed for other DBL-containing proteins such as EBA-175 and *Pv*DBP [147]. Therefore, it is possible that oligomerisation of DBLMSP and DBLMSP2 is a prerequisite for ligand recognition. Hodder et al. hypothesised that dimerisation via the SPAM fragments would orientate two DBL domains in a parallel fashion; however the presence of a flexible linker region between the DBL and SPAM fragments could permit variations in DBL orientation [147]. Resolving the crystal structure of full length DBLMSP and/or DBLMSP2 will help clarify how the SPAM domain could permit oligomerisation of these proteins.

In addition to hFcμR, DBLMSP and DBLMSP2 also interacted with hIgM bound to DC-SIGN. Since our previous research identified glycan residues on hIgM as the ligands for DC-SIGN [136], we wished to determine if DBLMSP and DBLMSP2 utilised glycans for hIgM binding. The removal of glycans did not block the binding of these proteins to hIgM, but rather marginally enhanced binding, possibly owing to the fact that the glycans are confined to the non-Ag binding face of hIgM due to its barrel-like structure [169]. The removal of glycans could therefore facilitate interactions between the DBLMSP proteins and the Cμ4 domain that were previously restricted due to steric hindrance. Together this data suggests that DBLMSP engage hIgM via

residues outside of the glycosylation regions, which may help to characterise how these proteins are able to interact with IgM bound to receptors such as hFcμR or DC-SIGN. As interactions between blood stage *Plasmodium* parasites and dendritic cells (DCs) are pivotal for priming adaptive immune responses against malaria [298], and since DBLMSP and DBLMSP2 do not bind the glycans recognised by DC-SIGN, it is tempting to speculate that these proteins may have evolved to permit interactions of merozoites with DCs. Since these malaria proteins do not appear to be involved in erythrocyte invasion, it may be more likely that they have evolved to interact with other cell types. This area requires further research to determine whether these proteins can bind to hIgM on DC cell surfaces, and what the consequence of this binding may be.

Immune dysregulation is characteristic of *P. falciparum* infections [123]. Since a high proportion of $CD19^+$ B cells bound DBLMSP and DBLMSP2, we hypothesised that binding of these proteins to hFcμR and/or IgM^+ BCR could induce cross-linking of receptors resulting in downstream effector functions, such as proliferation or apoptosis. This hypothesis supports previous findings that hFcμR initiates signalling pathways through conserved tyrosine and serine residues in its cytoplasmic tail [137, 140]. Although DBLMSP and DBLMSP2 bound to IgM^+ lymphocytes, the proteins did not induce proliferation or apoptosis of $CD19^+$ B cells, $CD4^+$/$CD8^+$ T cells, nor monocytic cell populations. However, *P. falciparum* culture pull-downs revealed that additional parasite proteins were also complexed to hIgM, possibly explaining why the use of recombinant DBLMSP and DBLMSP2 alone did not generate any functional effects *per se* in these experiments.

The finding that numerous parasite proteins immunoprecipitated with hIgM supports the hypothesis that merozoite surface proteins are able to form complexes [294]. Parasite proteins of ~250kDa, 100kDa, 53kDa, and 25kDa from ITGvar1 and ITGvar13 long-term cultures, and ~250kDa, 140kDa, 100kDa, 80kDa, and 36kDa from 3D7 long-term cultures, were isolated using IgM pull-downs. The observed band at ~100kDa was predicted to be the DBLMSP proteins, since it was of the correct corresponding MW, and anti-DBLMSP Abs identified a band of similar MW (Figure 4.18A; right panel). Although the identity of the additional proteins remain to be determined, immunoprecipitations using anti-$MSP1_{42}$ Abs captured proteins of

similar MW and identified them as two putative RAP proteins (~110 and 22kDa) and RhopH3 (~50kDa) by mass spectrometry [294]. As RhopH3 and RAP proteins have been implicated in parasite invasion of RBCs [294, 299], future research should aim to identify the additional parasite proteins by mass spectrometry, and investigate whether these proteins exist in complex with or can bind directly to IgM.

Another reason why the binding of recombinant DBLMSP to lymphocytes produced no functional effects could be owing to the use of non-native forms of the proteins. Hodder et al. identified two forms of DBLMSP and DBLMSP2; a mature form of corresponding MW to the full-length proteins (~75 and 100kDa, respectively), and a ~25kDa shorter protease-cleaved processed form [147]. The mature form was found in the culture supernatant of saponin-treated 3D7-infected erythrocytes, supporting the hypothesis that these proteins are present in the periphery, whereas the processed form was confined to the cell pellet [147]. They speculated that the unprocessed forms which are not incorporated into the merozoite membrane may act as immuno-decoys in the periphery to generate inappropriate immune responses [147]. However, confirmation is required to confirm the presence of the mature or processed forms of DBLMSP in the periphery, and determine whether they form complexes with hIgM. It will be of interest to repeat the functional assays with the processed form of DBLMSP and DBLMSP2 to see whether similar results are obtained.

Experiments investigating whether DBLMSP initiated inhibition of proliferation in lymphocytes produced some unexpected results. Inhibition of cellular proliferation was observed at saturating concentration with DBLMSP and the control protein Cd4-d3+4, and thus was attributed to a protein-loading effect. When investigating whether DBLMSP needed to be complexed to hIgM to initiate inhibition, high concentrations of IgM-DBLMSP complexes were observed to promote inhibition, as did saturating concentrations of hIgM. IgM is heavily mannosylated, and the ability of the oligomannose residues of hIgM to bind lectins such as mannose-binding lectin (MBL) has been well characterised [168, 293]. Therefore, an explanation for the observed inhibitory effect could be that IgM directly binds to the stimulants and thus prevents their interaction with cellular receptors. In support of this hypothesis, we observed significant binding of hIgM not only to PHA but also to PWM and LPS, but interestingly not CpG. LPS is an integral structural component of the outer

membrane of Gram negative bacteria, and potently induces innate immune responses through interactions with several host proteins [300]. Therefore, it is conceivable to speculate that the binding of hIgM to LPS is specific (e.g. Fab-mediated) and results from immunity to previous bacterial infections. This explanation cannot be extended for the binding of hIgM to PWM and PHA, since these are lectins found in plants. It is tempting to propose that IgM binds to PHA and PWM in a glycan-dependent manner. Repeating these experiments with endoglycosidase-treated IgM could help clarify the role of glycans in mediating binding of stimulants to IgM. These results are significant as they suggest that binding of stimulants by Igs should be considered for functional assay design.

Finally, the atomic model of the IgM/FcμR/DBLMSP interaction provided a physical means to explain the experimental data generated in this chapter. This model was built using the DBL domains of DBLMSP, which predicted maximal binding of two DBL domains to a single IgM monomer. As the oligomerisation status of full-length DBLMSP and/or DBLMSP2 is unknown, solving the crystal structure of these proteins will clarify how oligomerisation may influence the binding of DBL domains to pentameric IgM. Moreover, since IgM was found to immunoprecipitate from parasite cultures with numerous malaria proteins, the modelling should be updated once the identity of these additional malaria proteins is revealed to investigate how these proteins exist within the IgM/FcμR/DBLMSP. Future studies could adopt this model to investigate whether other IgM-binding malaria proteins can engage IgM on hFcμR, such as PfEMP1.

Chapter 5: Production of recombinant DBLMSP and DBLMSP2

5.1. Literature review

5.1.1. Role of the SPAM domain in oligomerisation

The expression of a SPAM domain is a key feature of the MSP3 gene family [148]. McColl et al. initially designated the polymorphic antigen MSP3 as the "secreted polymorphic antigen associated with merozoite" (SPAM) [266]. Analysis of the sequence encoding MSP3 revealed alanine heptad repeats in the N-terminus and a conserved glutamic acid-rich C-terminus featuring a leucine zipper-like sequence [266]. This C-terminal was shown to be conserved in more than 100 *P. falciparum* field isolates from different geographical locations [301]. Further analysis revealed that additional merozoite surface proteins shared similarities in the structural organisation of their C-terminal regions [148]. These proteins were grouped to form the MSP3-like gene family, which include MSP3 (MSP3.1), MSP6 (MSP3.2), H101 (MSP3.3), DBLMSP (MSP3.4), H103 (MSP3.7) and DBLMSP2 (MSP 3.8) [148]. The highly conserved C-terminus of the MSP3-gene family members was subsequently designated as the SPAM domain [148]. Common features of the SPAM domain of MSP3-like family members include:

- Glutamic acid-rich region [148]
- Leucine zipper-like sequence [147, 148]
- No GPI anchor [147, 266]

Relatively little is known about the function of the SPAM domain. The C-terminal regions of the MSP3-like family members elicit cross-reactive Abs capable of generating Ab-dependent cellular inhibition (ADCI) of parasite growth, highlighting their potential as vaccine candidates [148]. MSP3 has also been shown to form highly elongated oligomers via its C-terminal region [276, 302]. It was hypothesised that oligomer formation of MSP3-like proteins may permit long-distance interactions with erythrocyte receptors [147, 276]. In support of this, transmission electron microscopy and immuno-staining revealed that MSP3 formed self-assembled

filamentous structures on merozoite surfaces that associated with erythrocyte membranes [302]. Furthermore, MSP3 oligomerisation was recently proposed to confer a protective role for the parasite by binding to, and potential detoxifying, free haem in the periphery [302]. Intriguingly, a peptide region outside the SPAM domain of MSP3 (192-196 aa; YILGM) may also mediate oligomer formation [302]. Whether this region is a feature of the other MSP3-family members remains to be determined.

5.1.2. SPAM domain of DBLMSP and DBLMSP2

DBLMSP and DBLMSP2 feature a single SPAM domain in their C-termini [147, 149]. Due to the similarities with the C-terminal region of MSP3, these SPAM domains were predicted to mediate oligomerisation of these DBLMSP proteins [147]. A recent study which characterised DBLMSP and DBLMSP2 as IgM-binding proteins confirmed the ability of these proteins to form high molecular weight oligomers [146]. Individual DBL fragments were eluted as a single monodispersed peak by size exclusion chromatography, signifying monomer formation. In contrast, the C-terminal region of DBLMSP and DBLMSP2 composed of the SPAM and coiled-coil domains (SPAM fragment) exhibited a polydispersed elution prolife, consistent with tetramer and higher order complex formation [146]. Furthermore, full-length DBLMSP and DBLMSP2 proteins exhibited similar elution profiles to the individual SPAM fragments, suggesting that these also form higher-order oligomers via their C-terminus [146]. Curiously, the absence of the SPAM fragment in recombinant proteins reduced the binding affinity of DBLMSPs for IgM. Full length DBLMSP and DBLMSP2 interacted with IgM with very high equilibrium binding constants (K_d = 0.3 and 1.1 nM, respectively), thought to reflect the overall binding avidity due to the multimeric nature of both IgM and DBLMSPs [146]. However, monomeric DBL fragments of DBLMSP and DBLMSP2 bound IgM at 60nM and 600nM, respectively, signifying a 200- to 550-fold reduction in binding. As the SPAM fragment does not directly bind IgM, these weaker binding constants were proposed to result from a reduction in overall avidity since the DBL fragments could no longer oligomerise via the SPAM fragments. These data show the important role that the SPAM fragments play, not only in the oligomerisation of DBLMSP and DBLMSP2, but also how they enhance the binding of these proteins to IgM.

In Chapter 4, the function of the SPAM fragment in oligomerisation was supported by the findings that the DBL fragments alone were insufficient to mediate binding to IgM^+ lymphocytes. This signifies that the SPAM fragments are essential for this interaction, and therefore play an important role in mediating binding of malarial proteins to host receptors. It will be of interest to further characterise the role of the SPAM fragment in DBLMSP and DBLMSP2, as it may be possible to harvest its oligomerisation function for therapeutic advantage. For example, hexa-Fc is an oligomeric Fc-scaffold which was recently developed to enhance binding of IgG to low-affinity receptors, such as the human neonatal FcR, through avidity interactions [136]. Fc-fusions are well-established as therapeutics [303], and the hexa-Fc was proposed as a template Fc-fusion molecule which could be further engineered to create novel drugs and vaccines [136]. As the C-terminal region of the MSP3-like protein family has been implicated in generating cross-reactive Abs [148, 271], and has been shown to be immunogenic [148, 270], the incorporation of target malarial antigens (e.g. RTS,S/AS01, Basingin) onto the SPAM domains of DBLMSP and/or DBLMSP2 could produce highly immunogenic chimeric malarial antigens which could be used in vaccine design to prime immune responses. Alternatively, SPAM domains alone may be sufficient for the induction of immunity. By gaining further understanding of the SPAM domains of DBLMSP and DBLMSP2, future studies can harvest the potential of these fragments to generate highly efficient malaria vaccines. Whether the SPAM domain of DBLMSP and/or DBLMSP2 could also serve as a multimeric scaffold for drug and vaccine development is an exciting question.

In addition to therapeutics, recombinant DBLMSP and DBLMSP2 proteins could be utilised for other applications. Owing to their high affinity for hIgM, these proteins could be coupled to agarose beads to be used for IgM purification. In support of this, the well-characterised IgM-binding protein MBL is frequently used for IgM purification [168], although it has the disadvantage of not being able to purify all glyco-variants of IgM. This chapter aims to explore the oligomerisation status of DBLMSP and DBLMSP2 further, to ascertain how the SPAM domain may function to facilitate receptor binding.

5.2. Objectives

This chapter aims to determine the role of SPAM fragments in DBLMSP and DBLMSP2. The specific objectives include:

I. Produce full-length and DBL knock-out DBLMSP and DBLMSP2 recombinant proteins
II. Investigate the role of SPAM fragments in oligomerisation using recombinant DBL knock out proteins
III. Explore the possibility of a novel IgM purification method using recombinant DBLMSP-coated agarose beads

5.3. Results

5.3.1. Gene synthesis and mammalian expression vector construction

It has been proposed that the linker region of DBLMSP and DBLMSP2 plays a role in the flexibility of oligomers [147]. We therefore decided to create recombinant DBLMSP and DBLMSP2 proteins that lack the DBL domain (C = control) to further investigate the role of the SPAM domain in oligomerisation. Although individual SPAM domains had been looked at previously [146], these proteins (constructs) did not contain the flexible linker region which may influence the conformation and/or function of the proteins [147].

The genes for variants of the DBLMSP and DBLMSP2 proteins from the *P. falciparum* 3D7 strain (PF10_0348 and PF10_0355, respectively) were synthesised by Life Technologies, with the addition of two c-myc tags, a 6-histidine tag and a kozak sequence at the N-terminus to initiate translation.

Four new constructs were made (Life Technologies) using the mammalian expression vector pcDNA 3.1(+): DBLMSP-FL (DBL + SPAM domains); DBLMSP-C (SPAM only); DBLMSP2-FL (DBL + SPAM domains); DBLMSP2-C (SPAM only) (see Appendix II for vector maps and sequences). The coding regions including the c-myc and histidine tags were flanked by BamHI and XhoI restriction enzyme sites. Potential N-linked glycosylation sequons were mutated in these chemically synthesised genes to prevent inappropriate glycosylation of *Plasmodium* proteins, and these genes also codon-optimised for mammalian expression.

Restriction enzyme digests revealed bands that corresponded in predicted size to the four new constructs (Figure 5.1). Sequencing confirmed the correct insertion of DBLMSP-FL, DBLMSP-C, DBLMSP2-FL, and DBLMSP2-C into the mammalian expression vector pcDNA 3.1(+).

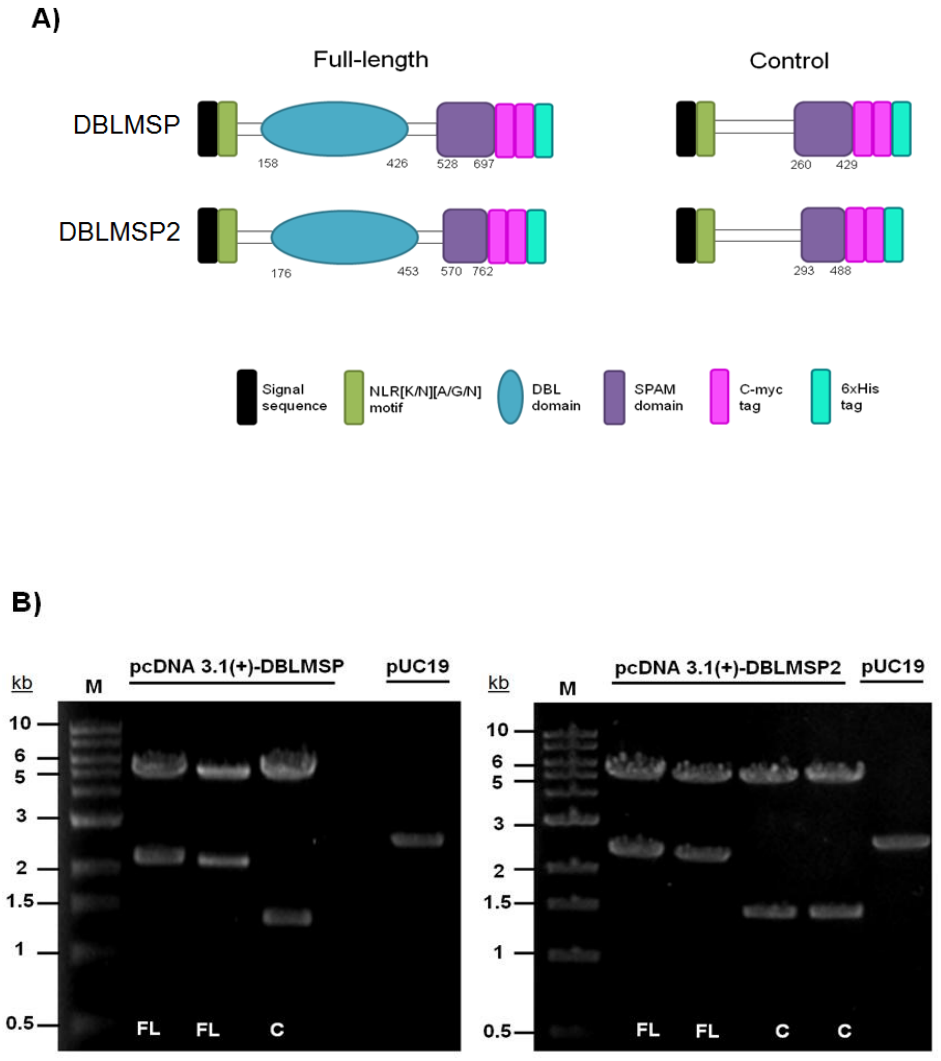

Figure 5.1 Diagnostic digest of mammalian expression vectors containing DBLMSP domains (A) Domain structures of DBLMSP and DBLMSP2 full-length and control (SPAM only) genes from the 3D7 *P. falciparum* clone. **(B)** Restriction enzyme digests confirmed the presence of inserts coding for the DBLMSP (left panel) and DBLMSP2 (right panel) synthesised genes. The predicted size of the inserts are 2199bp and 1374bp for DBLMSP-FL and –C respectively, and 2373bp and 1542bp for DBLMSP2-FL and –C respectively. Lanes left to right: **M** – 1kb plus marker (NEB), **FL** – full-length insert, **C** – SPAM-only control. pUC19 DNA (Life Technologies) was used as a positive control. Bands observed at >2kb correspond to full-length (FL) inserts and bands between 1-1.5kb correspond to SPAM-only (C) inserts released by double digest (BamHI/ XhoI). The plasmid vectors are designated as pcDNA 3.1(+)DBLMSP-FL or –C, and pcDNA 3.1(+)DBLMSP2-FL or –C. All constructs were analysed by Sanger sequencing (Source Bioscience) and the nucleotide sequences are shown in Appendix II.

5.3.2. Expression of pcDNA 3.1(+)-DBLMSP vectors in mammalian cells

Mammalian expression systems were employed for the transient expression of recombinant DBLMSP proteins, as this approach has been shown to be successful [146].

All four constructs were amplified by DNA maxiprep (Qiagen), resequenced, and transfected into Chinese Hamster Ovary (CHO-K1) cells using the FuGENE® 6 transfection reagent (see section 2.2.2 for details). As DBLMSP and DBLMSP2 proteins are expressed in a soluble form [146], culture supernatant was harvested after two weeks and tested for the presence of recombinant proteins. A pilot protein expression trial, using ELISA and immunoblotting in which anti-his Abs were used to detect the 6x histidine tag, revealed the lack of soluble recombinant DBLMSP-FL, DBLMSP-C, DBLMSP2-FL or DBLMSP2-C in culture media taken off the transfected CHO-K1 cells (Figure 5.2).

The failure to detect protein in the pilot trial was thought to be due to insufficient yield. To resolve this issue, transfected CHO-K1 cells were expanded and seeded to select for high-expressing cell colonies. As shown in Figure 5.3, no protein expression was observed in any of the screened transfected CHO-K1 cell clones (n= 20). Next, we sought to investigate whether an expanded polyclonal transfected cell culture contained detectable levels of recombinant proteins. For this, a c-myc column was used to purify proteins via the c-myc tags (Figure 5.4A). A peak was observed at fractions A6-A10 for DBLMSP-FL (~170 mAU) and smaller peaks at fractions A4-A7 and A2-A6 for DBLMSP2-FL and DBLMSP2-C (~15 and ~17 mAU, respectively). The chromatogram revealed that there was no protein produced for DBLMSP-C, and therefore this sample was not used in subsequent analysis. To confirm the identity of these eluted proteins, 20µl of each fraction was resolved under reducing conditions by SDS-PAGE. The predicted MW of DBLMSP-FL, DBLMSP-C, DBLMSP2-FL and DBLMSP2-C were 84kDa, 52kDa, 91kDa and 59kDa, respectively, as derived from the amino acid sequences submitted to ExPASY (http://web.expasy.org/compute_pi/). No bands were resolved by Coomassie staining for DBLMSP2-FL or –C, indicating that the protein quantities were too low to be detected by gel electrophoresis (Figure 5.4B).

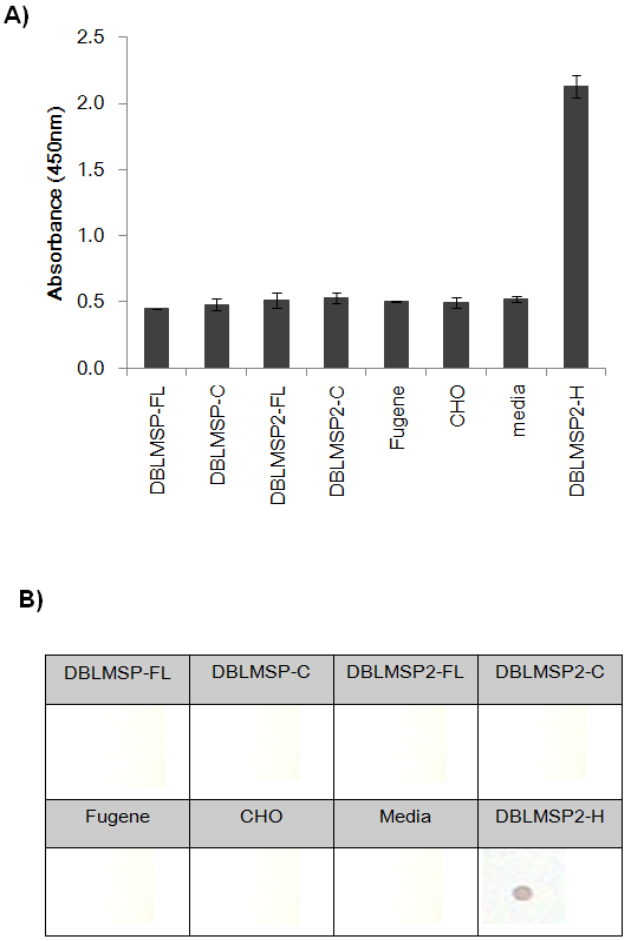

Figure 5.2 Pilot expression of DBLMSP and DBLMSP2 in CHO-K1 mammalian cells. (A) The expression of recombinant protein and its ability to bind hIgM was tested by ELISA. 10µg/ml human IgM was coated to microtitre wells (Nunc) in carbonate buffer (pH9.6) overnight at 4˚C. The wells were washed and blocked with PBST/ 5% milk powder for 1hr at RT, washed four times with PBST and incubated for 2hr at RT with 100µl of culture supernatant, or 10µg/ml recombinant his-tag DBLMSP2 (kindly provided by Dr. Cecile Crosnier, Sanger Institute) as a positive control, in duplicate. Wells were washed and incubated with anti-his-HRP (1:2000) for 1hr at RT, washed again then developed with 100µl of the TMB substrate (Sigma-Aldrich). Absorbance was measured at 450nm. The mean ± SD of duplicate reads is shown. **(B)** Immunoblots of culture supernatant from transfected CHO-K1 cells. 5µl of culture supernatants were blotted onto nitrocellulose membrane and allowed to dry for 30 min. The presence of protein was detected using anti-his-HRP (1:5000). DBLMSP-H and media were used as positive and negative controls, respectively.

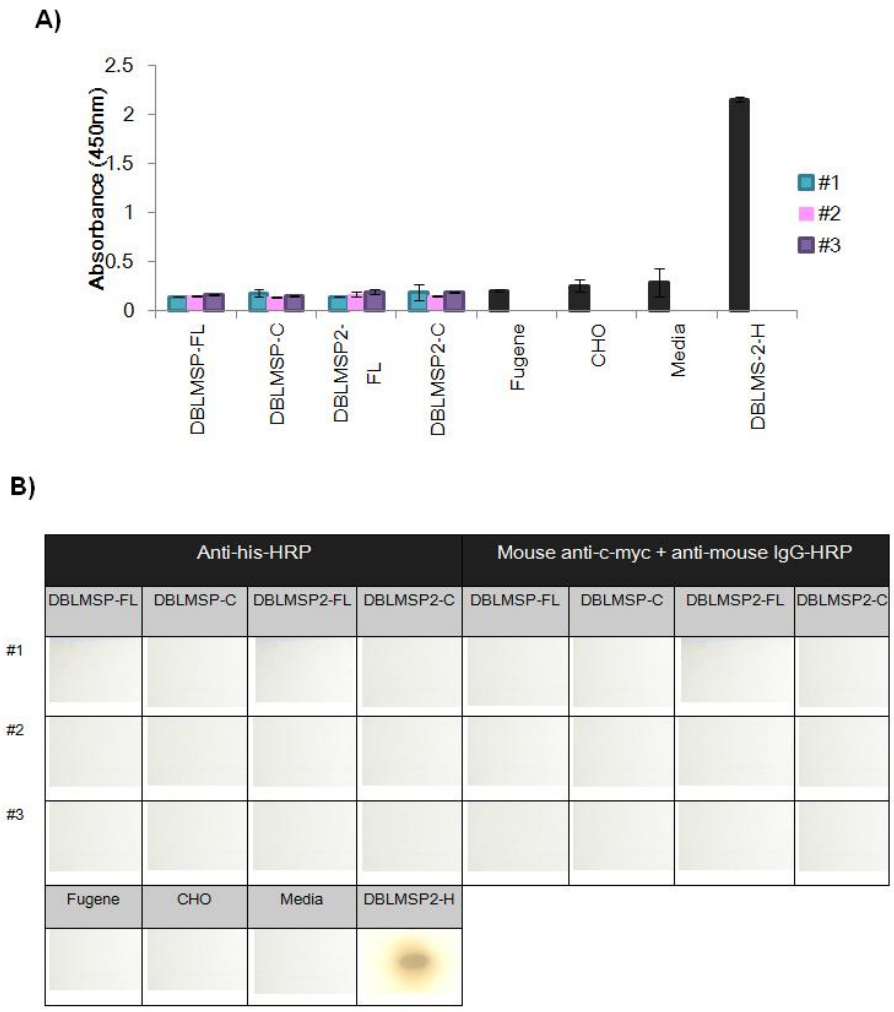

Figure 5.3 Screening transfected CHO-K1 cell clones for expression of DBLMSP and DBLMSP2. 20 cell colonies each of transfected CHO-K1 cells were seeded for DBLMSP-FL, DBLMSP-C, DBLMSP2-FL, and DBLMSP2-C. As similar results were observed for all colonies, only three from each cell line (#1-3) are shown for clarity. **(A)** The expression of recombinant protein and its ability to bind hIgM was tested by ELISA. 10µg/ml human IgM was coated in duplicate on microtitre wells (Nunc) in carbonate buffer (pH9.6) overnight at 4˚C. The wells were washed and blocked with PBST/ 5% milk powder for 1hr at RT, prior to washing with PBST and incubated for 2hr at RT with 100µl of culture supernatant, or 10µg/ml recombinant his-tag DBLMSP as a positive control. Wells were washed and incubated with anti-his-HRP (1:2000; Sigma-Aldrich) for 1hr at RT, washed and developed. Absorbance was measured at 450nm. The mean ± SD of duplicate reads is shown. **(B)** Immunoblots of culture supernatant from transfected CHO-K1 cells, which were developed using anti-his-HRP (1:5000). Recombinant his-tagged DBLMSP2 and media were used as positive and negative controls, respectively.

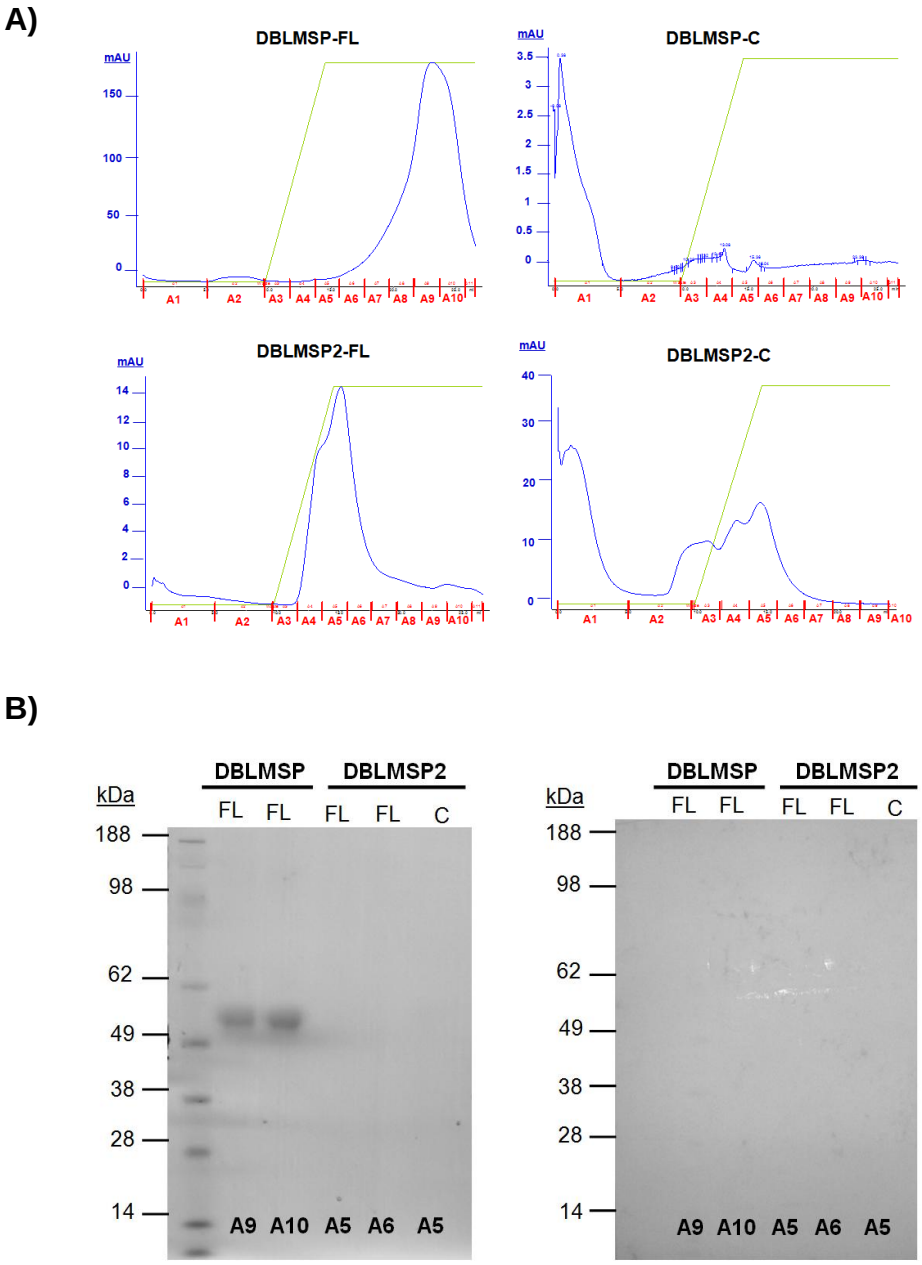

Figure 5.4 Small-scale purification of recombinant DBLMSP and DBLMSP2. (A) FPLC chromatogram showing the affinity purification of recombinant proteins (labelled) from 200ml polyclonal tissue culture supernatant using an anti-c-myc column. The blue line corresponds to eluted protein as determined by UV absorbance (OD 280nm) shown on the y-axis. The green line shows a linear increase in volume of 0.1M glycine (pH2) elution buffer. Fractions are shown in red on the x-axis. **(B)** Following elution, 20µl of fractions corresponding to peaks on chromatograms were separated under reducing conditions by SDS-PAGE and stained with Coomassie Brilliant Blue R-250 (left panel) or transferred to nitrocellulose by Western blotting (right panel). Nitrocellulose membranes were blocked with PBST/5% milk powder for 1hr, washed extensively and incubated with anti-his-HRP (1:5000; Sigma-Aldrich) for 3hr at RT. Blots were developed to detect for the presence of his-tagged recombinant proteins.

Bands were detected at ~54kDa for DBLMSP-FL (fractions A9-A10) (Figure 5.4B), which did not match the predicted MW of this recombinant protein. To confirm the identity of these proteins, Western blots were performed with anti-his-HRP to detect for recombinant proteins. No bands were detected for any of the proteins, indicating that the ~54kDa bands identified by Coomassie staining were not DBLMSP-FL, and the identity of these proteins is unknown.

Due to the lack of protein in the culture supernatants, transfected polyclonal CHO-K1 cells were expanded in attempts to increase the quantity of recombinant protein in culture supernatants. For this, 1L of transfected CHO-K1 cell culture was cultured at 37˚C for 21 days under selection prior to purification and/or protein expression trials. An ELISA confirmed the lack of protein expression (Figure 5.5). Therefore, despite numerous expression trials, no recombinant protein production was observed using the pcDNA 3.1(+)-DBLMSP vectors.

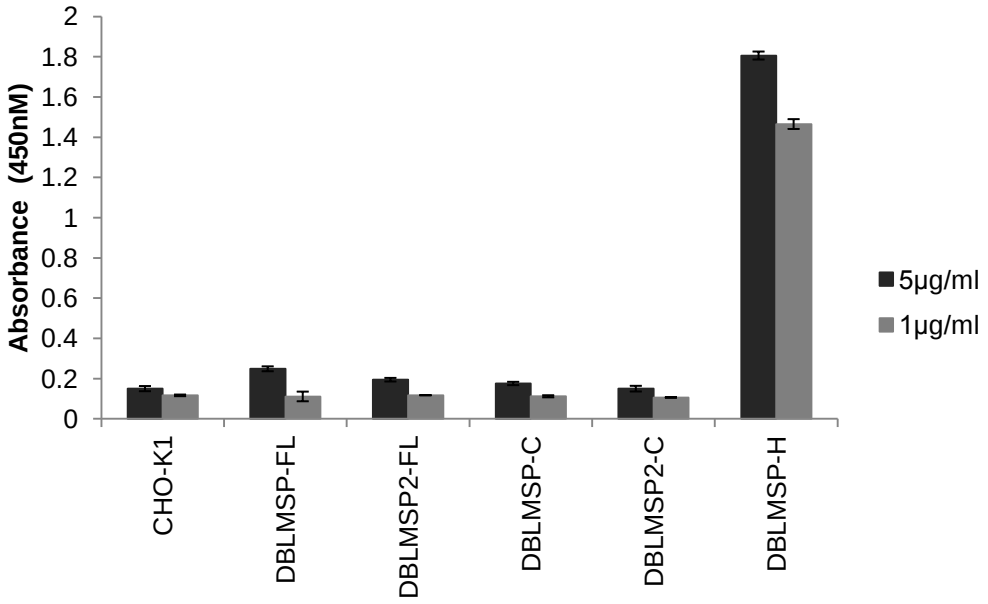

Figure 5.5 Large-scale purification of recombinant DBLMSP and DBLMSP2. The expression of recombinant protein and its ability to bind hIgM was tested by ELISA. For this, 5µg/ml or 1µg/ml human IgM was coated on microtitre wells (Nunc) in carbonate buffer (pH9.6) overnight at 4˚C. The wells were washed and blocked with PBST/ 5% milk powder for 1hr at RT, washed four times with PBST and incubated for 2hr at RT with 100µl of culture supernatant, or 10µg/ml DBLMSP-H as a positive control, in duplicate. Wells were washed and incubated with anti-his-HRP (1:2000) for 1hr at RT, washed again and then developed. Absorbance was measured at 450nm. The mean± SD of duplicate reads is shown.

5.3.3. Subcloning of DBLMSP fragments into a pFUSE mammalian expression vector

As there was no detectable expression of recombinant proteins using the pcDNA 3.1(+)-DBLMSP vectors, we decided to sub-clone DBLMSP-FL, DBLMSP-C, DBLMSP2-FL, and DBLMSP2-C DNA fragments into another mammalian expression vector. The pFUSE-hIgG1-Fc2 vector (InvivoGen) has previously been shown to produce high yields of recombinant proteins [185], and was therefore selected for sub-cloning. This vector features a IL-2 signal sequence at the 5' end of the cloned insert, which enhances the secretion of novel recombinant proteins [304].

As the pFUSE-hIgG1-Fc2 vector encodes for Fcγ–fusion proteins, which are unsuitable for use with lymphocytes owing to potential cross-reactivity with FcγRs, we designed a parking vector that lacks the Fcγ tag referred to as pFUSE- MCS (see Appendix II for vector map). To make this new vector, the hIgG1-Fc2 Fcγ insert was excised by restriction enzyme digestion (EcoRI/NheI) and replaced by a run of restriction sites, to create a multiple cloning site region only (pFUSE-MCS, synthesised by Eurofins). To isolate the DBLMSP-FL, DBLMSP-C, DBLMSP2-FL, and DBLMSP2-C inserts, restriction enzyme digests (BamHI/ XhoI) on the pcDNA 3.1(+)-DBLMSP vectors were performed (Figure 5.6).

The genes encoding DBLMSP-FL, DBLMSP-C, DBLMSP2-FL, and DBLMSP2-C were then subcloned into the pFUSE-MCS vector using the restriction enzyme sites BamHI and XhoI (Figure 5.7). All new constructs were confirmed by sequence analysis (Appendix II). Following unsuccessful miniprep screenings for all constructs, the same ligation mixture was retransformed into dam^-/dcm^- competent *E. coli* cells (C2925, New England Biolabs) to improve transformation efficiency. Although we did not assess the methylation status of the inserts, dam^-/dcm^- competent *E. coli* cells are known to be more accepting of foreign DNA.

Transformation efficiencies for pFUSE-MCS-DBLMSP2-FL and –C were significantly lower than those for pFUSE-MCS-DBLMSP-FL and –C, as more than 75 minipreps were screened for each prior to the identification of vectors containing correct inserts (confirmed by restriction enzyme digestion and sequencing), whereas only less than 10 minipreps were screened for the pFUSE-MCS-DBLMSP vectors.

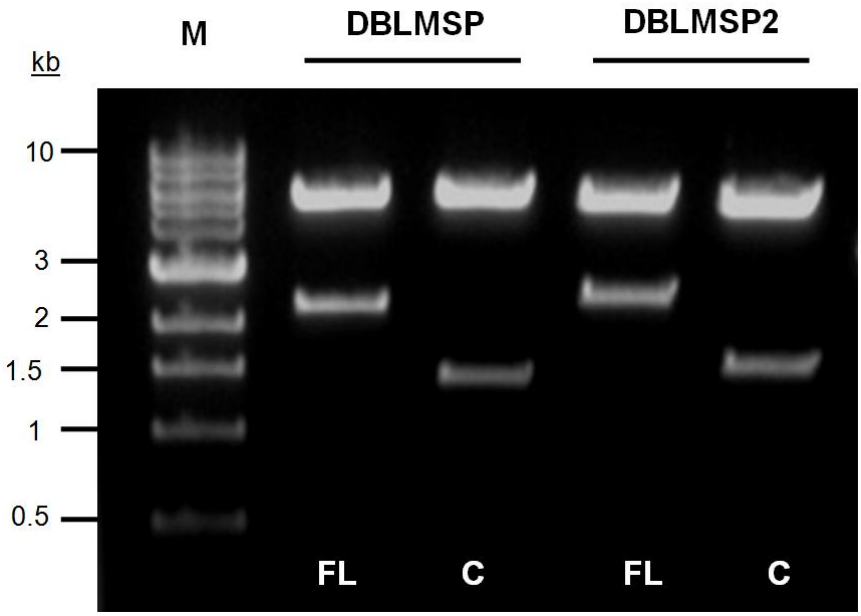

Figure 5.6 Restriction enzyme digestion of DNA fragments from pcDNA 3.1(+)-DBLMSP vectors. DNA fragments were excised from the pcDNA 3.1(+) vectors by digestion with BamHI/ XhoI restriction enzymes. 5µl of each digest was run on a 1% agarose gel. The predicted size of the inserts are 2199bp and 1374bp for DBLMSP-FL and –C respectively, and 2373bp and 1542bp for DBLMSP2-FL and –C respectively. Bands were observed at >2kb and at ~1.5kb, corresponding to full-length (FL) and SPAM-only (C) DBLMSP and DBLMSP2, respectively.

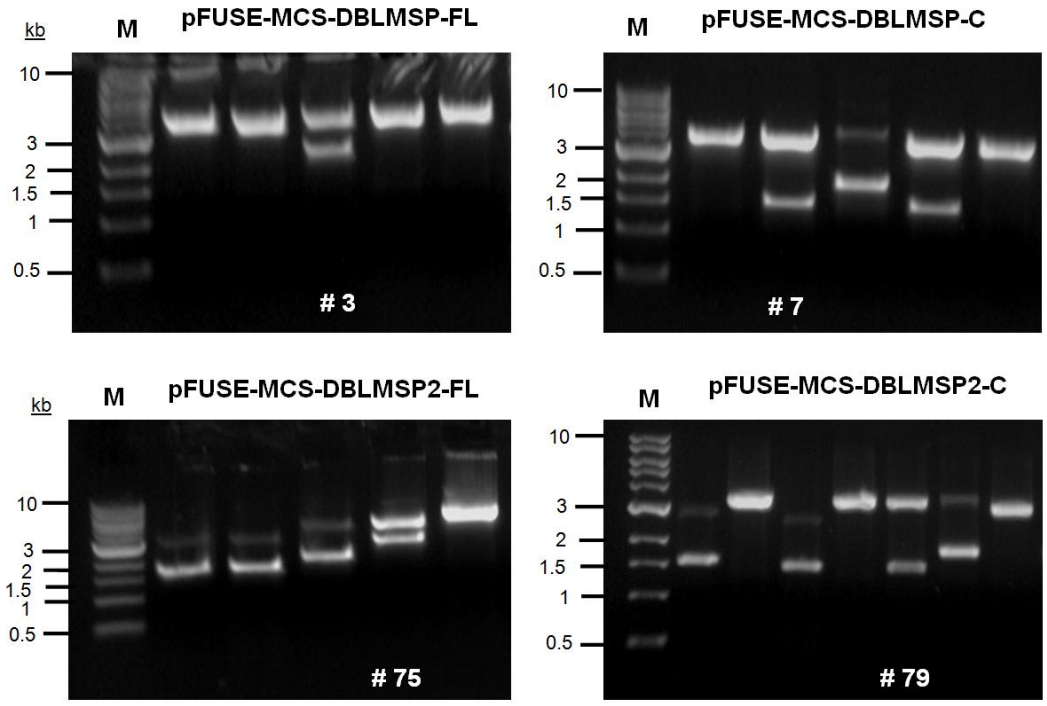

Figure 5.7 Generation of pFUSE-MCS-DBLMSP mammalian expression vectors. Diagnostic digestions of miniprep DNA of pFUSE-MCS-DBLMSP vectors to confirm the presence of inserts coding DBLMSP-FL and –C, and DBLMSP2-FL and –C. The predicted size of the inserts are 2199bp and 1374bp for DBLMSP-FL and –C respectively, and 2373bp and 1542bp for DBLMSP2-FL and –C respectively. Bands at ~3kb correspond to the pFUSE-MCS vector backbone released by double digestion with BamHI/ XhoI. The number of miniprep DNAs screened before identification of a positive vector is shown in white (#), and each lane represents individual clones. Bands at >2kb and ~1.5kb correspond to the FL- and C-DBLMSP fragments. Sequencing confirmed the generation of pFUSE-MCS-DBLMSP mammalian expression vectors (see Appendix II). The subcloning experiments were performed by Dr Pat Blundell.

5.3.4. Expression of pFUSE-MCS-DBLMSP vectors in mammalian cells

After confirming that all cloned inserts were correct, the pFUSE-MCS vectors were amplified and transfected into CHO-K1 cells (see section 2.2.2). After 21 days under selection, the polyclonal transfected cell culture media was harvested and filter sterilised. Production of recombinant DBLMSP-FL and DBLMSP-C in culture supernatants was tested by SDS-PAGE and Western blotting with anti-histidine and anti-c-myc Abs, respectively (Figure 5.8). Despite numerous transfections, CHO-K1 cells transformed with the pFUSE-MCS-DBLMSP2 vectors failed to grow. No protein was detected for either DBLMSP-FL or –C, as no bands were observed at the predicted MW for recombinant DBLMSP-FL and -C (~84kDa and 52kDa, respectively). Non-specific bands were observed at ~55kDa and ~78kDa for the anti-histidine Western blots, and ~38kDa for the anti-c-myc Western blot, in all samples tested. The presence of these bands for the negative control signifies that the detecting Abs may be cross-reacting with unidentified proteins present in the culture supernatants.

As protein production was unsuccessful in CHO-K1 cells, we next decided to transfect HEK293T mammalian cells as these cells have previously been shown to produce recombinant DBLMSPs [146]. Protein expression trials of polyclonal transfected cell culture media revealed that transfected HEK293T cells did not secrete any recombinant protein (Figure 5.9). As there was no positive control available for the capture ELISA in Figure 5.9 (e.g. a protein containing both a c-myc and 6x histidine tag), an IgM-binding ELISA was used to confirm that the negative results in Figure 5.9 were due to lack of protein rather than a failure of the c-myc mAb to capture the recombinant proteins. However, no expression of the recombinant proteins was observed (Figure 5.10).

Finally, whether the lack of protein expression was due to insoluble protein production was investigated. To confirm this, transfected HEK293T cells were lysed then probed for the presence of recombinant protein using Abs to detect the 6x histidine tag. As shown in Figure 5.11, there were no obvious differences between the control (HEK293T) and transfected HEK293T cells observed by Coomassie staining or Western blotting.

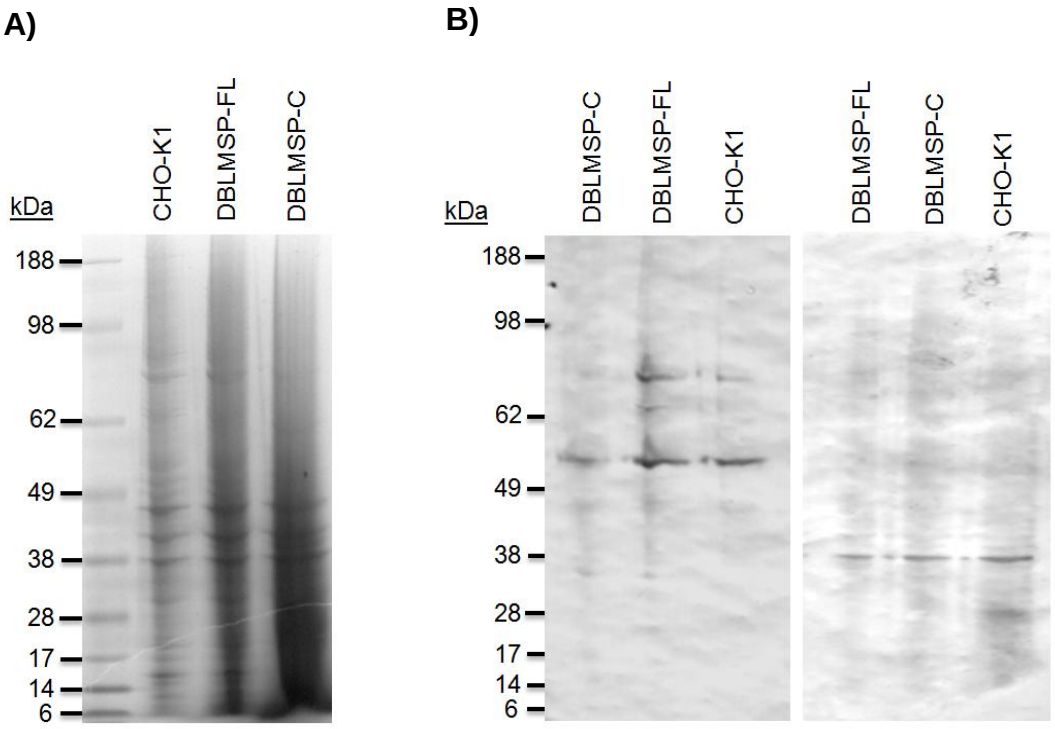

Figure 5.8 Protein expression trials of the pFUSE-MCS-DBLMSP vectors. The culture supernatant of CHO-K1 cells transfected with pFUSE-MCS-DBLMSP-FL and pFUSE-MCS-DBLMSP-C were harvested following 21 days under selection. The presence of secreted recombinant DBLMSP-FL and DBLMSP-C was investigated following gel electrophoresis by Coomassie Brilliant Blue R250 staining **(A)** and Western blotting **(B)** with anti-his-AP (left panel) and anti-c-myc-AP (right panel) Abs.

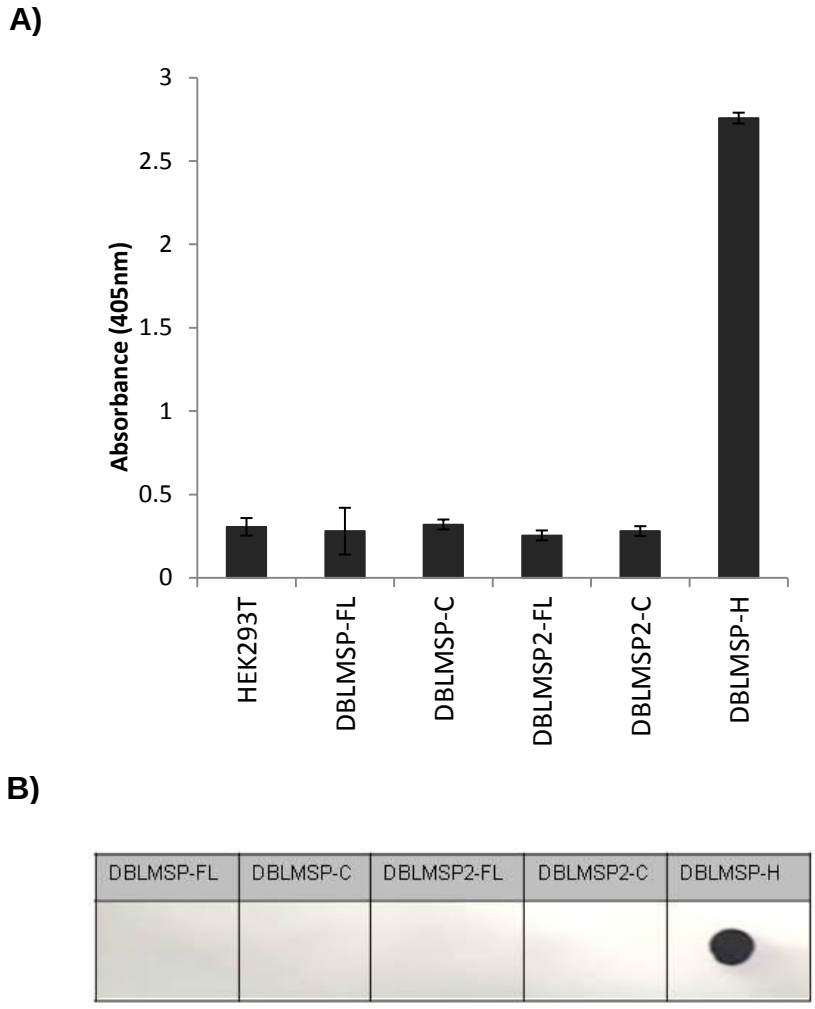

Figure 5.9 Protein expression trials of the pFUSE-MCS-DBLMSP vectors in HEK293T cells. (A) A capture ELISA was used to screen for soluble recombinant DBLMSP protein production in transfected cell culture supernatants. For this, 10µg/ml anti-c-myc mAb was coated in duplicate onto wells of a microtitre plate (Nunc). Following overnight incubation in carbonate bicarbonate buffer (pH9.6), the wells were washed three times and blocked for 1hr in PBST/5% milk powder. After three more washes, 100µl of transfected cell culture supernatants were added to each well and incubated for 3hr at RT, then extensively washed. To detect the presence of recombinant protein, anti-his-AP (1:5000) was added to wells for 3hr and then washed and developed. As a positive control, 10µg/ml of the recombinant his-tagged DBLMSP (DBLMSP-H) (kindly provided by Dr Cecile Crosnier, Sanger Institute) was also coated. The mean± SD of duplicate reads is shown. **(B)** Immunoblot analysis of transfected cell culture supernatant. 5µl of each culture supernatant was blotted onto nitrocellulose membrane and allowed to dry for 30 min. The membrane was blocked in PBST/5% milk powder for 1hr, washed extensively and incubated with anti-his-AP Abs in PBST (1:5000).

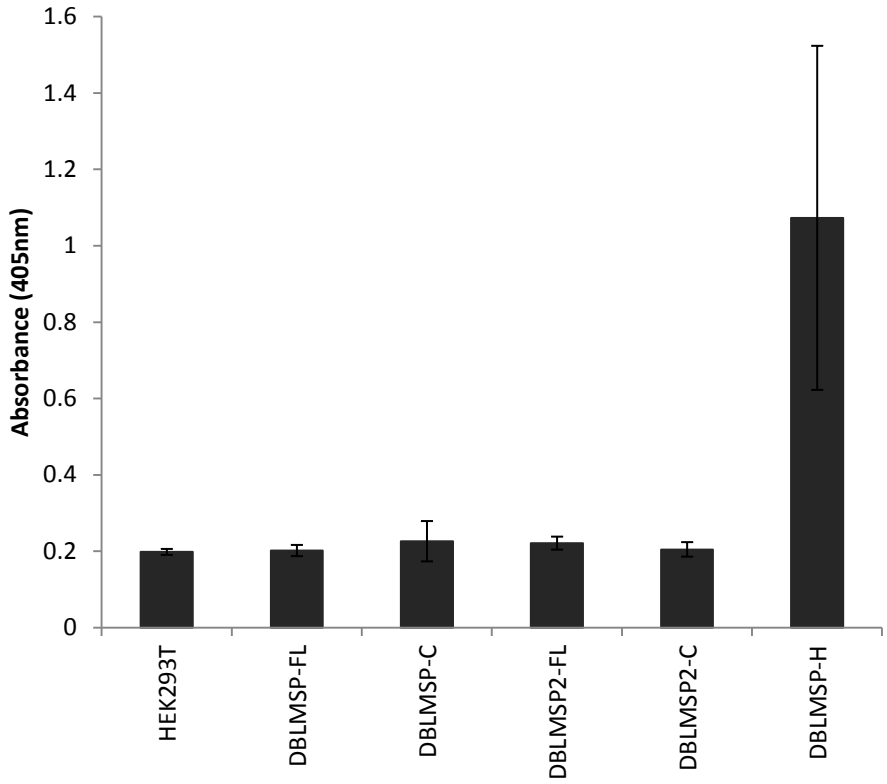

Figure 5.10 IgM-binding ELISA to detect recombinant protein production in HEK293T cells. (A) A capture ELISA was used to screen for soluble recombinant DBLMSP protein production in transfected cell culture supernatants. 10μg/ml hIgM (Sigma-Aldrich) was coated in duplicate onto wells of a microtitre plate (Nunc) and incubated overnight in carbonate bicarbonate buffer (pH9.6). The wells were then washed three times and blocked for 1hr in PBST/5% milk powder. After three more washes, 100μl of transfected cell culture supernatants were added to the wells and incubated for 3hr at RT, then extensively washed. To detect the presence of recombinant protein, anti-his-AP (1:5000) was added to the wells for 3hr, washed and developed. As a positive control, 10μg/ml recombinant his-tagged DBLMSP (DBLMSP-H) (kindly provided by Dr Cecile Crosnier, Sanger Institute) was also coated. The mean± SD of duplicate reads is shown.

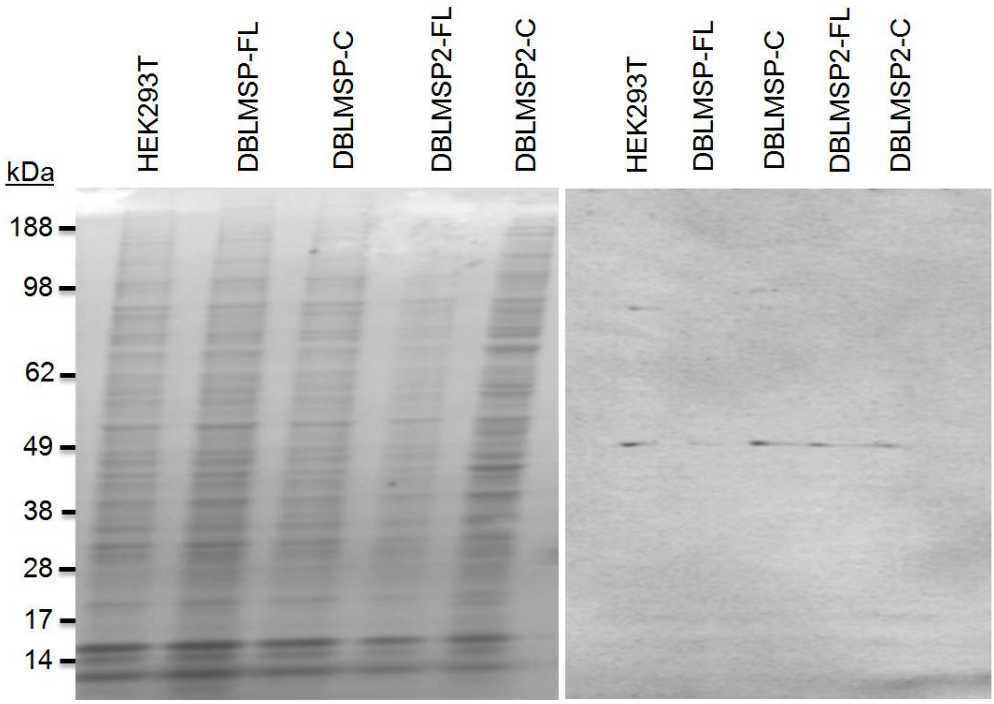

Figure 5.11 Lysis of pFUSE-MCS-DBLMSP-transfected HEK293T cells. To determine whether recombinant protein was trapped intracellularly, HEK293T cells transfected with pFUSE-MCS-DBLMSP-FL or -C, and pFUSE-MCS-DBLMSP2-FL or –C, or HEK293T cells alone were lysed. For this, cells (1x 10^6) were harvested, washed and pelleted by centrifugation. Cells were then resuspended in 300µl of 1x NuPAGE reducing buffer (Life Technologies), and boiled for 5 min at 95˚C. 20µl of this mixture was loaded into the wells of 4-12% Bis-Tris gels and proteins were separated by electrophoresis. Gels were either stained with Coomassie Brilliant Blue R250 (left panel) or transferred to a nitrocellulose membrane by Western blotting (right panel). The presence of recombinant protein on the membrane was detected using anti-his-AP (1:5000).

5.3.5. Subcloning of DBLMSP into pRSET bacterial expression vector

Since numerous expression trials were unsuccessful in mammalian cells, we decided to sub-clone the DBLMSP inserts into a bacterial expression vector. The commercial expression vector pRSET EmGFP (Life Technologies) was selected for use as it contained compatible restriction enzyme sites to the DBLMSP inserts. To prepare the vector for sub-cloning, the GFP gene was removed by double digestion with BamHI/ XhoI. The linearised vector was then dephosphorylated and inactivated to prevent re-ligation, and purified by gel elution (Figure 5.12).

The linear pRSET vector was ligated with *BamHI/XhoI* digested DBLMSP-FL, DBLMSP-C, DBLMSP2-FL, and DBLMSP2-C inserts at a 1:3 ratio. The resulting cloning vectors are referred to as pRSET-DBLMSP-FL, pRSET-DBLMSP-C, pRSET-DBLMSP2-FL, and pRSET-DBLMSP2-FL. Five microliters of each ligation mix was transformed into TOP10 competent *E. coli* cells (see section 2.1.7). Despite numerous attempts, transformation efficiencies were very low, as only pRSET-DBLMSP-C was successful (Figure 5.13). To resolve this issue, the same ligation mix was transformed into $dam^{-/}dcm^{-}$ competent bacteria (C2925). Positive clones for pRSET-DBLMSP-FL, pRSET-DBLMSP2-FL, and pRSET-DBLMSP2-FL were identified by restriction enzyme digestion and sequence analysis (Figure 5.14).

5.3.6. Expression of pRSET-DBLMSP vectors in BL21Star (DE3) *E. coli*

After confirming the presence of the cloned inserts by sequencing, the pRSET-DBLMSP vectors were amplified and transformed into BL21Star (DE3) *E. coli* cells using the heat-shock technique (section 2.1.7). Following transformation, small protein expression trials were initiated. For this, starter cultures of transformed cells were grown to mid-log phase (OD_{600}= 0.3-0.4) prior to initiating transcription with 1mM IPTG, as previously described [147].

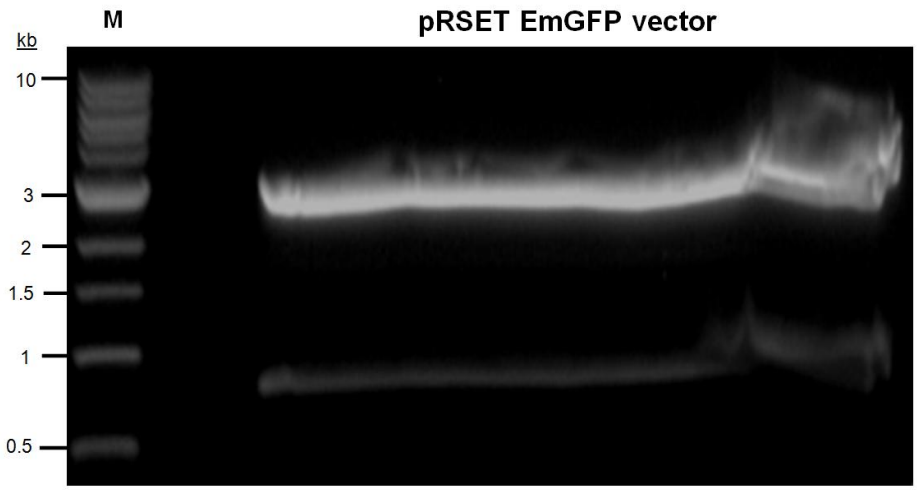

Figure 5.12 Digestion and linearisation of the pRSET EmGFP bacterial expression vector. The pRSET vector was double digested with BamHI/ XhoI restriction enzymes to release the green fluorescence protein (GFP) gene, shown as the lower band at ~738 bp. The upper band at ~2862 bp is the linearised pRSET vector backbone.

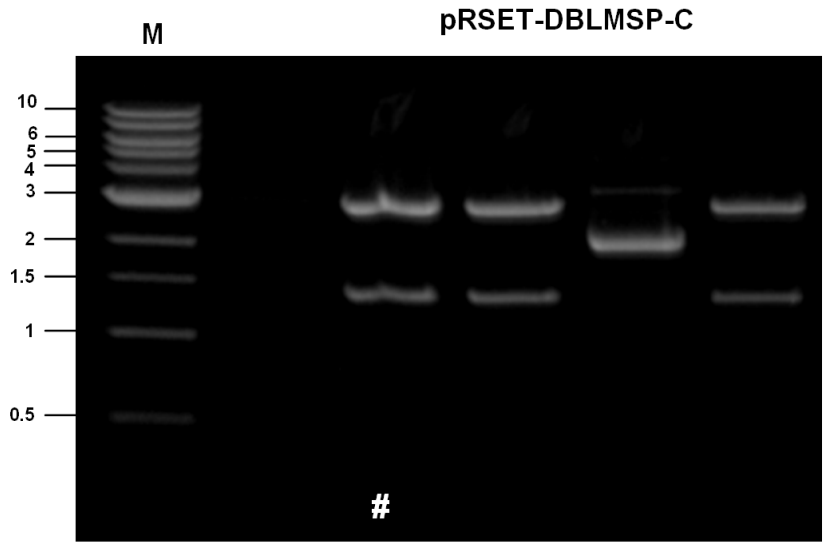

Figure 5.13 Transformation of TOP10 competent *E. coli* with pRSET-DBLMSP-C bacterial expression vector. pRSET-DBLMSP-C was transformed into TOP10 *E. coli* cells and incubated overnight at 37˚C on LB-ampicillin plates. Bacterial colonies were screened for the presence of the DBLMSP-C insert by restriction enzyme digestion (BamHI/XhoI) and agarose gel electrophoresis. Positive colonies were amplified and sent for sequencing. Colonies with the correct sequence are shown as # in lane 1. The subcloning experiments were performed by Dr Pat Blundell.

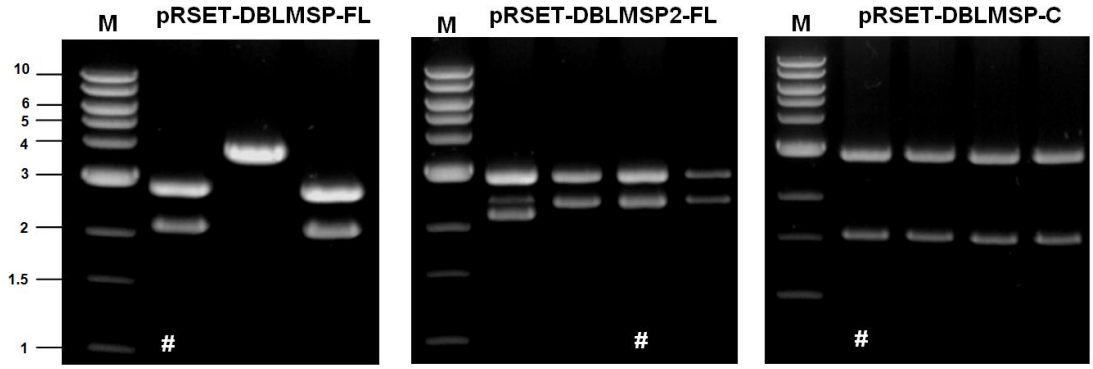

Figure 5.14 Generation of pRSET-DBLMSP mammalian expression vectors in dam$^-$/dcm$^-$ competent *E. coli* cells. Ligation mixes were transformed into dam-/dcm- cells following failed transformation into TOP10 *E. coli*. Colonies were screened for the presence of DBLMSP inserts in pRSET-DBLMSP vectors by restriction enzyme digestion (BamHI/XhoI) and agarose gel electrophoresis. Positive colonies were amplified and sent for sequencing. Colonies with the correct sequence are shown as #, and correspond to lanes 1, 3, and 1 for DBLMSP-FL, DBLMSP2-FL, and DBLMSP-C, respectively. The subcloning experiments were performed by Dr Pat Blundell.

Initial protein expression trials focussed on DBLMSP-FL and –C, as the growth of *E. coli* transformed with pSRET-DBLMSP2-FL and pSRET-DBLMSP2-C. As the recombinant proteins were predicted to form insoluble inclusion bodies, the cells were lysed by sonication and boiling in reducing buffer. The expression of recombinant protein was determined by Coomassie Brilliant Blue staining and Western blotting (Figure 5.15), which showed no obvious differences between the non-induced and induced samples for either pRSET-DBLMSP-FL or pRSET-DBLMSP-C. Furthermore, striking similarities were observed between DBLMSP-FL and DBLMSP-C (Figure 5.15, left panels). Bands of ~30kDa were observed in lane 2 for the non-induced and induced samples of DBLMSP-C (Figure 5.15B, left panel), which do not correspond to the predicted MW of DBLMSP-C (52kDa). This is most likely due to cross-reactivity of the detecting Ab, as previously observed in Figure 5.11.

Subsequent protein trials were performed with pRSET-DBLMSP-FL/-C and pRSET-DBLMSP2-FL/C vectors. In these experiments, the BL21Star (DE3) *E. coli* were also transformed with the pRSET-EmGFP original vector (see Appendix II for map) to investigate whether the GFP tag could be expressed, which has a predicted MW of 27kDa [305]. Expression of the GFP tag would indicate that the vector is sufficient for protein production, therefore confirming that the issues with recombinant protein expression are specific for the DBLMSP genes. In addition, protein expression was initiated with 1mM IPTG (1mM), which was incubated with cells for a longer period (6hr), to assess whether this had an effect on expression. As shown in Figure 5.16, there was expression of the GFP tag (lane A, highlighted with a black box) at ~30kDa but no expression of recombinant DBLMSP-FL/C or DBLMSP2-FL/C. Together, these results indicate that bacterial expression of recombinant DBLMSP proteins was unsuccessful.

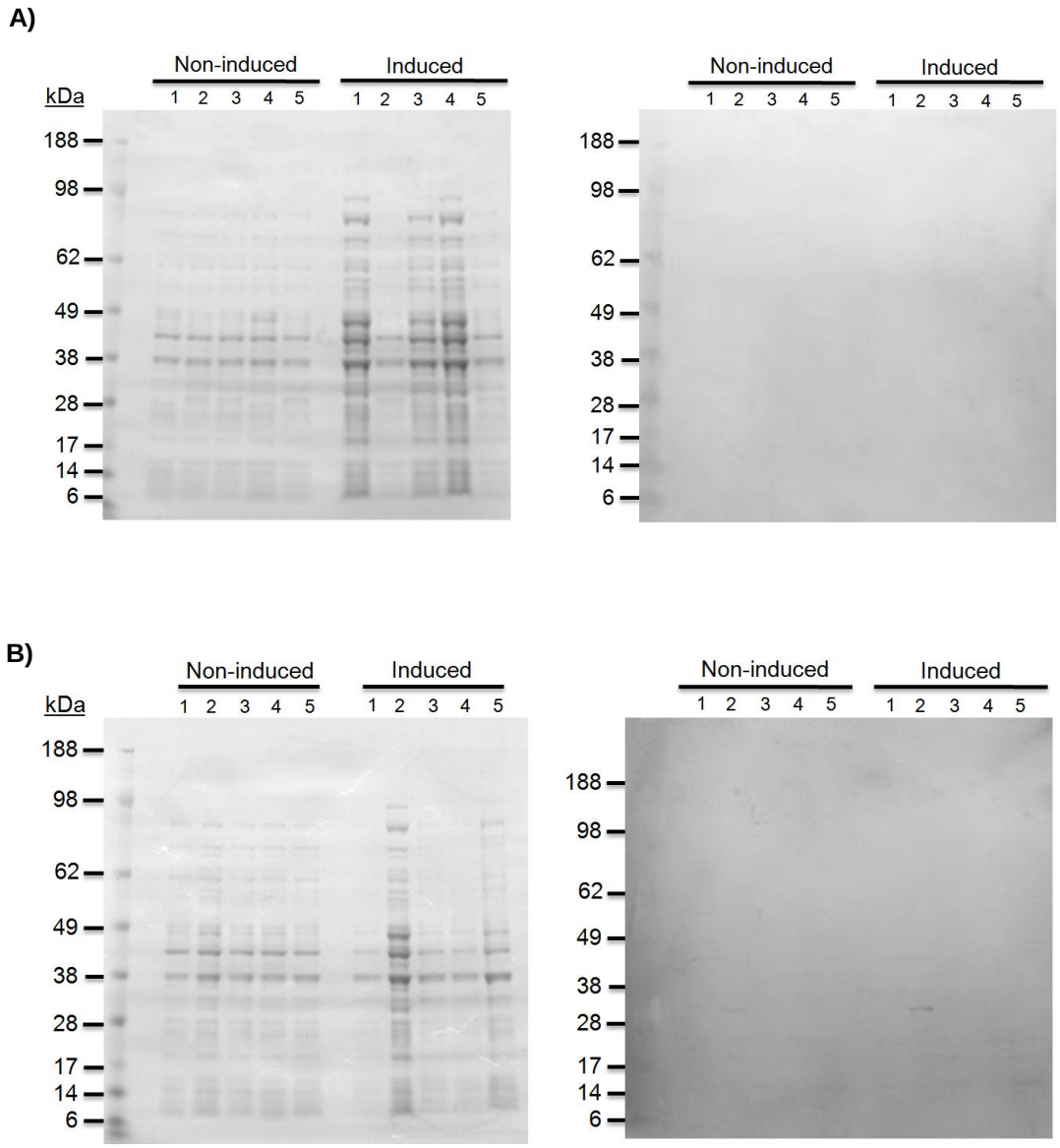

Figure 5.15 Small-scale protein production in BL21Star (DE3) *E. coli*. pRSET-DBLMSP-FL and pRSET-DBLMSP-C transformed *E. coli* were grown to mid-log phase (OD_{600} = 0.3-0.4). 1mM IPTG was used to initiate protein expression. Induced and non-induced cells were incubated for 3hr at 37˚C in a shaking incubator, and pelleted by centrifugation. The cells were resuspended in 40µl of 1x NuPAGE reducing buffer (Life Technologies), and boiled for 5 min at 95˚C. 5µl of this mixture was loaded into the wells of 4-12% Bis-Tris gels and visualised by Coomassie Brilliant Blue R250 staining (left panels) or Western blotting (right panels) with anti-his-AP Abs (1:5000). A total of five transformations were screened for each protein (lanes 1-5; non-induced and induced). No expression of recombinant DBLMSP-FL **(A)** or DBLMSP-C **(B)** was observed.

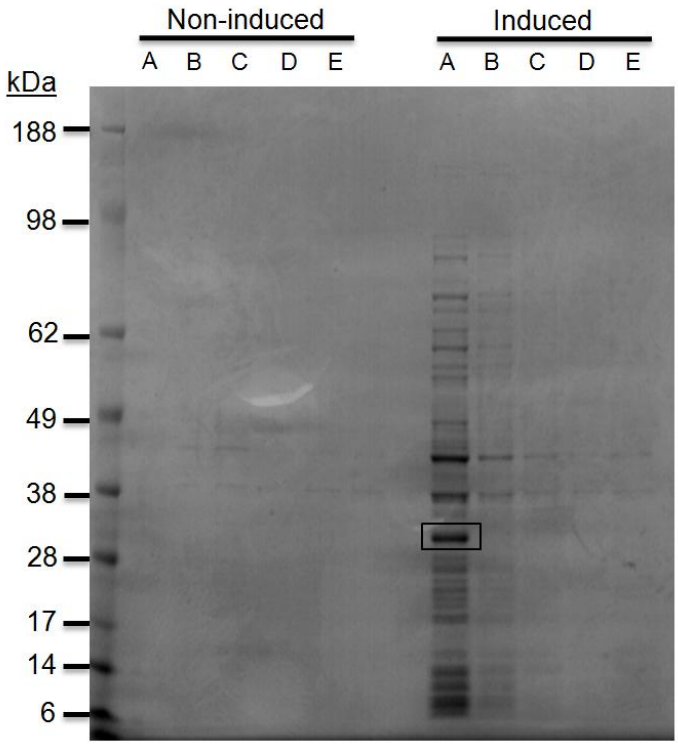

Figure 5.16 Protein expression trials of transformed BL21Star (DE3) *E. coli*. pRSET-EmGFP and pRSET-DBLMSP vectors transformed into *E. coli* were grown to mid-log phase ($0D_{600}$ = 0.3-0.4), prior to the addition of 1mM IPTG. Induced and non-induced bacteria were incubated for 6hr at 37˚C in a shaking incubator, and pelleted by centrifugation. The cells were resuspended in 40µl of 1x NuPAGE reducing buffer (Life Technologies), and boiled for 5 min at 95˚C. 5µl of this mixture was loaded into the wells of 4-12% Bis-Tris gels and visualised by Coomassie Brilliant Blue R250 staining. Lanes are as follows: **A**- pRSET-EmGFP; **B**- pRSET-DBLMSP-FL; **C**- pRSET-DBLMSP-C; **D**- pRSET-DBLMSP2-FL; **E** - pRSET-DBLMSP2-C. Expression of the GFP tag (~ 30kDa) is highlighted with a black box. Owing to the poor resolution of proteins from non-induced samples by Coomassie staining, a larger volume (>5µl) of mixture should be loaded onto gels in future expression trials.

5.3.7. Synthesis of the DBL fragments of DBLMSP and DBLMSP2 and sub-cloning into pRSET bacterial expression vector

The DBL domain of DBLMSP2 has been successfully cloned using bacterial expression systems [147]. Owing to the extreme difficulty in production of the DBLMSP2 proteins, we investigated whether the presence of the SPAM domain was inhibiting the expression of recombinant DBLMSP and DBLMSP2. For this, bacterial expression vectors containing genes encoding only the DBL domains of DBLMSP and DBLMSP2 from the 3D7 *P. falciparum* strain were designed. The DBL domains were synthesised and cloned into the pFUSE-MCS parking vector (Eurofins, see Appendix II for plasmid maps and sequences), digested with restriction enzymes to confirm correct insertion (Figure 5.17A), and checked by sequencing. The inserts were subcloned into the pRSET vector, which was linearised and dephosphorylated. The resulting vectors are referred to as pRSET-DBLMSP-DBL and pRSET-DBLMSP2-DBL, which were confirmed by sequencing (Figure 5.17B).

5.3.8. Expression of pRSET-DBL vectors in BL21Star (DE3) *E. coli*

The pRSET-DBLMSP/2-DBL vectors transformed into BL21Star (DE3) *E. coli*. Starter bacterial cultures were grown to mid-log phase, then grown for a further 6hr at 37˚C in a shaking incubator, in the presence or absence of 1mM IPTG. Protein expression was determined by Coomassie Brilliant Blue R250 staining and Western blotting. Western blot analysis revealed expression of the GFP tag (~30kDa) but not of the recombinant DBLMSP-DBL or DBLMSP2-DBL (Figure 5.18, right panel). No obvious differences were observed by Coomassie staining (Figure 5.18, left panel). These results indicate that bacterial expression of the DBL domains was unsuccessful.

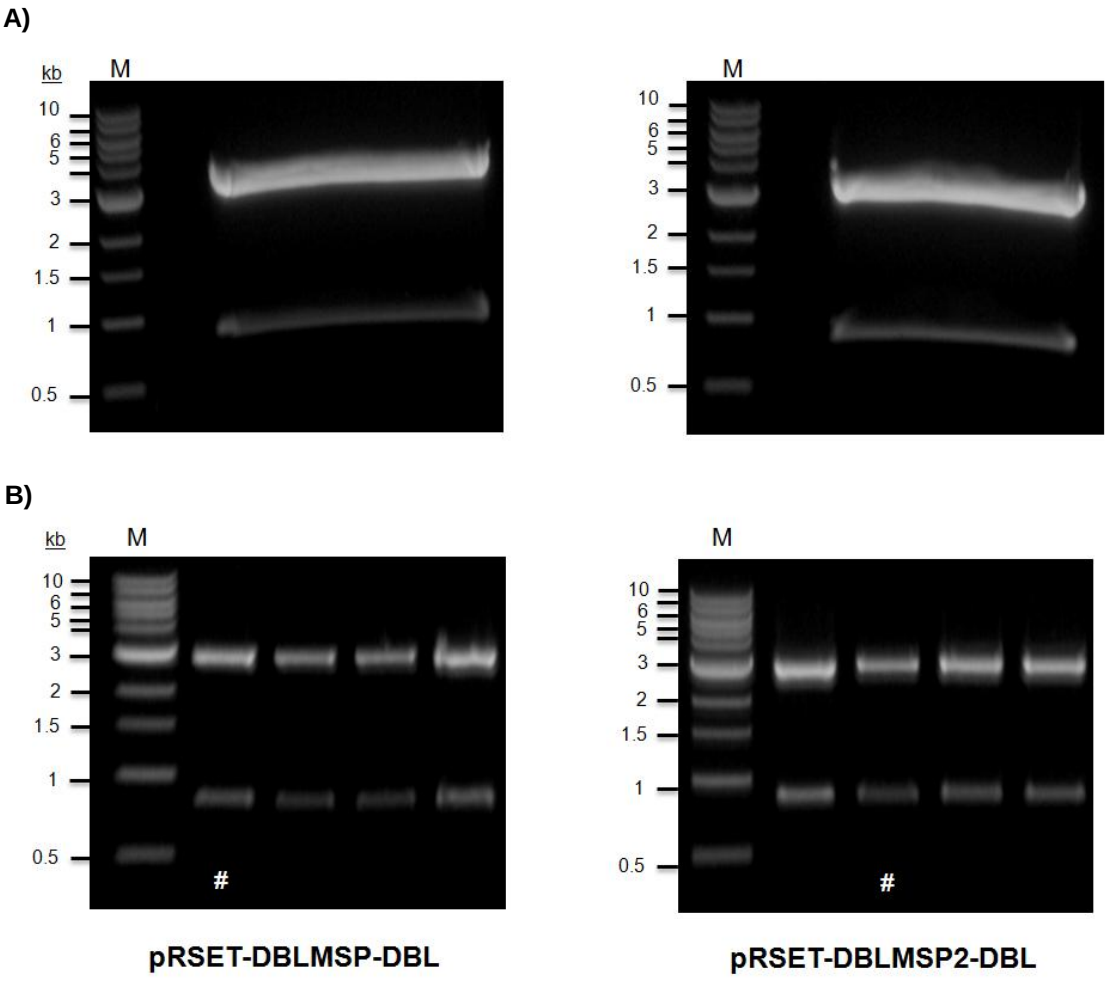

Figure 5.17 (A) Digestion and linearisation of the pRSET EmGFP bacterial expression vector. The pFUSE-MCS-DBLMSP/2-DBL vectors were double digested with BamHI/ XhoI restriction enzymes to release the genes encoding the DBL domains of DBLMSP and DBLMSP2, shown above as the lower band at ~800 and ~830bp, respectively. The upper band at >3000bp is the linearised pFUSE-MCS vector backbone. **(B) Generation of the pRSET-DBLMSP-DBL and pRSET-DBLMSP2-DBL vectors**. DBL inserts were subcloned into the pRSET vector linearised with BamHI/XhoI. The resulting pRSET-DBLMSP/2-DBL vectors were transformed into TOP10 *E. coli* cells and incubated overnight at 37˚C on LB-ampicillin plates. Bacterial colonies were screened for the presence of the DBL inserts by restriction enzyme digestion (BamHI/XhoI) and agarose gel electrophoresis. The upper bands represents the linearise pRSET vector (>3000bp) and the lower bands represent the DBLMSP/2-DBL inserts. Positive colonies were amplified and checked by sequencing. Colonies with the correct sequence are shown as #. The subcloning experiments were performed by Dr Pat Blundell.

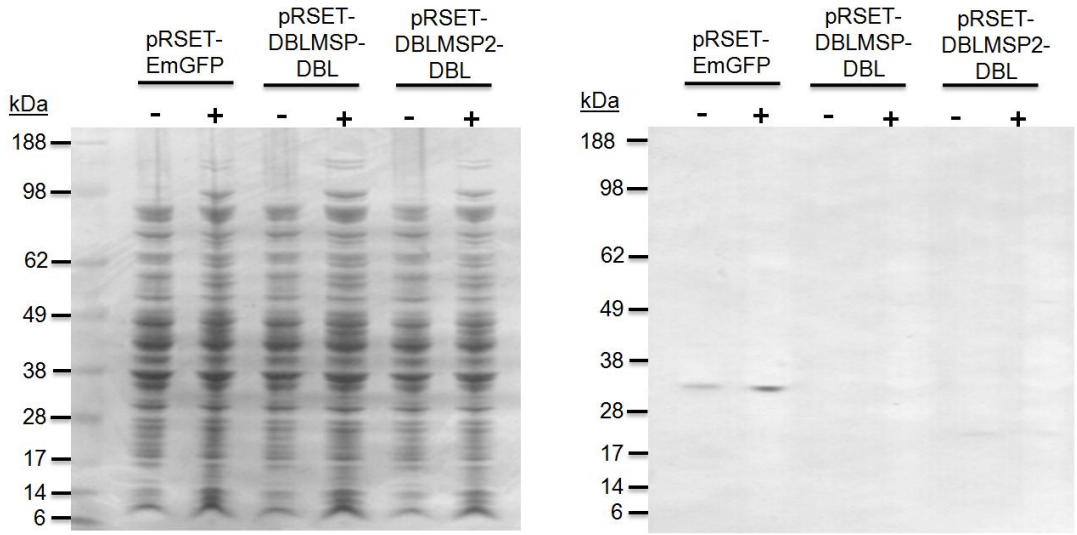

Figure 5.18 Expression of recombinant DBL domains of DBLMSP and DBLMSP2. pRSET-EmGFP and pRSET-DBLMSP/2-DBL vectors transformed *E. coli* were grown to mid-log phase (OD_{600}= 0.3-0.4), prior to the addition of 1mM IPTG. Induced (+) and non-induced (-) cells were incubated for 6hr at 37˚C in a shaking incubator, and pelleted by centrifugation. The cells were resuspended in 40µl of 1x NuPAGE reducing buffer (Life Technologies), and boiled for 5 min at 95˚C. 5µl of this mixture was loaded into the wells of 4-12% Bis-Tris gels and visualised by Coomassie Brilliant Blue R250 staining (left panel) or Western blotting using anti-his-AP (1:5000) (right panel). The Western blot reveals expression of the GFP tag (~30kDa) but not of the recombinant his-tagged DBL domains of DBLMSP and DBLMSP2.

5.3.9. Analysis of possible explanations for failed protein expression

The recurrent failure to produce recombinant protein via mammalian and bacterial systems led us to investigate possible explanations for this lack of protein expression. In the mammalian expression systems, our genes in two different plasmids (pcDNA 3.1(+) and pFUSE-MCS), and in two different cell lines (CHO-K1 and HEK293T) could not generate recombinant protein. There are several factors which can influence protein expression in mammalian systems, including the presence of the Kozak consensus sequence [306], signal peptide sequences [304], and fusion partners [307, 308]. The Kozak sequence (A/GxxATGG) was identified as the optimal sequence for initiation by eukaryotic ribosomes [306, 309]. Reanalysis of the synthesised gene sequences revealed that the Kozak sequence used here (ACCATG**A**; Appendix II) contained an adenine (A) at position-6 rather than a guanine (G; A/GxxATG**G**), possibly as a result of codon-optimisation. Base substitutions in the positions surrounding the ATG initiation codon can modulate its function [306], therefore, the substitution of an A for a G at position-6 could affect the efficiency of translation, potentially offering one explanation for the lack of recombinant protein expression observed.

Sakamoto et al. offered an alternative explanation by suggesting the possibility of RNA polymerase spillage at AT-rich areas in plasmodium genes, which may induce potential frameshifts during the transcription stage [281]. They identified three regions of adenine-repeat sequence areas of the *dblmsp* gene at positions 701-707bp, 1363-1370bp and 1871-1875/ 1901-1909bp, which were subject to site-directed mutagenesis during plasmid construction [281]. Using the assumptions described previously for the identification of adenine-repeat areas [281], we characterised six adenine-repeat regions (≥7 adenines) in the gene encoding DBLMSP2 (PF10_0355), as shown in Figure 5.19. However, analysis of the cloned inserts showed that these areas had been removed by codon-optimisation (see Appendix II). Sequence analysis revealed that the overall A-T content for the cloning inserts used in this chapter were ~46% (Table 5.1), thus this does not offer an explanation as to why DBLMSP2 was more difficult to produce.

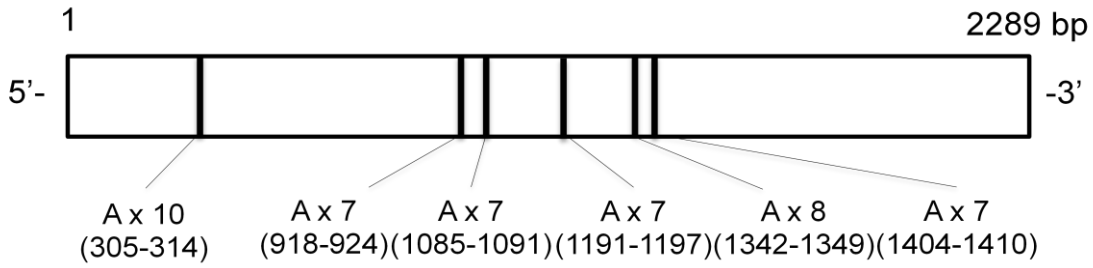

Figure 5.19 Schematic diagram of the adenine-repeat regions of DBLMSP2. Six vertical lines show the adenine-rich sites of the *dblmsp2* gene; 10 consecutive adenines (305-314bp); 7 consecutive adenines (918-924bp); 7 consecutive adenines (1085-1091bp); 7 consecutive adenines (1191-1197bp); 8 consecutive adenines (1342-1349bp) and 7 consecutive adenines (1404-1410bp). These regions were removed from the cloned inserts used in this chapter by codon-optimisation.

Table 5.1 Analysis of the A-T content of genes encoding DBLMSP and DBLMSP2. Counts of adenine (A) or thymine (T) base pairs were taken from the cloned inserts between the BamHI/ XhoI restriction enzyme sites. Percentage of A+T and G+C were calculated using the equation: (A+T or G+C counts/ total bp) x 100.

Genes	Base pairing	Counts (total bp)	Percentage of total bp (%)
DBLMSP-FL	A+T	1013 (2187)	46.3
	C+G	1174 (2187)	53.7
DBLMSP2-FL	A+T	1090 (2373)	45.9
	C+G	1283 (2373)	54.1
DBLMSP-C	A+T	646 (1374)	47
	C+G	728 (1374)	53
DBLMSP2- C	A+T	712 (1542)	46.2
	C+G	830 (1542)	53.8

Another factor contributing to the successful expression of recombinant proteins in mammalian cells is the use of a fusion partner. Fusion proteins have long been adopted for enhancing expression and solubility of recombinant proteins, in particular in prokaryotic expression systems which lack folding and chaperone machinery [308]. In mammalian systems, Fc regions of Abs and human serum albumin have been shown to enhance expression levels [308, 310]. Therefore, the difference in successful protein expression using the pFUSE-hIgG1-Fc2 and pFUSE-MCS could be due to the presence of the Fcγ-fusion partner in the former vector. However, this remains to be determined.

Expression of the genes encoding DBLMSP fragments in the bacterial expression vector was also unsuccessful. Initially, we hypothesised that the removal of the fluorescent protein sequence (209-928bp) from the pRSET-EmGFP may have cleaved the ribosome binding site (RBS), which would affect initiation of transcription. However, further analysis revealed the RBS to be upstream of the 6xhis tag at base pair position 76-81 (Life Technologies, personal communication). As the genes were codon-optimised for mammalian expression, the failed expression of recombinant DBLMSP proteins in contrast to the GFP tag could be due to suboptimal codon selection.

5.4. Discussion

The SPAM domain of MSP3-family proteins has been implicated in allowing the formation of oligomers [276]. Since the SPAM domains of DBLMSP and DBLMSP2 were shown to oligomerise [146], we sought to clarify whether DBLMSP and DBLMSP2 proteins lacking DBL domains (C= control, SPAM only) could also form high molecular weight oligomers, to clarify the potential involvement of regions outside of the SPAM domains in oligomerisation of these proteins.

To achieve this, we tried to produce full-length and SPAM-only recombinant DBLMSP and DBLMSP2 proteins. Mammalian expression systems were initially used, as this system was adopted by Crosnier et al. to generate recombinant DBLMSP and DBLMSP2 [146]. However, protein expression trials using the pcDNA 3.1(+)-DBLMSP vectors were unsuccessful. To determine whether this issue was due to vector selection, inserts were subcloned into the pFUSE-hIgG1-Fc2 vector which has previously been shown to produce high yields of protein [185]. Furthermore, expression of the DBL domains only had been successful using this vector (Shona Moore, personal communication). Despite numerous expression trials using two mammalian cell lines (CHO-K1 and HEK293T), we were unable to generate recombinant protein using this vector. Protein trials with cell lysate indicated that the lack of expression in HEK293T cells was not due to issues with protein secretion. These results were somewhat confounding, especially as the DBL domains were generated using identical methods. However, an adapted version of the pFUSE-hIgG1-Fc2 vector was used here (pFUSE-MCS) in which the sequence encoding the Fcγ tag was removed. This could contribute to the efficiency of protein expression, as Fcγ tags have been shown to dramatically increase the expression of recombinant proteins [308]. Intriguingly, a review of the previously published data on DBLMSP and/or DBLMSP2 protein expression showed that the majority of studies omitted the native plasmodium signal peptide in cloning procedures [147, 149, 281]. Whether the native signal peptide can affect protein expression in mammalian/ bacterial systems remains to be determined. Therefore, future protein expression trials could be repeated following cleavage of the native signal peptide from the *dblmsp* genes to clarify its role in protein expression.

Due to the failed expression in mammalian systems, we next sought to investigate whether these proteins could be produced via bacterial expression systems, similar to those used by Hodder et al. However, we were unable to express full-length, SPAM only, or DBL-only domains of DBLMSP and DBLMSP2 [147]. The expression of the GFP tag in bacteria was successful, suggesting that the issues with protein expression were governed by the inserts rather than the cloning vector. As discussed in section 5.3.9, the most likely explanation for the failed protein expression in bacterial systems was codon-optimisation for mammalian cells, and therefore subsequent experiments should be repeated with genes codon-optimised for bacterial systems or use a commercial *E. coli* strain that contains rare tRNAs such as Rosetta.

The production of DBLMSP2 was significantly more problematic compared to DBLMSP, as both mammalian and bacterial cells transfected with vectors containing DBLMSP2 were either slow growing or completely failed to grow. This observation was also confirmed for the DBL domain of DBLMSP2 produced by expression in the pFUSE-hIgG1-Fc2 vector (Shona Moore, personal communication). Sequence analysis of the *dblmsp2* gene revealed that codon-optimisation had removed numerous AT-rich regions which may have cause RNA polymerase spillage. Therefore, the stunted growth of the DBLMSP2-containing constructs in both mammalian and bacterial cells suggests that this gene is toxic to cells. Possible methods to resolve this issue include the use of lower incubation temperatures (25-30˚C) or repeating transformations with *E. coli* strains or vectors which exert tighter transcriptional control over the gene of interest.

Only one laboratory has been successful in expressing full-length DBLMSP and DBLMSP2 to date [146]. This success may have been due to the use of a more sophisticated cloning vector, the identity of which is currently unknown, or the use of bioreactors for large-scale protein production [311]. In addition, this study utilises the mouse variable K light chain leader sequence and a rat Cd4 domain 3 and 4 tag (Cd4-d3+4), both of which have been implicated in enhanced protein production [188-190]. There is plenty of scope for building on the protein production techniques used in this chapter. For example, subcloning inserts into expression vectors previously shown to generate recombinant DBLMSP proteins, improving signal peptide sequences or fusion partners, or the upscale of protein production through the use of

bioreactors. Unfortunately, limitations in time and resources prevented us from pursing these potential avenues.

The aim of this chapter was to determine the role of the SPAM domain in oligomerisation via the production of recombinant SPAM-only proteins. However, the present data indicates that full-length and SPAM-only recombinant DBLMSP and DBLMSP2 cannot be produced by the methods mentioned above. In addition to optimizing protein expression techniques, future studies could perform mRNA analysis to resolve whether the lack of protein expression was due to issues in the transcription or translation of the cloned inserts.

Chapter 6: Investigating the function of hFcμR

6.1. Literature review

6.1.1. Function of FcμR

The biological consequences of IgM binding to hFcμR remain unclear. However, genetically altered mice lacking FcμR (*Fcμ$R^{-/-}$*) have provided an insight into the function of this receptor. FcμR-deficiencies in mice resulted in significantly elevated serum IgM levels [138], altered differentiation of B cells [292], and increased production of autoAbs with age [312]. Furthermore, *Fcμ$R^{-/-}$* B cells were sensitive to apoptosis induced by B cell receptor (BCR) activation, suggesting that FcμR mediates enhanced B cell survival and proliferation following BCR cross-linking [138, 292]. The effect of FcμR on immune responses has also been investigated using knockout mice models, which revealed that FcμR ablation resulted in reduced Ab responses to thymus independent (TI) and thymus dependent (TD) antigens [138]. In addition, reduced Ab responses were accompanied by reduced germinal centre formation in FcμR-deficient mice immunised with TD antigen [138]. Together, the data implicates murine FcμR in generation of immune responses, IgM homeostasis, and in the negative regulation of autoimmunity.

6.1.2. Expression of human FcμR

Although insights have been made into the function of FcμR in mice, differential expression of the receptor in mice and human poses the question whether the receptor serves a different function(s) in humans. In mice, FcμR is expressed on B cells but not T cells, dendritic cells and macrophages, whereas human FcμR is expressed on adaptive immune cells including B cells, T cells and at low densities on NK cells [137]. The finding that overnight incubation of PBMCs in serum-free media enhanced the expression of hFcμR indicates that exogenous levels of IgM may influence the expression of the receptor [137]. T cells were particularly susceptible to enhancement, and the effect was more prominent for tonsillar and splenic lymphocytes compared to blood lymphocytes [137].

Cellular activation was shown to influence FcμR expression. B cell stimulants PMA and anti-μ mAb promoted a ~2.2-fold increase in cell-surface hFcμR expression after 24hr, whereas PMA or anti-CD3 mAb treatment of T cells reduced the expression of hFcμR by ~90% after 24-72hr [137]. Murakami et al. supported these findings and concluded that interleukin (IL)-2 induced downregulated hFcμR expression on T cells and NK cells in a dynamic and reversible process [140]. Furthermore, they found hFcμR expression on $CD4^+$ T cells was downregulated through TCR activation, which supported the observation of lower receptor expression on effector and memory T cells when compared to naive T cells [140]. However, this study used mouse IgM as a ligand for hFcμR owing to its increased binding ability [140]. Therefore, these results should be viewed with caution as mouse IgM could induce alternative effector mechanisms, possibly owing to structural and biochemical differences between mouse and human IgM. Future studies should therefore focus on using human IgM to resolve the function of hFcμR. The expression of hFcμR in chronic lymphocytic leukaemia (CLL) cells was dramatically down-regulated within 24hr following culture with the toll-like receptor (TLR)-7 agonist imiquimod and the TLR9 agonist CpG-ODN [183]. The contrasting effect of stimulation on hFcμR expression between B cells and T cells could be due to the receptor performing differential functions on these cells.

An intriguing finding was that hFcμR expression was selectively overexpressed on malignant B cells in CLL disease [178]. CLL is a malignancy of IgM^+ IgD^+ mature B cells which are poly-reactive and are resistant to Fas-mediated apoptosis, although the mechanisms governing this resistance are unknown [313, 314]. The mechanisms involved in CLL ontogeny are unclear, however Ag-stimulation has been proposed as a key pathway for CLL cell expansion [315]. Given that BCR stimulation was found to increase the expression of hFcμR on CLL cells [137, 177], and the finding that BCR signalling influences hFcμR expression [137], the overexpression of hFcμR in CLL may be indicative of prolonged BCR activation [183]. However, this remains to be determined. In addition to enhanced expression, serum titres of soluble FcμR (~40kDa) were also elevated in CLL patients, which strongly correlated with blood lymphocyte counts [313]. Healthy donors did not exhibit increased serum titres of soluble FcμR, which identified a soluble form of FcμR encoded by a *FCMR* splice

variant. CLL B cells and non-CLL B cells, but not T cells, secrete ~40kDa soluble FcμR [313]. The significance of soluble FcμR in CLL disease remains unknown.

6.1.3. Function of human FcμR

The overexpression of hFcμR in CLL cells was initially associated with resistance to Fas-induced apoptosis, as determined by gene ontology analysis [178]. Subsequent studies investigated the role of hFcμR in protection for apoptosis, and revealed that isolated FcμR cDNA is identical to that of the previously described human Fas apoptotic inhibitory molecule 3 (FAIM3). Hitoshi et al. identified FAIM3 as a potent inhibitor of Fas/CD95-induced apoptotic signalling within activated T cells using a retroviral cDNA library-based functional assay [316]. In contrast, Kubagawa et al. dismissed hFcμR role in the inhibition of Fas-induced signalling as inhibition of apoptosis was only observed when anti-Fas IgM (and not IgG) Abs were used [137, 312]. Despite the controversy over the role of FcμR as an anti-apoptotic receptor, numerous studies have since discounted the role of hFcμR as an anti-apoptotic receptor [137, 140, 312, 317].

The finding that serum levels of IgM are significantly raised in $Fc\mu R^{-/-}$ mice implies a role for the FcμR in IgM homeostasis [138]. Peritoneal B1 cell populations are considered a major source of IgM [318]. However, as these populations were not expanded in FcμR-deficient mice, the elevated IgM levels are unlikely to be a consequence of increased IgM production. Further, the expression of FcμR on B cell surfaces inversely correlated with serum levels of IgM. Intriguingly, serum IgM levels were unaltered in pIgR- and Fcα/μR-deficient mice, signifying FcμR as the sole receptor modulating the homeostasis of IgM [138]. Administered exogenous monoclonal IgM exhibited a similar half life in WT and $Fc\mu R^{-/-}$ mice, indicating that FcμR is not involved in maintaining the half-life of IgM in mice [138]. Alternatively, the similar half-life may be owing to the down modulation of FcμR expression on B cells, as FcμR expression is sensitive to exogenous IgM levels [137]. These similarities in half-life may indicate that FcμR is not involved in IgM clearance under steady-state conditions, although it is feasible that the ligation of IgM-immune complexes to FcμR during immune responses could lead to their catabolism [138].

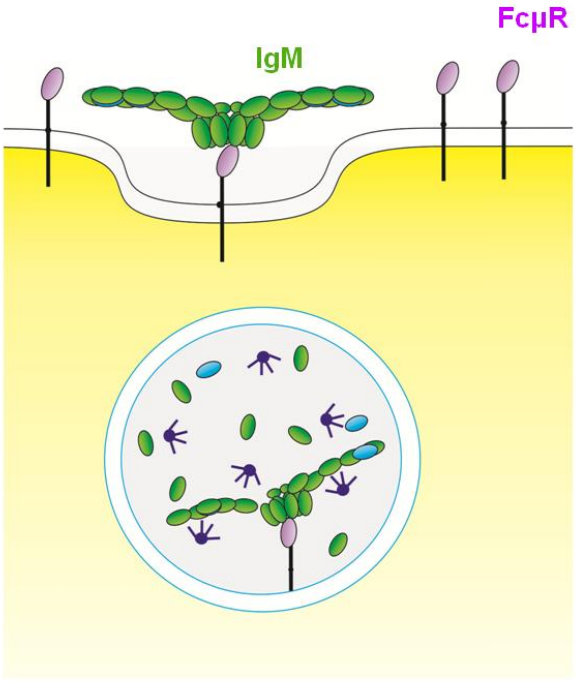

Figure 6.1 Schematic diagram depicting FcμR-mediated endocytosis of human IgM. The cross-linking of FcμR by IgM induces rapid internalisation of FcμR-bound IgM. Within 60 min of internalisation, IgM is shuttled to lysosomes (represented as blue vesicle) via the endocytic pathway for degradation by hydrolytic enzymes (represented in navy blue) adapted from [183]. Since FcμR expression was dramatically down-regulated by TLR activation, it was hypothesised that FcμR may function to shuttle IgM-opsonised immune complexes to lysosomes where TLR activation may ensue [183].

Further studies are required to evaluate the role of IgM and FcμR during *in vivo* immune responses.

Initial studies reported that HeLa cells expressing mouse and human FcμR internalised microbeads coupled with mouse IgM, suggesting human FcμR may also serve as an endocytosis receptor for IgM-opsonised antigens by B cells [175]. The cross-linking of hFcμR on CLL cells by IgM results in the rapid internalisation of IgM, which occurred within 1 minute [183]. Following internalisation, IgM is shuttled through the endocytic pathway to lysosomes, whereby IgM is proposed to be degraded [183], as depicted in Figure 6.1. Inhibition of clathrin-dependent endocytosis by phenylarsine oxide (PAO) decreased IgM internalisation by more than half, signifying that IgM internalisation by CLL cells is partially mediated by a clathrin-dependent mechanism [183]. In the absence of IgM, basal FcμR recycling and degradation from the plasma membrane is slow. Therefore, it is thought that FcμR does not recycle from membrane to the trans-golgi network (TGN) without ligation of natural ligand [183]. A panel of FcμR deletion mutants revealed that internalisation is controlled by a YXXφ motif [183]. Together, these results identify hFcμR as an endocytotic receptor for hIgM on B cells.

Despite these insights into the effector functions of FcμR, there are still gaps in the current knowledge regarding the role of human FcμR. For example, it is not known how cellular activation or immune complex formation can affect the internalisation of IgM via hFcμR, or what characteristics of IgM are required for internalisation. This chapter confirmed the role of hFcμR as an endocytic receptor for IgM, and investigated what additional factors contribute to this mechanism.

6.2. Objectives

This chapter presents experiments that were done with the aim of determining the function of FcμR in humans. The specific objectives were:

I. Investigate whether FcμR functions as an endocytic receptor for IgM
II. Determine the requirements for FcμR-mediated internalisation of IgM
III. Characterise the expression of hFcμR on lymphocyte subsets

6.3. Results

6.3.1. Human FcμR mediates endocytosis of IgM into FcμR expressing cell lines

The role for FcμR in the internalisation of IgM molecules has been highlighted previously [183]. As this previous study focused on human FcμR overexpressed on CLL cells, the ability of human FcμR to function as an endocytic receptor for IgM was investigated here by flow cytometry.

The internalisation of IgM by FcμR was assessed by flow cytometry as previously described with minor modifications [183]. Briefly, hFcμR-transfected cell lines were opsonised with hIgM and washed prior to incubation at 37°C to induce receptor internalisation. IgM internalisation into untransfected BW5147 T cell lines was also investigated, and the values of which were subtracted from the data obtained for the hFcμR-transfected cell lines. As shown in Figure 6.2, there was marked internalisation of IgM within 5 min of incubation at 37°C, with ~50% reduction of IgM levels on cell surfaces. Cell surface IgM was further internalised until ~30% of IgM remained on the surfaces following 1hr at 37°C (Figure 6.2). This data suggests that upon ligand binding, hFcμR rapidly internalises bound IgM. Similarities in internalisation dynamics between purified human IgM (Sigma-Aldrich) and human serum suggests that additional serum components are not necessary to mediate IgM internalisation (Figure 6.2B; $p = 0.746$).

To determine if IgM-immune complexes were also internalised by hFcμR, hFcμR-transfected cell lines were opsonised with heat-aggregated IgM prior to incubation at 37°C. Intriguingly, IgM-immune complexes (ICs) exhibited significantly enhanced binding and internalisation by hFcμR when compared to untreated IgM molecules (Figure 6.3 & Table 6.1), most likely owing to receptor cross-linking. The enhanced internalised of IgM-ICs suggests that hFcμR may play a role in the internalisation and presentation of immune complexes during immune responses.

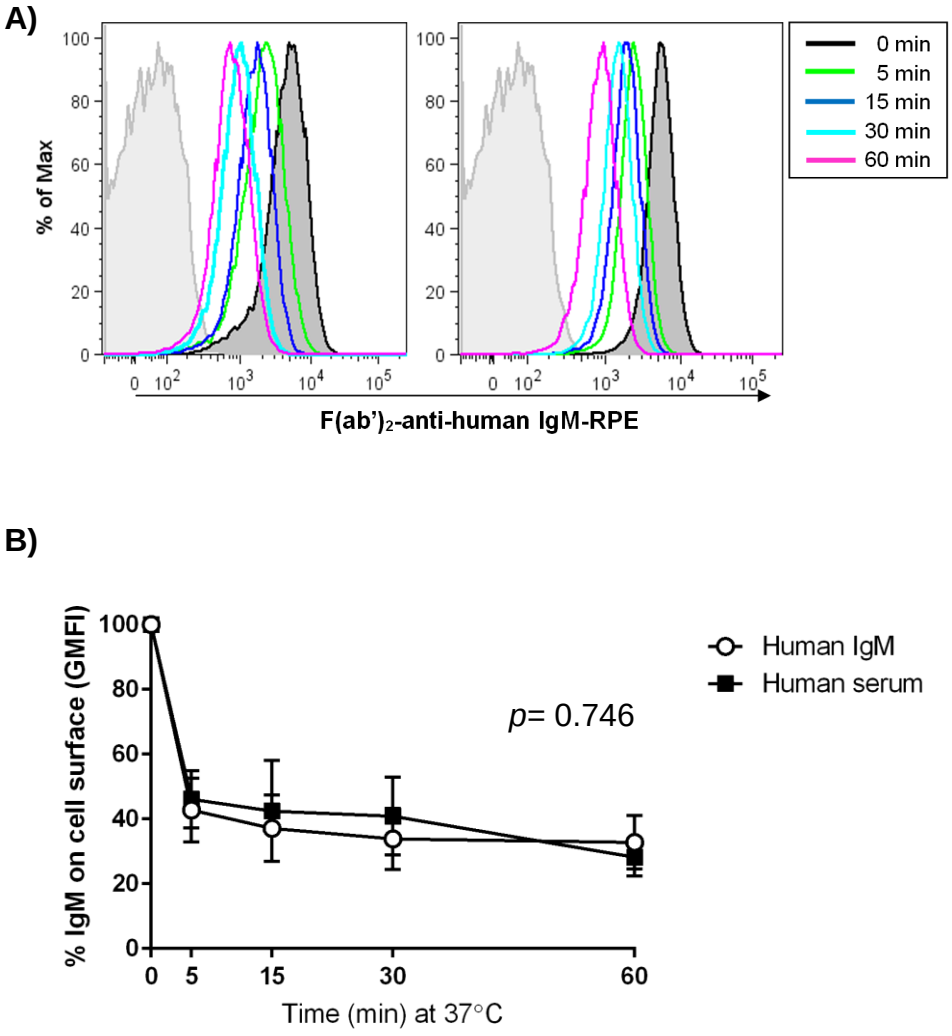

Figure 6.2 Human FcμR mediates endocytosis of IgM. (A) Human FcμR-transfected cell lines were incubated with media alone (grey filled trace) or media supplemented with 15μg/ml purified hIgM (left panel) or 10% human serum (right panel) for 1hr at 4°C, followed by extensive washing at 4°C to remove unbound IgM. Subsequently, the cells were either left at 4°C (black filled trace) or incubated at 37°C for the indicated times. Internalisation was halted with the addition of ice-cold media and immediate incubation on ice for 10min. Cells were then washed and labelled with F(ab')$_2$-anti-human IgM-RPE for 1hr on ice to detect the presence of IgM bound to the cell surface, and analyzed by flow cytometry. IgM mean intensity fluorescence (MFI) shown for indicated time points are representative of five independent experiments. **(B)** IgM cell surface levels (geometric MFI) assessed in *(A)* and normalised to time 0. The mean ± SD from five independent experiments is shown. Mann-Whitney test was used for the comparison of % IgM on cell surface (GMFI) values for human IgM and human serum. Statistically significance was regarded as $p < 0.05$.

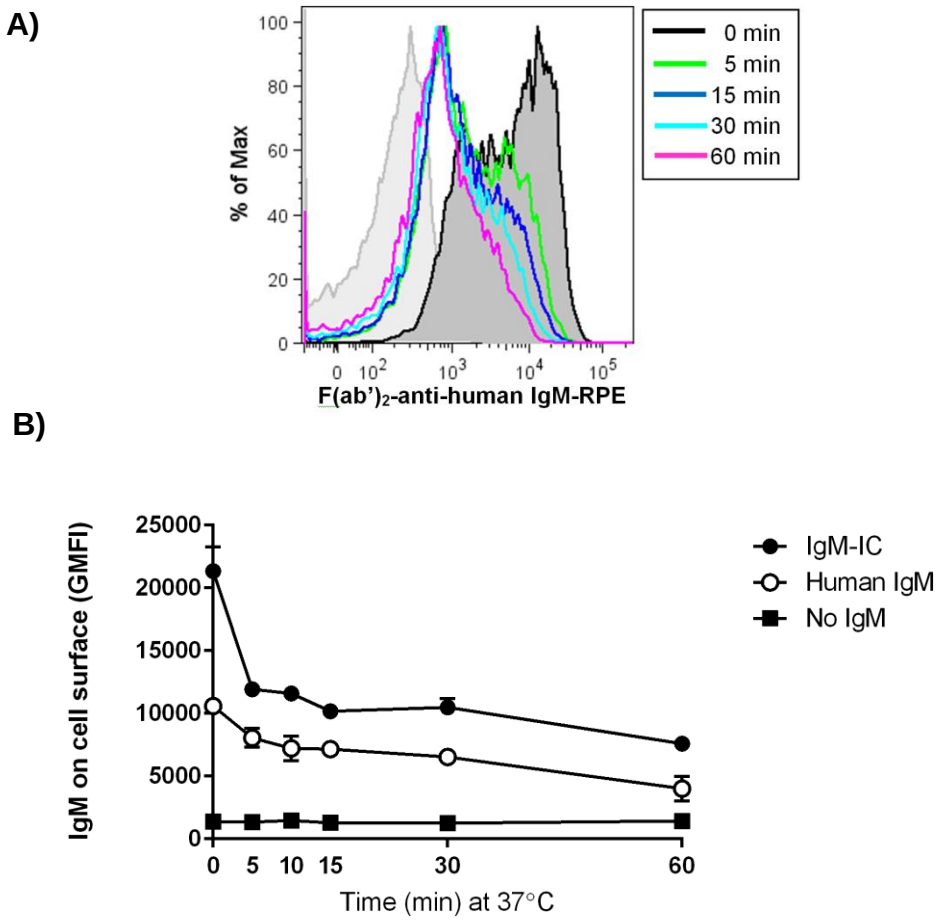

Figure 6.3 FcμR-mediated internalisation of IgM immune-complexes. (A) hFcμR-transfected cell lines were incubated with media alone (grey filled trace) or media supplemented with 15μg/ml heat-aggregated hIgM (IgM-IC) or hIgM for 1hr at 4°C, prior to incubation either at 4°C (black filled trace) or at 37°C for the indicated times. Cells were then washed, labelled with F(ab')$_2$-anti-human IgM-RPE for 1hr on ice, and analyzed by flow cytometry. Data shown are representative of three repeat experiments. **(B)** IgM cell surface levels (GMFI) indicate enhanced binding of IgM-IC to hFcμR-transfected cell lines followed by rapid internalisation of IgM-IC. The mean ± SD from three independent experiments is shown.

Table 6.1 The P values for the difference in internalisation of no IgM, human IgM, or IgM-IC. Mann-Whitney tests for the comparison of IgM on cell surface (GMFI) values for no IgM, human IgM and IgM-IC. Significant results are shown as red ($p < 0.05$).

P value	Human IgM	IgM-IC
No IgM	**0.002**	**0.002**
Human IgM		**0.026**

To confirm the role of hFcμR as an endocytosis receptor for IgM, we next attempted to monitor internalisation of FcμR. First, the expression of hFcμR on cell surfaces was assessed. FcμR was found to be strongly expressed on hFcμR-transfected cell lines (Figure 6.4A), which was shown to co-localise with hIgM binding (Figure 6.4B). No expression of hFcμR was observed on untransfected cell lines (Appendix III; Figure A2). Next, internalisation of FcμR was tracked using a commercially available anti-hFcμR mAb (Abnova). As shown in Figure 6.5, cell surface levels of hFcμR decrease upon incubation at 37°C, supporting basal levels of internalisation of this receptor. However upon IgM binding, internalisation of FcμR was dramatically increased (Figure 6.5), FcμR levels were reduced ~50% within 1hr in the presence of exogenous IgM, compared to a ~25% reduction in the absence of exogenous IgM. This data supports the role of hFcμR as an endocytic receptor for IgM.

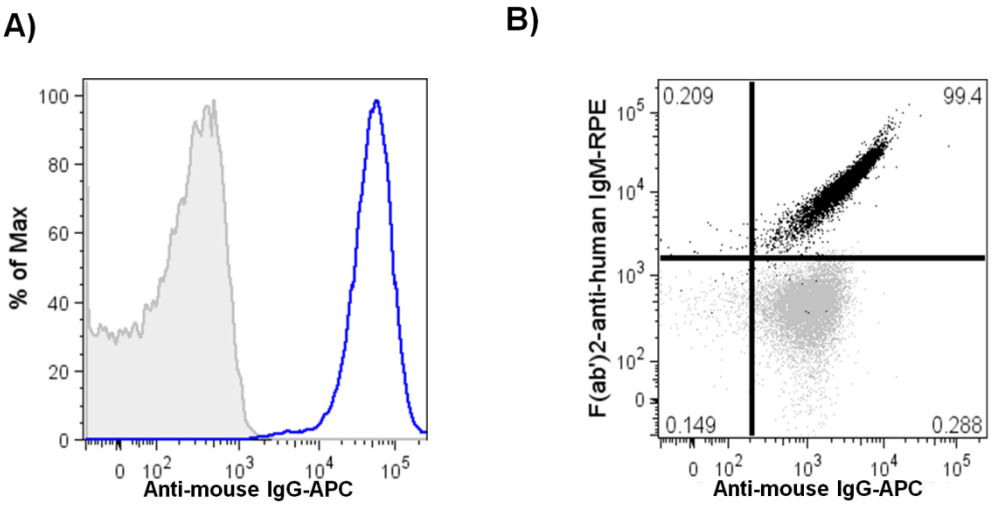

Figure 6.4 IgM binding co-localises with the expression of FcμR on cell surfaces. (A) hFcμR-transfected cell lines were incubated with media in the presence (blue trace) or absence (grey trace) of 1μg mouse anti-hFcμR mAb (Abnova) for 1hr at 4°C, followed by extensive washing in ice-cold media and labelling with anti-mouse IgG-APC for 1hr at 4°C. Labelled cells were analyzed by flow cytometry. **(B)** IgM co-localises with hFcμR expression on cell surfaces. For this, hFcμR-transfected cells were incubated in the presence or absence of 15μg/ml hIgM (shown as black or grey dots, respectively) prior to labelling with anti-hFcμR mAb, anti-mouse IgG-APC, and $F(ab')_2$-anti-human IgM-RPE. Co-localisation of hIgM and hFcμR on cell surfaces was then assessed by flow cytometry (n=2).

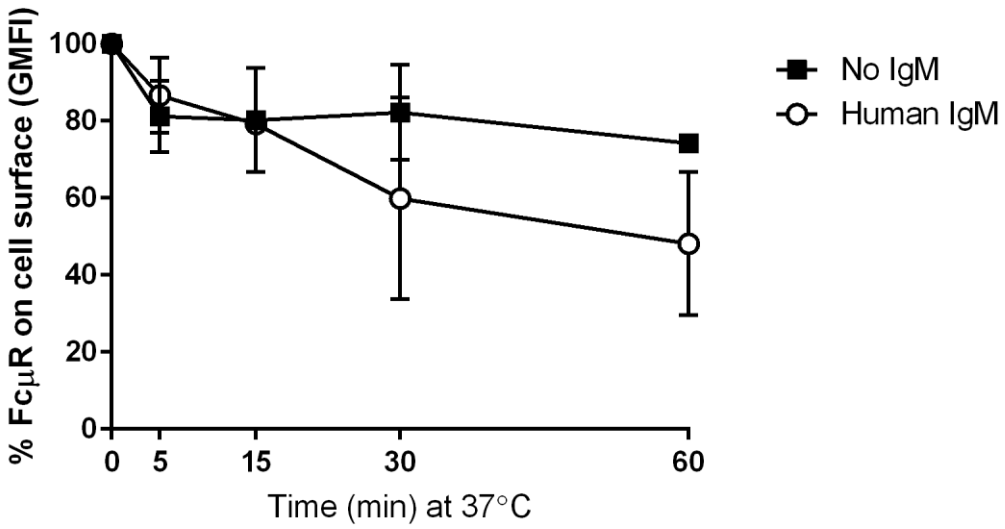

Figure 6.5 FcμR is internalised upon IgM binding. hFcμR-transfected cells were labelled with anti-hFcμR mAb (1μg), washed, then incubated in the presence or absence of 15μg/ml hIgM (shown as black squares or white dots, respectively) for 1hr at 4°C. Internalisation assays were then performed as above. Following internalisation, cells were washed, labelled with anti-mouse IgG-APC and analysed by flow cytometry. Background values were removed from FcμR cell surface levels (GMFI) values, which were then normalised to time 0 for both samples. The mean ± SD of two experiments is shown.

6.3.2. Human IgM is internalised into human lymphocytes

Since hIgM was internalised by hFcμR-transfected cells, IgM internalisation into lymphocyte subsets known to express FcμR was next investigated. For this, PBMCs were labelled with markers to differentiate B cells, T cells and NK cells (Figure 6.6). Surface levels of IgM on gated lymphocyte surfaces was detected by staining with $F(ab')_2$-anti-human IgM-RPE in the presence or absence of IgM (Figure 6.7). As lymphocytes were found to be purified with IgM on their cell surfaces (see Chapter 3), internalisation of endogenous surface IgM was detected with the addition of the anti-human IgM-RPE Ab only (no IgM).

As lymphocytes express a multitude of receptors, the binding of additional components in human serum (e.g. complement, lectins) to receptors expressed on lymphocyte surface could affect the internalisation of IgM. To determine if additional serum components affected internalisation, some assays were performed using both purified hIgM (Sigma-Aldrich) and human serum as a source of IgM. There was no significant difference in IgM internalisation between two IgM sources (Appendix III; Figure A3), and therefore human serum was used for subsequent internalisation assays.

We then investigated IgM internalisation on lymphocyte subsets. As shown in Figure 6.7, exogenous IgM was internalised into B cells, $CD4^+$ and $CD8^+$ T cells, and NK cells following incubation at 37°C. For T cells, $CD8^+$ subsets were shown to internalise IgM better than $CD4^+$, with ~75% reduction in cell surface levels of IgM in $CD8^+$ T cells within 5 min at 37°C compared to ~60% reduction in $CD4^+$ T cells (Figure 6.7). In the absence of exogenous IgM, incubation at 37°C still initiates a reduction of cell surface IgM, albeit at a slower rate (~20% and ~18% vs. ~75% and 60% reductions after 5 min for $CD8^+$ and $CD4^+$ cells, respectively). In NK cells, surface levels of IgM were reduced by ~85% within 5 min in cells incubated with human serum and ~25% in cells incubated with media alone (Figure 6.7). However, these values were highly variable between donors as reflected by the high error bars (Figure 6.7). B cells exhibit high levels of IgM on cell surfaces upon purification, likely owing to the expression of IgM^+ BCR, which resulted in difficulty differentiating between IgM bound to FcμR and IgM^+ BCRs. Despite this, there was a noticeable reduction in cell surface IgM levels upon incubation in cells incubated

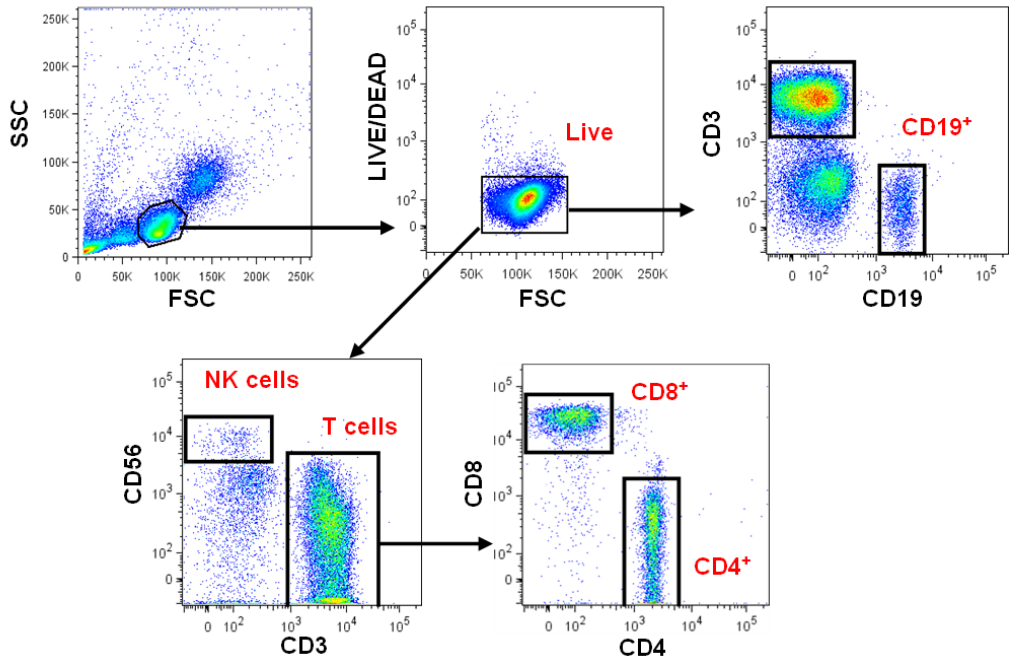

Figure 6.6 Gating strategy for lymphocyte subsets expressing hFcμR. PBMCs were washed and labelled with 1uM LIVE/DEAD® Aqua Dead Cell stain in PBS at 4°C for 30 min. Cells were washed and incubated with anti-human CD3-Brilliant Violet™ 421, anti-human CD56-Alexa Fluor 700, anti-human CD8-PerCp, and anti-human CD4-FITC for 1hr at 4°C. To differentiate B cells, LIVE/DEAD stained PBMCs were incubated with anti-human CD3-Brilliant Violet™ 421 and anti-human CD19-FITC. Labelled cells were washed extensively and analyzed by flow cytometry. Lymphocytes were gated from the PBMC population based on side (SSC) and forward (FSC) profiles, which was further gated into live cells based on LIVE/DEAD® and FSC staining. Live cell population was further gated into B cells ($CD3^-CD19^+$), T cell ($CD3^+CD56^-$) and NK cell ($CD3^-CD56^+$) populations, and the T cell population was divided into $CD4^+$ ($CD3^+CD4^+$) and $CD8^+$ ($CD3^+CD8^+$) T cell subsets.

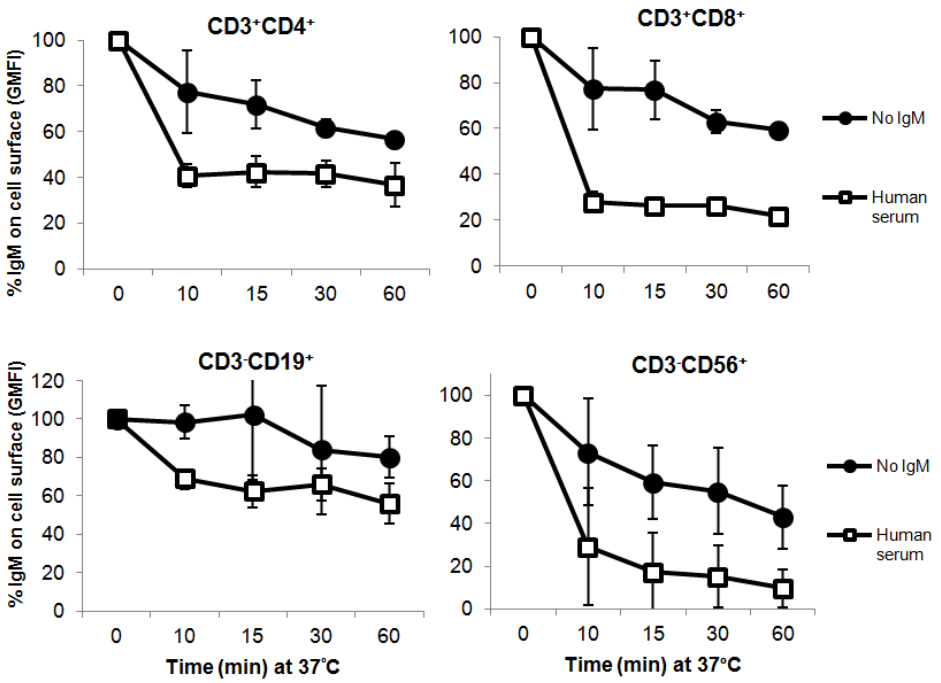

Figure 6.7 Internalisation of IgM on lymphocyte subsets. PBMCs were washed and incubated with media alone or supplemented with human serum for 1hr at 4°C. Cells were extensively washed and incubated at 37°C for the indicated times to induce receptor internalisation, then washed extensively to remove unbound IgM. Cells were labelled with lymphocyte markers (see Figure 6.6) and analysed by flow cytometry. Surface levels of IgM on gated lymphocytes levels (geometric MFI) is represented assessed was assessed and normalised to time 0. The mean ± SD of four independent repeats is shown.

with human serum compared to those incubated with media alone (Figure 6.7). Together, these results suggest that exogenous IgM is rapidly internalised into B cells, T cells, and NK cells upon binding to hFcμR.

6.3.3. IgM sialylation and internalisation

The μ chain of IgM contains five N-linked glycosylation sites (see Figure 1.6), which are predominantly occupied by complex glycans terminating in sialic acid or galactose, or oligomannose glycans [168]. In Chapter 3, we showed that de-glycosylation of IgM did not affect its binding to hFcμR. However, a recent study depicted a role for sialylated N-linked glycans in the internalisation of human IgM by T cells [286]. The authors of this paper hypothesised that hFcμR could bind sialylated IgM and mediate its internalisation.

To clarify the role of glycans in IgM internalisation by hFcμR, N-linked glycans were initially removed from human IgM using PNGase F and neuraminidase (Figure 6.8). De-glycosylation of IgM by PNGase F resulted in a decrease in MW of the IgM heavy chain (from ~62kDa to ~55kDa) and light chain (~25kDa to ~23kDa), and reductions in MW for the heavy chain with neuraminidase treatment (~62kDa to ~60kDa), which signify the removal of glycans from IgM. Next, the ability of hFcμR to internalise de-glycosylated IgM was investigated by flow cytometry (Figure 6.9). De-glycosylation of IgM had no effect on its internalisation by hFcμR-transfected cells (Figure 6.9; $p= 0.746$), demonstrating that PNGase F or neuraminidase susceptible glycan(s), such as the N-linked or sialic acid-terminating glycans, do not contribute to the internalisation of IgM by hFcμR, while also supporting our previous observations that deglycosylated IgM can still bind human FcμR.

In addition to FcμR, human lymphocytes express numerous ligands which have been shown to bind glycans, including lectins such as CD62L or CD33 (Siglec-3) [319, 320]. Moreover, the lectin CD22 (Siglec-2) on B cells binds α2,6-linked sialic acid residues of soluble IgM, resulting in the induction of negative feedback for B cell activation [233]. However, it is not known whether CD22 can mediate internalisation of IgM. To rule out the involvement of glycans and/or the possible involvement of

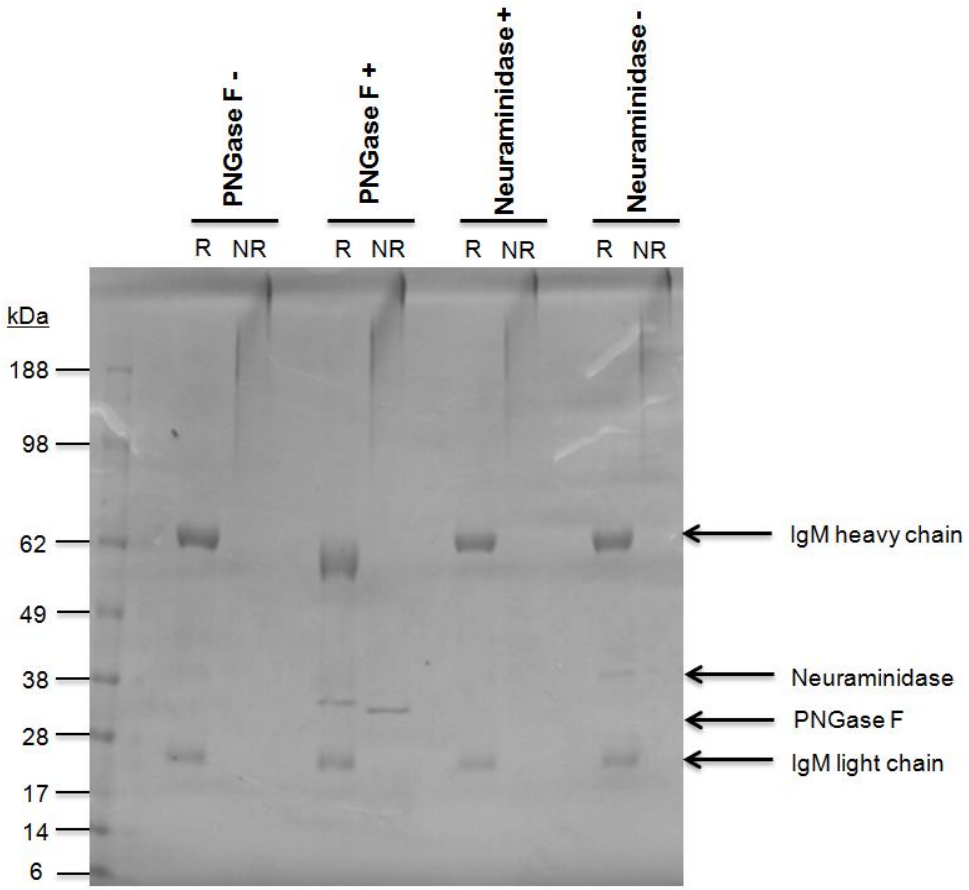

Figure 6.8 Endoglycosidase digestion of human IgM. Human IgM (50µg; Sigma-Aldrich) was digested in the presence (+) or absence (-) of 10µl (5,000 units) of PNGase F or neuraminidase according to manufacturer's instructions (NEB). After overnight incubation at 37˚C, 5µg of each Ab preparation was run under reducing (R) or non-reducing (NR) conditions into wells of a 4-12% Bis-Tris gradient gel (Novex).

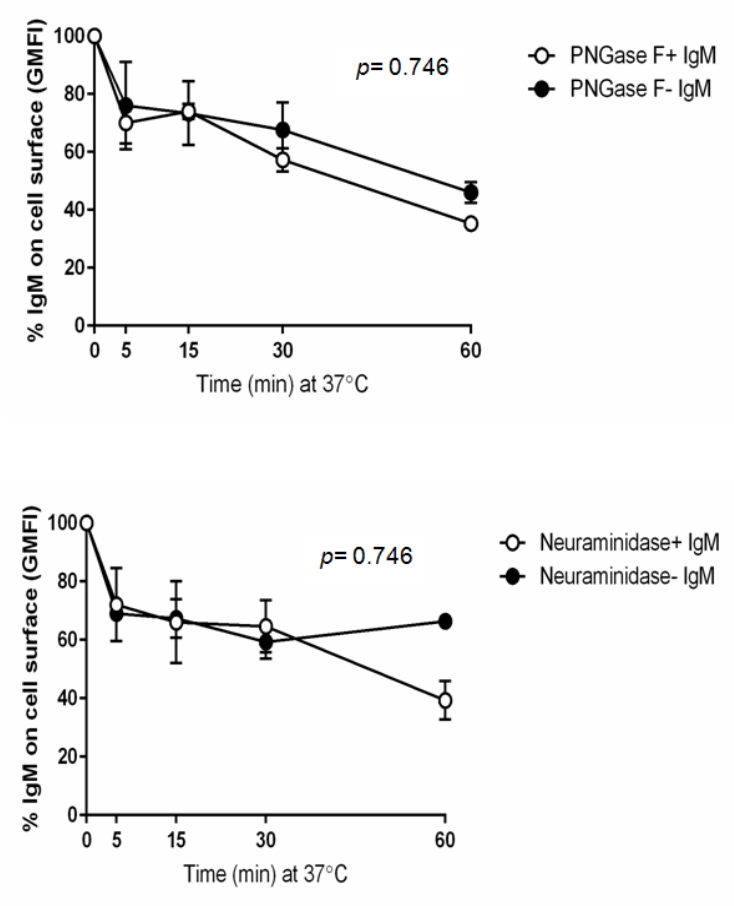

Figure 6.9 Effect of de-glycosylation on FcμR-mediated IgM internalisation. hFcμR-transfected cell lines were incubated with media supplemented with endoglycosidase-treated (Neuraminidase+/PNGase F+) and non-treated (Neuraminidase-/PNGase F-) hIgM (15μg/ml) for 1hr on ice. Internalisation assays were performed as described previously. IgM cell surface levels (GMFI) were normalised to time 0 for both samples. The mean ± SD of two independent repeats is shown. Mann-Whitney test was performed for the comparison of % IgM on cell surface (GMFI) values for endoglycosidase-treated (Neuraminidase+/ PNGase F+) and non-treated (Neuraminidase-/PNGase F-) hIgM. Statistical significance was regarded as $p < 0.05$.

CD22 in IgM internalisation by lymphocytes, we repeated the internalisation assays with the de-glycosylated IgM.

As shown in Figure 6.10, de-glycosylated IgM is still internalised by T cells ($CD4^+$ and $CD8^+$) and B cells. Indeed there was a trend to increased uptake of hIgM when the glycans were removed (Figure 6.10). This effect was observed within 5 min at 37˚C for T cells and was more prominent for B cells following 30 min at 37˚C (Figure 6.10; PNGase+). However, there was no significant difference in the internalisation of de-glycosylated IgM compared to normal IgM by lymphocytes (Table 6.2). Together, these results demonstrate that PNGase F or neuraminidase susceptible glycan(s) do not contribute to the binding or internalization of hIgM by hFcμR.

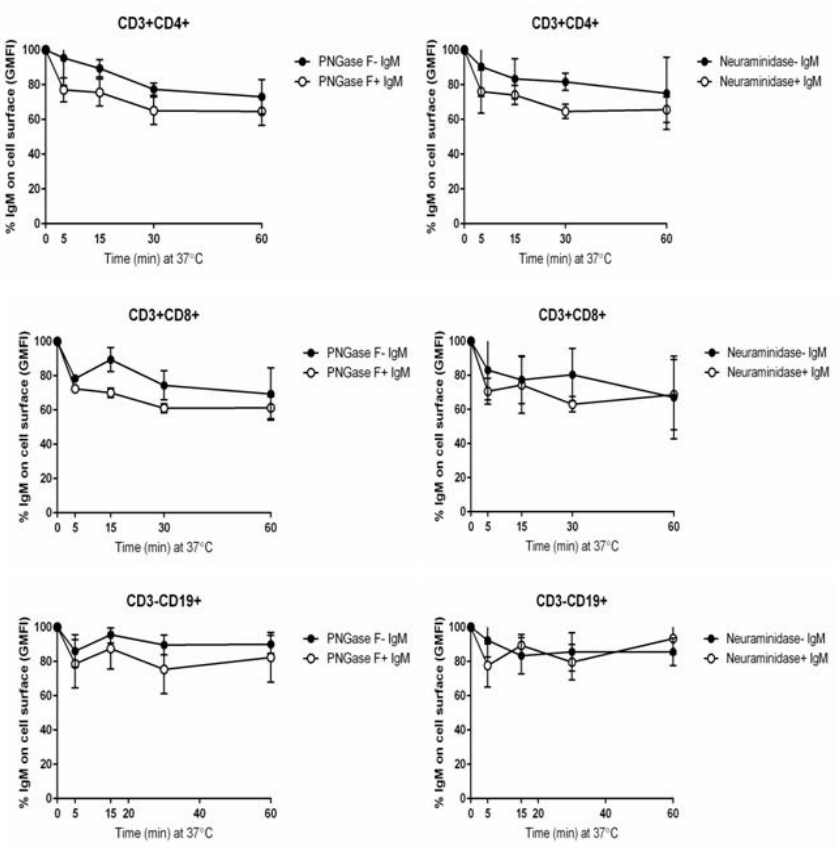

Figure 6.10 Effect of de-glycosylation on IgM internalisation by lymphocytes. PBMCs were washed and incubated with media supplemented with endoglycosidase-treated (Neuraminidase+/PNGase F+) and –non-treated (Neuraminidase-/PNGase F-) hIgM (15µg/ml) for 1hr on ice, prior to internalisation assays. Levels of IgM on lymphocyte surfaces were determined by flow cytometry using Abs specific for CD3, CD4, CD8, CD19, and hIgM. IgM cell surface levels (GMFI) were normalised to time 0 for both samples. The mean ± SD of three repeats is shown.

Table 6.2 The P values for the affect of glycosylation on IgM internalisation by lymphocytes. Mann-Whitney tests were performed for the comparison of % IgM on cell surface (GMFI) values (Neuraminidase+/PNGase F+) for endoglycosidase-treated and –non-treated (Neuraminidase-/PNGase F-) human IgM samples. Statistically significance was regarded as $p < 0.05$ (shown in red).

P value	$CD3^+CD4^+$	$CD3^+CD8^+$	$CD3^-CD19^+$
Neuraminidase- IgM vs. neuraminidase+ IgM	**0.1587**	**0.3333**	**0.8968**
PNGase F- vs. PNGase F+	**0.2381**	**0.2381**	**0.1587**

6.3.4. Cellular activation affects IgM internalisation

IgM is the first Ab to be produced during humoral immune responses. The recognition and agglutination of pathogens by IgM is pivotal for primary responses against invading pathogens, and the ability of IgM to activate complement is important for priming adaptive immune responses [155, 156]. Fc receptors for IgM have also been implicated in priming adaptive immune responses, as Fcα/μR was shown to mediate endocytosis of IgM-coated *Staphylococcus aureus* into splenic B cells [143]. Given the importance of IgM in immunity, and the findings that IgM-immune complexes were internalised via FcμR, the effect of cellular activation on IgM internalisation was determined.

A panel of different stimulants were used to activate lymphocytes (see Figure 6.6 for gating strategy). These stimulants were initially titrated to determine the optimum concentration to induce cellular proliferation of lymphocytes (see Chapter 2). B cells were stimulated with CpG and LPS. T cells were stimulated with PHA and anti-CD3 mAb. In addition, anti-μ mAb was used to investigate the effects of cross-linking IgM on hFcμR for both B cells and T cells (and/or IgM^+ BCR on B cells), and anti-human IgA+IgG+IgM Abs were used for the cross-linking of surface Igs. To mimic activation *in vivo*, the assay was conducted in 10% human serum. The presence of stimulants in IgM internalisation assays resulted in marginally decreased levels of cell surface IgM on B cells when compared to the unstimulated controls (Figure 6.11A). The effects of CpG, LPS, and anti-human IgA+IgG+IgM on IgM internalisation were observed following 30 min at 37˚C, whereby there were further decreases in levels of surface IgM (Figure 6.11A). However, anti-human IgM $Fc_{5\mu}$ fragment-specific Abs appeared to affect the internalisation of IgM following 15 min at 37˚C, and appeared to have a more pronounced affect on internalisation (~65% reduction in surface IgM levels). For T cells, anti-human IgM $Fc_{5\mu}$ fragment specific Abs appeared to have no effect on the internalisation of IgM (Figure 6.11B). There was a slight increase in IgM internalisation with anti-human IgA+IgG+IgM stimulation, notable following 10 min at 37˚C. Curiously, stimulation of T cells with both PHA and anti-CD3-mAb resulted in increased levels of surface IgM; however the effect was more striking in PHA-stimulated T cells. As the effect of cellular activation on IgM internalisation was only assessed for one donor, the data presented here should be viewed as preliminary.

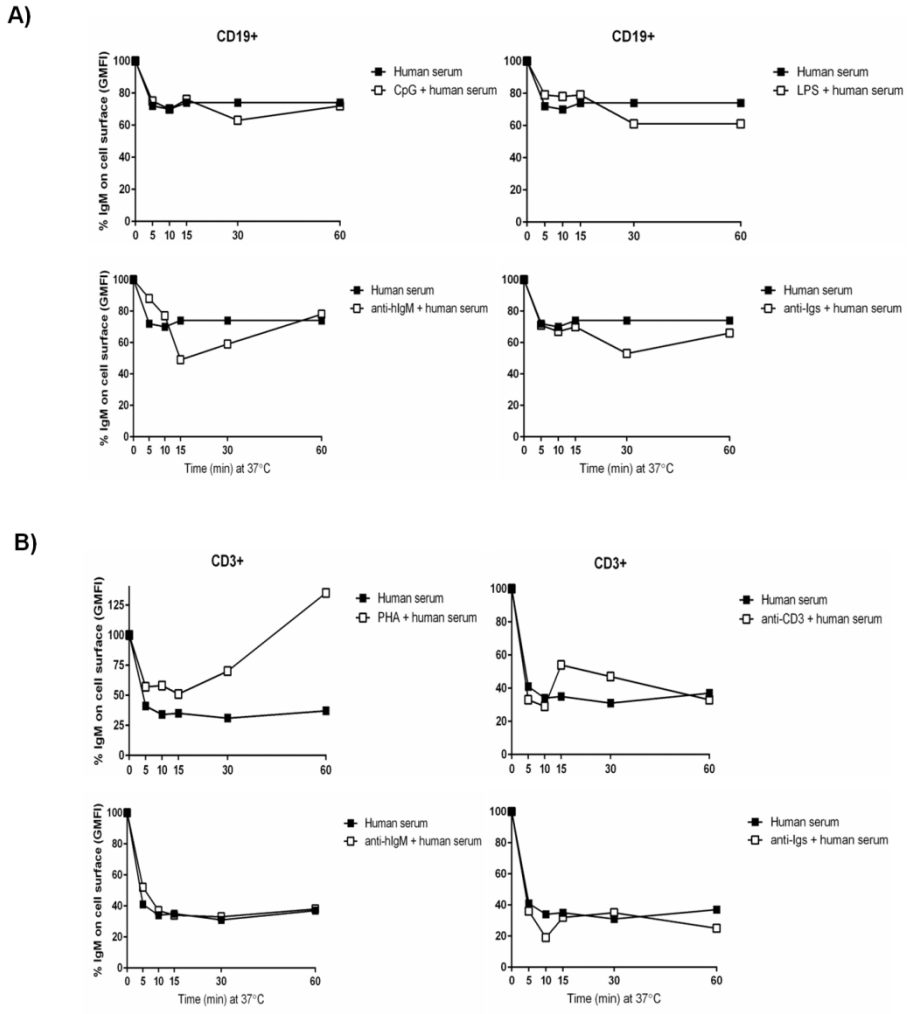

Figure 6.11 Cellular activation affects IgM internalisation by lymphocytes. PBMCs (2 x 10^5) isolated from a healthy donor were washed and incubated with media supplemented with 10% human serum for 1hr at 4˚C. Cells were washed extensively to remove unbound IgM and incubated with media supplemented with PHA (5μg/ml), CpG (1μg/ml), LPS (10μg/ml), anti-CD3-mAb (1:3000), anti-human IgM $Fc_{5\mu}$ fragment specific (hIgM) Abs (2μg/ml), anti-human IgA+IgG+IgM (Igs) Abs (2μg/ml) for 5 min on ice prior to incubation at 37˚C for the indicated times. Following incubation, cells were washed three times and stained with anti-CD3-APC and anti-CD19-Brilliant Violet™-421 Abs for 1hr at 4˚C. Levels of IgM on cell surface of B cells **(A)** and T cells **(B)** were analysed by flow cytometry, and normalised to time 0. Data are from one donor.

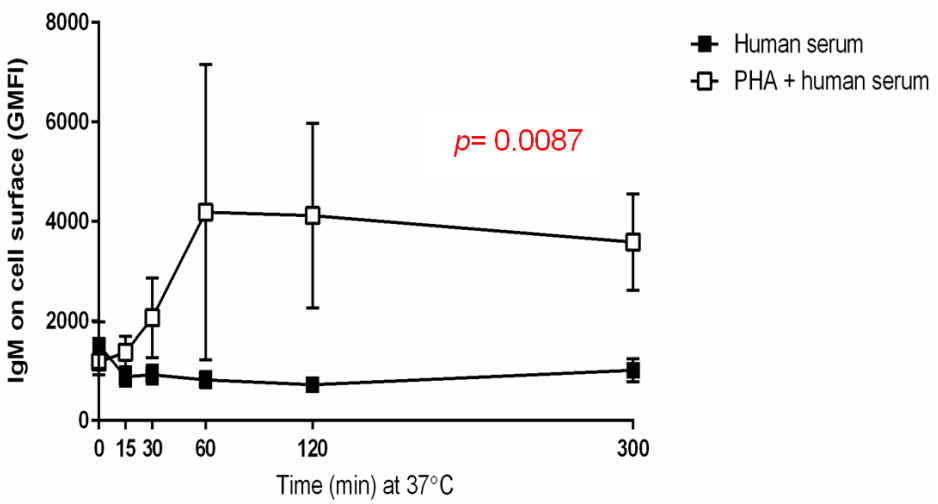

Figure 6.12 PHA induces externalisation of human IgM on gated T cells. PBMCs were incubated with 10% human serum for 1hr at 4°C. Cells were then washed twice and resuspended in medium. PHA (1µg/ml) was added to cells immediately prior to incubation at 37°C for the indicated times. Following internalisation, cells were washed twice to remove unbound IgM. Subsequently, cells were labelled with $F(ab')_2$-anti-human IgM-RPE and anti-CD3-APC. IgM levels on cell surfaces were determined by the geometric mean fluorescence intensity of RPE (*n*= 3). Mann-Whitney test was done for the comparison of IgM on cell surface (GMFI) values for human serum and PHA + human serum samples. Statistical significance was regarded as $p < 0.05$, and are shown as red.

Given the striking observation that PHA induced increased levels of IgM on T cell surfaces (Figure 6.11B), we repeated the internalisation assay to confirm whether this effect could be reproduced with additional donors. The incubation periods were also extended in these experiments to investigate whether the levels of surface IgM returned to baseline.

As shown in Figure 6.12, PHA activation of T cells resulted in the dramatic increase of IgM surface levels after 15 min at physiological temperature ($p= 0.0087$). Levels of IgM were seen to plateau following 60 min, but failed to reach basal levels within 5hr (300 min) at physiological temperature as IgM levels remained ~2-fold higher than those at time 0. This data reveals a hitherto unknown effect of PHA on T cells; the induction of raised surface IgM levels on activated T cells.

6.3.5. IgM inhibits lymphocyte proliferation

In Chapter 4, IgM was shown to inhibit proliferation in T cells stimulated with PHA. To further investigate this intriguing feature, we repeated the inhibition of proliferation assays previously performed with varying concentrations of human IgM, utilizing PHA and CpG to induce proliferation of T cells and B cells, respectively. In these assays, matching concentrations of bovine serum albumin (BSA) were used to confirm the specificity of this inhibitory affect.

As shown in Figure 6.13, incubations of PBMCs with hIgM or BSA alone did not induce proliferation of T cells or B cells. However, hIgM was observed to strongly inhibit both PHA- and CpG-induced proliferation of T cells and B cells respectively (Figure 6.13). There were significant decreases in proliferation of $CD4^+$ and $CD8^+$ T cells ($p= 0.0278$ and $p= 0.0469$, respectively) in cells incubated in the presence of hIgM and PHA, when compared to incubation with PHA alone (Figure 6.13; top panel). No significant inhibition of $CD4^+$ and $CD8^+$ T cell proliferation was observed with similar concentrations of BSA ($p= 0.2128$ and $p= 0.4632$, respectively). Furthermore, there was a highly significant decrease in B cell proliferation in the presence of CpG and hIgM but not BSA ($p= 0.0050$ and $p= 0.2689$, respectively), suggesting that the inhibitory effect is specific for hIgM.

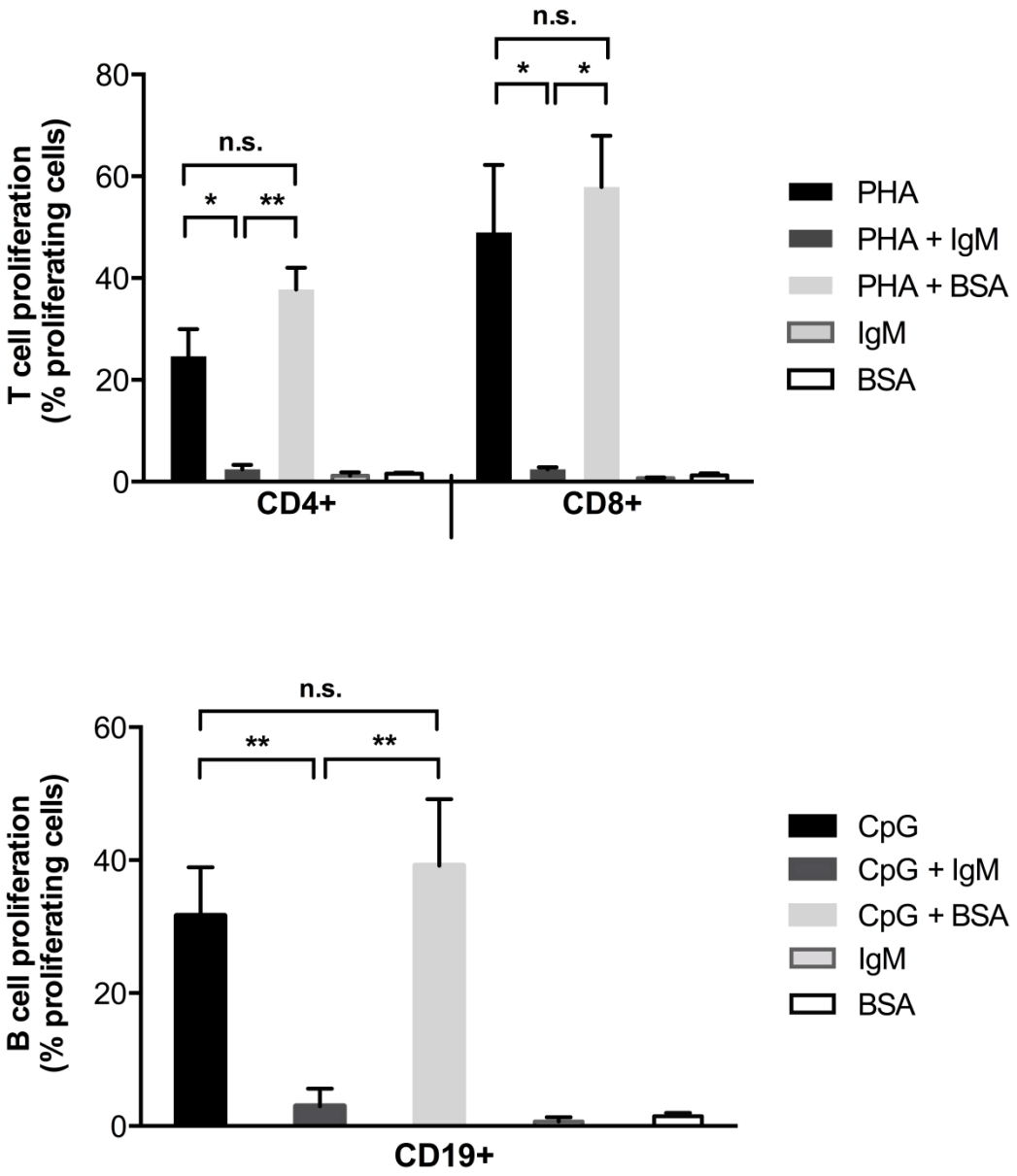

<u>Figure 6.13</u> IgM inhibits T cell and B cell proliferation. Varying concentrations of IgM or BSA were incubated with 5μg/ml PHA or 1μg/ml CpG for 30 min at 4˚C, prior to 5 day incubation with CellTrace™ Violet-labelled PBMCs at 37˚C. The ability of IgM or BSA (50μg/ml) to inhibit proliferation of gated lymphocytes was investigated by flow cytometry. Data are represented as mean ± SD of two independent experiments. Multiple unpaired t-tests were used to determine significant differences in cellular proliferation (% proliferating cells) between samples. Significance was determined as; * = $p < 0.05$, ** = $p < 0.01$, n.s. = not significant.

Lower concentrations of hIgM (but not BSA) also inhibited lymphocyte proliferation, albeit at a reduced rate, signifying that the inhibition is also titratable (Appendix III; Figure A4). Together these results show that hIgM can potently inhibit T cell and B cell proliferative responses.

6.3.6. Expression of human FcμR on lymphocytes

Finally, we sought to characterise the expression of FcμR on lymphocyte subsets by flow cytometry. For this, lymphocytes were gated on the forward versus side scatter profile. NK cells were defined as $CD3^{-}CD56^{+}$ and T cells as $CD3^{+}CD56^{-}$. T cells were further gated into $CD4^{+}$ ($CD3^{+}CD4^{+}$) and $CD8^{+}$ ($CD3^{+}CD8^{+}$) populations (Figure 6.6). B cell subsets were gated as follows: mature B cells were identified as $CD19^{+}CD10^{-}$ cells, which were further gated into naive B cells ($CD19^{+}CD10^{-}CD21^{+}CD27^{-}$), resting memory B cells ($CD19^{+}CD10^{-}CD21^{+}CD27^{+}$), atypical memory B cells ($CD19^{+}CD10^{-}CD21^{-}CD27^{-}$), and activated memory B cells ($CD19^{+}CD10^{-}CD21^{-}CD27^{+}$) (Figure 6.14). Plasmablasts were gated as $CD19^{+}CD27^{+}CD38^{+}$ cells (Figure 6.14).

Cell-surface hFcμR expression was investigated using a commercially available receptor-specific mAb (anti-hFcμR; Abnova). In normal adult blood samples, hFcμR was expressed on $CD4^{+}$ and $CD8^{+}$ T cells and $CD56^{+}$ NK cells (Figure 6.15).The expression of hFcμR on isolated T cells was relatively low, with ~10% of the total $CD4^{+}$ T cell population staining positive for hFcμR and ~5% of the total $CD8^{+}$ T cell population (Figure 6.15). NK cells were found to contain two populations of cells; those expressing low levels (10-15%) and those expressing high levels (~80-95%) of cell surface hFcμR (Figure 6.15). For blood B cells, cell surface levels of hFcμR were found to follow the hierarchy: naive < resting memory < activated memory B cells < and atypical memory B cells < plasmablasts (Figure 6.16). Expression of hFcμR on atypical memory B cells and plasmablasts was split into distinct populations with low and high levels of hFcμR (Figure 6.16), similar to that observed for NK cells (Figure 6.15). However, the high levels of surface hFcμR on plasmablasts may be contributed to the small total cell counts, which may skew the geometric mean intensity fluorescence (GMFI) values.

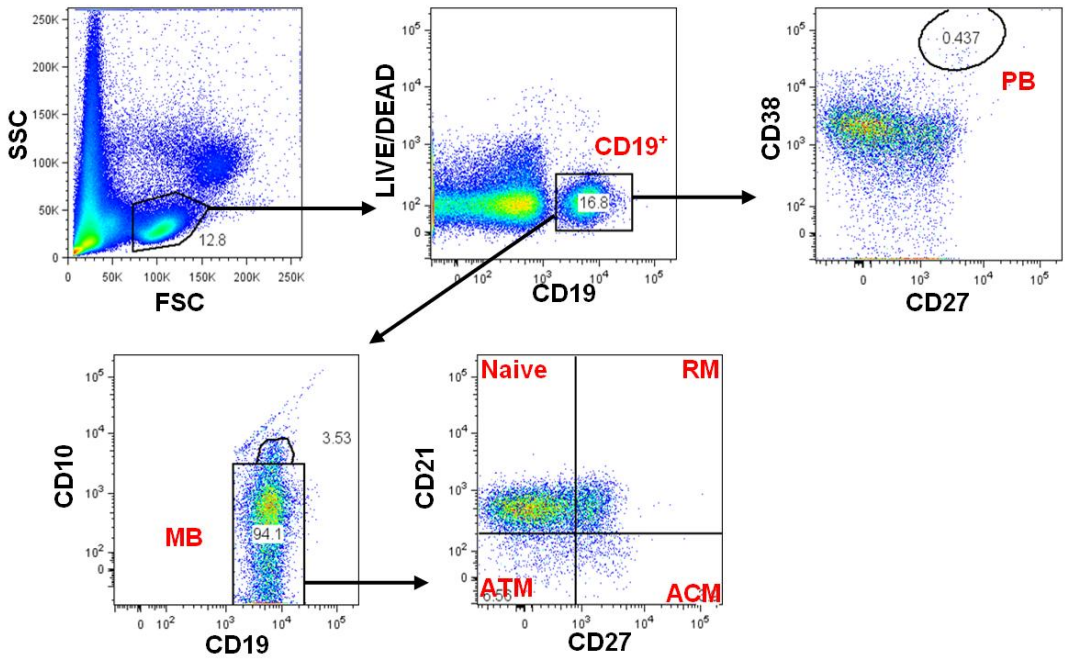

Figure 6.14 Gating strategy for B cell panel. Freshly isolated PBMCs were washed and labelled with 1uM LIVE/DEAD® Aqua Dead Cell stain in PBS at 4°C for 30 min. Cells were washed and incubated with anti-human CD19-PE-CF594, anti-human CD10-PE, anti-human CD38-Alexa Fluor® 700, anti-human CD27-APC-Cy7 and anti-human CD21-Brilliant Violet™ 421 for 1hr at 4°C. Labelled cells were washed extensively and analyzed by flow cytometry. Lymphocytes were gated from the PBMC population based on side (SSC) and forward (FSC) profiles, which was further gated into live $CD19^+$ B cells based on LIVE/DEAD® and anti-human CD19 staining. Plasmablasts (PB) were gated as $CD19^+CD27^+CD38^+$ cells. Mature B cells (MB) were identified as $CD19^+CD10^-$ cells, which were further gated into naive B cells ($CD19^+CD10^-CD21^+CD27^-$), resting memory B cells (RM; $CD19^+CD10^-CD21^+CD27^+$), atypical memory B cells (ATM; $CD19^+CD10^-CD21^-CD27^-$), and activated memory B cells (ATM; $CD19^+CD10^-CD21^-CD27^+$).

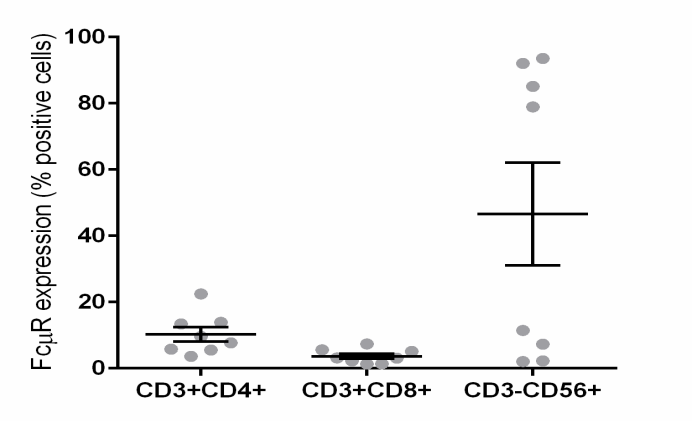

Figure 6.15 FcμR expression on T cells and NK cells. Freshly isolated PBMCs were washed and labelled with 1uM LIVE/DEAD® Aqua Dead Cell stain in PBS at 4°C for 30 min. Following extensive washing, cells were incubated with media in the presence or absence of 1μg mouse anti-hFcμR mAb at 4°C for 1hr. Cells were then washed three times and labelled with anti-mouse IgG-APC to detect the expression of hFcμR. Subsequently, PBMCs were labelled with the T/NK cell Ab panel (see Chapter 2) and analysed by flow cytometry. Lymphocyte subsets were gated as above and the expression of hFcμR was assessed as % cells positive for hFcμR (background removed). Averages are shown for eight independent donors, error bars indicate SEM.

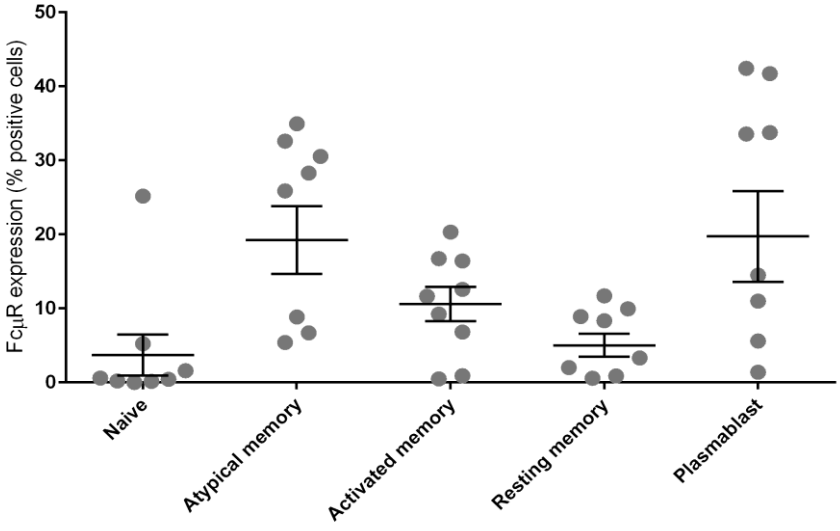

Figure 6.16 FcμR expression on B cell subsets. PBMCs labelled with 1μg mouse anti-hFcμR mAb (Abnova) at 4°C for 1hr, washed three times and labelled with anti-mouse IgG-APC. Subsequently, PBMCs were labelled with B cell panel Abs and analysed by flow cytometry. B cell subsets were gated as in Figure 6.14, and the expression of hFcμR was assessed as % cells positive for hFcμR (minus background). Averages are shown for nine independent donors, error bars indicate SEM.

Previous studies hypothesised that hFcμR expression is sensitive to exogenous levels of IgM, as hFcμR levels were significantly raised on mononuclear cell surfaces following overnight culture in serum-free conditions [137]. We sought to investigate whether these results could be duplicated using the commercially available anti-hFcμR mAb. Overnight culture of PBMCs in serum-free medium resulted in no significant increase expression of hFcμR on naive and activated memory B cells ($p= 0.60$ and $p= 0.76$, respectively) (Figure 6.17). The expression of hFcμR was reduced on atypical memory B cells and on resting memory B cells and levels on plasmablast remain relatively constant (Figure 6.17). Together, these results indicate that exogenous IgM concentrations had no significant effect on the expression of hFcμR on PBMCs.

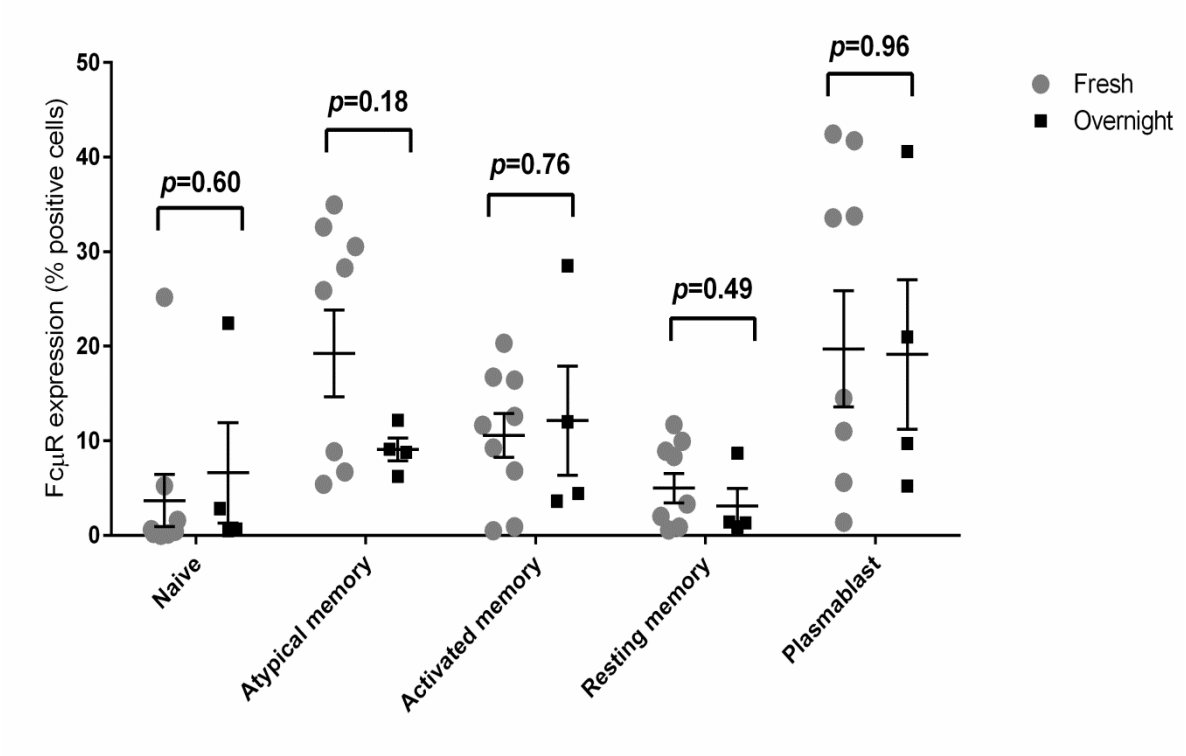

Figure 6.17 Comparing FcμR expression on freshly isolated vs. serum-starved B cell subsets. Levels of hFcμR on B cell surfaces was investigated on freshly isolated PBMCs (shown as fresh) or PBMCs cultured in serum-free media overnight (shown as overnight), in order to investigate whether FcμR expression is sensitive to exogenous IgM concentrations. Averages are shown for nine independent donors, error bars indicate SEM. Statistical analysis was done by multiple t-tests using the Graphpad Prism 6 software, whereby *p* values less than 0.05 were regarded as significant.

6.4. Discussion

In this chapter, possible effector function(s) of hFcμR were investigated. We identified several key findings: (1) hFcμR is an endocytosis receptor for IgM. (2) Glycosylation does not influence IgM internalisation by hFcμR or by PBMCs (3) Cellular activation affects IgM internalisation by lymphocytes. (4) hFcμR is expressed on a variety of lymphocyte subsets, including B cells, T cells and NK cells.

FcμR has been implicated in IgM homeostasis [137, 138], and one study showed receptor cross-linking promoted the rapid internalisation of IgM and FcμR [183]. Here, we confirm that hFcμR mediates the endocytosis of both pentameric IgM and IgM immune-complexes, and that hFcμR is also internalised upon ligand binding. This supports the hypothesis that IgM is degraded upon internalisation and shuttling to lysosomes [183], however future studies could expand these findings by tracking the internalisation dynamics of IgM by confocal microscopy.

To our knowledge, this is the first report of human IgM-immune complexes (IC) being internalised by hFcμR. However, HeLa cells expressing hFcμR were previously shown to internalise mouse IgM-conjugated microbeads [175]. IgM Abs are the first to be produced during immune responses, and are pivotal for pathogen opsonisation and complement activation [156]. Therefore, internalisation of IgM-IC by hFcμR could be implicated in the primary stages of adaptive immune responses, through bridging immune complexes with adaptive immune cells. Whether hFcμR can indeed mediate the internalisation and cross-presentation of IgM-coated pathogens and/ or IgM-Ag complexes, and what effect this could have on immune responses, remains to be determined. Given that FcμR has been implicated in enhancing B cell proliferation and survival following BCR cross-linking in mice [138], it will be of interest to see whether specific IgM-Ag can influence B cell proliferation or signalling as a result of BCR and/ or hFcμR cross-linking. Recently, the ability hFcμR to internalise IgM was utilised in cancer immunotherapy [321]. Vire et al. used the IgM-Fc (Fcμ) as a scaffold to deliver cytotoxic drugs to CLL cells overexpressing hFcμR [321]. The internalisation of these Fcμ-drug candidates resulted in selective toxicity of CLL cells [321], highlighting the potential use of hFcμR in therapeutic design.

IgM internalisation was sensitive to the activation status of lymphocytes. The preliminary data presented here revealed that activation resulted in increased IgM internalisation by B cells. B cells are antigen presenting cells which prime T cell responses through the presentation of foreign antigens via MHC molecules [322]. Therefore, it is tempting to speculate that increased internalisation following activation may function to endocytose foreign antigens bound to IgM and mediate their cross-presentation. However, this remains to be resolved. Curiously, activation of T cells with PHA and anti-CD3 Abs promoted externalisation of IgM following initial internalisation. It is still unknown whether this effect was due to the direct externalisation of IgM-FcμR complexes, or whether cellular activation promotes the upregulation of a hitherto unidentified IgM^+ receptor on T cells. Since no exogenous IgM was available during the internalisation assays, it is likely that the externalised IgM comes from within the cell. In support of this, Vire et al. showed that hFcμR accumulates in the trans-golgi network (TGN), and hypothesised that the TGN serves as an intracellular storage site for hFcμR so that the receptor can be released quickly under certain circumstances, such as cellular activation [321]. As both PHA and anti-CD3 mAbs were able to generate externalisation of IgM by T cells, it is tempting to speculate that this mechanism is important in governing T cell immunity. For example, the upregulation of IgM on activated T cell surfaces could promote cell-cell interactions between cells expressing hFcμR, as previously suggested [100, 137]. Evaluating the internalisation dynamics of hFcμR alongside IgM could be one way of deciphering the role of the receptor in IgM internalisation and externalisation following cellular activation.

De-glycosylation of IgM molecules had no effect on its internalisation by hFcμR-transfected cell lines, T cells ($CD4^+$ and $CD8^+$) or B cells. This contradicted an earlier study that demonstrated that the FcμR mediated internalisation was dependent on sialylation of IgM [286]. The findings presented here, as well as previous findings [183], suggest that IgM is rapidly internalised by hFcμR. As Colucci et al. investigated internalisation of desialylated IgM at 72 hr, it is possible that an alternative receptor is mediating the sialic-acid-dependent internalisation of IgM by T cells [286]. Numerous glycan receptors are expressed on human T cells, including CD62L (L-selectin) and members of the glycan-binding galectin family [323]. The galectin family appear to have the greatest potential as the receptor mediating the internalisation of

sialylated IgM, as galectins are essentially expressed on all adaptive immune cells and have been implicated in the fine-tuning of T cell signalling and activation [323]. Further, galectin 9 has been shown to bind to the heavy chain of serum IgM [324]. The use of anti-galectin Abs to block interactions between IgM and galectins during internalisation assays could help clarify the role of galectins in IgM internalisation by T cells.

Another interesting feature reported here was that IgM inhibited activation of both B cells and T cells. Similar results were described for T cells previously, whereby the sialic acid-dependent internalisation of IgM contributed to augmentation of T cell inhibition [286]. However, we discounted the role for sialic-acid in mediating the internalisation of IgM by hFcμR. One possible explanation for the T cell inhibition could be that IgM directly binds to PHA (see Chapter 4), and thus prevents its interaction with cell surface receptors to initiate T cell activation. Alternatively, the binding of IgM to galectins on T cell surfaces could potentially mediate the inhibitory effect [323]. Galectins are also expressed on B cells and have been implicated in the inhibition of B cell proliferation [325, 326]. Likewise, the binding of IgM to the inhibitory glycan receptor CD22 could be responsible for the observed inhibition [233]. Future studies should aim to characterise what receptor is governing the IgM-dependent inhibition of lymphocytes, possibly through the use of blocking Abs specific for CD22- and/or galectin.

Since glycosylation did not impact on IgM internalisation by hFcμR, there is scope to modify this multivalent immunoglobulin for therapeutic application. The addition of α2,6-linked sialic acid glycans to Fcμ-drug candidates for CLL [321] could also function to induce a negative feedback loop for CLL proliferation through CD22 binding [233]. A similar approach was adopted for the Bruton tyrosine kinase (BTK) inhibitor drug ibrutinib, which was shown to down-regulate BCR signalling in CLL cells resulting in significantly decreased tumour proliferation [327]. Alternatively, as sialylation of IgM was implicated recently in T cell inhibition [286], the excessive sialylation of IgM could be used to inhibit auto-reactive T cells governing certain autoimmune diseases [328, 329]. This interesting topic is discussed further in Chapter 7.

FcμR is unique from other FcR in its exclusive expression on adaptive immune cells [137]. Here, we confirmed the expression of hFcμR on B cells, T cells, and NK cells

using the commercially available anti-FAIM3 mAb. In addition, we further characterised expression of hFcμR on B cell subsets and characterised the hierarchy of expression on B cells in blood: naive < resting memory < activated memory B cells < and atypical memory B cells < plasmablasts. This hierarchy differs from previous data which characterised hFcμR downmodulation upon B cell activation [137, 288]. Plasmablasts were found to fall into two populations; those expressing high levels of hFcμR and those expressing low levels, which supports the findings that subpopulations of plasma cells ($CD38^{hi}$) express hFcμR [288]. In addition, we did not observe enhanced cell surface levels of FcμR on B cell subsets following overnight culture in serum-free media, contrasting previous findings [137]. Possible explanations for the differences in hFcμR expression reported here could be owing to the use of a commercial anti-FAIM3 (hFcμR) mAb, different gating strategies for lymphocyte subsets, different serum-free media, or the lack of a FcγR-blocking method used previously [137]. Therefore, future studies should duplicate the staining methods used by Kubagawa et al. with the anti-FAIM3 mAb to determine what is governing these differences in expression [137].

Chapter 7: Discussion and conclusion

7.1. Objectives

Why *P. falciparum* express IgM-binding proteins has received considerable attention over the last decade. Although the IgM-binding properties of PfEMP1 expressed on the surface of infected erythrocytes has been well characterised [120, 123, 130, 284], significantly less is known about two IgM-binding proteins expressed on the surface of the merozoite. The expression of DBLMSP and DBLMSP2 on merozoites has been linked to permitting interactions with erythrocytes [147], complement activation and camouflaging critical epitopes from immune responses [146]. However, whether the binding of these molecules to the Fc portion of IgM could affect subsequent interactions with IgM receptors had not been investigated. Moreover, the mechanism of IgM binding to and the function of human FcμR, as well as the identification of novel IgM receptors remain unclear.

The overall aim of this study was to characterise the DBLMSP-IgM interaction, and to determine why *P. falciparum* merozoites express DBL domains that bind non-immune human IgM. In particular, the specific objectives included:

I. Assess the structural and biochemical requirements for IgM binding to IgM-receptors
II. Investigate the requirements for DBLMSP and DBLMSP2 binding to human IgM
III. Determine if IgM-binding by DBLMSP and/or DBLMSP2 mediates immune evasion by:
    - Blocking interactions of IgM with receptors
    - Targeting IgM on hFcμR expressed on human lymphocytes
    - Promoting immunomodulation through binding lymphocytes
IV. Characterise the function(s) of human FcμR

7.2. Main findings and significance

Improving our understanding of the host-parasite relationship is crucial to develop better methods for controlling malaria. Strategies to overcome the extensive immune evasion mechanisms employed by *P. falciparum* will aid in the development of highly effective vaccines, which has so far been difficult to attain.

Here, we show for the first time that merozoite surface proteins are able to bind to adaptive immune cells. Intriguingly, the DBL domains alone were unable to bind IgM on hFcμR, implying a role for the SPAM domains in oligomerisation of the full-length proteins. Even though we were unable to characterise any biological consequences of DBLMSP and DBLMSP2 binding to lymphocytes, the data generated in this study indicates that these proteins do not function to block interactions between IgM and hFcμR. Furthermore, we show the potential of DBLMSP and DBLMSP2 to engage dendritic cells via interactions with IgM on DC-SIGN. Since these malaria proteins do not appear to be involved in erythrocyte invasion, or mediate functional effects by binding IgM-positive lymphocytes, it may be more likely that they have evolved to interact with other cell types such as dendritic cells. However, the lack of functionality of these proteins on lymphocytes could be owing to the fact that additional malarial proteins are in native IgM-DBLMSP complexes. The presence of additional parasite proteins within the IgM-DBLMSP complex does not affect its binding to hFcμR, supporting the potential of IgM-DBLMSP complexes to engage hFcμR on expressed lymphocytes *in vivo*.

In addition, this study provided some insight into the requirements for IgM binding by hFcμR. The Cμ4 domain of hIgM was identified as the domain which bound hFcμR, with a partial contribution made by the Cμ2 and/or Cμ3 domain. This interaction was not dependent on the glycosylation of IgM. Both IgM and IgM-immune complexes were seen to bind to hFcμR, confirming hFcμR as a *bona fide* receptor for IgM and signifying the receptor may play a role in initial immune responses. Through the assessment of IgM binding to lymphocyte subsets known to express hFcμR, we also observed binding of IgM to monocytes. As far as we are aware, there has been no characterisation of an IgM receptor expressed on monocytes to date, although IgM is known to bind murine monocytes and macrophages [226]. The identification of DC-SIGN as a novel ligand for IgM could offer one explanation as

to how monocytes bind hIgM. DC-SIGN bound IgM-Fc at high affinity (K_d ~0.26μM), which was found to be dependent on IgM glycosylation. Although a subset of monocytes express DC-SIGN [167, 237], whether the expression of DC-SIGN by monocytes can account for the observed IgM binding is still unknown.

As there is currently no crystal structure for hFcμR, molecular dynamic simulations were used to provide structural insights into how IgM engages FcμR. The models generated using the Phyre2 Server suggested that hFcμR is expressed as a dimer, owing to its striking homology to the transmembrane region of the epidermal growth factor receptor erbb1, which exists as a dimer on cell surfaces [241]. Moreover, the integration of the DBL domains of DBLMSP into this model revealed that these proteins might bind to a different region of the Cμ4 domain of IgM than that bound by hFcμR. The Cμ2/Cμ4 interface was predicted as the target of FcμR, as the Cμ3/Cμ4 interface is completely buried by the DBLMSP domains, and the FcμR interaction with IgM does not completely prevent DBLMSP interaction with IgM. A similar association of dimeric FcμR with this Cμ2/Cμ4 interface also shows partial overlap with the DBLMSP, thus the model(s) confirmed that it is structurally viable for the DBLMSP proteins to bind to IgM bound to hFcμR, and provides an explanation as to why there is a reduction, but not complete blocking, of IgM-DBLMSP complexes to hFcμR. Due to the steric constraints imposed by the experimental data, the model could aid the identification of the IgM-binding domain of DBLMSP/DBLMSP2.

In order to gain a better understand into how the binding of DBLMSP and/or DBLMSP2 to hFcμR could possibly benefit parasite survival, the role of receptor was further investigated. Here, we confirmed that hFcμR is expressed on adaptive immune cells and mediates the endocytosis of IgM and artificially-induced IgM-immune complexes. IgM was not recycled to the cell surface following internalisation, supporting previous findings that internalised IgM is shuttled through the endocytic pathway to lysosomes for degradation [183]. Taken together, the findings presented here strengthen the previous data generated in FcμR-deficient mice which implicated the receptor in the homeostasis of IgM [138]. The data showed that IgM internalisation is enhanced upon lymphocyte activation, implying the importance of the mechanism in early immune responses, such as the cross-presentation of foreign

antigens via MHC molecules or by delivering antigens to TLR receptors (e.g. TLR7/9) which also residue within lysosomes [183]. However, T cell activation resulted in the externalisation of IgM following initial internalisation. This surprising result was observed using two different stimuli (PHA and anti-CD3 Abs) and was hypothesised to occur due to the rapid release of intracellular stores of hFcμR-IgM complexes [183]. Although this is yet to be determined, the presence of IgM on activated T cell surfaces could function to facilitate T and B cell interactions which could help enhance B cell activation, as previously described [137].

Finally, we showed a role for IgM in the inhibition of B cell and T cell proliferation. Whether or not this inhibitory effect was owing to the interaction of IgM with hFcμR remains to be determined. Despite this, these results confirmed previous findings that IgM inhibited T cell activation [286]. The authors concluded that the sialic acid-dependent inhibitory effect of IgM on T cell activation may have been a result of the internalisation of IgM by hFcμR. However, we showed that glycosylation of IgM had no effect on the initial internalisation of IgM by hFcμR-transfected cells or lymphocytes known to express the receptor. Therefore, we hypothesise that the inhibitory effects of IgM are governed through interactions with unidentified receptors, most likely galectins on T cells [323, 324, 326] or the inhibitory receptor CD22 on B cells [233]. Alternatively, the direct binding of IgM to stimulants such as PHA or PWM could prevent their binding to receptors on lymphocyte surfaces, thus preventing the initiation of activation.

7.3. Applications

The fact that the DBL domains alone were unable to engage IgM bound to cell-surface receptors signified a role of the SPAM domain in the oligomerisation of malaria proteins. Therefore, the fusion of SPAM domains to malaria vaccine candidate antigens could promote their oligomerisation, thus increasing the overall size of the complex which in turn could enhance its immunogenicity, as shown for other vaccines [330, 331]. Moreover, the SPAM domain itself has been shown to elicit cross-reactive Abs capable of generating Ab-dependent cellular inhibition of parasite growth [148]. Therefore, there is potential for the SPAM domain of DBLMSP and/or DBLMSP2 to be utilised in vaccine design. In addition, the ability of hFcμR to

internalise both IgM and IgM-immune complexes could be exploited to deliver therapeutic targets to adaptive immune cells. This concept has already been explored by Vire et al., who used IgM-Fc as a scaffold to deliver cytotoxic drugs to CLL cells which overexpress hFcμR [321].

Glycosylation of immunoglobulins can dramatically alter their function. Excessive sialylation of immunoglobulins stimulates immune suppression as demonstrated by the anti-inflammatory effects of IVIG, which are commonly used as a therapeutic for certain autoimmune and inflammatory diseases [303, 332, 333]. In light of the recent report of the effect of sialylation of IgM on T cell activation [286], the excessive sialylation of IgM could be used to inhibit auto-reactive T cells implicated in pathologies such as diabetes mellitus [328, 329] and multiple sclerosis [334, 335]. Further, the addition of α2,6-linked glycans to IgM could permit B cell inhibition through cross-linking of the inhibitory receptor CD22 [233], which could be used for treatment of hypergammaglobulinemia. As CLL cells overexpress hFcμR [178, 313], the addition of α2,6-linked sialic acid glycans to IgM-Fc could promote cross-linking of hFcμR and CD22 [233], which in turn could induce a negative feedback loop for B cell activation resulting in decreased tumour proliferation. Although IgM is heavily glycosylated [168], de-glycosylation did not affect the binding or internalisation of IgM to hFcμR. Therefore, modifying the glycans on the IgM-Fc to enhance its binding to glycan receptors would not interfere with IgM-hFcμR interactions. Further work is required to evaluate the potential of glycosylated IgM-fusions in therapeutics.

7.4. Limitations

A major limitation in this study was the inability to produce recombinant DBLMSP and DBLMSP2. The downstream effects of lack of protein meant that we were unable to further explore the immune subsets binding DBLMSP and/ or DBLMSP2, to determine whether binding of these proteins correlated with hFcμR expression, to repeat assays to determine the function of these proteins, or to investigate the biological consequences of binding to NK cells. In addition, the inability to produce recombinant DBLMSP and/or DBLMSP2 proteins lacking DBL domains meant that we were unable to confirm the role of the SPAM domain in oligomerisation.

Another limitation included the restricted assays we were able to perform to determine the function of hFcμR. Previous studies have utilised genetically altered mice lacking the expression of FcμR to investigate the function of the receptor. Here, we focused on investigating the ability of the receptor to internalise IgM by monitoring levels of IgM and/or hFcμR on cell surfaces. However, the expression of the IgM^+ BCR on B cells resulted in high levels of background staining when detecting for cell surface levels of IgM. Therefore, future studies may want to utilise RNA interference technology to knock out the expression of hFcμR on lymphocytes to further clarify its role in humans. Another limiting factor was that only one anti-hFcμR (FAIM3) Ab is available commercially, which is not directly conjugated to a fluorochrome. It is possible that difference in hFcμR expression on B cell subset featured here compared to that described previously [137] was attributed to the use of different anti-hFcμR mAbs.

7.5. Future work

Although this thesis has provided an insight into the role of IgM-binding proteins in malaria, there are still a number of outstanding questions. For example, it is still unclear at what concentration DBLMSP and DBLMSP2 are present in the periphery of an individual with high parasitemia, or what proportion of these proteins complex with IgM. It is important to evaluate this to understand how these complexes may interact with hFcμR. As hFcμR was characterised as an endocytosis receptor, it will be interesting to determine whether the binding of DBLMSP and/or DBLMSP2 to IgM can prevent its internalisation by hFcμR. As these proteins are expected to form complexes with IgM in the periphery, their function may be to block internalisation of IgM-opsonised antigens in order to delay immune detection. Alternatively, internalisation of native IgM-immune complexes containing malarial proteins could promote TLR activation within lysosomes resulting in excessive B cell and/ or T cell activation.

Another outstanding question is the identity of the additional malarial proteins contained within the IgM-DBLMSP complex. Characterizing these proteins by mass spectrometry will enable a better understanding of the interaction between merozoite surface proteins, and could help identify novel IgM-binding proteins expressed on

the surface of merozoites. Future studies should repeat the functional assays performed here to determine whether the presence of these unidentified proteins within IgM-complexes serve to bind to receptors on lymphocytes, which could initiate biological consequences such as proliferation or apoptosis.

References

1. Cowman, A.F. & Crabb, B.S. Invasion of Red Blood Cells by Malaria Parasites. *Cell* **124**, 755-766 (2006).
2. Singh, B. et al. A Large Focus of Naturally Acquired Plasmodium knowlesi Infections in Human Beings. *The Lancet* **363**, 1017-1024 (2004).
3. Wiesenfeld, S.L. Sickle-cell Trait in Human Biological and Cultural Evolution. *Science* **157**, 1134-1140 (1967).
4. Joy, D.A. et al. Early Origin and Recent Expansion of Plasmodium falciparum. *Science* **300**, 318-321 (2003).
5. World Health Organisation (World Health Organization, Geneva, Switzerland; 2013).
6. Amino, R. et al. Quantitative Imaging of Plasmodium Transmission from Mosquito to Mammal. *Nature Medicine* **12**, 220-224 (2006).
7. Sidjanski, S. & Vanderberg, J.P. Delayed Migration of Plasmodium Sporozoites from the Mosquito Bite Site to the Blood. *The American Journal of Tropical Medicine and Hygiene* **57**, 426-429 (1997).
8. Medica, D.L. & Sinnis, P. Quantitative Dynamics of Plasmodium yoelii Sporozoite Transmission by Infected Anopheline Mosquitoes. *Infection and Immunity* **73**, 4363-4369 (2005).
9. Vanderberg, J.P. & Frevert, U. Intravital Microscopy Demonstrating Antibody-mediated Immobilisation of Plasmodium berghei Sporozoites Injected into Skin by Mosquitoes. *International Journal for Parasitology* **34**, 991-996 (2004).
10. Vaughan, J.A., Scheller, L.F., Wirtz, R.A. & Azad, A.F. Infectivity of Plasmodium berghei Sporozoites Delivered by Intravenous Inoculation versus Mosquito Bite: Implications for Sporozoite Vaccine Trials. *Infection and Immunity* **67**, 4285-4289 (1999).
11. Krettli, A.U. & Dantas, L.A.B. Which Routes Do Plasmodium Sporozoites Use for Successful Infections of Vertebrates? *Infection and Immunity* **68**, 3064-3065 (2000).
12. Frevert, U., Usynin, I., Baer, K. & Klotz, C. Nomadic or Sessile: Can Kupffer Cells Function as Portals for Malaria Sporozoites to the Liver? *Cellular Microbiology* **8**, 1537-1546 (2006).
13. Cerami, C. et al. The Basolateral Domain of the Hepatocyte Plasma Membrane Bears Receptors for the Circumsporozoite Protein of Plasmodium falciparum Sporozoites. *Cell* **70**, 1021-1033 (1992).
14. Frevert, U. et al. Malaria Circumsporozoite Protein Binds to Heparan Sulfate Proteoglycans Associated with the Surface Membrane of Hepatocytes. *The Journal of Experimental Medicine* **177**, 1287-1298 (1993).
15. Pradel, G., Garapaty, S. & Frevert, U. Proteoglycans Mediate Malaria Sporozoite Targeting to the Liver. *Molecular Microbiology* **45**, 637-651 (2002).
16. Mota, M.M. et al. Migration of Plasmodium Sporozoites Through Cells Before Infection. *Science* **291**, 141-144 (2001).
17. Sturm, A. et al. Manipulation of Host Hepatocytes by the Malaria Parasite for Delivery into Liver Sinusoids. *Science* **313**, 1287-1290 (2006).
18. Augustine, A.D. et al. NIAID Workshop on Immunity to Malaria: Addressing Immunological Challenges. *Nature Immunology* **10**, 673-678 (2009).
19. Jones, M.K. & Good, M.F. Malaria Parasites Up Close. *Nature Medicine* **12**, 170-171 (2006).
20. Joice, R. et al. *Plasmodium falciparum* Transmission Stages Accumulate in the Human Bone Marrow. *Science translational medicine* **6**, 244re245-244re245 (2014).
21. Muirhead-Thomson, R.C. The Malarial Infectivity of an African Village Population to Mosquitoes (Anopheles Gambiae): A Random Xenodiagnostic Survey. *The American Journal of Tropical Medicine and Hygiene* **6**, 971-979 (1957).

22. Salmon, B.L., Oksman, A. & Goldberg, D.E. Malaria Parasite Exit from the Host Erythrocyte: A Two-step Process Requiring Extraerythrocytic Proteolysis. *Proceedings of the National Academy of Sciences* **98**, 271-276 (2001).
23. Chandramohanadas, R. et al. Apicomplexan Parasites Co-Opt Host Calpains to Facilitate Their Escape from Infected Cells. *Science* **324**, 794-797 (2009).
24. Boyle, M.J., Richards, J.S., Gilson, P.R., Chai, W. & Beeson, J.G. Interactions with Heparin-Like Molecules During Erythrocyte Invasion by Plasmodium falciparum Merozoites. *Blood* **115**, 4559-4568 (2010).
25. Crosnier, C. et al. Basigin is a Receptor Essential for Erythrocyte Invasion by Plasmodium falciparum. *Nature* **480**, 534-537 (2011).
26. Duraisingh, M.T. et al. Phenotypic Ariation of Plasmodium falciparum Merozoite Proteins Directs Receptor Targeting for Invasion of Human Erythrocytes. *The EMBO Journal* **22**, 1047-1057 (2003).
27. Sim, B.K., Chitnis, C.E., Wasniowska, K., Hadley, T.J. & Miller, L.H. Receptor and Ligand Domains for Invasion of Erythrocytes by Plasmodium falciparum. *Science* **264**, 1941-1944 (1994).
28. Cowman, A.F., Berry, D. & Baum, J. The Cellular and Molecular Basis for Malaria Parasite Invasion of the Human Red Blood Cell. *The Journal of Cell Biology* **198**, 961-971 (2012).
29. Singh, S., Alam, M.M., Pal-Bhowmick, I., Brzostowski, J.A. & Chitnis, C.E. Distinct External Signals Trigger Sequential Release of Apical Organelles during Erythrocyte Invasion by Malaria Parasites. *PLoS Pathogens* **6**, e1000746 (2010).
30. Srinivasan, P. et al. Binding of Plasmodium Merozoite Proteins RON2 and AMA1 Triggers Commitment to Invasion. *Proceedings of the National Academy of Sciences* **108**, 13275-13280 (2011).
31. Mitchell, G.H., Thomas, A.W., Margos, G., Dluzewski, A.R. & Bannister, L.H. Apical Membrane Antigen 1, a Major Malaria Vaccine Candidate, Mediates the Close Attachment of Invasive Merozoites to Host Red Blood Cells. *Infection and Immunity* **72**, 154-158 (2004).
32. Riglar, D.T. et al. Super-Resolution Dissection of Coordinated Events during Malaria Parasite Invasion of the Human Erythrocyte. *Cell Host & Microbe* **9**, 9-20 (2011).
33. O'Donnell, R.A. & Blackman, M.J. The Role of Malaria Merozoite Proteases in Red Blood Cell Invasion. *Current Opinion in Microbiology* **8**, 422-427 (2005).
34. Gilles, H.M. & Warrell, D.A. Bruce-Chwatt. *Essential Malariology* (1993).
35. Gething, P. et al. A New World Malaria mMap: Plasmodium falciparum Endemicity in 2010. *Malaria Journal* **10**, 378 (2011).
36. Hay, S.I. et al. Developing Global Maps of the Dominant *Anopheles* Vectors of Human Malaria. *PLoS Medicine* **7**, e1000209 (2010).
37. Eckhoff, P. Malaria Parasite Diversity and Transmission Intensity Affect Development of Parasitological Immunity in a Mathematical Model. *Malaria Journal* **11**, 419 (2012).
38. Jepson, A.P. et al. Genetic Regulation of Fever in Plasmodium falciparum Malaria in Gambian Twin Children. *Journal of Infectious Diseases* **172**, 316-319 (1995).
39. Mackinnon, M.J. et al. Quantifying Genetic and Nongenetic Contributions to Malarial Infection in a Sri Lankan Population. *Proceedings of the National Academy of Sciences* **97**, 12661-12666 (2000).
40. Haldane, J.B.S. The Rate of Mutation of Human Genes. *Hereditas* **35**, 267-273 (1949).
41. Willcox, M. The Haemoglobin Pattern of Sickle Cell and Haemoglobin C Beta +-thalassaemia in Liberia. *Journal of Medical Genetics* **20**, 430-432 (1983).
42. Luzzatto, L., Nwachuku-Jarrett, E.S. & Reddy, S. Increased Sickling of Parasitised Erythrocytes as Mechanism of Resistance Against Malaria in the Sickle-cell Trait. *The Lancet* **295**, 319-322 (1970).

43. Hill, A.V.S. et al. Common West African HLA Antigens are Associated with Protection from Severe Malaria. *Nature* **352**, 595-600 (1991).
44. Hill, A.V.S. et al. Molecular Analysis of the Association of HLA-B53 and Resistance to Severe Malaria. *Nature* **360**, 434-439 (1992).
45. May, J. et al. HLA Class II Factors Associated with Plasmodium falciparum Merozoite Surface Antigen Allele Families. *Journal of Infectious Diseases* **179**, 1042-1045 (1999).
46. May, J., Lell, B., Luty, A.J.F., Meyer, C.G. & Kremsner, P.G. HLA-DQB1*0501-Restricted Th1 Type Immune Responses to Plasmodium falciparum Liver Stage Antigen 1 Protect against Malaria Anemia and Reinfections. *Journal of Infectious Diseases* **183**, 168-172 (2001).
47. Lyke, K.E. et al. Association of HLA Alleles with Plasmodium falciparum Severity in Malian Children. *Tissue Antigens* **77**, 562-571 (2011).
48. Adu, B. et al. Fc Gamma Receptor IIIB (FcγRIIIB) Polymorphisms Are Associated with Clinical Malaria in Ghanaian Children. *PLoS ONE* **7**, e46197 (2012).
49. Zhao, J. et al. Association Between Fc-gamma Receptor IIa (CD32) Gene Polymorphism and Malaria Susceptibility: A Meta-analysis Based on 6928 Subjects. *Infection, Genetics and Evolution* **23**, 169-175 (2014).
50. Abu-Raddad, L.J., Patnaik, P. & Kublin, J.G. Dual Infection with HIV and Malaria Fuels the Spread of Both Diseases in Sub-Saharan Africa. *Science* **314**, 1603-1606 (2006).
51. van den Bogaart, E. et al. Prevalence, Features and Risk Factors for Malaria Co-Infections amongst Visceral Leishmaniasis Patients from Amudat Hospital, Uganda. *PLoS Neglected Tropical Disease* **6**, e1617 (2012).
52. Cunnington, A.J., de Souza, J.B., Walther, M. & Riley, E.M. Malaria Impairs Resistance to Salmonella Through Heme- and Heme Oxygenase-dependent Dysfunctional Granulocyte Mobilization. *Nature Medicine* **18**, 120-127 (2012).
53. Fernando, S.D. et al. The Impact of Repeated Malaria Attacks on the School Performance of Children. *The American Journal of Tropical Medicine and Hygiene* **69**, 582-588 (2003).
54. Carter, J.A. et al. Developmental Impairments Following Severe Falciparum Malaria in Children. *Tropical Medicine & International Health* **10**, 3-10 (2005).
55. Sachs, J. & Malaney, P. The Economic and Social Burden of Malaria. *Nature* **415**, 680-685 (2002).
56. Steketee, R.W., Nahlen, B.L., Parise, M.E. & Menendez, C. The Burden of Malaria in Pregnancy in Malaria-endemic Areas. *The American Journal of Tropical Medicine and Hygiene* **64**, 28-35 (2001).
57. Guyatt, H.L. & Snow, R.W. Malaria in Pgnancy as an Idirect Cuse of Ifant Mrtality in Sb-Saharan Africa. *Transactions of The Royal Society of Tropical Medicine and Hygiene* **95**, 569-576 (2001).
58. Wellems, T.E. & Miller, L.H. Two Worlds of Malaria. *New England Journal of Medicine* **349**, 1496-1498 (2003).
59. Franco-Paredes, C. & Santos-Preciado, J.I. Problem Pathogens: Prevention of Malaria in Travellers. *The Lancet Infectious Diseases* **6**, 139-149 (2006).
60. Trampuz, A., Jereb, M., Muzlovic, I. & Prabhu, R.M. Clinical Review: Severe Malaria. *Critical Care* **7**, 315-323 (2003).
61. WHO Severe falciparum malaria. World Health Organization, Communicable Diseases Cluster. *Transactions of The Royal Society of Tropical Medicine and Hygiene* **94**, S1-S90 (2000).
62. Marsh, K. et al. Indicators of Life-Threatening Malaria in African Children. *New England Journal of Medicine* **332**, 1399-1404 (1995).
63. Dondorp, A.M., Pongponratn, E. & White, N.J. Reduced Microcirculatory Flow in Severe Falciparum Malaria: Pathophysiology and Electron-microscopic Pathology. *Acta Tropica* **89**, 309-317 (2004).

64. Abdalla, S., Weatherall, D.J., Wickramasinghe, S.N. & Hughes, M. The Anaemia of *P. falciparum* Malaria. *British Journal of Haematology* **46**, 171-183 (1980).
65. Dondorp, A.M. et al. Red Blood Cell Deformability as a Predictor of Anemia in Severe Falciparum Malaria. *The American Journal of Tropical Medicine and Hygiene* **60**, 733-737 (1999).
66. Miller, L.H., Good, M.F. & Milon, G. Malaria Pathogenesis. *Science* **264**, 1878-1883 (1994).
67. UNICEF. (ed. U.a.T.R.B.M. Partnership) (UNICEF, 2009).
68. Mendis, K. et al. From Malaria Control to Eradication: The WHO Perspective. *Tropical Medicine & International Health* **14**, 802-809 (2009).
69. Tulloch, J., David, B., Newman, R.D. & Meek, S. Artemisinin-resistant Malaria in the Asia-Pacific Region. *The Lancet* **381**, e16-e17 (2013).
70. EANMAT The Efficacy of Antimalarial Monotherapies, Sulphadoxine–pyrimethamine and Amodiaquine in East Africa: Implications for Sub-regional Policy. *Trop Med Int Health* **8**, 860-867 (2003).
71. Makanga, M. & Krudsood, S. The Clinical Efficacy of Artemether/Lumefantrine (Coartem(R)). *Malaria Journal* **8**, S5 (2009).
72. 4ABC, T.F.A.-B.C.S.G. A Head-to-Head Comparison of Four Artemisinin-Based Combinations for Treating Uncomplicated Malaria in African Children: A Randomized Trial. *PLoS Medicine* **8**, e1001119 (2011).
73. Ranson, H. et al. Pyrethroid Resistance in African Anopheline Mosquitoes: What are the Implications for Malaria Control? *Trends in Parasitology* **27**, 91-98 (2011).
74. Sallusto, F., Lanzavecchia, A., Araki, K. & Ahmed, R. From Vaccines to Memory and Back. *Immunity* **33**, 451-463 (2010).
75. Alonso, P.L. et al. Efficacy of the RTS,S/AS02A Vaccine Against *Plasmodium falciparum* Infection and Disease in Young African Children: Randomised Controlled Trial. *The Lancet* **364**, 1411-1420 (2004).
76. Olotu, A. et al. Four-Year Efficacy of RTS,S/AS01E and Its Interaction with Malaria Exposure. *New England Journal of Medicine* **368**, 1111-1120 (2013).
77. Arama, C. & Troye-Blomberg, M. The Path of Malaria Vaccine Development: Challenges and Perspectives. *Journal of Internal Medicine* **275**, 456-466 (2014).
78. Crompton, P.D., Pierce, S.K. & Miller, L.H. Advances and Challenges in Malaria Vaccine Development. *The Journal of Clinical Investigation* **120**, 4168-4178 (2010).
79. Langhorne, J., Ndungu, F.M., Sponaas, A.-M. & Marsh, K. Immunity to Malaria: More Questions than Answers. *Nature Immunology* **9**, 725-732 (2008).
80. Owusu-Agyei, S. et al. Incidence of Symptomatic and Asymptomatic Plasmodium falciparum Infection Following Curative Therapy in Adult Residents of Northern Ghana. *The American Journal of Tropical Medicine and Hygiene* **65**, 197-203 (2001).
81. Hoffman, S.L. et al. Protection of Humans against Malaria by Immunization with Radiation-Attenuated Plasmodium falciparum Sporozoites. *Journal of Infectious Diseases* **185**, 1155-1164 (2002).
82. Alonso, P.L. et al. Duration of Protection with RTS,S/AS02A Malaria Vaccine in Prevention of *Plasmodium falciparum* Disease in Mozambican Children: Single-blind Extended Follow-up of a Randomised Controlled Trial. *The Lancet* **366**, 2012-2018 (2005).
83. Stoute, J.A. et al. A Preliminary Evaluation of a Recombinant Circumsporozoite Protein Vaccine against Plasmodium falciparum Malaria. *New England Journal of Medicine* **336**, 86-91 (1997).
84. Campo, J.J. et al. Duration of Vaccine Efficacy Against Malaria: 5th Year of Follow-up in Children Vaccinated with RTS,S/AS02 in Mozambique. *Vaccine* **32**, 2209-2216 (2014).
85. Ofori, M.F. et al. Malaria-Induced Acquisition of Antibodies to Plasmodium falciparum Variant Surface Antigens. *Infection and Immunity* **70**, 2982-2988 (2002).

86. Bull, P.C. et al. Parasite Antigens on the Infected Red Cell Surface are Targets for Naturally Acquired Immunity to Malaria. *Nature Medicine* **4**, 358-360 (1998).
87. Cohen, S., McGregor, I.A. & Carrington, S. Gamma-Globulin and Acquired Immunity to Human Malaria. *Nature* **192**, 733-737 (1961).
88. Sabchareon, A. et al. Parasitologic and Clinical Human Response to Immunoglobulin Administration in Falciparum Malaria. *The American Journal of Tropical Medicine and Hygiene* **45**, 297-308 (1991).
89. Osier, F.H.A. et al. Breadth and Magnitude of Antibody Responses to Multiple Plasmodium falciparum Merozoite Antigens Are Associated with Protection from Clinical Malaria. *Infection and Immunity* **76**, 2240-2248 (2008).
90. Blackman, M.J., Heidrich, H.G., Donachie, S., McBride, J.S. & Holder, A.A. A Single Fragment of a Malaria Merozoite Surface Protein Remains on the Parasite During Red Cell Invasion and is the Target of Invasion-Inhibiting Antibodies. *The Journal of Experimental Medicine* **172**, 379-382 (1990).
91. Bouharoun-Tayoun, H., Oeuvray, C., Lunel, F. & Druilhe, P. Mechanisms Underlying the Monocyte-mediated Antibody-dependent Killing of Plasmodium falciparum Asexual Blood Stages. *The Journal of Experimental Medicine* **182**, 409-418 (1995).
92. Felgner, P.L. et al. Pre-erythrocytic Antibody Profiles Induced by Controlled Human Malaria Infections in Healthy Volunteers Under Chloroquine Prophylaxis. *Scientific Reports* **3** (2013).
93. Roestenberg, M. et al. Protection against a Malaria Challenge by Sporozoite Inoculation. *New England Journal of Medicine* **361**, 468-477 (2009).
94. Beeson, J.G., Osier, F.H.A. & Engwerda, C.R. Recent Insights Into Humoral and Cellular Immune Responses Against Malaria. *Trends in Parasitology* **24**, 578-584 (2008).
95. Moormann, A.M. et al. Humoral and Cellular Immunity to Plasmodium falciparum Merozoite Surface Protein 1 and Protection From Infection With Blood-Stage Parasites. *Journal of Infectious Diseases* **208**, 149-158 (2013).
96. Casares, S. & Richie, T.L. Immune Evasion by Malaria Parasites: A Challenge for Vaccine Development. *Current Opinion in Immunology* **21**, 321-330 (2009).
97. Hisaeda, H., Yasutomo, K. & Himeno, K. Malaria: Immune Evasion by Parasites. *The International Journal of Biochemistry and Cell Biology* **37**, 700-706 (2005).
98. Craig, A. & Scherf, A. Molecules on the Surface of the Plasmodium falciparum Infected Erythrocyte and Their Role in Malaria Pathogenesis and Immune Evasion. *Molecular and Biochemical Parasitology* **115**, 129-143 (2001).
99. Beeson, J.G., Reeder, J.C., Rogerson, S.J. & Brown, G.V. Parasite Adhesion and Immune Evasion in Placental Malaria. *Trends in Parasitology* **17**, 331-337 (2001).
100. Czajkowsky, D.M. et al. IgM, FcμRs, and Malarial Immune Evasion. *The Journal of Immunology* **184**, 4597-4603 (2010).
101. Scherf, A., Lopez-Rubio, J.J. & Riviere, L. Antigenic Variation in Plasmodium falciparum. *Annual Review of Microbiology* **62**, 445-470 (2008).
102. Qari, S.H. et al. Predicted and Observed Alleles of Plasmodium falciparum Merozoite Surface Protein-1 (MSP-1), A Potential Malaria Vaccine Antigen. *Molecular and Biochemical Parasitology* **92**, 241-252 (1998).
103. Biggs, B.A. et al. Adherence of infected erythrocytes to venular endothelium selects for antigenic variants of Plasmodium falciparum. *The Journal of Immunology* **149**, 2047-2054 (1992).
104. Bronke, C. et al. HIV Escape Mutations Occur Preferentially at HLA-binding Sites of CD8 T-cell Epitopes. *AIDS* **27**, 899-905 (2013).
105. Kelleher, A.D. et al. Clustered Mutations in HIV-1 Gag Are Consistently Required for Escape from Hla-B27–Restricted Cytotoxic T Lymphocyte Responses. *The Journal of Experimental Medicine* **193**, 375-386 (2001).

106. Bianco, A.E. et al. A repetitive antigen of Plasmodium falciparum that is homologous to heat shock protein 70 of Drosophila melanogaster. *Proc Natl Acad Sci USA* **83**, 8713-8717 (1986).
107. Smith, J.D. et al. Switches in Expression of Plasmodium falciparum Var Genes Correlate with Changes in Antigenic and Cytoadherent Phenotypes of Infected Erythrocytes. *Cell* **82**, 101-110 (1995).
108. Pouvelle, B., Buffet, P.A., Lepolard, C., Scherf, A. & Gysin, J. Cytoadhesion of Plasmodium falciparum ring-stage-infected erythrocytes. *Nature Medicine* **6**, 1264-1268 (2000).
109. Hernandez-Rivas, R. et al. Expressed var genes are found in Plasmodium falciparum subtelomeric regions. *Molecular and Cellular Biology* **17**, 604-611 (1997).
110. Gardner, M.J. et al. Genome Sequence of the Human Malaria Parasite Plasmodium falciparum. *Nature* **419**, 498-511 (2002).
111. Scherf, A. et al. Antigenic variation in malaria: in situ switching, relaxed and mutually exclusive transcription of var genes during intra-erythrocytic development in Plasmodium falciparum. *The EMBO Journal* **17**, 5418-5426 (1998).
112. Roberts, D.J. et al. Rapid switching to multiple antigenic and adhesive phenotypes in malaria. *Nature* **357**, 689-692 (1992).
113. Rowe, J.A., Claessens, A., Corrigan, R.A. & Arman, M. Adhesion of Plasmodium falciparum-infected erythrocytes to human cells: molecular mechanisms and therapeutic implications. *Expert Reviews in Molecular Medicine* **11**, null-null (2009).
114. Turner, L. et al. Severe Malaria is Associated with Parasite Binding to Endothelial Protein C Receptor. *Nature* **498**, 502-505 (2013).
115. Laclette, J.P. et al. Paramyosin Inhibits Complement C1. *The Journal of Immunology* **148**, 124-128 (1992).
116. Lubinski, J.M., Lazear, H.M., Awasthi, S., Wang, F. & Friedman, H.M. The herpes simplex virus 1 IgG fc receptor blocks antibody-mediated complement activation and antibody-dependent cellular cytotoxicity in vivo. *Journal of virology* **85**, 3239-3249 (2011).
117. Sprague, E.R., Wang, C., Baker, D. & Bjorkman, P.J. Crystal Structure of the HSV-1 Fc Receptor Bound to Fc Reveals a Mechanism for Antibody Bipolar Bridging. *PLoS Biol* **4**, e148 (2006).
118. Stevenson, L. et al. Investigating the Function of Fc-specific Binding of IgM to Plasmodium falciparum Erythrocyte Membrane Protein 1 Mediating Erythrocyte Rosetting. *Cellular Microbiology* (2014).
119. Barfod, L. et al. Evasion of immunity to Plasmodium falciparum malaria by IgM masking of protective IgG epitopes in infected erythrocyte surface-exposed PfEMP1. *Proceedings of the National Academy of Sciences* (2011).
120. Ghumra, A. et al. Identification of Residues in the Cμ4 Domain of Polymeric IgM Essential for Interaction with Plasmodium falciparum Erythrocyte Membrane Protein 1 (PfEMP1). *The Journal of Immunology* **181**, 1988-2000 (2008).
121. Rowe, J.A., Moulds, J.M., Newbold, C. & Miller, L.H. P. falciparum rosetting mediated by a parasite-variant erythrocyte membrane protein and complement-receptor 1. *Nature* **388**, 292-295 (1997).
122. Scholander, C., Treutiger, C.J., Hultenby, K. & Wahlgren, M. Novel Fibrillar Structure Confers Adhesive Property to Malaria-Infected Erythrocytes. *Nature Medicine* **2**, 204-208 (1996).
123. Donati, D. et al. Identification of a Polyclonal B-Cell Activator in Plasmodium falciparum. *Infection and Immunity* **72**, 5412-5418 (2004).
124. Rowe, J.A., Shafi, J., Kai, O.K., Marsh, K. & Raza, A. Nonimmune IgM, but not IgG Binds to the Surface of Plasmodium falciparum-Infected Erythrocytes and Correlates with Rosetting and Severe Malaria. *The American Journal of Tropical Medicine and Hygiene* **66**, 692-699 (2002).

125. Creasey, A.M., Staalsoe, T., Raza, A., Arnot, D.E. & Rowe, J.A. Nonspecific Immunoglobulin M Binding and Chondroitin Sulfate A Binding Are Linked Phenotypes of Plasmodium falciparum Isolates Implicated in Malaria during Pregnancy. *Infection and Immunity* **71**, 4767-4771 (2003).
126. Fried, M. & Duffy, P.E. Adherence of Plasmodium falciparum to Chondroitin Sulfate A in the Human Placenta. *Science* **272**, 1502-1504 (1996).
127. Somner, E.A., Black, J. & Pasvol, G. Multiple Human Serum Components Act as Bridging Molecules in Rosette Formation by Plasmodium falciparum-Infected Erythrocytes. *Blood* **95**, 674-682 (2000).
128. Ghumra, A. et al. Induction of Strain-Transcending Antibodies Against Group A PfEMP1 Surface Antigens from Virulent Malaria Parasites. *PLoS Pathogens* **8**, e1002665 (2012).
129. Salanti, A. et al. Evidence for the Involvement of VAR2CSA in Pregnancy-associated Malaria. *The Journal of Experimental Medicine* **200**, 1197-1203 (2004).
130. Semblat, J.-P., Raza, A., Kyes, S.A. & Rowe, J.A. Identification of Plasmodium falciparum Var1CSA and Var2CSA Domains that Bind IgM Natural Antibodies. *Molecular and Biochemical Parasitology* **146**, 192-197 (2006).
131. Scholzen, A. & Sauerwein, R.W. How Malaria Modulates Memory: Activation and Dysregulation of B Cells in Plasmodium Infection. *Trends in Parasitology* **29**, 252-262 (2013).
132. Donati, D. et al. Clearance of Circulating Epstein-Barr Virus DNA in Children with Acute Malaria after Antimalaria Treatment. *Journal of Infectious Diseases* **193**, 971-977 (2006).
133. Donati, D. et al. Increased B Cell Survival and Preferential Activation of the Memory Compartment by a Malaria Polyclonal B Cell Activator. *The Journal of Immunology* **177**, 3035-3044 (2006).
134. Simone, O. et al. TLRs Innate Immunereceptors and Plasmodium falciparum Erythrocyte Membrane Protein 1 (PfEMP1) CIDR1α-driven Human Polyclonal B-cell Activation. *Acta Tropica* **119**, 144-150 (2011).
135. Czajkowsky, D.M. & Shao, Z. The Human IgM Pentamer is a Mushroom-Shaped Molecule with a Flexural Bias. *Proceedings of the National Academy of Sciences* **106**, 14960-14965 (2009).
136. Czajkowsky, D.M. et al. Developing the IVIG Biomimetic, Hexa-Fc, for Drug and Vaccine Applications. *Nature Scientific Reports* **5**, 1-11 (2015).
137. Kubagawa, H. et al. Identity of the Elusive IgM Fc Receptor (FcμR) in Humans. *The Journal of Experimental Medicine* **206**, 2779-2793 (2009).
138. Ouchida, R. et al. Critical Role of the IgM Fc Receptor in IgM Homeostasis, B-cell Survival, and Humoral Immune Responses. *Proceedings of the National Academy of Sciences* **109**, E2699–E2706 (2012).
139. Greenwood, B.M. & Vick, R.M. Evidence for a Malaria Mitogen in Human Malaria. *Nature* **257**, 592-594 (1975).
140. Murakami, Y. et al. Toso, a Functional IgM Receptor, Is Regulated by IL-2 in T and NK Cells. *The Journal of Immunology* **189**, 587-597 (2012).
141. McCall, M.B.B. et al. Memory-like IFN-γ Response by NK Cells Following Malaria Infection Reveals the Crucial Role of T Cells in NK Cell Activation by P. falciparum. *European Journal of Immunology* **40**, 3472-3477 (2010).
142. Agudelo, O., Bueno, J., Villa, A. & Maestre, A. High IFN-gamma and TNF Production by Peripheral NK Cells of Colombian Patients with Different Clinical Presentation of Plasmodium falciparum. *Malaria Journal* **11**, 38 (2012).
143. Shibuya, A. et al. Fcα/μ Receptor Mediates Endocytosis of IgM-Coated Microbes. *Nature Immunology* **1**, 441-446 (2000).
144. Bartholdson, S.J. et al. Semaphorin-7A Is an Erythrocyte Receptor for *P. falciparum* Merozoite-Specific TRAP Homolog, MTRAP. *PLoS Pathogens* **8**, e1003031 (2012).

145. Chen, F.H. et al. Domain-switched Mouse IgM/IgG2b Hybrids Indicate Individual Roles for C mu 2, C mu 3, and C mu 4 Domains in the Regulation of the Interaction of IgM with Complement C1q. *The Journal of Immunology* **159**, 3354-3363 (1997).
146. Crosnier, C. et al. 1-302015).
147. Hodder, A.N. et al. Insights into Duffy Binding-like Domains through the Crystal Structure and Function of the Merozoite Surface Protein MSPDBL2 from Plasmodium falciparum. *Journal of Biological Chemistry* **287**, 32922-32939 (2012).
148. Singh, S. et al. A Conserved Multi-Gene Family Induces Cross-Reactive Antibodies Effective in Defense against *Plasmodium falciparum*. *PLoS ONE* **4**, e5410 (2009).
149. Wickramarachchi, T. et al. A Novel Plasmodium falciparum Erythrocyte Binding Protein Associated with the Merozoite Surface, PfDBLMSP. *International Journal for Parasitology* **39**, 763-773 (2009).
150. Gondeau, C. et al. The C-terminal domain of Plasmodium falciparum merozoite surface protein 3 self-assembles into alpha-helical coiled coil tetramer. *Molecular and biochemical parasitology* **165**, 153-161 (2009).
151. Amambua-Ngwa, A. et al. Population genomic scan for candidate signatures of balancing selection to guide antigen characterization in malaria parasites. *PLoS genetics* **8**, e1002992 (2012).
152. Ochola, L.I. et al. Allele frequency-based and polymorphism-versus-divergence indices of balancing selection in a new filtered set of polymorphic genes in Plasmodium falciparum. *Molecular biology and evolution* **27**, 2344-2351 (2010).
153. Tetteh, K.K. et al. Prospective identification of malaria parasite genes under balancing selection. *PloS one* **4**, e5568 (2009).
154. Fellah, J.S., Wiles, M.V., Charlemagne, J. & Schwager, J. Evolution of Vertebrate IgM: Complete Amino Acid Sequence of the Constant Region of Ambystoma mexicanum μ Chain Deduced from cDNA Sequence. *European Journal of Immunology* **22**, 2595-2601 (1992).
155. Klimovich, V.B. IgM and Its Receptors: Structural and Functional Aspects. *Biochemistry* **76**, 534-549 (2011).
156. Ehrenstein, M.R. & Notley, C.A. The Importance of Natural IgM: Scavenger, Protector and Regulator. *Nature Review Immunology* **10**, 778-786 (2010).
157. Rapaka, R.R. et al. Conserved Natural IgM Antibodies Mediate Innate and Adaptive Immunity Against the Opportunistic Fungus Pneumocystis murina. *The Journal of Experimental Medicine* **207**, 2907-2919 (2010).
158. Vollmers, H.P. & Brändlein, S. Natural IgM Antibodies: The Orphaned Molecules in Immune Surveillance. *Advanced Drug Delivery Reviews* **58**, 755-765 (2006).
159. Randall, T.D., Brewer, J.W. & Corley, R.B. Direct Evidence that J Chain Regulates the Polymeric Structure of IgM in Antibody-secreting B Cells. *Journal of Biological Chemistry* **267**, 18002-18007 (1992).
160. Cattaneo, A. & Neuberger, M.S. Polymeric Immunologbulin M is Secreted by Transfectants of Non-lymphoid Cells in the Absence of Immunoglobulin J Chain. *The EMBO Journal* **6**, 2753-2758 (1987).
161. Sørensen, V., Rasmussen, I.B., Sundvold, V., Michaelsen, T.E. & Sandlie, I. Structural Requirements for Incorporation of J Chain into Human IgM and IgA. *International Immunology* **12**, 19-27 (2000).
162. Chapuis, R.M. & Koshland, M.E. Mechanism of IgM Polymerization. *Proceedings of the National Academy of Sciences* **71**, 657-661 (1974).
163. Brandtzaeg, P. & Prydz, H. Direct Evidence for an Integrated Function of J Chain and Secretory Component in Epithelial Transport of Immunoglobulins. *Nature* **311**, 71-73 (1984).
164. Randall, T.D., King, L.B. & Corley, R.B. The Biological Effects of IgM Hexamer Formation. *European Journal of Immunology* **20**, 1971-1979 (1990).
165. Wiersma, E.J., Collins, C., Fazel, S. & Shulman, M.J. Structural and Functional Analysis of J Chain-Deficient IgM. *The Journal of Immunology* **160**, 5979-5989 (1998).

166. Johansen, Braathen & Brandtzaeg Role of J Chain in Secretory Immunoglobulin Formation. *Scandinavian Journal of Immunology* **52**, 240-248 (2000).
167. Müller, R. et al. High-resolution Structures of the IgM Fc Domains Reveal Principles of its Hexamer Formation. *Proceedings of the National Academy of Sciences* **110**, 10183-10188 (2013).
168. Arnold, J.N. et al. Human Serum IgM Glycosylation: Identification of Glycoforms that can Bind to Mannan-Binding Lectin. *Journal of Biological Chemistry* **280**, 29080-29087 (2005).
169. Arnold, J.N., Wormald, M.R., Sim, R.B., Rudd, P.M. & Dwek, R.A. The Impact of Glycosylation on the Biological Function and Structure of Human Immunoglobulins. *Annual Review of Immunology* **25**, 21-50 (2007).
170. Kaetzel, C.S. The polymeric immunoglobulin receptor: bridging innate and adaptive immune responses at mucosal surfaces. *Immunological reviews* **206**, 83-99 (2005).
171. Tissot, J.D. et al. IgM are Associated to Sp Alpha (CD5 Antigen-like). *Electrophoresis* **23**, 1203-1206 (2002).
172. Mallery, D.L. et al. Antibodies Mediate Intracellular Immunity Through Tripartite Motif-containing 21 (TRIM21). *Proceedings of the National Academy of Sciences* **107**, 19985-19990 (2010).
173. Shibuya, A. et al. Fc alpha/mu receptor mediates endocytosis of IgM-coated microbes. *Nature immunology* **1**, 441-446 (2000).
174. Adachi, T. et al. CD22 serves as a receptor for soluble IgM. *European journal of immunology* (2011).
175. Shima, H. et al. Identification of TOSO/FAIM3 as an Fc Receptor for IgM. *International Immunology* **22**, 149-156 (2010).
176. Li, F.J. et al. Enhanced Levels of Both the Membrane-bound and Soluble Forms of IgM Fc Receptor (FcμR) in Patients with Chronic Lymphocytic Leukemia. *Blood* **118**, 4902-4909 (2011).
177. Pallasch, C.P. et al. Overexpression of TOSO in CLL is Triggered by B-Cell Receptor Signaling and Associated with Progressive Disease. *Blood* **112**, 4213-4219 (2008).
178. Proto-Siqueira, R. et al. SAGE Analysis Demonstrates Increased Expression of TOSO Contributing to Fas-mediated Resistance in CLL. *Blood* **112**, 394-397 (2008).
179. Honjo, K., Kubagawa, Y. & Kubagawa, H. Is Toso/IgM Fc Receptor (FcμR) Expressed by Innate Immune Cells? *Proceedings of the National Academy of Sciences* **110**, E2540-E2541 (2013).
180. Lang, K.S. et al. Involvement of Toso in Activation of Monocytes, Macrophages, and Granulocytes. *Proceedings of the National Academy of Sciences* **110**, 2593-2598 (2013).
181. Brenner, D. et al. Toso Controls Encephalitogenic Immune Responses by Dendritic Cells and Regulatory T Cells. *Proceedings of the National Academy of Sciences* **111**, 1060-1065 (2014).
182. Honjo, K. et al. Altered Ig Levels and Antibody Responses in Mice Deficient for the Fc Receptor for IgM (FcμR). *Proceedings of the National Academy of Sciences* **109**, 15882-15887 (2012).
183. Vire, B., David, A. & Wiestner, A. TOSO, the Fcμ Receptor, Is Highly Expressed on Chronic Lymphocytic Leukemia B Cells, Internalizes upon IgM Binding, Shuttles to the Lysosome, and Is Downregulated in Response to TLR Activation. *The Journal of Immunology* **187**, 4040-4050 (2011).
184. Mitchell, D.A., Fadden, A.J. & Drickamer, K. A novel mechanism of carbohydrate recognition by the C-type lectins DC-SIGN and DC-SIGNR. Subunit organization and binding to multivalent ligands. *The Journal of biological chemistry* **276**, 28939-28945 (2001).
185. Mekhaiel, D.N.A. et al. Polymeric Human Fc-fusion Proteins with Modified Effector Functions. *Scientific Reports* **1** (2011).

186. Maier, A. & Rug, M. in Malaria, Vol. 923. (ed. R. Ménard) 3-15 (Humana Press, 2013).
187. Lambros, C. & Vanderberg, J.P. Synchronization of Plasmodium falciparum Erythrocytic Stages in Culture. *Journal of Parasitology* **65**, 418-420 (1979).
188. Crosnier, C. et al. A Library of Functional Recombinant Cell-surface and Secreted P. falciparum Merozoite Proteins. *Molecular & Cellular Proteomics* **12**, 3976-3986 (2013).
189. Crosnier, C., Staudt, N. & Wright, G. A Rapid and Scalable Method for Selecting Recombinant Mouse Monoclonal Antibodies. *BMC Biology* **8**, 76 (2010).
190. Brown, M.H. & Barclay, A.N. Expression of Immunoglobulin and Scavenger Receptor Superfamily Domains as Chimeric Proteins with Domains 3 and 4 of CD4 for Ligand Analysis. *Protein Engineering* **7**, 515-521 (1994).
191. Bushell, K.M., Söllner, C., Schuster-Boeckler, B., Bateman, A. & Wright, G.J. Large-scale screening for novel low-affinity extracellular protein interactions. *Genome Research* **18**, 622-630 (2008).
192. Nordström, T., Jendholm, J., Samuelsson, M., Forsgren, A. & Riesbeck, K. The IgD-binding Domain of the Moraxella IgD-binding Protein MID (MID962-1200) Activates Human B Cells in the Presence of T Cell Cytokines. *Journal of Leukocyte Biology* **79**, 319-329 (2006).
193. Kang, Y.-H., Urban, B.C., Sim, R.B. & Kishore, U. Human Complement Factor H Modulates C1q-mediated Phagocytosis of Apoptotic Cells. *Immunobiology* **217**, 455-464 (2012).
194. Ostreiko, K.K., Tumanovam, I.A. & Sykulev, Y. Production and Characterization of Heat-Aggregated IgG Complexes with Pre-determined Molecular Masses: Light-scattering Study. *Immunology Letters* **15**, 311-316 (1987).
195. Higgins, M.K. The structure of a chondroitin sulfate-binding domain important in placental malaria. *The Journal of biological chemistry* **283**, 21842-21846 (2008).
196. Khunrae, P., Philip, J.M.D., Bull, D.R. & Higgins, M.K. Structural Comparison of Two CSPG-Binding DBL Domains from the VAR2CSA Protein Important in Malaria during Pregnancy. *Journal of molecular biology* **393**, 202-213 (2009).
197. Czajkowsky, D.M. & Shao, Z. The human IgM pentamer is a mushroom-shaped molecule with a flexural bias. *Proceedings of the National Academy of Sciences of the United States of America* **106**, 14960-14965 (2009).
198. Czajkowsky, D.M. et al. IgM, Fc mu Rs, and malarial immune evasion. *J Immunol* **184**, 4597-4603 (2010).
199. Kelley, L.A. & Sternberg, M.J.E. Protein Structure Prediction on the Web: A Case Study using the Phyre Server. *Nature Protocols* **4**, 363-371 (2009).
200. Kubagawa, H. et al. The long elusive IgM Fc receptor, FcmuR. *Journal of clinical immunology* **34 Suppl 1**, S35-45 (2014).
201. Mineev, K.S. et al. Spatial Structure of the Transmembrane Domain Heterodimer of ErbB1 and ErbB2 Receptor Tyrosine Kinases. *Journal of Molecular Biology* **400**, 231-243 (2010).
202. Gautam, S. & Loh, K.-C. Human pIgR mimetic peptidic ligand for affinity purification of IgM. *Separation and Purification Technology* **102**, 173-179 (2013).
203. Yang, X., Zhao, Q., Zhu, L. & Zhang, W. The three complementarity-determining region-like loops in the second extracellular domain of human Fc alpha/mu receptor contribute to its binding of IgA and IgM. *Immunobiology* **218**, 798-809 (2013).
204. Pincetic, A. et al. Type I and type II Fc receptors regulate innate and adaptive immunity. *Nature immunology* **15**, 707-716 (2014).
205. Marquez, J.A. et al. The crystal structure of the extracellular domain of the inhibitor receptor expressed on myeloid cells IREM-1. *Journal of molecular biology* **367**, 310-318 (2007).
206. Herr, A.B., Ballister, E.R. & Bjorkman, P.J. Insights into IgA-mediated Immune Responses from the Crystal Structures of Human FcαRI and its Complex with IgA1-Fc. *Nature* **423**, 614-620 (2003).

207. W, H., A, D. & K, S. - VMD: visual molecular dynamics. *D - 9014762*, - 33-38, 27-38 (1996).
208. MacKerell, A.D. et al. All-Atom Empirical Potential for Molecular Modeling and Dynamics Studies of Proteins. *The Journal of Physical Chemistry B* **102**, 3586-3616 (1998).
209. Phillips, J.C. et al. Scalable Molecular Dynamics with NAMD. *Journal of Computational Chemistry* **26**, 1781-1802 (2005).
210. Song, Y. & Jacob, C.O. The Mouse Cell Surface Protein TOSO Regulates Fas/Fas Ligand-induced Apoptosis through Its Binding to Fas-associated Death Domain. *Journal of Biological Chemistry* **280**, 9618-9626 (2005).
211. Boes, M. et al. Enhanced B-1 Cell Development, But Impaired IgG Antibody Responses in Mice Deficient in Secreted IgM. *The Journal of Immunology* **160**, 4776-4787 (1998).
212. Ehrenstein, M.R., O'Keefe, T.L., Davies, S.L. & Neuberger, M.S. Targeted Gene Disruption Reveals a Role for Natural Secretory IgM in the Maturation of the Primary Immune Response. *Proceedings of the National Academy of Sciences* **95**, 10089-10093 (1998).
213. Baumgarth, N. et al. B-1 and B-2 Cell–Derived Immunoglobulin M Antibodies Are Nonredundant Components of the Protective Response to Influenza Virus Infection. *The Journal of Experimental Medicine* **192**, 271-280 (2000).
214. Malkiel, S., Kuhlow, C.J., Mena, P. & Benach, J.L. The Loss and Gain of Marginal Zone and Peritoneal B Cells Is Different in Response to Relapsing Fever and Lyme Disease Borrelia. *The Journal of Immunology* **182**, 498-506 (2009).
215. Rajan, B., Ramalingam, T. & Rajan, T.V. Critical Role for IgM in Host Protection in Experimental Filarial Infection. *The Journal of Immunology* **175**, 1827-1833 (2005).
216. Subramaniam, K.S., Datta, K., Marks, M.S. & Pirofski, L.-a. Improved Survival of Mice Deficient in Secretory Immunoglobulin M following Systemic Infection with Cryptococcus neoformans. *Infection and Immunity* **78**, 441-452 (2010).
217. Subramaniam, K.S. et al. The Absence of Serum IgM Enhances the Susceptibility of Mice to Pulmonary Challenge with Cryptococcus neoformans. *The Journal of Immunology* **184**, 5755-5767 (2010).
218. Boes, M., Prodeus, A.P., Schmidt, T., Carroll, M.C. & Chen, J. A Critical Role of Natural Immunoglobulin M in Immediate Defense Against Systemic Bacterial Infection. *The Journal of Experimental Medicine* **188**, 2381-2386 (1998).
219. Kinoshita, M. et al. Restoration of Natural IgM Production from Liver B Cells by Exogenous IL-18 Improves the Survival of Burn-Injured Mice Infected with Pseudomonas aeruginosa. *The Journal of Immunology* **177**, 4627-4635 (2006).
220. Ehrenstein, M.R., Cook, H.T. & Neuberger, M.S. Deficiency in Serum Immunoglobulin (Ig)m Predisposes to Development of Igg Autoantibodies. *The Journal of Experimental Medicine* **191**, 1253-1258 (2000).
221. Baker, N. & Ehrenstein, M.R. Cutting Edge: Selection of B Lymphocyte Subsets Is Regulated by Natural IgM. *The Journal of Immunology* **169**, 6686-6690 (2002).
222. Notley, C.A., Baker, N. & Ehrenstein, M.R. Secreted IgM Enhances B Cell Receptor Signaling and Promotes Splenic but Impairs Peritoneal B Cell Survival. *The Journal of Immunology* **184**, 3386-3393 (2010).
223. Myles, A., Tuteja, A. & Aggarwal, A. Synovial Fluid Mononuclear Cell Gene Expression Profiling Suggests Dysregulation of Innate Immune Genes in Enthesitis-related Arthritis Patients. *Rheumatology* **51**, 1785-1789 (2012).
224. Nguyen, X.-H. et al. Response: Antiapoptotic Function of Toso (Faim3) in Death Receptor Signaling. *Blood* **119**, 1790-1791 (2012).
225. Kaetzel, C.S. Polymeric Ig Receptor: Defender of the Fort or Trojan Horse? *Current Biology* **11**, R35-R38 (2001).
226. Litvack, M.L., Post, M. & Palaniyar, N. IgM Promotes the Clearance of Small Particles and Apoptotic Microparticles by Macrophages. *PLoS ONE* **6**, e17223 (2011).

227. Kaveri, S.V., Silverman, G.J. & Bayry, J. Natural IgM in Immune Equilibrium and Harnessing Their Therapeutic Potential. *J Immunol* **188**, 939-945 (2012).
228. Vas, J., Gronwall, C. & Silverman, G.J. Fundamental roles of the innate-like repertoire of natural antibodies in immune homeostasis. *Frontiers in immunology* **4**, 4 (2013).
229. Richter, G.H.S., Mollweide, A., Hanewinkel, K., Zobywalski, C. & Burdach, S. CD25 Blockade protects T Cells from Activation-induced Cell Death (AICD) via Maintenance of TOSO Expression. *Scandinavian Journal of Immunology* **70**, 206-215 (2009).
230. Boes, M. et al. Accelerated Development of IgG Autoantibodies and Autoimmune Disease in the Absence of Secreted IgM. *Proceedings of the National Academy of Sciences* **97**, 1184-1189 (2000).
231. Daëron, M. Fc Receptor Biology. *Annual Review of Immunology* **15**, 203-234 (1997).
232. Garman, S.C., Wurzburg, B.A., Tarchevskaya, S.S., Kinet, J.-P. & Jardetzky, T.S. Structure of the Fc Fragment of Human IgE Bound to its High-Affinity Receptor FcεRIα. *Nature* **406**, 259-266 (2000).
233. Adachi, T. et al. CD22 Serves as a Receptor for Soluble IgM. *European Journal of Immunology* **42**, 241-247 (2011).
234. Sigruener, A. et al. E-LDL Upregulates TOSO Expression and Enhances the Survival of Human Macrophages. *Biochemical and Biophysical Research Communications* **359**, 723-728 (2007).
235. Lang, K.S. et al. Reply to Honjo et al.: Functional Relevant Expression of Toso on Granulocytes. *Proceedings of the National Academy of Sciences* **110**, E2542-E2543 (2013).
236. Haury, M. et al. The Repertoire of Serum IgM in Normal Mice is Largely Independent of External Antigenic Contact. *European Journal of Immunology* **27**, 1557-1563 (1997).
237. Murphy, K., Paul, T., Mark, W. & Charles, J. Janeway's immunobiology. (Garland Science, New York; 2012).
238. Mekhaiel, D.N. et al. Polymeric human Fc-fusion proteins with modified effector functions. *Scientific reports* **1**, 124 (2011).
239. Hoffman, J.N. et al. Immunoglobulin M-enriched human intravenous immunoglobulins reduce leukocyte-endothelial cell interactions and attenuate microvascular perfusion failure in normotensive endotoxemia. *Shock* **29**, 133-139 (2008).
240. Mitchell, D.A., Fadden, A.J. & Drickamer, K. A Novel Mechanism of Carbohydrate Recognition by the C-type Lectins DC-SIGN and DC-SIGNR: Subunit Organization and Binding to Multivalent Ligands. *Journal of Biological Chemistry* **276**, 28939-28945 (2001).
241. Low-Nam, S.T. et al. ErbB1 Dimerization is Promoted by Domain Co-confinement and Stabilized by Ligand Binding. *Nature Structural and Molecular Biology* **18**, 1244-1249 (2011).
242. Kubagawa, H. et al. The Long Elusive IgM Fc Receptor, FcμR. *J Clin Immunol* **34**, 35-45 (2014).
243. Gautam, S. & Loh, K.-C. Human pIgR mimetic peptidic ligand for affinity purification of IgM Part II: Ligand binding characteristics. *Separation and Purification Technology* **102**, 43-49 (2013).
244. Pincetic, A. et al. Type I and type II Fc receptors regulate innate and adaptive immunity. *Nat Immunol* **15**, 707-716 (2014).
245. Sakamoto, N. et al. A Novel Fc Receptor for IgA and IgM is Expressed on both Hematopoietic and Non-hematopoietic Tissues. *European Journal of Immunology* **31**, 1310-1316 (2001).
246. Nimmerjahn, F. & Ravetch, J.V. Fc[gamma] receptors as regulators of immune responses. *Nat Rev Immunol* **8**, 34-47 (2008).

247. Ghumra, A. et al. Structural Requirements for the Interaction of Human IgM and IgA with the Human Fcα/μ Receptor. *European Journal of Immunology* **39**, 1147-1156 (2009).
248. Braathen, R., Sørensen, V., Brandtzaeg, P., Sandlie, I. & Johansen, F.-E. The Carboxyl-terminal Domains of IgA and IgM Direct Isotype-specific Polymerization and Interaction with the Polymeric Immunoglobulin Receptor. *Journal of Biological Chemistry* **277**, 42755-42762 (2002).
249. Sørensen, V., Sundvold, V., Michaelsen, T.E. & Sandlie, I. Polymerization of IgA and IgM: Roles of Cys309/Cys414 and the Secretory Tailpiece. *The Journal of Immunology* **162**, 3448-3455 (1999).
250. Feinstein, A. & Munn, E.A. Conformation of the Free and Antigen-bound IgM Antibody Molecules. *Nature* **224**, 1307-1309 (1969).
251. Haegert, D.G. Phagocytic Peripheral Blood Monocytes from Rabbits and Humans Express Membrane Receptors Specific for IgM Molecules: Evidence that Incubation with Neuraminidase Exposes Cryptic IgM (Fc) Receptors. *Clinical & Experimental Immunology* **35**, 484-490 (1979).
252. Öhlander, C. & Perlmann, P. Role of IgM in Human Monocyte-Mediated Target Cell Destruction in Vitro. *Scandinavian Journal of Immunology* **15**, 363-370 (1982).
253. Bouhlel, M.A. et al. PPARγ Activation Primes Human Monocytes into Alternative M2 Macrophages with Anti-inflammatory Properties. *Cell Metabolism* **6**, 137-143 (2007).
254. Scott, D.W. et al. Role of Endothelial N-Glycan Mannose Residues in Monocyte Recruitment During Atherogenesis. *Arteriosclerosis, Thrombosis, and Vascular Biology* **32**, e51-e59 (2012).
255. Gazi, U. & Martinez-Pomares, L. Influence of the Mannose Receptor in Host Immune Responses. *Immunobiology* **214**, 554-561 (2009).
256. Chieppa, M. et al. Cross-Linking of the Mannose Receptor on Monocyte-Derived Dendritic Cells Activates an Anti-Inflammatory Immunosuppressive Program. *The Journal of Immunology* **171**, 4552-4560 (2003).
257. Gage, E., Hernandez, M.O., O'Hara, J.M., McCarthy, E.A. & Mantis, N.J. Role of the Mannose Receptor (CD206) in Innate Immunity to Ricin Toxin. *Toxins* **3**, 1131-1145 (2011).
258. Foxall, C. et al. The Three Members of the Selectin Receptor Family Recognize a Common Carbohydrate Epitope, the Sialyl Lewis(x) Oligosaccharide. *The Journal of Cell Biology* **117**, 895-902 (1992).
259. Gbarah, A., Gahmberg, C.G., Ofek, I., Jacobi, U. & Sharon, N. Identification of the Leukocyte Adhesion Molecules CD11 and CD18 as Receptors for Type 1-Fimbriated (Mannose-Specific) Escherichia coli. *Infection and Immunity* **59**, 4524-4530 (1991).
260. Park, K.-H. et al. Effects of Mannosylated Glycopolymers on Specific Interaction to Bone Marrow Hematopoietic and Progenitor Cells Derived from Murine Species. *Journal of Biomedical Materials Research Part A* **82A**, 281-287 (2007).
261. Adachi, T. et al. CD22 serves as a receptor for soluble IgM. *European journal of immunology* **42**, 241-247 (2012).
262. O'Reilly, M.K. et al. Bifunctional CD22 ligands use multimeric immunoglobulins as protein scaffolds in assembly of immune complexes on B cells. *Journal of the American Chemical Society* **130**, 7736-7745 (2008).
263. Munn, E.A., Bachmann, L. & Feinstein, A. Structure of Hydrated Immunoglobulins and Antigen-Antibody Complexes. Electron Microscopy of Spray-freeze-etched Specimens. *Biochimica et Biophysica Acta* **625**, 1-9 (1980).
264. Voll, R.E. et al. Immunosuppressive Effects of Apoptotic Cells. *Nature* **390**, 350-351 (1997).
265. McColl, D.J. & Anders, R.F. Conservation of Structural Motifs and Antigenic Diversity in the Plasmodium falciparum Merozoite Surface Protein-3 (MSP-3). *Molecular and Biochemical Parasitology* **90**, 21-31 (1997).

266. McColl, D.J. et al. Molecular Variation in a Novel Polymorphic Antigen Associated with Plasmodium falciparum Merozoites. *Molecular and Biochemical Parasitology* **68**, 53-67 (1994).
267. Richards, J.S. & Beeson, J.G. The Future for Blood-stage Vaccines Against Malaria. *Immunology and cell biology* **87**, 377-390 (2009).
268. Escalante, A.A., Lal, A.A. & Ayala, F.J. Genetic Polymorphism and Natural Selection in the Malaria Parasite Plasmodium falciparum. *Genetics* **149**, 189-202 (1998).
269. Mills, K.E., Pearce, J.A., Crabb, B.S. & Cowman, A.F. Truncation of Merozoite Surface Protein 3 Disrupts its Trafficking and that of Acidic–Basic Repeat Protein to the Surface of Plasmodium falciparum Merozoites. *Molecular Microbiology* **43**, 1401-1411 (2002).
270. Demanga, C.G. et al. Toward the Rational Design of a Malaria Vaccine Construct Using the MSP3 Family as an Example: Contribution of Antigenicity Studies in Humans. *Infection and Immunity* **78**, 486-494 (2010).
271. Singh, S. et al. Identification of a Conserved Region of Plasmodium falciparum MSP3 Targeted by Biologically Active Antibodies to Improve Vaccine Design. *Journal of Infectious Diseases* **190**, 1010-1018 (2004).
272. Polley, S.D. et al. Plasmodium falciparum Merozoite Surface Protein 3 Is a Target of Allele-Specific Immunity and Alleles Are Maintained by Natural Selection. *Journal of Infectious Diseases* **195**, 279-287 (2007).
273. Soe, S., Theisen, M., Roussilhon, C., Aye, K.-S. & Druilhe, P. Association between Protection against Clinical Malaria and Antibodies to Merozoite Surface Antigens in an Area of Hyperendemicity in Myanmar: Complementarity between Responses to Merozoite Surface Protein 3 and the 220-Kilodalton Glutamate-Rich Protein. *Infection and Immunity* **72**, 247-252 (2004).
274. Roussilhon, C. et al. Long-Term Clinical Protection from Falciparum Malaria Is Strongly Associated with IgG3 Antibodies to Merozoite Surface Protein 3. *PLoS Med* **4**, e320 (2007).
275. Singh, S.K., Hora, R., Belrhali, H., Chitnis, C.E. & Sharma, A. Structural Basis for Duffy Recognition by the Malaria Parasite Duffy-Binding-Like Domain. *Nature* **439**, 741-744 (2006).
276. Burgess, B.R., Schuck, P. & Garboczi, D.N. Dissection of Merozoite Surface Protein 3, a Representative of a Family of Plasmodium falciparum Surface Proteins, Reveals an Oligomeric and Highly Elongated Molecule. *Journal of Biological Chemistry* **280**, 37236-37245 (2005).
277. Tolia, N.H., Enemark, E.J., Sim, B.K.L. & Joshua-Tor, L. Structural Basis for the EBA-175 Erythrocyte Invasion Pathway of the Malaria Parasite Plasmodium falciparum. *Cell* **122**, 183-193 (2005).
278. Kauth, C.W., Epp, C., Bujard, H. & Lutz, R. The Merozoite Surface Protein 1 Complex of Human Malaria Parasite Plasmodium falciparum: Interactions and Arrangements of Subunits. *Journal of Biological Chemistry* **278**, 22257-22264 (2003).
279. Silmon de Monerri, N.C. et al. Global Identification of Multiple Substrates for Plasmodium falciparum SUB1, an Essential Malarial Processing Protease. *Infection and Immunity* **79**, 1086-1097 (2011).
280. Ochola, L.I. et al. Allele Frequency–Based and Polymorphism-Versus-Divergence Indices of Balancing Selection in a New Filtered Set of Polymorphic Genes in Plasmodium falciparum. *Molecular Biology and Evolution* **27**, 2344-2351 (2010).
281. Sakamoto, H. et al. Antibodies Against a Plasmodium falciparum Antigen PfMSPDBL1 Inhibit Merozoite Invasion into Human Erythrocytes. *Vaccine* **30**, 1972-1980 (2012).
282. Wright, G.J. & Rayner, J.C. *Plasmodium falciparum* Erythrocyte Invasion: Combining Function with Immune Evasion. *PLoS Pathogens* **10**, e1003943 (2014).

283. Duraisingh, M.T., Maier, A.G., Triglia, T. & Cowman, A.F. Erythrocyte-binding Antigen 175 Mediates Invasion in Plasmodium falciparum Utilizing Sialic Acid-dependent and -independent Pathways. *Proceedings of the National Academy of Sciences* **100**, 4796-4801 (2003).
284. Barfod, L. et al. Evasion of Immunity to *Plasmodium falciparum* Malaria by IgM Masking of Protective IgG Epitopes in Infected Erythrocyte Surface-Exposed PfEMP1. *Proceedings of the National Academy of Sciences* **108**, 12485-12490 (2011).
285. von Itzstein, M., Plebanski, M., Cooke, B.M. & Coppel, R.L. Hot, Sweet and Sticky: The Glycobiology of Plasmodium falciparum. *Trends in Parasitology* **24**, 210-218 (2008).
286. Colucci, M. et al. Sialylation of N-Linked Glycans Influences the Immunomodulatory Effects of IgM on T Cells. *The Journal of Immunology* (2014).
287. Smilovich, D. et al. Differential Expression of Galα1,3Gal Epitope in Polymeric and Monomeric IgM Secreted by Mouse Myeloma Cells Deficient in α2,6-sialyltransferase. *Glycobiology* **8**, 841-848 (1998).
288. Kubagawa, H. et al. in Fc Receptors, Vol. 382. (eds. M. Daeron & F. Nimmerjahn) 3-28 (Springer International Publishing, 2014).
289. Illingworth, J. et al. Chronic exposure to Plasmodium falciparum is associated with phenotypic evidence of B and T cell exhaustion. *J Immunol* **190**, 1038-1047 (2013).
290. Torgbor, C. et al. A multifactorial role for P. falciparum malaria in endemic Burkitt's lymphoma pathogenesis. *PLoS pathogens* **10**, e1004170 (2014).
291. Pinzon-Charry, A. et al. Apoptosis and dysfunction of blood dendritic cells in patients with falciparum and vivax malaria. *The Journal of experimental medicine* **210**, 1635-1646 (2013).
292. Choi, S.-C. et al. Mouse IgM Fc Receptor, FCMR, Promotes B Cell Development and Modulates Antigen-Driven Immune Responses. *The Journal of Immunology* **190**, 987-996 (2013).
293. Perkins, S.J., Nealis, A.S., Sutton, B.J. & Feinstein, A. Solution Structure of Human and Mouse Immunoglobulin M by Synchrotron X-Ray Scattering and Molecular Graphics Modelling: A Possible Mechanism for Complement Activation. *Journal of Molecular Biology* **221**, 1345-1366 (1991).
294. Ranjan, R. et al. Proteome Analysis Reveals a Large Merozoite Surface Protein-1 Associated Complex on the Plasmodium falciparum Merozoite Surface. *Journal of Proteome Research* **10**, 680-691 (2010).
295. Higgins, M.K. The Structure of a Chondroitin Sulfate-binding Domain Important in Placental Malaria. *Journal of Biological Chemistry* **283**, 21842-21846 (2008).
296. Asito, A. et al. Alterations on Peripheral B Cell Subsets Following an Acute Uncomplicated Clinical Malaria Infection in Children. *Malaria Journal* **7**, 238 (2008).
297. Weiss, G.E. et al. Atypical Memory B Cells Are Greatly Expanded in Individuals Living in a Malaria-Endemic Area. *The Journal of Immunology* **183**, 2176-2182 (2009).
298. Seixas, E., Cross, C., Quin, S. & Langhorne, J. Direct Activation of Dendritic Cells by the Malaria Parasite, Plasmodium chabaudi chabaudi. *European Journal of Immunology* **31**, 2970 - 2978 (2001).
299. Patarroyo, M.E., Cifuentes, G., Bermúdez, A. & Patarroyo, M.A. Strategies for Developing Multi-epitope, Subunit-based, Chemically Synthesized Anti-malarial Vaccines. *Journal of Cellular and Molecular Medicine* **12**, 1915-1935 (2008).
300. Bryant, C.E., Spring, D.R., Gangloff, M. & Gay, N.J. The Molecular Basis of the Host Response to Lipopolysaccharide. *Nature Review Microbiology* **8**, 8-14 (2010).
301. Oeuvray, C. et al. Merozoite Surface Protein-3: A Malaria Protein Inducing Antibodies that Promote Plasmodium falciparum Killing by Cooperation with Blood Monocytes. *Blood* **84**, 1594-1602 (1994b).

302. Imam, M., Singh, S., Kaushik, N.K. & Chauhan, V.S. Plasmodium falciparum Merozoite Surface Protein 3: Oligomerization, Self-assembly and Heme Complex Formation. *Journal of Biological Chemistry* **289**, 3856-3868 (2014).
303. Czajkowsky, D.M., Hu, J., Shao, Z. & Pleass, R.J. Fc-fusion proteins: New Developments and Future Perspectives. *EMBO Molecular Medicine* **4**, 1015-1028 (2012).
304. Zhang, L., Leng, Q. & Mixson, A.J. Alteration in the IL-2 Signal Peptide Affects Secretion of Proteins In vitro and In vivo. *The Journal of Gene Medicine* **7**, 354-365 (2005).
305. Feilmeier, B.J., Iseminger, G., Schroeder, D., Webber, H. & Phillips, G.J. Green Fluorescent Protein Functions as a Reporter for Protein Localization in Escherichia coli. *Journal of Bacteriology* **182**, 4068-4076 (2000).
306. Kozak, M. Point Mutations Define a Sequence Flanking the AUG Initiator Codon that Modulates Translation by Eukaryotic Ribosomes. *Cell* **44**, 283-292 (1986).
307. Peroutka, R.J., Elshourbagy, N., Piech, T. & Butt, T.R. Enhanced Protein Expression in Mammalian Cells Using Engineered SUMO Fusions: Secreted Phospholipase A2. *Protein Science* **17**, 1586-1595 (2008).
308. Carter, J. et al. Fusion Partners Can Increase the Expression of Recombinant Interleukins Via Transient Transfection in 2936E Cells. *Protein Science* **19**, 357-362 (2010).
309. Kozak, M. At Least Six Nucleotides Preceding the AUG Initiator Codon Enhance Translation in Mammalian Cells. *Journal of Molecular Biology* **196**, 947-950 (1987).
310. Lo, K.M. et al. High Level Expression and Secretion of Fc-X Fusion Proteins in Mammalian Cells. *Protein Engineering* **11**, 495-500 (1998).
311. Durocher, Y., Perret, S. & Kamen, A. High-level and High-throughput Recombinant Protein Production by Transient Transfection of Suspension-growing Human 293-EBNA1 Cells. *Nucleic Acids Research* **30**, e9-e9 (2002).
312. Honjo, K., Kubagawa, Y. & Kubagawa, H. Is Toso an Antiapoptotic Protein or an Fc Receptor for IgM? *Blood* **119**, 1789-1790 (2012).
313. Li, F.J. et al. Enhanced Levels of Both Membrane-Bound and Soluble Forms of IgM Fc Receptor in Patients with Chronic Lymphocytic Leukemia. *Blood* (2011).
314. Hancer, V.S., Diz-Kucukkaya, R. & Aktan, M. Overexpression of Fc mu Receptor (FCMR, TOSO) Gene in Chronic Lymphocytic Leukemia Patients. *Medical oncology* **29**, 1068-1072 (2012).
315. Herishanu, Y. et al. The Lymph Node Microenvironment Promotes B-cell Receptor Signaling, NF-κB Activation, and Tumor Proliferation in Chronic Lymphocytic Leukemia, Vol. 117. (2011).
316. Hitoshi, Y. et al. Toso, a Cell Surface, Specific Regulator of Fas-Induced Apoptosis in T Cells. *Immunity* **8**, 461-471 (1998).
317. Ouchida, R., Mori, H., Ohno, H. & Wang, J.-Y. FcμR (Toso/Faim3) is Not an Inhibitor of Fas-mediated Cell Death in Mouse T and B Cells. *Blood* **121**, 2368-2370 (2013).
318. Baumgarth, N., Tung, J. & Herzenberg, L. Inherent Specificities in Natural Antibodies: A Key to Immune Defense Against Pathogen Invasion. *Springer Semin Immun* **26**, 347-362 (2005).
319. Yang, S., Liu, F., Wang, Q.J., Rosenberg, S.A. & Morgan, R.A. The Shedding of CD62L (L-Selectin) Regulates the Acquisition of Lytic Activity in Human Tumor Reactive T Lymphocytes. *PLoS ONE* **6**, e22560 (2011).
320. Hernández-Caselles, T. et al. A Study of CD33 (SIGLEC-3) Antigen Expression and Function on Activated Human T and NK Cells: Two Isoforms of CD33 are Generated by Alternative Splicing. *Journal of Leukocyte Biology* **79**, 46-58 (2006).
321. Vire, B. et al. Harnessing the Fcμ Receptor for Potent and Selective Cytotoxic Therapy of Chronic Lymphocytic Leukemia. *Cancer Research* **74**, 7510-7520 (2014).

322. Hon, H., Oran, A., Brocker, T. & Jacob, J. B Lymphocytes Participate in Cross-Presentation of Antigen following Gene Gun Vaccination. *The Journal of Immunology* **174**, 5233-5242 (2005).
323. Rabinovich, G.A. & Toscano, M.A. Turning 'Sweet' on Immunity: Galectin-glycan Interactions in Immune Tolerance and Inflammation. *Nature Review Immunology* **9**, 338-352 (2009).
324. Cederfur, C. et al. Different Affinity of Galectins for Human Serum Glycoproteins: Galectin-3 Binds Many Protease Inhibitors and Acute Phase Proteins. *Glycobiology* **18**, 384-394 (2008).
325. Clark, A.G., Weston, M.L. & Foster, M.H. Lack of Galectin-1 or Galectin-3 Alters B Cell Deletion and Anergy in an Autoantibody Transgene Model. *Glycobiology* **23**, 893-903 (2013).
326. Zuñiga, E., Rabinovich, G.A., Iglesias, M.M. & Gruppi, A. Regulated Expression of Galectin-1 During B-cell Activation and Implications for T-cell Apoptosis. *Journal of Leukocyte Biology* **70**, 73-79 (2001).
327. Herman, S.E.M. et al. Ibrutinib Inhibits BCR and NF-κB Signaling and Reduces Tumor Proliferation in Tissue-resident Cells of Patients with CLL, Vol. 123. (2014).
328. Monti, P., Heninger, A.-K. & Bonifacio, E. Differentiation, Expansion, and Homeostasis of Autoreactive T Cells in Type 1 Diabetes Mellitus. *Curr Diab Rep* **9**, 113-118 (2009).
329. Arif, S. et al. Autoreactive T Cell Responses Show Proinflammatory Polarization in Diabetes but a Regulatory Phenotype in Health. *Journal of Clinical Investigation* **113**, 451-463 (2004).
330. Spencer, A.J. et al. Fusion of the *Mycobacterium tuberculosis* Antigen 85A to an Oligomerization Domain Enhances Its Immunogenicity in Both Mice and Non-Human Primates. *PLoS ONE* **7**, e33555 (2012).
331. Weldon, W.C. et al. Enhanced Immunogenicity of Stabilized Trimeric Soluble Influenza Hemagglutinin. *PLoS ONE* **5**, e12466 (2010).
332. Schwab, I. & Nimmerjahn, F. Intravenous Immunoglobulin Therapy: How Does IgG Modulate the Immune System? *Nature Review Immunology* **13**, 176-189 (2013).
333. von Gunten, S. et al. IVIG Pluripotency and the Concept of Fc-sialylation: Challenges to the Scientist. *Nature Review Immunology* **14**, 349-349 (2014).
334. Costantino, C., Baecher-Allan, C. & Hafler, D. Multiple Sclerosis and Regulatory T Cells. *J Clin Immunol* **28**, 697-706 (2008).
335. Olsson, T. et al. Autoreactive T Lymphocytes in Multiple Sclerosis Determined by Antigen-induced Secretion of Interferon-gamma. *Journal of Clinical Investigation* **86**, 981-985 (1990).

Appendix I

DBLMSP and DBLMSP2 sequences (Dr Cecile Crosnier, Welcome Trust Sanger Institute)

P. falciparum 3D7 DBLMSP amino acid sequence

Red=DBL domain Green= SPAM domain

MKKIYSIFFSLFILNLHIYIKNIKCNDLINYNDSNLRNGLLNNSLDLTNGLNNKDNSFIDSKIEEHEN
KSYQNKDNNISIVGQDVPITSVYSSKIINANDLEGNSIDDTKGLSVTNSGFDDGSAFGGGLPFSGYSP
LQGNHNKCPDENFCKGIKNVLSCPPKNSTGRNGDWISVAVKESSTTNKGVLVPPRRTKLCLRNINKVW
HRIKDEKNFKEEFVKVALGESNALMKHYKEKNLNALTAIKYGFSDMGDIIKGTDLIDYQITKNINRAL
DKILRNETSNDKIKKRVDWWEANKSAFWDAFMCGYKVHIGNKPCPEHDNMDRIPQYLRWFREWGTYVC
SEYKNKFEDVIKLCNIQQFTNQDDSQLLEISKKDKCKEALKHYEEWVNRRRPEWKGQCDKFEKEKSKY
EDTKSITAEKYLKEICSECDCKYKDLDNTFKEFKDNVTLLKAVIDNKKNQDSLTTTSLSTSINSVRDS
SNLDQRGNITTSQGNSHRATVVQQVDQTNRLDNVNSVTQRGNNNYNNNLERGLGSGALPGTNIITEEK
YSLELIKLTSKDEEDIIKHNEDVREEIEEQQEDIEEDEEELENEGEETKEEDDEEKNETNDTEDTDDT
EDTEDIEEENKEKELSNQQQSEKKSISKVDEDSYRILSVSYKDNNEVKNVAESIVKKLFSLFNDNNNL
ETIFKGLTEDMTDLFQK

P. falciparum 3D7 DBLMSP2 amino acid sequence

Red=DBL domain Green= SPAM domain

MIYILSIVFYIFFLHIDIYVNIYSTCFVVNEGNPNLRNNIINDDELKGKAYNNTIDANNQNIEYNKNL
KHNVNSSHISKFSDIMDQEDKGDNENSHDIKFEEKKNINKSLDAESNYGINEISITGNDSNSDNSNQN
IFPDGSELAGGIPRSIYTINLGFNKCPTEEICKDFSNLPQCRKNVHERNNWLGSSVKNFSSDNKGVLV
PPRRQSLCLRITLQDFRTKKKKEGDFEKFIYSYASSEARKLRTIHNNNLEKAHQAIRYSFADIGNIIR
GDDMMDTPTSKETITYLEKVLKIYNENNDKPKDAKKWWTENRHHVWEAMMCGYQSAQKDNQCTGYGNI
DDIPQFLRWFREWGTYVCEESEKNMNTLKAVCFPKQPRTEANPALTVHENEMCSSTLKKYEEWYNKRK
TEWTEQSIKYNNDKINYTDIKTLSPSEYLIEKCPECKCTKKNLQDVFELTFDGKALLEKLKKEESPVS
NSVNALPEPGQITLPDPSLKQTTQQENQPVVETPVTTAVINEHQGQTEPNKGDNNNERENHESNVGSI
QEVNQGSVSEESHSKTIDPSKIDDRLELSSGSSSLEQHSKEDVKKGCALELVPLSLSDIEQIANESED
VLEEIEEEINTDGEIEYITEEEIKEDIEEETEEDIEEETEEETEEETEEETEEADEETVKEIEDKPEQEIK
NKSLEEKQIDKNTDTSEKKGFNNSEKDEKARNLISKNYKNYNELDKNVHTLVNSIISLLEEGNGSDST
LNSLSKDITNLFKN

Appendix II

Vector maps and sequences

Creation of pcDNA 3.1(+) vector containing DBLMSP and DBLMSP2

Full-length DBLMSP and DBLMSP2 (FL), and DBLMSP and DBLMSP lacking DBL domains (C), were synthesised and cloned into pcDNA 3.1(+) vector with flanking BamHI and XhoI cloning sites (LifeTechnologies).

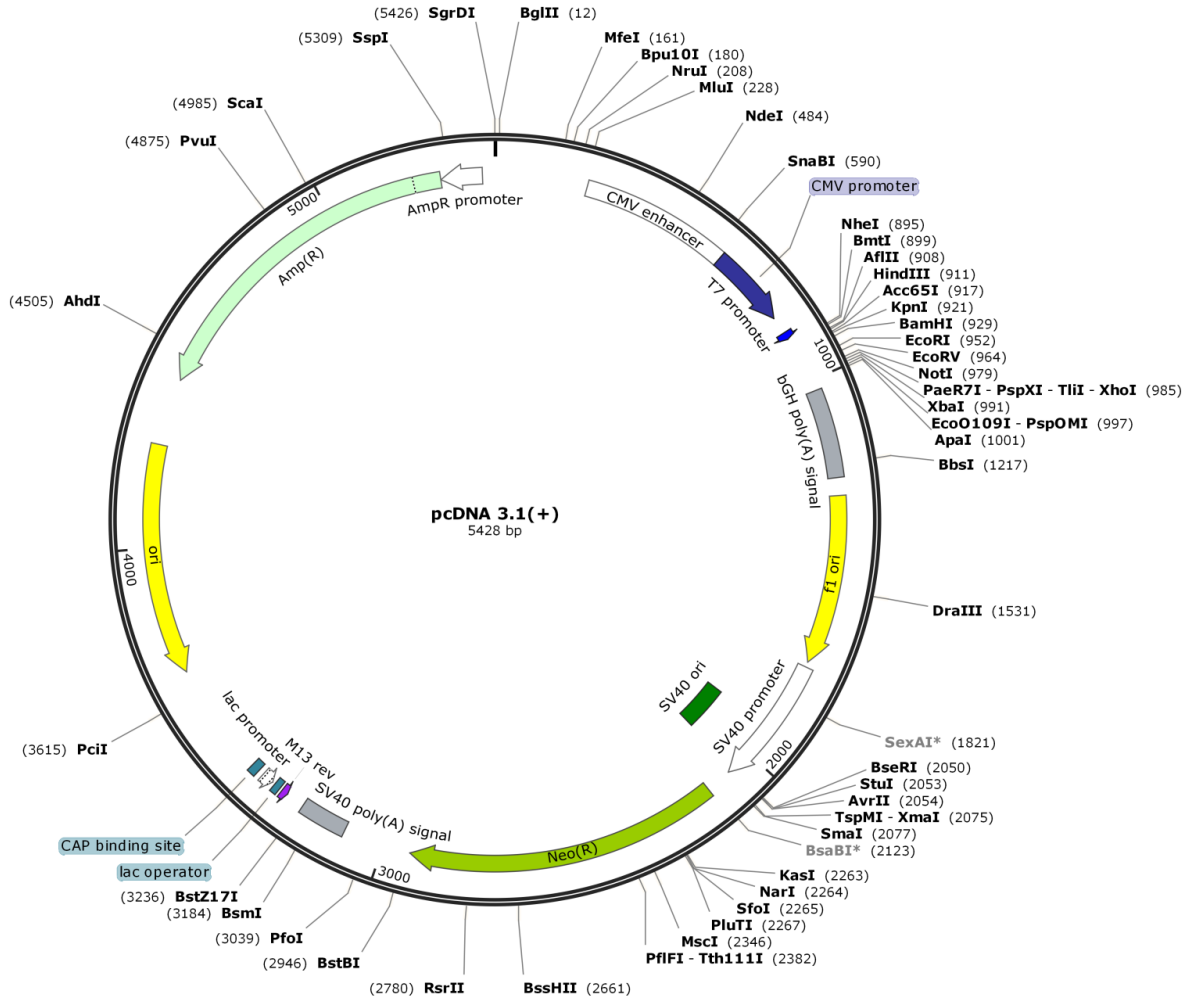

pcDNA 3.1(+)-DBLMSP-FL

BamHI Insert DBL SPAM 2x c-myc 6x His XhoI

GGATCCGCCACCATGAAGAAGATCTACTCCATCTTCTTCTCCCTGTTCATCCTGAACCTGCACATCTACATCAAGA
ACATCAAGTGCAACGACCTGATCAACTACAACGACAGCAACCTGAGAAACGGCCTGCTGAACAACAGCCTGGACCT
GACCAACGGCCTGAACAACAAGGACAACAGCTTCATCGACAGCAAGATCGAGGAACACGAGAACAAGAGCTACCAG
AACAAGGATAACAACATCAGCATCGTGGGCCAGGACGTGCCCATCACCAGCGTGTACAGCTCCAAGATCATCAACG
CCAACGATCTGGAAGGCAACAGCATCGACGACACCAAGGGCCTGAGCGTGACCAACAGCGGCTTCGACGATGGCTC
TGCTTTCGGCGGAGGCCTGCCTTTCAGCGGCTACAGTCCTCTGCAGGGCAACCACAACAAGTGCCCCGACGAGAAC
TTCTGCAAGGGAATCAAGAACGTGCTGAGCTGCCCCCCCAAGAACAGCACCGGCAGAAACGGCGACTGGATCAGCG
TGGCCGTGAAAGAGAGCAGCACCACCAACAAGGGCGTGCTGGTGCCCCCTAGAAGGACCAAGCTGTGCCTGAGGAA
CATCAACAAAGTGTGGCACAGGATCAAGGACGAGAAGAACTTCAAAGAGGAATTCGTGAAGGTGGCCCTGGGCGAG
AGCAACGCCCTGATGAAGCACTACAAAGAGAAGAACCTGAACGCTCTGACCGCCATTAAGTACGGCTTCAGCGACA
TGGGCGACATCATCAAGGGCACAGATCTGATCGACTACCAGATCACCAAGAATATCAACCGGGCCCTGGACAAGAT
CCTGCGGAACGAGACAAGCAACGACAAGATCAAGAAACGAGTGGATTGGTGGGAGGCCAACAAGAGCGCCTTCTGG
GACGCCTTCATGTGCGGCTACAAGGTGCACATCGGCAACAAGCCCTGCCCCGAGCACGACAACATGGACAGAATCC
CCCAGTACCTGAGATGGTTCCGCGAGTGGGGCACCTACGTGTGCAGCGAGTACAAGAACAAGTTCGAGGACGTGAT
CAAGCTGTGTAACATCCAGCAGTTCACCAACCAGGACGACAGCCAGCTGCTGGAAATCAGCAAGAAAGACAAGTGC
AAAGAGGCCCTGAAACACTACGAGGAATGGGTCAACAGACGCAGACCCGAGTGGAAGGGCCAGTGCGATAAGTTCG
AGAAAGAGAAGTCTAAGTACGAGGACACCAAGAGCATCACCGCCGAGAAGTATCTGAAAGAAATCTGCTCCGAGTG
CGACTGCAAGTACAAGGACCTGGACAACACATTCAAAGAATTCAAGGACAATGTGACCCTGCTGAAGGCCGTGATC
GACAACAAGAAGAACCAGGACAGCCTGACCACCACCAGCCTGAGCACCTCCATCAACTCCGTGCGGGACTCCTCCA
ACCTGGACCAGAGAGGCAACATCACCACCTCCCAGGGCAACAGCCACAGAGCCACAGTGGTGCAGCAGGTGGACCA
GACAAACAGACTGGACAACGTGAACAGCGTGACCCAGCGGGGCAACAACAATTACAACAACAACCTGGAAAGGGGC
CTGGGCTCTGGCGCTCTGCCTGGCACCAACATCATCACCGAGGAAAAGTACTCCCTGGAACTGATTAAGCTGACCA
GCAAGGACGAAGAGGATATCATCAAGCACAATGAGGACGTGCGGGAAGAGATTGAGGAACAGCAGGAAGATATTGA
AGAGGACGAGGAAGAACTGGAAAACGAGGGCGAGGAAACAAAAGAAGAGGACGACGAGGAAAAGAACGAGACAAAC
GACACCGAGGACACCGACGATACAGAGGATACCGAAGATATCGAGGAAGAGAACAAAGAAAAAGAGCTGAGCAACC
AGCAGCAGAGCGAGAAGAAATCCATCAGCAAGGTGGACGAGGACAGCTACAGAATCCTGTCCGTGTCCTACAAAGA
CAACAACGAAGTGAAGAACGTGGCCGAGAGCATCGTGAAGAAGCTGTTCAGCCTGTTCAACGACAACAACAATCTG
GAAACCATCTTCAAGGGCCTGACCGAGGACATGACCGACCTGTTCCAGAAGGCCGAGCAGAAGCTGATCTCCGAAG
AGGACCTGGCTGAACAGAAACTGATCAGCGAGGAAGATCTGGCC**CACCACCACCATCACCAC**TGA**CTCGAG**

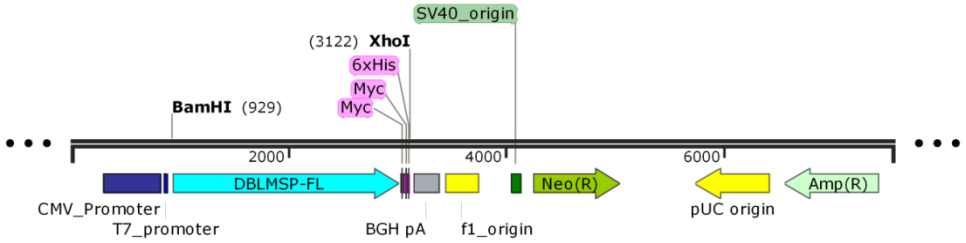

pcDNA 3.1(+)-DBLMSP-C

GGATCCGCCACCATGAAGAAGATCTACTCCATCTTCTTCTCCCTGTTCATCCTGAACCTGCACATCTACATCAAGA
ACATCAAGTGCAACGACCTGATCAACTACAACGACAGCAACCTGAGAAACGGCCTGCTGAACAACAGCCTGGACCT
GACCAACGGCCTGAACAACAAGGACAACAGCTTCATCGACAGCAAGATCGAGGAACACGAGAACAAGAGCTACCAG
AACAAGGATAACAACATCAGCATCGTGGGCCAGGACGTGCCCATCACCAGCGTGTACAGCTCCAAGATCATCAACG
CCAACGATCTGGAAGGCAACAGCATCGACGACACCAAGGGCCTGAGCGTGACCAACAGCGGCTTCGACGATGGCTC
TGCTTTCGGCGGAGGCCTGCCTTTCAGCGGCTACAGTCCTCTGCAGGGCAACCACAACAAGTGCCCCGACGAGAAC
TTCTGCAAGGGAATCAAGAACGTGCTGAGCTGCGACTGCAAGTACAAGGACCTGGACAACACATTCAAAGAATTCA
AGGACAATGTGACCCTGCTGAAGGCCGTGATCGACAACAAGAAGAACCAGGACAGCCTGACCACCACCAGCCTGAG
CACCTCCATCAACTCCGTGCGGGACTCCTCCAACCTGGACCAGAGAGGCAACATCACCACCTCCCAGGGCAACAGC
CACAGAGCCACAGTGGTGCAGCAGGTGGACCAGACAAACAGACTGGACAACGTGAACAGCGTGACCCAGCGGGGCA
ACAACAATTACAACAACAACCTGGAAAGGGGCCTGGGCTCTGGCGCTCTGCCTGGCACCAACATCATCACCGAGGA
AAAGTACTCCCTGGAACTGATCAAGCTGACCAGCAAGGACGAAGAGGACATCATCAAGCACAATGAGGACGTGCGG
GAAGAGATCGAAGAACAGCAGGAAGATATTGAAGAGGACGAGGAAGAACTGGAAAACGAGGGCGAGGAAACAAAAG
AAGAGGACGACGAGGAAAAGAACGAGACAAACGACACCGAGGACACAGACGATACAGAGGACACTGAGGACATCGA
AGAGGAAAACAAAGAGAAAGAGCTGAGCAACCAGCAGCAGAGCGAGAAGAAATCCATCAGCAAGGTGGACGAGGAC
AGCTACAGAATCCTGTCCGTGTCCTACAAAGACAACAACGAAGTGAAGAACGTGGCCGAGAGCATCGTGAAGAAGC
TGTTCAGCCTGTTCAACGACAACAACAATCTGGAAACCATCTTCAAGGGCCTGACCGAGGACATGACCGACCTGTT
CCAGAAAGAGCAGAAGCTGATCTCCGAAGAGGACCTGGAACAGAAACTGATCAGCGAGGAAGATCTGCACCACCAT
CACCATCACTGACTCGAG

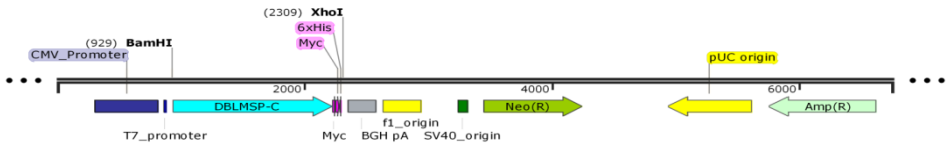

pcDNA 3.1(+)-DBLMSP2-C

GGATCCGCCACCATGATCTACATCCTGTCTATCGTGTTCTACATCTTCTTTCTGCACATCGACATCTACGTGAACA
TCTACAGCACCTGTTTCGTCGTGAACGAGGGCAACCCCAACCTGAGAAACAACATCATCAACGACGACGAGCTGAA
GGGCAAGGCCTACAACAACACCATCGACGCCAACAACCAGAACATCGAGTACAACAAGAACCTGAAGCACAACGTG
AACAGCAGCCACATCAGCAAGTTCAGCGACATCATGGACCAGGAAGATAAGGGCGACAACGAGAACTCCCACGACA
TCAAGTTCGAGGAAAAGAAGAACATCAACAAGAGCCTGGACGCCGAGAGCAACTACGGCATCAACGAGATCAGCAT
CACCGGCAACGACAGCAACAGCGACAACAGCAACCAGAATATCTTCCCCGACGGCAGCGAGCTGGCTGGCGGCATC
CCTAGATCCATCTACACCATCAACCTGGGCTTCAACAAGTGCCCCACCGAGGAAATCTGCAAGGACTTCAGCAACC
TGCCCCAGGTGTTCGAGCTGACCTTCGACGGCAAGGCCCTGCTGGAAAAGCTGAAGAAAGAGGAATCCCCCGTGTC
CAACAGCGTGAACGCCCTGCCTGAGCCTGGCCAGATCACACTGCCTGACCCCAGCCTGAAGCAGACCACCCAGCAG
GAAAACCAGCCCGTGGTGGAAACCCCTGTGACCACCGCCGTGATCAACGAGCACCAGGGCCAGACCGAGCCCAACA
AGGGCGATAACAACAACGAGAGAGAGAACCACGAGTCCAACGTGGGCAGCATCCAGGAAGTGAACCAGGGCAGCGT
GTCCGAGGAAAGCCACAGCAAGACCATCGACCCCAGCAAGATCGACGACAGACTGGAACTGAGCAGCGGCAGCAGC
AGCCTGGAACAGCACAGCAAAGAAGATGTGAAGAAGGGCTGCGCCCTGGAACTGGTGCCTCTGAGCCTGAGCGACA
TCGAGCAGATCGCCAACGAGAGCGAGGACGTGCTGGAAGAGATCGAGGAAGAGATTAACACCGACGGCGAGATCGA
GTATATCACCGAAGAGGAAATCAAAGAGGACATCGAAGAAGAGACAGAAGAGGATATTGAGGAAGAAACCGAAGAA
GAAACTGAGGAAGAGACAGAGGAAGAGGCCGACGAGGAAACCGTGAAAGAAATCGAGGACAAGCCCGAGCAGGAAA
TCAAGAACAAGTCCCTGGAAGAGAAGCAGATCGACAAGAACACCGACACCAGCGAGAAGAAGGGATTCAACAACTC
CGAGAAGGACGAGAAGGCCAGAAACCTGATCAGCAAGAACTACAAGAATTACAACGAGCTGGACAAGAACGTGCAC
ACCCTCGTGAACTCCATCATTAGCCTGCTGGAAGAAGGCAACGGCAGCGACAGCACCCTGAACAGCCTGAGCAAGG
ACATCACAAACCTGTTCAAGAACGAGCAGAAGCTGATCTCTGAAGAGGATCTGGAACAGAAACTGATTAGCGAAGA
GGACCTGCACCACCACCATCACCACTGACTCGAG

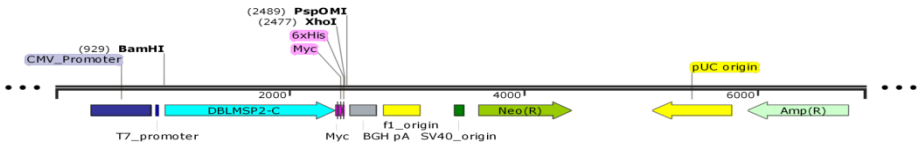

pcDNA 3.1(+)-DBLMSP2-FL

GGATCCGCCACCATGATCTACATCCTGTCTATCGTGTTCTACATCTTCTTTCTGCACATCGACATCTACGTGAACA
TCTACAGCACCTGTTTCGTCGTGAACGAGGGCAACCCCAACCTGAGAAACAACATCATCAACGACGACGAGCTGAA
GGGCAAGGCCTACAACAACACCATCGACGCCAACAACCAGAACATCGAGTACAACAAGAACCTGAAGCACAACGTG
AACAGCAGCCACATCAGCAAGTTCAGCGACATCATGGACCAGGAAGATAAGGGCGACAACGAGAACTCCCACGACA
TCAAGTTCGAGGAAAAGAAGAACATCAACAAGAGCCTGGACGCCGAGAGCAACTACGGCATCAACGAGATCAGCAT
CACCGGCAACGACAGCAACAGCGACAACAGCAACCAGAATATCTTCCCCGACGGCAGCGAGCTGGCTGGCGGCATC
CCTAGATCCATCTACACCATCAACCTGGGCTTCAACAAGTGCCCCACCGAGGAAATCTGCAAGGACTTCAGCAACC
TGCCCCAGTGCCGGAAGAACGTGCACGAGAGGAACAACTGGCTGGGCAGCAGCGTGAAGAACTTCAGCTCCGACAA
CAAGGGCGTGCTGGTGCCCCCTAGAAGGCAGAGCCTGTGCCTGAGAATCACCCTGCAGGACTTCCGCACCAAGAAG
AAGAAAGAGGGCGACTTCGAGAAGTTCATCTACTCCTACGCCAGCAGCGAGGCCAGAAAGCTGAGAACCATCCACA
ACAACAATCTGGAAAAGGCCCACCAGGCCATCAGATACAGCTTCGCCGACATCGGCAATATCATCAGAGGCGACGA
CATGATGGACACCCCCACCAGCAAAGAGACAATCACCTACCTGGAAAAAGTGCTGAAGATCTACAATGAGAACAAC
GACAAGCCCAAGGACGCCAAGAAGTGGTGGACCGAGAACAGACACCACGTGTGGGAGGCCATGATGTGCGGCTACC
AGAGCGCCCAGAAAGACAACCAGTGCACCGGCTACGGCAACATCGACGATATCCCCCAGTTCCTGAGATGGTTCCG
CGAGTGGGGCACCTACGTGTGCGAGGAATCCGAGAAGAATATGAACACCCTGAAGGCCGTGTGCTTCCCCAAGCAG
CCTAGAACCGAGGCCAACCCTGCCCTGACCGTGCACGAAAACGAGATGTGCAGCAGCACACTGAAGAAATACGAGG
AATGGTATAACAAGCGCAAGACCGAGTGGACAGAGCAGTCCATCAAGTATAACAACGATAAGATCAACTACACAGA
CATCAAGACCCTGAGCCCCAGCGAGTACCTGATCGAGAAGTGCCCCGAGTGCAAGTGCACCAAAAAGAACCTGCAG
GATGTGTTCGAGCTGACCTTCGACGGCAAGGCCCTGCTGGAAAAGCTGAAAAAAGAGGAATCCCCCGTGTCCAACA
GCGTGAACGCCCTGCCTGAGCCTGGCCAGATCACACTGCCTGACCCCAGCCTGAAGCAGACCACCCAGCAGGAAAA
CCAGCCCGTGGTGGAAACCCCTGTGACCACCGCCGTGATCAACGAGCACCAGGGCCAGACCGAGCCCAACAAGGGG
GATAACAACAACGAGAGAGAGAACCACGAGTCCAACGTGGGCAGCATCCAGGAAGTGAACCAGGGCAGCGTGTCCG
AGGAAAGCCACAGCAAGACCATCGACCCCAGCAAGATCGACGACAGACTGGAACTGAGCAGCGGCAGCAGCAGCCT
GGAACAGCACAGCAAAGAAGATGTGAAGAAGGGCTGCGCCCTGGAACTGGTGCCTCTGAGCCTGAGCGACATCGAG
CAGATCGCCAACGAGAGCGAGGACGTGCTGGAAGAGATCGAGGAAGAGATTAACACCGACGGCGAGATCGAGTATA
TCACCGAAGAGGAAATCAAAGAGGACATCGAAGAAGAGACAGAAGAGGATATTGAGGAAGAAACTGAAGAAGAAAC
AGAGGAAGAGACTGAGGAAGAGGCCGACGAGGAAACCGTGAAAGAGATTGAGGACAAGCCCGAGCAGGAAATCAAG
AACAAGTCCCTGGAAGAGAAGCAGATCGACAAGAACACCGACACCAGCGAGAAGAAGGGATTCAACAACTCCGAGA
AGGACGAGAAGGCCCGGAACCTGATCAGCAAGAACTACAAGAATTACAACGAGCTGGACAAGAATGTGCACACACT
CGTGAACTCCATCATTAGCCTGCTGGAAGAAGGCAACGGCAGCGACAGCACCCTGAACAGCCTGAGCAAGGACATC
ACAAACCTGTTCAAGAACGAGCAGAAGCTGATCTCTGAAGAGGATCTGGAACAGAAACTGATCAGCGAAGAGGACC
TGCACCACCACCATCACCACTGACTCGAG

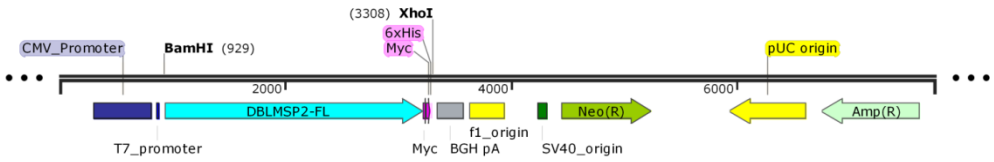

Creation of pFUSE-MCS vector containing DBLMSP and DBLMSP2

The sequences encoding full-length DBLMSP and DBLMSP2 (FL), and DBLMSP and DBLMSP lacking DBL domains (C), were subcloned into the pFUSE-MCS vector (Invivogen) to create the pFUSE-DBLMSP-FL, pFUSE-DBLMSP-C, pFUSE-DBLMSP2-FL, pFUSE-DBLMSP2-C expression vectors.

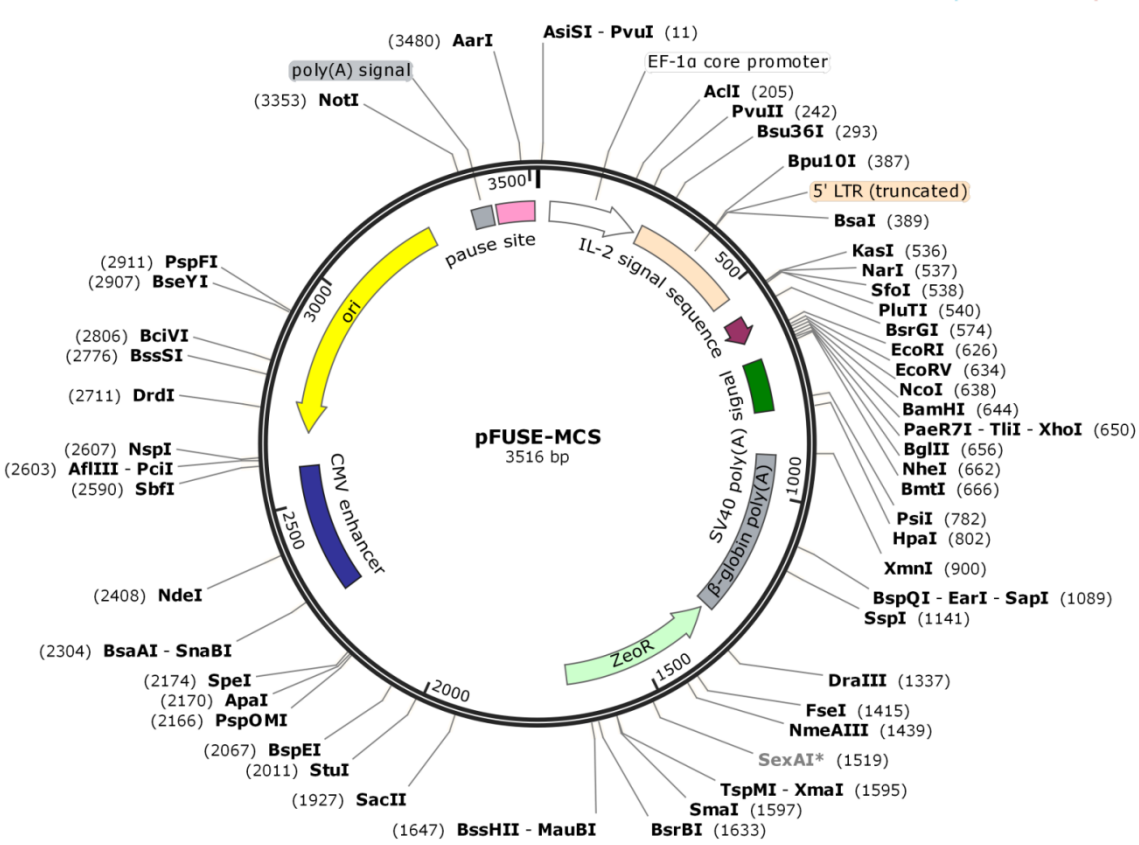

pFUSE-MCS-DBLMSP-FL

GGATCCCGCCACCATGAAGAAGATCTACTCCATCTTCTTCTCCCTGTTCATCCTGAACCTGCACATCTACATCAAGA
ACATCAAGTGCAACGACCTGATCAACTACAACGACAGCAACCTGAGAAACGGCCTGCTGAACAACAGCCTGGACCTG
ACCAACGGCCTGAACAACAAGGACAACAGCTTCATCGACAGCAAGATCGAGGAACACGAGAACAAGAGCTACCAGAA
CAAGGATAACAACATCAGCATCGTGGGCCAGGACGTGCCCATCACCAGCGTGTACAGCTCCAAGATCATCAACGCCA
ACGATCTGGAAGGCAACAGCATCGACGACACCAAGGGCCTGAGCGTGACCAACAGCGGCTTCGACGATGGCTCTGCT
TTCGGCGGAGGCCTGCCTTTCAGCGGCTACAGTCCTCTGCAGGGCAACCACAACAAGTGCCCCGACGAGAACTTCTG
CAAGGGAATCAAGAACGTGCTGAGCTGCCCCCCCAAGAACAGCACCGGCAGAAACGGCGACTGGATCAGCGTGGCCG
TGAAAGAGAGCAGCACCACCAACAAGGGCGTGCTGGTGCCCCCTAGAAGGACCAAGCTGTGCCTGAGGAACATCAAC
AAAGTGTGGCACAGGATCAAGGACGAGAAGAACTTCAAAGAGGAATTCGTGAAGGTGGCCCTGGGCGAGAGCAACGC
CCTGATGAAGCACTACAAAGAGAAGAACCTGAACGCTCTGACCGCCATTAAGTACGGCTTCAGCGACATGGGCGACA
TCATCAAGGGCACAGATCTGATCGACTACCAGATCACCAAGAATATCAACCGGGCCCTGGACAAGATCCTGCGGAAC
GAGACAAGCAACGACAAGATCAAGAAACGAGTGGATTGGTGGGAGGCCAACAAGAGCGCCTTCTGGGACGCCTTCAT
GTGCGGCTACAAGGTGCACATCGGCAACAAGCCCTGCCCCGAGCACGACAACATGGACAGAATCCCCCAGTACCTGA
GATGGTTCCGCGAGTGGGGCACCTACGTGTGCAGCGAGTACAAGAACAAGTTCGAGGACGTGATCAAGCTGTGTAAC
ATCCAGCAGTTCACCAACCAGGACGACAGCCAGCTGCTGGAAATCAGCAAGAAAGACAAGTGCAAAGAGGCCCTGAA
ACACTACGAGGAATGGGTCAACAGACGCAGACCCGAGTGGAAGGGCCAGTGCGATAAGTTCGAGAAAGAGAAGTCTA
AGTACGAGGACACCAAGAGCATCACCGCCGAGAAGTATCTGAAAGAAATCTGCTCCGAGTGCGACTGCAAGTACAAG
GACCTGGACAACACATTCAAAGAATTCAAGGACAATGTGACCCTGCTGAAGGCCGTGATCGACAACAAGAAGAACCA
GGACAGCCTGACCACCACCAGCCTGAGCACCTCCATCAACTCCGTGCGGGACTCCTCCAACCTGGACCAGAGAGGCA
ACATCACCACCTCCCAGGGCAACAGCCACAGAGCCACAGTGGTGCAGCAGGTGGACCAGACAAACAGACTGGACAAC
GTGAACAGCGTGACCCAGCGGGGCAACAACAATTACAACAACAACCTGGAAAGGGGCCTGGGCTCTGGCGCTCTGCC
TGGCACCAACATCATCACCGAGGAAAAGTACTCCCTGGAACTGATTAAGCTGACCAGCAAGGACGAAGAGGATATCA
TCAAGCACAATGAGGACGTGCGGGAAGAGATTGAGGAACAGCAGGAAGATATTGAAGAGGACGAGGAAGAACTGGAA
AACGAGGGCGAGGAAACAAAAGAAGAGGACGACGAGGAAAAGAACGAGACAAACGACACCGAGGACACCGACGATAC
AGAGGATACCGAAGATATCGAGGAAGAGAACAAAGAAAAAGAGCTGAGCAACCAGCAGCAGAGCGAGAAGAAATCCA
TCAGCAAGGTGGACGAGGACAGCTACAGAATCCTGTCCGTGTCCTACAAAGACAACAACGAAGTGAAGAACGTGGCC
GAGAGCATCGTGAAGAAGCTGTTCAGCCTGTTCAACGACAACAACAATCTGGAAACCATCTTCAAGGGCCTGACCGA
GGACATGACCGACCTGTTCCAGAAGGCCGAGCAGAAGCTGATCTCCGAAGAGGACCTGGCTGAACAGAAACTGATCA
GCGAGGAAGATCTGGCCCACCACCACCATCACCACTGACTCGAG

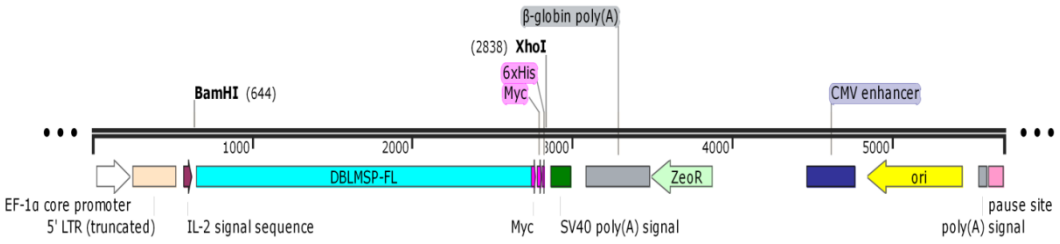

pFUSE-MCS-DBLMSP2-FL

GGATCCGCCACCATGATCTACATCCTGTCTATCGTGTTCTACATCTTCTTTCTGCACATCGACATCTACGTGAACAT
CTACAGCACCTGTTTCGTCGTGAACGAGGGCAACCCCAACCTGAGAAACAACATCATCAACGACGACGAGCTGAAGG
GCAAGGCCTACAACAACACCATCGACGCCAACAACCAGAACATCGAGTACAACAAGAACCTGAAGCACAACGTGAAC
AGCAGCCACATCAGCAAGTTCAGCGACATCATGGACCAGGAAGATAAGGGCGACAACGAGAACTCCCACGACATCAA
GTTCGAGGAAAAGAAGAACATCAACAAGAGCCTGGACGCCGAGAGCAACTACGGCATCAACGAGATCAGCATCACCG
GCAACGACAGCAACAGCGACAACAGCAACCAGAATATCTTCCCCGACGGCAGCGAGCTGGCTGGCGGCATCCCTAGA
TCCATCTACACCATCAACCTGGGCTTCAACAAGTGCCCCACCGAGGAAATCTGCAAGGACTTCAGCAACCTGCCCCA
GTGCCGGAAGAACGTGCACGAGAGGAACAACTGGCTGGGCAGCAGCGTGAAGAACTTCAGCTCCGACAACAAGGGCG
TGCTGGTGCCCCCTAGAAGGCAGAGCCTGTGCCTGAGAATCACCCTGCAGGACTTCCGCACCAAGAAGAAGAAAGAG
GGCGACTTCGAGAAGTTCATCTACTCCTACGCCAGCAGCGAGGCCAGAAAGCTGAGAACCATCCACAACAACAATCT
GGAAAAGGCCCACCAGGCCATCAGATACAGCTTCGCCGACATCGGCAATATCATCAGAGGCGACGACATGATGGACA
CCCCCACCAGCAAAGAGACAATCACCTACCTGGAAAAAGTGCTGAAGATCTACAATGAGAACAACGACAAGCCCAAG
GACGCCAAGAAGTGGTGGACCGAGAACAGACACCACGTGTGGGAGGCCATGATGTGCGGCTACCAGAGCGCCCAGAA
AGACAACCAGTGCACCGGCTACGGCAACATCGACGATATCCCCCAGTTCCTGAGATGGTTCCGCGAGTGGGGCACCT
ACGTGTGCGAGGAATCCGAGAAGAATATGAACACCCTGAAGGCCGTGTGCTTCCCCAAGCAGCCTAGAACCGAGGCC
AACCCTGCCCTGACCGTGCACGAAAACGAGATGTGCAGCAGCACACTGAAGAAATACGAGGAATGGTATAACAAGCG
CAAGACCGAGTGGACAGAGCAGTCCATCAAGTATAACAACGATAAGATCAACTACACAGACATCAAGACCCTGAGCC
CCAGCGAGTACCTGATCGAGAAGTGCCCCGAGTGCAAGTGCACCAAAAAGAACCTGCAGGATGTGTTCGAGCTGACC
TTCGACGGCAAGGCCCTGCTGGAAAAGCTGAAAAAAGAGGAATCCCCCGTGTCCAACAGCGTGAACGCCCTGCCTGA
GCCTGGCCAGATCACACTGCCTGACCCCAGCCTGAAGCAGACCACCCAGCAGGAAAACCAGCCCGTGGTGGAAACCC
CTGTGACCACCGCCGTGATCAACGAGCACCAGGGCCAGACCGAGCCCAACAAGGGGGATAACAACAACGAGAGAGAG
AACCACGAGTCCAACGTGGGCAGCATCCAGGAAGTGAACCAGGGCAGCGTGTCCGAGGAAAGCCACAGCAAGACCAT
CGACCCCAGCAAGATCGACGACAGACTGGAACTGAGCAGCGGCAGCAGCAGCCTGGAACAGCACAGCAAAGAAGATG
TGAAGAAGGGCTGCGCCCTGGAACTGGTGCCTCTGAGCCTGAGCGACATCGAGCAGATCGCCAACGAGAGCGAGGAC
GTGCTGGAAGAGATCGAGGAAGAGATTAACACCGACGGCGAGATCGAGTATATCACCGAAGAGGAAATCAAAGAGGA
CATCGAAGAAGAGACAGAAGAGGATATTGAGGAAGAAACTGAAGAAGAAACAGAGGAAGAGACTGAGGAAGAGGCCG
ACGAGGAAACCGTGAAAGAGATTGAGGACAAGCCCGAGCAGGAAATCAAGAACAAGTCCCTGGAAGAGAAGCAGATC
GACAAGAACACCGACACCAGCGAGAAGAAGGGATTCAACAACTCCGAGAAGGACGAGAAGGCCCGGAACCTGATCAG
CAAGAACTACAAGAATTACAACGAGCTGGACAAGAATGTGCACACACTCGTGAACTCCATCATTAGCCTGCTGGAAG
AAGGCAACGGCAGCGACAGCACCCTGAACAGCCTGAGCAAGGACATCACAAACCTGTTCAAGAACGAGCAGAAGCTG
ATCTCTGAAGAGGATCTGGAACAGAAACTGATCAGCGAAGAGGACCTGCACCACCACCATCACCACTGACTCGAG

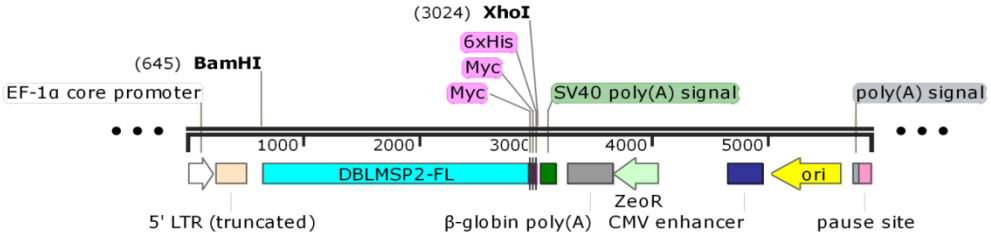

pFUSE-MCS-DBLMSP-C

GGATCCGCCACCATGAAGAAGATCTACTCCATCTTCTTCTCCCTGTTCATCCTGAACCTGCACATCTACATCAAGAA
CATCAAGTGCAACGACCTGATCAACTACAACGACAGCAACCTGAGAAACGGCCTGCTGAACAACAGCCTGGACCTGA
CCAACGGCCTGAACAACAAGGACAACAGCTTCATCGACAGCAAGATCGAGGAACACGAGAACAAGAGCTACCAGAAC
AAGGATAACAACATCAGCATCGTGGGCCAGGACGTGCCCATCACCAGCGTGTACAGCTCCAAGATCATCAACGCCAA
CGATCTGGAAGGCAACAGCATCGACGACACCAAGGGCCTGAGCGTGACCAACAGCGGCTTCGACGATGGCTCTGCTT
TCGGCGGAGGCCTGCCTTTCAGCGGCTACAGTCCTCTGCAGGGCAACCACAACAAGTGCCCCGACGAGAACTTCTGC
AAGGGAATCAAGAACGTGCTGAGCTGCGACTGCAAGTACAAGGACCTGGACAACACATTCAAAGAATTCAAGGACAA
TGTGACCCTGCTGAAGGCCGTGATCGACAACAAGAAGAACCAGGACAGCCTGACCACCACCAGCCTGAGCACCTCCA
TCAACTCCGTGCGGGACTCCTCCAACCTGGACCAGAGAGGCAACATCACCACCTCCCAGGGCAACAGCCACAGAGCC
ACAGTGGTGCAGCAGGTGGACCAGACAAACAGACTGGACAACGTGAACAGCGTGACCCAGCGGGGCAACAACAATTA
CAACAACAACCTGGAAAGGGGCCTGGGCTCTGGCGCTCTGCCTGGCACCAACATCATCACCGAGGAAAAGTACTCCC
TGGAACTGATCAAGCTGACCAGCAAGGACGAAGAGGACATCATCAAGCACAATGAGGACGTGCGGGAAGAGATCGAA
GAACAGCAGGAAGATATTGAAGAGGACGAGGAAGAACTGGAAAACGAGGGCGAGGAAACAAAAGAAGAGGACGACGA
GGAAAAGAACGAGACAAACGACACCGAGGACACAGACGATACAGAGGACACTGAGGACATCGAAGAGGAAAACAAAG
AGAAAGAGCTGAGCAACCAGCAGCAGAGCGAGAAGAAATCCATCAGCAAGGTGGACGAGGACAGCTACAGAATCCTG
TCCGTGTCCTACAAAGACAACAACGAAGTGAAGAACGTGGCCGAGAGCATCGTGAAGAAGCTGTTCAGCCTGTTCAA
CGACAACAACAATCTGGAAACCATCTTCAAGGGCCTGACCGAGGACATGACCGACCTGTTCCAGAAAGAGCAGAAGC
TGATCTCCGAAGAGGACCTGGAACAGAAACTGATCAGCGAGGAAGATCTGCACCACCATCACCATCACTGACTCGAG

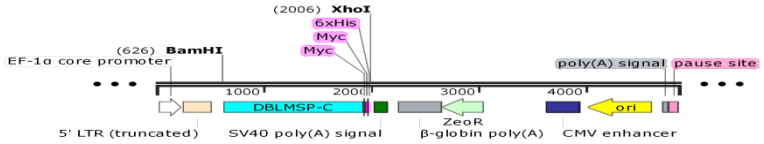

pFUSE-MCS-DBLMSP2-C

GGATCCGCCACCATGATCTACATCCTGTCTATCGTGTTCTACATCTTCTTTCTGCACATCGACATCTACGTGAACA
TCTACAGCACCTGTTTCGTCGTGAACGAGGGCAACCCCAACCTGAGAAACAACATCATCAACGACGACGAGCTGAA
GGGCAAGGCCTACAACAACACCATCGACGCCAACAACCAGAACATCGAGTACAACAAGAACCTGAAGCACAACGTG
AACAGCAGCCACATCAGCAAGTTCAGCGACATCATGGACCAGGAAGATAAGGGCGACAACGAGAACTCCCACGACA
TCAAGTTCGAGGAAAAGAAGAACATCAACAAGAGCCTGGACGCCGAGAGCAACTACGGCATCAACGAGATCAGCAT
CACCGGCAACGACAGCAACAGCGACAACAGCAACCAGAATATCTTCCCCGACGGCAGCGAGCTGGCTGGCGGCATC
CCTAGATCCATCTACACCATCAACCTGGGCTTCAACAAGTGCCCCACCGAGGAAATCTGCAAGGACTTCAGCAACC
TGCCCCAGGTGTTCGAGCTGACCTTCGACGGCAAGGCCCTGCTGGAAAAGCTGAAGAAAGAGGAATCCCCCGTGTC
CAACAGCGTGAACGCCCTGCCTGAGCCTGGCCAGATCACACTGCCTGACCCCAGCCTGAAGCAGACCACCCAGCAG
GAAAACCAGCCCGTGGTGGAAACCCCTGTGACCACCGCCGTGATCAACGAGCACCAGGGCCAGACCGAGCCCAACA
AGGGCGATAACAACAACGAGAGAGAGAACCACGAGTCCAACGTGGGCAGCATCCAGGAAGTGAACCAGGGCAGCGT
GTCCGAGGAAAGCCACAGCAAGACCATCGACCCCAGCAAGATCGACGACAGACTGGAACTGAGCAGCGGCAGCAGC
AGCCTGGAACAGCACAGCAAAGAAGATGTGAAGAAGGGCTGCGCCCTGGAACTGGTGCCTCTGAGCCTGAGCGACA
TCGAGCAGATCGCCAACGAGAGCGAGGACGTGCTGGAAGAGATCGAGGAAGAGATTAACACCGACGGCGAGATCGA
GTATATCACCGAAGAGGAAATCAAAGAGGACATCGAAGAAGAGACAGAAGAGGATATTGAGGAAGAAACCGAAGAA
GAAACTGAGGAAGAGACAGAGGAAGAGGCCGACGAGGAAACCGTGAAAGAAATCGAGGACAAGCCCGAGCAGGAAA
TCAAGAACAAGTCCCTGGAAGAGAAGCAGATCGACAAGAACACCGACACCAGCGAGAAGAAGGGATTCAACAACTC
CGAGAAGGACGAGAAGGCCAGAAACCTGATCAGCAAGAACTACAAGAATTACAACGAGCTAGACAAGAACGTGCAC
ACCCTCGTGAACTCCATCATTAGCCTGCTGGAAGAAGGCAACGGCAGCGACAGCACCCTGAACAGCCTGAGCAAGG
ACATCACAAACCTGTTCAAGAACGAGCAGAAGCTGATCTCTGAAGAGGATCTGGAACAGAAACTGATTAGCGAAGA
GGACCTGCACCACCACCATCACCACTGACTCGAG

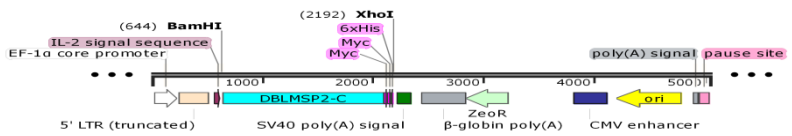

Creation of pRSET EmGFP bacterial expression vector containing DBLMSP and DBLMSP2

The sequences encoding full-length DBLMSP and DBLMSP2 (FL), and DBLMSP and DBLMSP lacking DBL domains (C), were subcloned into the pRSET-GFP bacterial expression vector (Invitrogen) to create the pRSET-DBLMSP-FL, pRSET-DBLMSP-C, pRSET-DBLMSP2-FL, pRSET-DBLMSP2-C expression vectors.

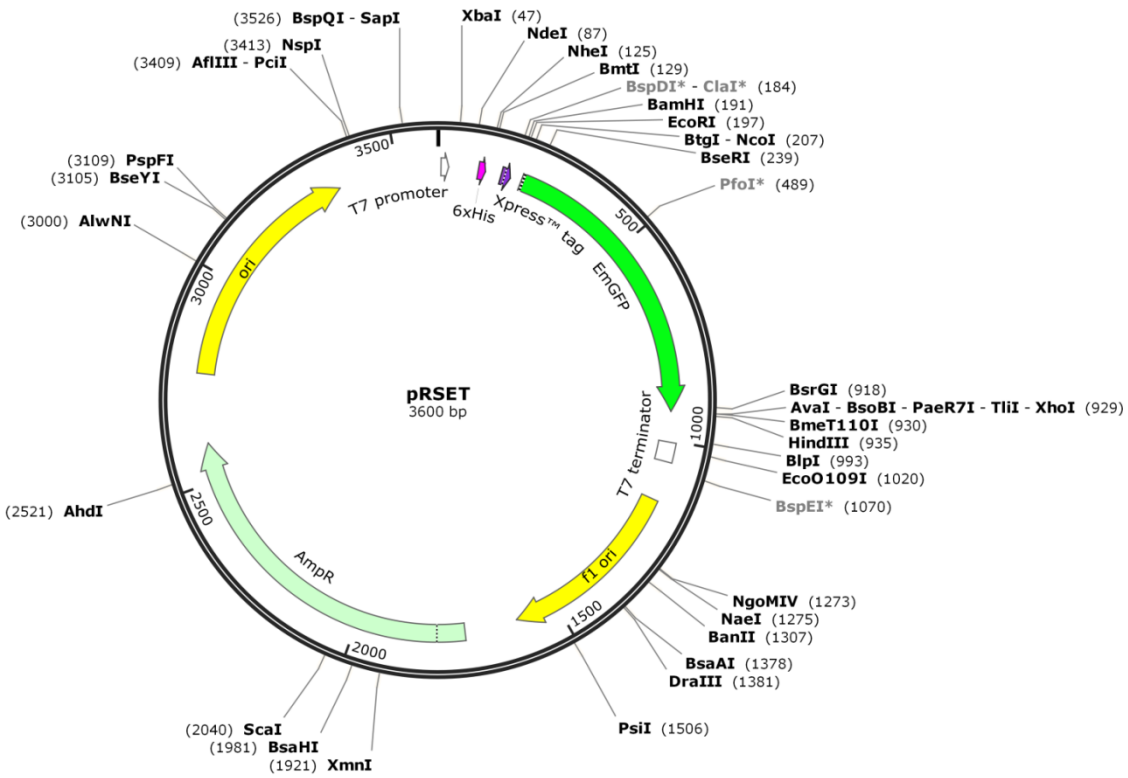

pRSET-DBLMSP-FL

GGATCCCGCCACCATGAAGAAGATCTACTCCATCTTCTTCTCCCTGTTCATCCTGAACCTGCACATCTACATCAAG
AACATCAAGTGCAACGACCTGATCAACTACAACGACAGCAACCTGAGAAACGGCCTGCTGAACAACAGCCTGGACC
TGACCAACGGCCTGAACAACAAGGACAACAGCTTCATCGACAGCAAGATCGAGGAACACGAGAACAAGAGCTACCA
GAACAAGGATAACAACATCAGCATCGTGGGCCAGGACGTGCCCATCACCAGCGTGTACAGCTCCAAGATCATCAAC
GCCAACGATCTGGAAGGCAACAGCATCGACGACACCAAGGGCCTGAGCGTGACCAACAGCGGCTTCGACGATGGCT
CTGCTTTCGGCGGAGGCCTGCCTTTCAGCGGCTACAGTCCTCTGCAGGGCAACCACAACAAGTGCCCCGACGAGAA
CTTCTGCAAGGGAATCAAGAACGTGCTGAGCTGCCCCCCCAAGAACAGCACCGGCAGAAACGGCGACTGGATCAGC
GTGGCCGTGAAAGAGAGCAGCACCACCAACAAGGGCGTGCTGGTGCCCCCTAGAAGGACCAAGCTGTGCCTGAGGA
ACATCAACAAAGTGTGGCACAGGATCAAGGACGAGAAGAACTTCAAAGAGGAATTCGTGAAGGTGGCCCTGGGCGA
GAGCAACGCCCTGATGAAGCACTACAAAGAGAAGAACCTGAACGCTCTGACCGCCATTAAGTACGGCTTCAGCGAC
ATGGGCGACATCATCAAGGGCACAGATCTGATCGACTACCAGATCACCAAGAATATCAACCGGGCCCTGGACAAGA
TCCTGCGGAACGAGACAAGCAACGACAAGATCAAGAAACGAGTGGATTGGTGGGAGGCCAACAAGAGCGCCTTCTG
GGACGCCTTCATGTGCGGCTACAAGGTGCACATCGGCAACAAGCCCTGCCCCGAGCACGACAACATGGACAGAATC
CCCCAGTACCTGAGATGGTTCCGCGAGTGGGGCACCTACGTGTGCAGCGAGTACAAGAACAAGTTCGAGGACGTGA
TCAAGCTGTGTAACATCCAGCAGTTCACCAACCAGGACGACAGCCAGCTGCTGGAAATCAGCAAGAAAGACAAGTG
CAAAGAGGCCCTGAAACACTACGAGGAATGGGTCAACAGACGCAGACCCGAGTGGAAGGGCCAGTGCGATAAGTTC
GAGAAAGAGAAGTCTAAGTACGAGGACACCAAGAGCATCACCGCCGAGAAGTATCTGAAAGAAATCTGCTCCGAGT
GCGACTGCAAGTACAAGGACCTGGACAACACATTCAAAGAATTCAAGGACAATGTGACCCTGCTGAAGGCCGTGAT
CGACAACAAGAAGAACCAGGACAGCCTGACCACCACCAGCCTGAGCACCTCCATCAACTCCGTGCGGGACTCCTCC
AACCTGGACCAGAGAGGCAACATCACCACCTCCCAGGGCAACAGCCACAGAGCCACAGTGGTGCAGCAGGTGGACC
AGACAAACAGACTGGACAACGTGAACAGCGTGACCCAGCGGGGCAACAACAATTACAACAACAACCTGGAAAGGGG
CCTGGGCTCTGGCGCTCTGCCTGGCACCAACATCATCACCGAGGAAAAGTACTCCCTGGAACTGATTAAGCTGACC
AGCAAGGACGAAGAGGATATCATCAAGCACAATGAGGACGTGCGGGAAGAGATTGAGGAACAGCAGGAAGATATTG
AAGAGGACGAGGAAGAACTGGAAAACGAGGGCGAGGAAACAAAAGAAGAGGACGACGAGGAAAAGAACGAGACAAA
CGACACCGAGGACACCGACGATACAGAGGATACCGAAGATATCGAGGAAGAGAACAAAGAAAAAGAGCTGAGCAAC
CAGCAGCAGAGCGAGAAGAAATCCATCAGCAAGGTGGACGAGGACAGCTACAGAATCCTGTCCGTGTCCTACAAAG
ACAACAACGAAGTGAAGAACGTGGCCGAGAGCATCGTGAAGAAGCTGTTCAGCCTGTTCAACGACAACAACAATCT
GGAAACCATCTTCAAGGGCCTGACCGAGGACATGACCGACCTGTTCCAGAAGGCCGAGCAGAAGCTGATCTCCGAA
GAGGACCTGGCTGAACAGAAACTGATCAGCGAGGAAGATCTGGCCCACCACCACCATCACCACTGA**CTCGAG**

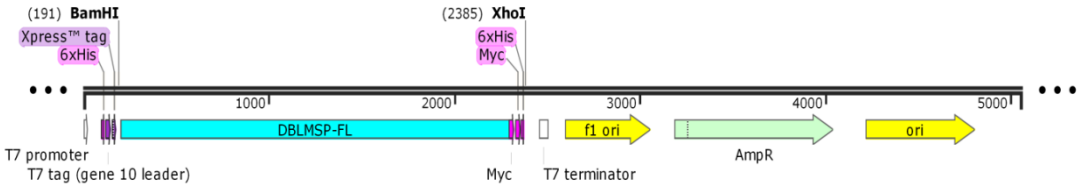

pRSET-DBLMSP2-FL

GGATCCGCCACCATGATCTACATCCTGTCTATCGTGTTCTACATCTTCTTTCTGCACATCGACATCTACGTGAACA
TCTACAGCACCTGTTTCGTCGTGAACGAGGGCAACCCCAACCTGAGAAACAACATCATCAACGACGACGAGCTGAA
GGGCAAGGCCTACAACAACACCATCGACGCCAACAACCAGAACATCGAGTACAACAAGAACCTGAAGCACAACGTG
AACAGCAGCCACATCAGCAAGTTCAGCGACATCATGGACCAGGAAGATAAGGGCGACAACGAGAACTCCCACGACA
TCAAGTTCGAGGAAAAGAAGAACATCAACAAGAGCCTGGACGCCGAGAGCAACTACGGCATCAACGAGATCAGCAT
CACCGGCAACGACAGCAACAGCGACAACAGCAACCAGAATATCTTCCCCGACGGCAGCGAGCTGGCTGGCGGCATC
CCTAGATCCATCTACACCATCAACCTGGGCTTCAACAAGTGCCCCACCGAGGAAATCTGCAAGGACTTCAGCAACC
TGCCCCAGTGCCGGAAGAACGTGCACGAGAGGAACAACTGGCTGGGCAGCAGCGTGAAGAACTTCAGCTCCGACAA
CAAGGGCGTGCTGGTGCCCCCTAGAAGGCAGAGCCTGTGCCTGAGAATCACCCTGCAGGACTTCCGCACCAAGAAG
AAGAAAGAGGGCGACTTCGAGAAGTTCATCTACTCCTACGCCAGCAGCGAGGCCAGAAAGCTGAGAACCATCCACA
ACAACAATCTGGAAAAGGCCCACCAGGCCATCAGATACAGCTTCGCCGACATCGGCAATATCATCAGAGGCGACGA
CATGATGGACACCCCCACCAGCAAAGAGACAATCACCTACCTGGAAAAAGTGCTGAAGATCTACAATGAGAACAAC
GACAAGCCCAAGGACGCCAAGAAGTGGTGGACCGAGAACAGACACCACGTGTGGGAGGCCATGATGTGCGGCTACC
AGAGCGCCCAGAAAGACAACCAGTGCACCGGCTACGGCAACATCGACGATATCCCCCAGTTCCTGAGATGGTTCCG
CGAGTGGGGCACCTACGTGTGCGAGGAATCCGAGAAGAATATGAACACCCTGAAGGCCGTGTGCTTCCCCAAGCAG
CCTAGAACCGAGGCCAACCCTGCCCTGACCGTGCACGAAAACGAGATGTGCAGCAGCACACTGAAGAAATACGAGG
AATGGTATAACAAGCGCAAGACCGAGTGGACAGAGCAGTCCATCAAGTATAACAACGATAAGATCAACTACACAGA
CATCAAGACCCTGAGCCCCAGCGAGTACCTGATCGAGAAGTGCCCCGAGTGCAAGTGCACCAAAAAGAACCTGCAG
GATGTGTTCGAGCTGACCTTCGACGGCAAGGCCCTGCTGGAAAAGCTGAAAAAAGAGGAATCCCCCGTGTCCAACA
GCGTGAACGCCCTGCCTGAGCCTGGCCAGATCACACTGCCTGACCCCAGCCTGAAGCAGACCACCCAGCAGGAAAA
CCAGCCCGTGGTGGAAACCCCTGTGACCACCGCCGTGATCAACGAGCACCAGGGCCAGACCGAGCCCAACAAGGGG
GATAACAACAACGAGAGAGAGAACCACGAGTCCAACGTGGGCAGCATCCAGGAAGTGAACCAGGGCAGCGTGTCCG
AGGAAAGCCACAGCAAGACCATCGACCCCAGCAAGATCGACGACAGACTGGAACTGAGCAGCGGCAGCAGCAGCCT
GGAACAGCACAGCAAAGAAGATGTGAAGAAGGGCTGCGCCCTGGAACTGGTGCCTCTGAGCCTGAGCGACATCGAG
CAGATCGCCAACGAGAGCGAGGACGTGCTGGAAGAGATCGAGGAAGAGATTAACACCGACGGCGAGATCGAGTATA
TCACCGAAGAGGAAATCAAAGAGGACATCGAAGAAGAGACAGAAGAGGATATTGAGGAAGAAACTGAAGAAGAAAC
AGAGGAAGAGACTGAGGAAGAGGCCGACGAGGAAACCGTGAAAGAGATTGAGGACAAGCCCGAGCAGGAAATCAAG
AACAAGTCCCTGGAAGAGAAGCAGATCGACAAGAACACCGACACCAGCGAGAAGAAGGGATTCAACAACTCCGAGA
AGGACGAGAAGGCCCGGAACCTGATCAGCAAGAACTACAAGAATTACAACGAGCTGGACAAGAATGTGCACACACT
CGTGAACTCCATCATTAGCCTGCTGGAAGAAGGCAACGGCAGCGACAGCACCCTGAACAGCCTGAGCAAGGACATC
ACAAACCTGTTCAAGAACGAGCAGAAGCTGATCTCTGAAGAGGATCTGGAACAGAAACTGATCAGCGAAGAGGACC
TGCACCACCACCATCACCACTGACTCGAG

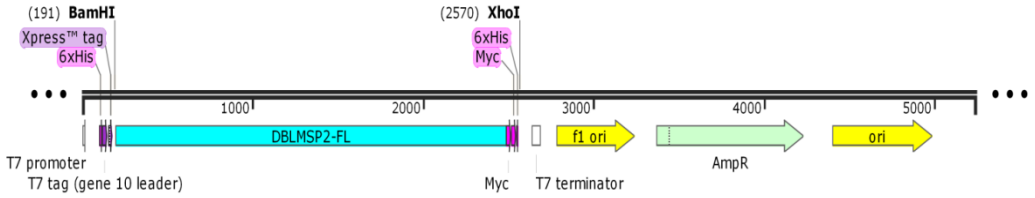

pRSET-DBLMSP-C

GGATCCGCCACCATGAAGAAGATCTACTCCATCTTCTTCTCCCTGTTCATCCTGAACCTGCACATCTACATCAAGA
ACATCAAGTGCAACGACCTGATCAACTACAACGACAGCAACCTGAGAAACGGCCTGCTGAACAACAGCCTGGACCT
GACCAACGGCCTGAACAACAAGGACAACAGCTTCATCGACAGCAAGATCGAGGAACACGAGAACAAGAGCTACCAG
AACAAGGATAACAACATCAGCATCGTGGGCCAGGACGTGCCCATCACCAGCGTGTACAGCTCCAAGATCATCAACG
CCAACGATCTGGAAGGCAACAGCATCGACGACACCAAGGGCCTGAGCGTGACCAACAGCGGCTTCGACGATGGCTC
TGCTTTCGGCGGAGGCCTGCCTTTCAGCGGCTACAGTCCTCTGCAGGGCAACCACAACAAGTGCCCCGACGAGAAC
TTCTGCAAGGGAATCAAGAACGTGCTGAGCTGCGACTGCAAGTACAAGGACCTGGACAACACATTCAAAGAATTCA
AGGACAATGTGACCCTGCTGAAGGCCGTGATCGACAACAAGAAGAACCAGGACAGCCTGACCACCACCAGCCTGAG
CACCTCCATCAACTCCGTGCGGGACTCCTCCAACCTGGACCAGAGAGGCAACATCACCACCTCCCAGGGCAACAGC
CACAGAGCCACAGTGGTGCAGCAGGTGGACCAGACAAACAGACTGGACAACGTGAACAGCGTGACCCAGCGGGGCA
ACAACAATTACAACAACAACCTGGAAAGGGGCCTGGGCTCTGGCGCTCTGCCTGGCACCAACATCATCACCGAGGA
AAAGTACTCCCTGGAACTGATCAAGCTGACCAGCAAGGACGAAGAGGACATCATCAAGCACAATGAGGACGTGCGG
GAAGAGATCGAAGAACAGCAGGAAGATATTGAAGAGGACGAGGAAGAACTGGAAAACGAGGGCGAGGAAACAAAAG
AAGAGGACGACGAGGAAAAGAACGAGACAAACGACACCGAGGACACAGACGATACAGAGGACACTGAGGACATCGA
AGAGGAAAACAAAGAGAAAGAGCTGAGCAACCAGCAGCAGAGCGAGAAGAAATCCATCAGCAAGGTGGACGAGGAC
AGCTACAGAATCCTGTCCGTGTCCTACAAAGACAACAACGAAGTGAAGAACGTGGCCGAGAGCATCGTGAAGAAGC
TGTTCAGCCTGTTCAACGACAACAACAATCTGGAAACCATCTTCAAGGGCCTGACCGAGGACATGACCGACCTGTT
CCAGAAAGAGCAGAAGCTGATCTCCGAAGAGGACCTGGAACAGAAACTGATCAGCGAGGAAGATCTGCACCACCAT
CACCATCACTGA**CTCGAG**

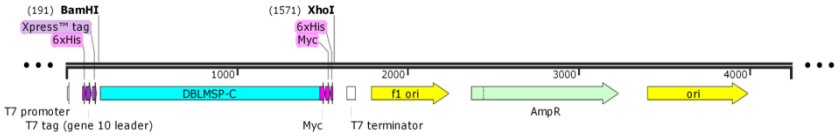

pRSET-DBLMSP2-C

GGATCCGCCACCATGAAGAAGATCTACTCCATCTTCTTCTCCCTGTTCATCCTGAACCTGCACATCTACATCAAGA
ACATCAAGTGCAACGACCTGATCAACTACAACGACAGCAACCTGAGAAACGGCCTGCTGAACAACAGCCTGGACCT
GACCAACGGCCTGAACAACAAGGACAACAGCTTCATCGACAGCAAGATCGAGGAACACGAGAACAAGAGCTACCAG
AACAAGGATAACAACATCAGCATCGTGGGCCAGGACGTGCCCATCACCAGCGTGTACAGCTCCAAGATCATCAACG
CCAACGATCTGGAAGGCAACAGCATCGACGACACCAAGGGCCTGAGCGTGACCAACAGCGGCTTCGACGATGGCTC
TGCTTTCGGCGGAGGCCTGCCTTTCAGCGGCTACAGTCCTCTGCAGGGCAACCACAACAAGTGCCCCGACGAGAAC
TTCTGCAAGGGAATCAAGAACGTGCTGAGCTGCGACTGCAAGTACAAGGACCTGGACAACACATTCAAAGAATTCA
AGGACAATGTGACCCTGCTGAAGGCCGTGATCGACAACAAGAAGAACCAGGACAGCCTGACCACCACCAGCCTGAG
CACCTCCATCAACTCCGTGCGGGACTCCTCCAACCTGGACCAGAGAGGCAACATCACCACCTCCCAGGGCAACAGC
CACAGAGCCACAGTGGTGCAGCAGGTGGACCAGACAAACAGACTGGACAACGTGAACAGCGTGACCCAGCGGGGCA
ACAACAATTACAACAACAACCTGGAAAGGGGCCTGGGCTCTGGCGCTCTGCCTGGCACCAACATCATCACCGAGGA
AAAGTACTCCCTGGAACTGATCAAGCTGACCAGCAAGGACGAAGAGGACATCATCAAGCACAATGAGGACGTGCGG
GAAGAGATCGAAGAACAGCAGGAAGATATTGAAGAGGACGAGGAAGAACTGGAAAACGAGGGCGAGGAAACAAAAG
AAGAGGACGACGAGGAAAAGAACGAGACAAACGACACCGAGGACACAGACGATACAGAGGACACTGAGGACATCGA
AGAGGAAAACAAAGAGAAAGAGCTGAGCAACCAGCAGCAGAGCGAGAAGAAATCCATCAGCAAGGTGGACGAGGAC
AGCTACAGAATCCTGTCCGTGTCCTACAAAGACAACAACGAAGTGAAGAACGTGGCCGAGAGCATCGTGAAGAAGC
TGTTCAGCCTGTTCAACGACAACAACAATCTGGAAACCATCTTCAAGGGCCTGACCGAGGACATGACCGACCTGTT
CCAGAAAGAGCAGAAGCTGATCTCCGAAGAGGACCTGGAACAGAAACTGATCAGCGAGGAAGATCTGCACCACCAT
CACCATCACTGA**CTCGAG**

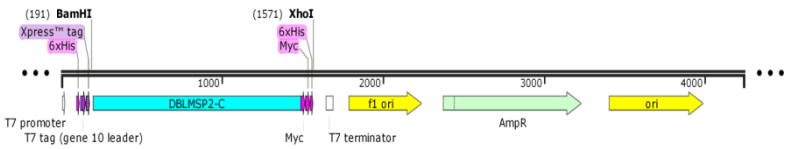

Appendix III

Supplementary data

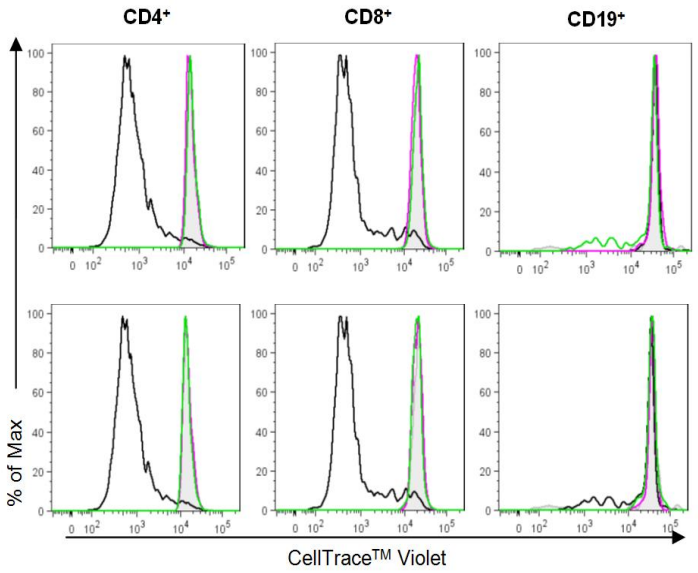

Figure A1 IgM/DBLMSP immune complexes did not induce proliferation. Purified CellTrace™ Violet-labelled PBMCs were cultured on 96-well plates (Nunc) coated with 50µg/ml of his-tagged DBLMSP or Cd4-d3+4 proteins, or IgM/DBLMSP or IgM/ Cd4-d3+4 immune complexes (1:5 ratio) for 5d at 37˚C/ 5% CO_2. Proliferation was not induced in CellTrace™ Violet labelled PBMCs incubated with DBLMSP (pink trace, top panel), Cd4-d3+4 (green trace, top panel), IgM/DBLMSP (pink trace, lower panel), or IgM/Cd4-d3+4 (green trace, lower panel), whereas it was induced in cells incubated with PHA (black trace). Data shown is one of two repeat experiments.

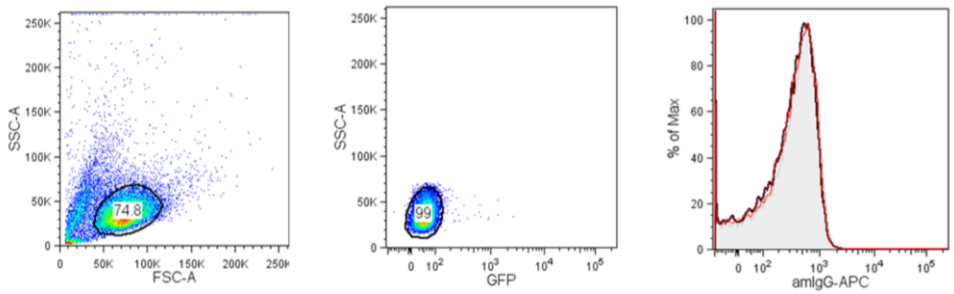

Figure A2 hFcμR is not expressed on untransfected BW5147 cells. Untransfected BW5147 cells were washed and incubated with 1μg anti-FcμR mAb (Abnova) or medium alone for 1hr at 4˚C. Cells were then washed and labelled with anti-mouse IgG-APC for 1hr at 4˚C prior to subsequent washing and analysis by flow cytometry. Live cells were gated based on the *SSC* and *FSC* prolife (left panel), and were further gated into GFP-negative cells (middle gate). Expression of FcμR was investigated by staining with anti-mIgG-APC (right panel). Cells incubated with medium alone are shown as a grey trace, cells incubated with anti-mIgG-APC are shown as a black trace, and cells incubated with anti-mAb and anti-mIgG-APC are shown as a red trace (n= 3).

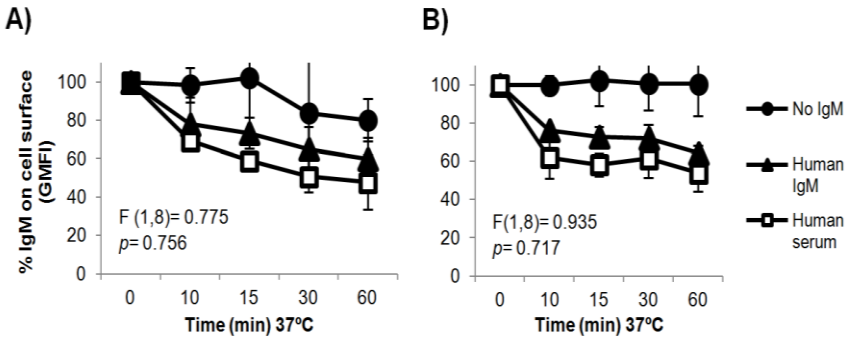

Figure A3 IgM is internalised into lymphocytes. PBMCs were isolated from healthy donors were washed and incubated with media alone or supplemented with human IgM or human serum for 1hr at 4˚C. Cells were washed and incubated at 37˚C for the indicated times. Cells were then washed extensively and labelled with markers specific for human IgM, CD3, and CD19. Surface levels of IgM on gated lymphocytes were determined by flow cytometry. IgM geometric mean fluorescence intensities (GMFI) were normalised to time 0 for T cells **(A)** and B cells **(B)**. There was no significant differences in internalisation between cells incubated purified IgM or human serum ($p > 0.05$), as determined by one-way ANOVA. The mean ± SD of five independent repeats is shown.

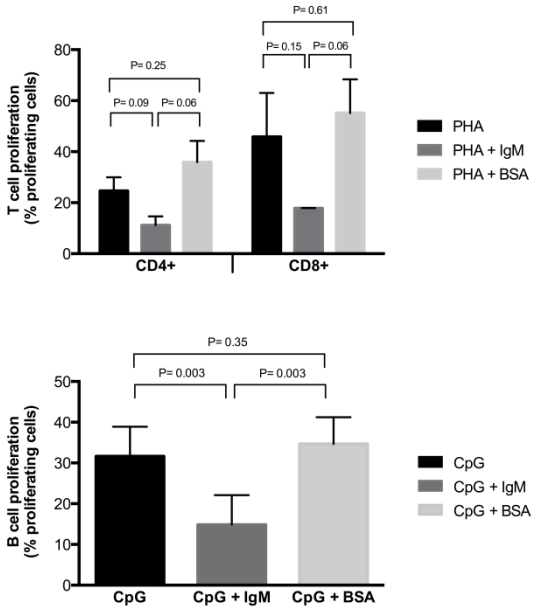

Figure A4 Lower concentrations of IgM induce inhibition of T cell and B cell proliferation. The ability of IgM or BSA (10µg/ml) to inhibit proliferation of CellTrace™ Violet-labelled gated lymphocytes was investigated by flow cytometry. Data are represented as mean ± SD of two independent experiments. Multiple unpaired t-tests were used to determine significant differences in cellular proliferation (% proliferating cells) between samples. Statistical significance was determined as $p < 0.05$.

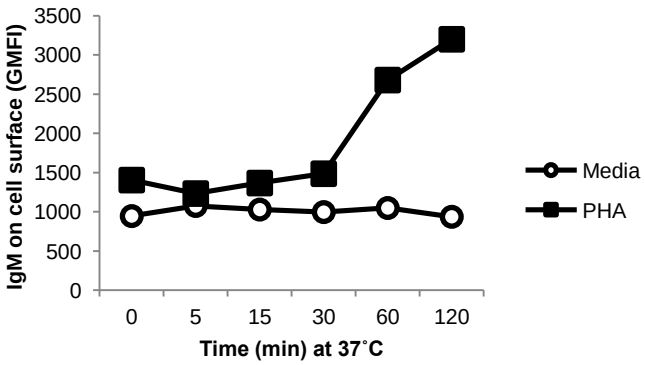

Figure A5 PHA activation induces externalisation of IgM on gated T cells. PBMCs were incubated with medium alone or medium supplemented with 1µg/ml PHA for 5 min at 4˚C, prior to incubation at 37˚C for the indicated times. Following internalisation, cells were washed twice to remove unbound IgM. Subsequently, cells were labelled with $F(ab')_2$-anti-human IgM-RPE and anti-CD3-APC. IgM levels on cell surfaces were determined by the geometric mean fluorescence intensity of RPE. Data shown is from one donor.

Appendix IV

Publications

Developing the IVIG biomimetic, Hexa-Fc, for drug and vaccine applications

Daniel M. Czajkowsky[1], Jan Terje Andersen[2], Anja Fuchs[3], Timothy J. Wilson[3], David Mekhaiel[4], Marco Colonna[3], Jianfeng He[1], Zhifeng Shao[1], Daniel A. Mitchell[5], Gang Wu[6], Anne Dell[6], Stuart Haslam[6], Katy A. Lloyd[4], Shona C. Moore[4], Inger Sandlie[2,7], Patricia A. Blundell[4] and Richard J. Pleass[4*]

1 – Bio-ID Center, School of Biomedical Engineering, Shanghai Jiao Tong University, Shanghai, 200240 P. R. China.
2 - Centre for Immune Regulation (CIR) and Department of Immunology, Oslo University Hospital Rikshospitalet, P.O. Box 4956, Oslo N-0424, Norway.
3 - Department of Pathology and Immunology, Washington University School of Medicine, St. Louis,MO 63110, USA
4 - Liverpool School of Tropical Medicine, Pembroke Place, Liverpool, L3 5QA, UK
5 - Clinical Sciences Research Laboratories, Warwick Medical School, University of Warwick, Coventry CV2 2DX, UK
6 - Department of Life Sciences, Imperial College London, South Kensington Campus, London SW7
7 CIR and Department of Biosciences, University of Oslo, N-0316 Oslo, Norway
*Corresponding author E-mail address: rpleass@liv.ac.uk Telephone: +44 151 705 3315

Abstract

The remarkable clinical success of Fc-fusion proteins has driven intense investigation for even more potent replacements. Using quality-by-design (QbD) approaches, we generated hexameric-Fc (hexa-Fc), a ~20nm oligomeric Fcbased scaffold that we here show binds low-affinity inhibitory receptors (FcRL5,FcγRIIb, and DC-SIGN) with high avidity and specificity, whilst eliminating significant clinical limitations of monomeric Fc-fusions for vaccine and/or cancer therapies, in particular their poor ability to activate complement. Mass spectroscopy of hexa-Fc reveals high-mannose, low-sialic acid content, suggesting that interactions with these receptors are influenced by the mannose-containing Fc. Molecular dynamics (MD) simulations provide insight into the mechanisms of hexa-Fc interaction with these receptors and reveals an unexpected orientation of high-mannose glycans on the human Fc that provide greater accessibility to potential binding partners. Finally, we show that this biosynthetic nanoparticle can be engineered to enhance interactions with the human neonatal Fc receptor (FcRn) without loss of the oligomeric structure, a crucial modification for these molecules in therapy and/or vaccine strategies where a long plasma half-life is critical.

Key words: hexa-Fc; glycosylation; complement; FcRL5; FcγRIIb; DC-SIGN.